ISTITUTO NAZIONALE DI FISICA NUCLEARE
Laboratori Nazionali di Frascati

FRASCATI PHYSICS SERIES

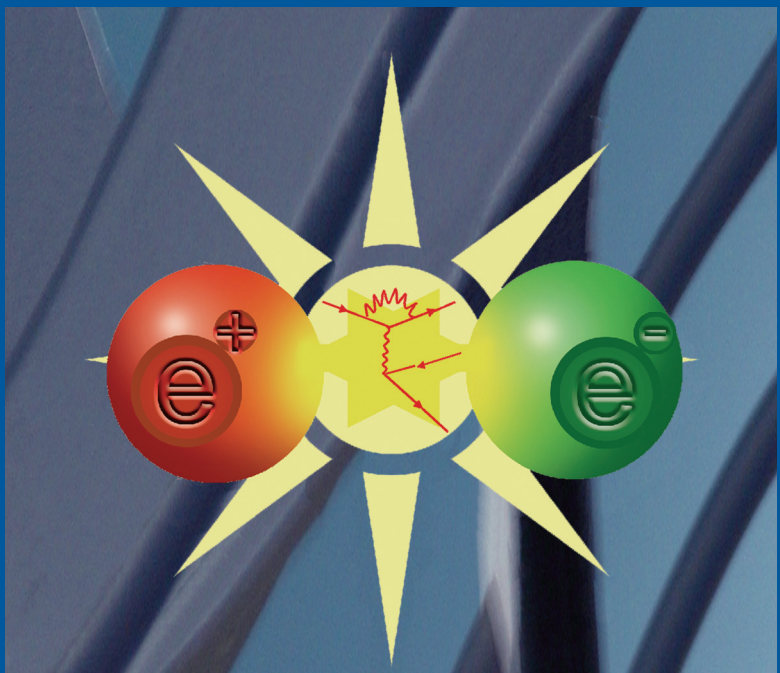

INTERNATIONAL WORKSHOP ON DISCOVERIES IN FLAVOUR PHYSICS AT e^+e^- COLLIDERS

Editors:
L.Benussi, S. Bianco, C. Bloise, R. de Sangro,
C. Gatti, G. Isidori, M. Martini, F. Mescia, S. Miscetti

INTERNATIONAL WORKSHOP ON DISCOVERIES IN FLAVOUR PHYSICS AT e^+e^- COLLIDERS

FRASCATI PHYSICS SERIES

Series Editor
Stefano Bianco

Technical Editor
Luigina Invidia

Volume XLI

Istituto Nazionale di Fisica Nucleare – Laboratori Nazionali di Frascati
Divisione Ricerca – SIS – Ufficio Pubblicazioni
P.O. Box 13, I–00044 Frascati (Roma) Italy
email: sis.publications@lnf.infn.it

FRASCATI PHYSICS SERIES
DISCOVERIES IN FLAVOUR PHYSICS AT e^+e^- COLLIDERS

ISBN — 88–86409–51–6

Printed in Italy by Poligrafica Laziale, P.le della Stazione 1, 00044 Frascati

FRASCATI PHYSICS SERIES

Volume XLI

DISCOVERIES IN FLAVOUR PHYSICS AT e^+e^- COLLIDERS

DIF06

Editors
L. Benussi, S. Bianco, C. Bloise, R. de Sangro,
C. Gatti, G. Isidori, M. Martini, F. Mescia, S. Miscetti

Laboratori Nazionali dell'INFN, Frascati (Italy)
February 28th - March 3rd, 2006

International Advisory Committee

J. Alexander	*(Cornell U., USA)*
I. Bigi	*(University of Notre Dame, USA)*
T.E. Browder	*(University of Hawaii, USA)*
A.J. Buras	*(TU München, Germany)*
G. Capon	*(INFN-Frascati, Italy)*
K.T. Chao	*(Peking University, China)*
F.L. Fabbri	*(INFN-Frascati, Italy*
F. Ferroni	*(University of Roma 1, Italy*
M. Giorgi	*(INFN and University of Pisa, Italy)*
J.L. Hewett	*(SLAC, USA)*
D.G. Hitlin	*(California Institute of Technology, USA)*
W.G. Li	*(IHEP, Russia)*
V. Luth	*(SLAC, USA)*
M. Mangano	*(CERN, Switzerland)*
A. Masiero	*(University of Padova, Italy)*
C. Matteuzzi	*(INFN and University of Milano-Bicocca, Italy)*
A. Palano	*(INFN Bari, Italy)*
M.L. Perl	*(SLAC, USA)*
A. Pich	*(Valencia University, Spain)*
I. Shipsey	*(Purdue University, USA)*
H. Yamamoto	*(Tohoku University, Japan)*

Local Organizing Committee

S. Bianco
C. Bloise
R. de Sangro
G. Isidori
S. Miscetti

Scientific Secretaries

F. Anulli
L. Benussi
C. Gatti
M. Martini
F. Mescia

Secretaries

R. Bertelli
M.C. D'Amato
A. Pelagalli

PREFACE

About one hundred physicists from thirteen Countries gathered at the end of February 2006 in Frascati Laboratories for a four-day full immersion in the future, and an ambitious goal: to ascertain the importance of future e+e- colliders in the era of LHC. No other place was better suited to host the meeting. Frascati Laboratories are the home of AdA, the very first e+e- collider ever built, invented by Bruno Touschek in 1960.

The Workshop turned out to be a riddle of questions, some answered, some other not: is flavour physics important to complement the discoveries in New Physics we expect for the LHC? Do electron-positron colliders have a future in flavour physics? What is the relevance of kaon physics? Do we need a tau-charm factory? Are we interested in tau physics for discoveries? Are we better off with taus at the upsilon resonance or at production threshold? Some of these questions indeed trickled to the very lively round table held on the last day. The meeting nicely fitted in the work done this year to define a INFN roadmap and, even more importantly, a sustainable development plan for Frascati in the long-term future. The Workshop ended with a common agreement on the importance of a flavour factory able to cover a multifaceted programme, from the $\phi(1020)$ meson to the $\Upsilon(4s)$.

Last but not least, we enjoyed gathering for celebrating Paolo Franzini's lifelong achievements in the special Kaon Symposium that opened the Workshop.

On behalf of the LOC we thank Frascati Director Mario Calvetti for enthusiastic encouragement and support, and all those who worked to make this meeting a success. We cherish the idea of having contributed with, at the very least, the raising of precise and provocative questions.

Frascati, September 2006 Stefano Bianco and Gino Isidori

CONTENTS

Bottom-Quark Physics I

τ-Lepton Physics

Bottom-Quark Physics II

SYMPOSIUM IN HONOUR OF PROF. PAOLO FRANZINI

Frascati Physics Series Vol. XLI (2006), pp. 3-14
DISCOVERIES IN FLAVOUR PHYSICS AT e^+e^- COLLIDERS
Frascati, February 28th - March 3rd, 2006

THE PHYSICS OF PAOLO FRANZINI

Nicola Cabibbo
Physics Department, University of Rome "La Sapienza"
and INFN, Sezione di Roma

Abstract

I review some of the highlights in the career of Paolo Franzini since the early bubble chamber work to the recent results obtained with the Kloe experiment at Frascati.

I am only a few years younger than Paolo Franzini, but that made a huge difference in 1956, when Lee and Yang proposed parity violation: I was then in my third year, while Paolo had already graduated and took part, with the Pisa group led by Marcello Conversi, in an experiment at the Brookhaven Cosmotron [1] that demonstrated parity violation in the decay of a Λ^0 hyperon, $\Lambda^0 \to p + \pi^-$. The Italian groups of Pisa and Bologna (I remember a seminar in Rome by Giampiero Puppi on this important result) had been collaborating with the group at Columbia University, led by Jack Steinberger and Mel Schwartz, and the Michigan group led by Don Glaser, the inventor of the bubble chamber. This was probably the first important result obtained with bubble chambers.

After moving to Columbia University as a Fulbright Fellow Paolo continued his bubble chamber work at the Cosmotron, and discovered the first

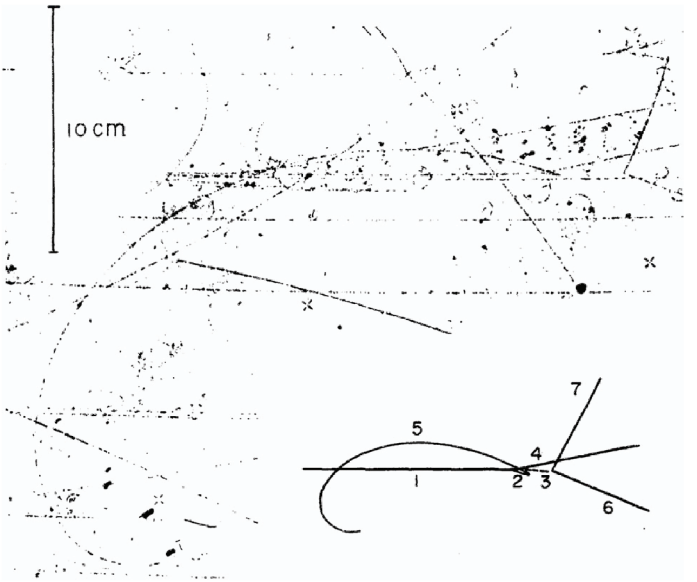

Figure 1: Paolo's $\Sigma^{\pm} \to \Lambda e^{\pm} \nu$ event.

example [2] of an hyperon leptonic decay, $\Sigma^- \to n e^- \bar{\nu}$. This was a very clean event: it confirmed the existence of leptonic decay modes of the hyperons, but at the same time demonstrated that the rate of these decays was much smaller than expected by the V-A theory of weak interactions.

At Columbia Paolo engaged in a new experiment, that used the Nevis cyclotron to measure the polarization of the μ^- in pion decay [3] and demonstrated that the electron and muon neutrinos have the same helicity. The question remained open whether the two particles were or not identical, and was only settled by high energy neutrino experiments. The team was small: Paolo, Marcel Bardon and Juliet Lee, and this experiment was the beginning of a lifelong collaboration with Juliet. In October 1962 I moved from Frascati to CERN, and there I found Paolo working on the hyperon data from the Saclay 81 cm hydrogen bubble chamber. At this point Paolo had decided to pursue a career in the United States, but the rules of the Fulbright Fellowship required that he had to spend two years outside of the country. We had met shortly

in Frascati, but at CERN we became very close friends, and we collaborated on a study [4] of the strangeness conserving leptonic decays $\Sigma^{\pm} \to \Lambda e^{\pm} \nu$. In 1960 I had written a paper [5] with Raul Gatto pointing out that these decays offer an excellent test of the Conserved Vector Current (CVC) hypothesis. In fact CVC implies that the allowed contribution of the vector current obeys a $\Delta I = 0$ selection rule, so that it should be absent in these decays, where $\Delta I = 1$. Paolo's group was collecting a sample of these decays, and we decided to work out other consequences of CVC, in particular with respect to the weak magnetism terms, where the Σ triplet offers a CVC test fully comparable to that proposed by Feynman and Gell-Mann for the $B^{12} - C^{12} - N^{12}$ triplet in nuclear beta decay. The first tests of these predictions was presented in 1972 [6] by collecting 186 events from different experiments.

My collaboration with Paolo in the winter of 1962-63 had an invaluable impact on the development of my own work [7] on the universality of weak interactions, both for his encouragement "Nicola, why don't you do something fundamental?", and for the many discussions we had on his work that kept me focused on the problem posed by the low rates of the hyperon leptonic decays. With Raul Gatto I had studied [8] the role of SU(3) symmetry in weak interactions, and we had worked out some of the tools that entered in my '63 paper, such as the F and D parameters for axial currents. It was however clear that SU(3) alone would not solve the problem of the low rate of $\Delta S = 1$ leptonic decays, and some new ingredient was needed. Until 1962, however, the available data was based on low-statistics experiments, with a handful of interesting events, such as the one found by Paolo in 1961. Now Paolo's experiment [9] was collecting hundreds of thousands of hyperon decays among which tens of leptonic events of the different types, especially those with $\Delta S = 1$: $\Sigma^- \to n e^- \bar{\nu}$ and $\Lambda^0 \to p e^- \bar{\nu}$, so that the perspective of having well measured branching ratios for these modes appeared imminent.

Getting a feeling for the results coming out of the Saclay bubble chamber was important from another point of view. In 1962 Walter Barkas and his collaborators at Berkeley had published [10] a $\Sigma^+ \to n \mu^+ \nu$ event, obtained in a sample of 120 Σ^+ observed in nuclear emulsions. The paper analysed the possibility that this event was due to some form of background and concluded

Figure 2: Paolo and Juliet in 1966, with Charles Baltay, Lawrence Kirsch and the IBM 7090.

that this had a very low probability, a few parts in 10^{-5}. This was a serious problem: it suggested the existence of a weak current with $\Delta S = -\Delta Q$, forbidden by the SU(3) octet scheme. The CERN experiment had collected a thousand time more events, and no $\Delta S = -\Delta Q$ event was emerging, and this implied a dilution of the significance of the Barkas event. I thus decided to go ahead with the octet hypothesis. The limit on $\Delta S = -\Delta Q$ currents has been improving with time, but the interpretation of the Barkas event remains somewhat mysterious.

Before returning to the US Paolo was for a short time in Pisa, where he engaged with Luigi Radicati in an analysis [11] of the validity of Wigner's SU(4) supermultiplet model in nuclear physics. Wigner's SU(4) was obtained from a mixture of ordinary spin and isotopic spin. This work had a seminal influence on Radicati's subsequent work with Feza Gursey on the SU(6) model of hadron multiplets, that in turn had a large role in the acceptance of the quark model.

Over the following years we kept meeting, sometimes in Italy, but more often in the United States where I was a frequent visitor. I met Paolo and Juliet in a Brookhaven conference in the fall of 1963, and they married the next year. Over the following years I was many times in their beautiful green house in Westchester. I remember with pleasure our meeting at Fermilab in the winter of 1975: Paolo and Juliet where engaged in a precision measurement [12] of the diffractive hadron production in very high energy proton-proton scattering. As is typical of the Franzini experiments it used a very sophisticated technique, that included a gas target in the circulating beam. At the same time it was a small experiment, carried on by Juliet and Paolo with three graduate students, all of them living as a small community in a house in the Fermilab village. Paula, then 10 years old, was an integral part of the group, always intent on a huge computer terminal.

Only two years after this visit Paolo and Juliet launched the Columbia – Stony Brook collaboration, CUSB. The discovery of the Υ state at Fermilab [13] was announced in July 1977, and in December of the same year the CUSB proposal was submitted to the Cornell Electron Storage Ring and was approved in record time. The collaboration was, by the standard of High Energy Physics, a small one, that at its peak barely reached thirty physicists, the apparatus was compact, aiming at rapid deployment and simplicity of the data analysis, and these choices paid off handsomely, as the installation of the detector could start in less than two years, in the fall of 1979. Before the year was over, while still incomplete, CUSB had observed the first three Υ states and produced a major discovery [14], the $\Upsilon(4S)$. The relatively large width indicated that this state was above the $B - \bar{B}$ threshold. The $\Upsilon(4S)$ proved to be the perfect tool for the study of B mesons. The recent work at the B-factories working at the $\Upsilon(4S)$ peak has led to the unraveling of the CP violation phenomena in the framework of the Standard Model.

Among the many important results obtained by CUSB I wish to remember the first studies of the electron and muon spetra in B decays that helped fix the value of the B mass and led to stringent limits on the $b \to u$ transition, the discovery of the B^*, the determination of the B^* amd B_s masses. A notable achievement was the detailed study of the spectrum of $b - \bar{b}$ states, on which

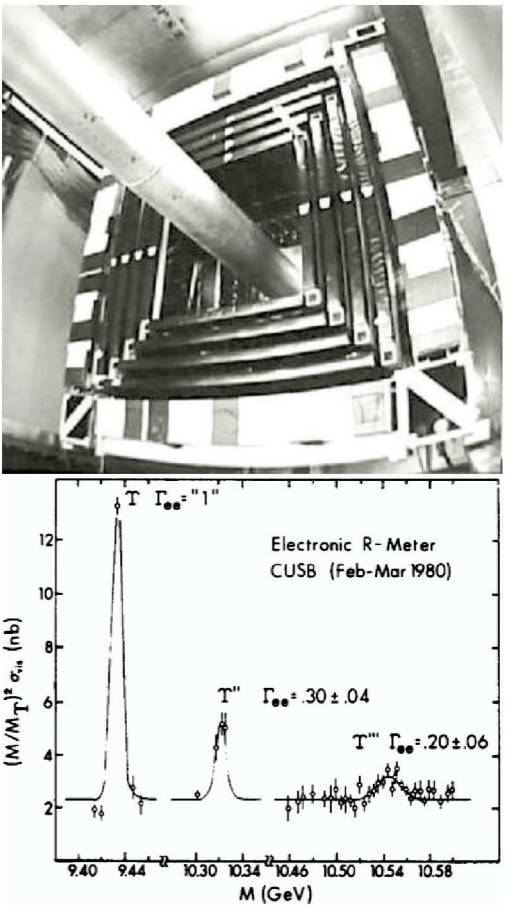

Figure 3: CUSB in 1979, with only half of the NaI crystals installed, and the discovery of the $\Upsilon(4S)$.

many theoreticians are still working to tune our understanding of heavy quark dynamics in QCD. Other important results are a precision determination of the QCD coupling $\alpha_s(m_b)$ and the determination of the b-quark contribution in the continuum region that definitely identified the absolute value of its charge to be $e/3$. A review of the CUSB history and achievements, with extensive references, has been presented by Juliet [15] at the Symposium "Twenty Beautiful Years of Bottom Physics", held in 1997 at the Illinois Institute of Technology in Chicago.

While CUSB was still in full swing Paolo and Juliet decided to engage their Columbia and Stony-Brook groups in the D0 experiment at Fermilab. Paolo gave a fundamental personal contribution to the design of the detector, with the development and evaluation of its most characteristic element, the uranium – liquid argon calorimeter [16, 17]. D0 was a very large collaboration, growing larger by the year: the final test of the calorimeters [18] was signed in 1992 by physicists from 25 institutions; three years later the paper announcing the observation of the top quark [19] was signed by more than 400 physicists from 42 institutions, and in recent D0 papers the number of participating institutions has nearly doubled. Paolo and Juliet had left the collaboration since a few years and moved to Frascati.

When CUSB was nearing the end of its running period at Cornell, and D0 about to begin its data-taking phase, Paolo started to explore ideas for a new line of research which he could develop, as he likes to do, from start to end with a tight group of collaborators. He started looking at the open problems in precision studies of low energy $e^+ - e^-$ collisions, a line of thought that led to the Dafne – Kloe project. When he was invited to speak at Les Arcs in 1989, he choose to discuss these ideas, in particular the possibility and necessity of improving the precision of the cross sections for $e^+ - e^-$ annihilations into pions at low energies to nail down the hadronic contribution to the muon anomalous magnetic moment [20].

The Daphne Φ-factory and the Kloe detector are well known here in Frascati, and I will not insist on the central role that Paolo had in their conception and development. The first open presentation of the project was held in the Daphne workshop of 1991, where Paolo presented the prospects of a Φ-factory

for CP physics [21]. During the same year he promoted the Daphne project at the Lake Louise Winter Institute, at the Vancouver Meeting of the Division of Particles & Fields of the APS, and in Italy at La Thuile.

I would like to conclude this talk by recalling two recent results obtained by Kloe. The first is an accurate determination of the low energy cross section for $e^+ - e^-$ hadronic annihilations, that Paolo had considered in 1989. To avoid a lenghty energy scan for which Daphne was not really designed, and would also lead to the possibility of energy dependent systematic errors, the measurement was executed by the radiative return method [22]. The idea is to measure, at a fixed energy for the colliding $e^+ - e^-$ beams, the cross section for $e^+ - e^- \rightarrow \gamma +$ pions as a function of the energy of the extra gamma ray. The differential cross section with respect to the invariant mass of the pion pair, s_π, is directly related to the annihilation cross section, as shown in Fig. 4,

$$s_\pi \frac{d\sigma_{\pi^+\pi^-\gamma}}{ds_\pi} = \sigma_{\pi^+\pi^-}(s_\pi) H(s_\pi), \tag{1}$$

Where $H(s_\pi)$ is a known function.

The first results of this measurements yeld a correction to the muon anomaly

$$a_\mu^{\pi\pi}(0.35, 0.95) = (388.7 \pm 0.8_{\rm stat} \pm 3.5_{\rm syst} \pm 3.5_{\rm th}) 10^{-10} \tag{2}$$

To put this result in perspective, the discrepancy between the expected value of the anomaly and the result of the recent Brookhaven experiment [23] is $\Delta a_\mu = 25.5(9.2) \times 10^{-10}$. After the Kloe results, the pion contribution is not any more the leading uncertainty in the expected value of the anomaly.

Many results from the Kloe collaboration have improved our knowledge on the properties and decay modes of the light mesons: the η and η', the light scalars $f(0)(980)$, $a(0)(980)$ and of course the Φ itself. But Kloe's greatest contribution is in the study of K-meson decay modes. What makes Kloe unique is the production of $K - \bar{K}$ pairs with very low velocity, and the ability to use tagged kaons. This allows studying the development in time of both charged and neutral K mesons and the direct determination of absolute decay rates and branching ratios for the different modes. Up to 2003-2004 the branching ratios for different kaon decay modes were obtained by the Particke Data Group in an

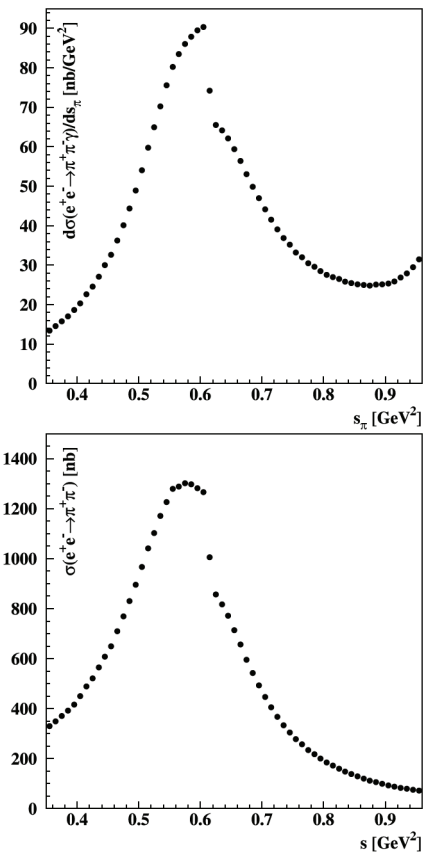

Figure 4: Left: differential cross section for the $e^+e^- \to \pi^+\pi^-\gamma$ process, inclusive in θ_π and with $\theta_{\pi\pi} < 15^\circ$ ($\theta_{\pi\pi} > 165^\circ$). Right: cross section for $e^+e^- \to \pi^+\pi^-$.

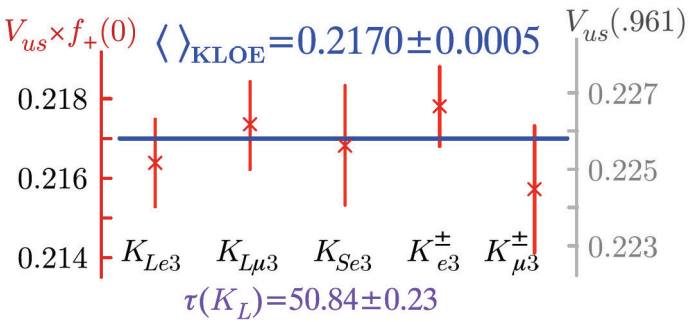

Figure 5: The V_{us} values obtained by Kloe from five $K_{\ell 3}$ decay modes.

indirect way by combining measurements of relative branching ratios, i.e, ratios of branching ratios, from different experiments. As emphasized by Paolo [24], this is dangerous as it requires a normalization procedure to ensure that the sum of the branching ratios add up to 1, so that a small error in the branching ratio of one of the leading modes, e.g. $K^+ \to \mu^+ + \nu$, can be reflected in a large error for smaller-rate modes. The tagged-kaon method used by Kloe makes it possible to directly and simultaneously measure *absolute* branching ratios.

For a long time the branching ratios for K-meson semileptonic decays, in particular the $K \to \pi e \nu$ modes, posed a serious problem as they led to a value for $V_{us} = 0.2200 \pm 0.0026$, lower than required by unitarity of the CKM matrix. The Kloe collaboration has published a new value for the lifetime of K_L [25] and the branching fractions for its main decay modes [26]. Kloe has also for the first time measured [27, 28] the branching ratio of $K_S \to \pi e \nu$, and in the International Europhysics Conference on High Energy Physics of 2005 in Lisbon [29] has presented preliminary results for K^+_{e3} and $K^+_{\mu 3}$.

As shown in Figure 5 the five measurements concur to a new value, $|V_{\rm us} f_+(0)| = 0.2170 \pm 0.0005$ that, using the Leutwyler-Roos value [30] $f_+(0) = 0.961 \pm 0.008$ leads to $V_{us} = 0.2258 \pm 0.0022$, a value in agreement with the CKM unitarity sum rule. While solving a long standing problem, the new measurements represent a challenge to the theoreticians as the experimental error is now smaller than the theoretical uncertainty on $f_+(0)$. A first step for

meeting this challenge with lattice QCD is very encouraging [31] as it results to be fully compatible with the Leutwyler-Roos value and there is ample space for an improvement. Kloe is also publishing precise measurements of the slope of the vector form-factor [32].

There is no end to this story. We all hope that Paolo will continue to lead the search for innovative ways to look at the world of elementary particles. His recent foray into the future of the Daphne-Kloe project indicates that this is already happening. Thanks, Paolo!

References

1. F. Eisler *et al.*, Phys. Rev. **108** (1957) 1353.
2. Paolo Franzini and Jack Steinberger, Phys. Rev. Lett. **6** (1961) 281.
3. Marcel Bardon, Paolo Franzini, and Juliet Lee, Phys. Rev. Lett. **7** (1961) 23.
4. Nicola Cabibbo and Paolo Franzini, Phys. Letters **3** (1963) 217.
5. Nicola Cabibbo and Raul Gatto, Nuovo Cimento **15** (1960) 159.
6. P. Franzini *et al.*, Phys. Rev. D **6** (1972) 2417.
7. Nicola Cabibbo, Phys. Rev. Lett. **10** (1963) 531.
8. Nicola Cabibbo and Raul Gatto, Nuovo Cimento **21** (1961) 872.
9. W. Willis *et al.*, Phys. Rev. Lett. **13** (1964) 291.
10. A. Barbaro-Galtieri *et al.*, Phys. Rev. Lett. **9** (1962) 26.
11. P. Franzini and L. A. Radicati, Phys. Letters **6** (1963) 322.
12. R. D. Schamberger, J. Lee-Franzini, R. Mccarthy, S. Childress and P. Franzini, Phys. Rev. Lett. **34** (1975) 1121.
13. S. W. Herb *et al.*, Phys. Rev. Lett. **39** (1977) 252.
14. G. Finocchiaro *et al.*, Phys. Rev. Lett. **45** (1980) 222.
15. Juliet Lee-Franzini in "Twenty beautiful years of bottom physics", editors, Ray A. Burnstein, Daniel M. Kaplan, Howard A. Rubin, AIP Press (1998); arXiv:hep-ex/9709025.
16. S. Aronson *et al.* [D0 Collaboration], Nucl. Instrum. Meth. A **269** (1988) 492 [Erratum-ibid. A **273** (1988) 453].

17. P. Franzini, Nucl. Instrum. Meth. A **263** (1988) 78.

18. S. Abachi *et al.* [D0 Collaboration], Nucl. Instrum. Meth. A **324** (1993) 53.

19. S. Abachi *et al.* [D0 Collaboration], Phys. Rev. Lett. **74**, 2632 (1995) [arXiv:hep-ex/9503003].

20. P. Franzini, "The Muon Gyromagnetic Ratio And E+ E- Annihilations," in Les Arcs 1989, Proceedings, Electroweak interactions and unified theories 159-164.

21. P. Franzini, LNF-91-045-R *Presented at Workshop on Physics and Detectors for DAPHNE, Frascati, Italy, Apr f9-12, 1991*

22. A. Aloisio *et al.* [KLOE Collaboration], Phys. Lett. B **606** (2005) 12 [arXiv:hep-ex/0407048].

23. G.W. Bennet, et al., Phys. Rev. Lett. **92**, (2004) 161802

24. P. Franzini, "Kaon decays and V(us)," presented at the XXIV Physics in Collision Conference, Boston, June27-29, 2004. eConf **C0406271** (2004) SUNT05 [arXiv:hep-ex/0408150].

25. F. Ambrosino *et al.* [KLOE Collaboration], Phys. Lett. B **626** (2005) 15 [arXiv:hep-ex/0507088].

26. F. Ambrosino *et al.* [KLOE Collaboration], Phys. Lett. B **632** (2006) 43 [arXiv:hep-ex/0508027].

27. A. Aloisio *et al.* [KLOE Collaboration], Phys. Lett. B **535** (2002) 37 [arXiv:hep-ph/0203232].

28. F. Ambrosino *et al.* [KLOE Collaboration], Phys. Lett. B **636** (2006) 173 [arXiv:hep-ex/0601026].

29. F. Ambrosino *et al.* [KLOE Collaboration], PoS **HEP2005** (2006) 287 [arXiv:hep-ex/0510028].

30. H. Leutwyler and M. Roos, Z. Phys. **C25** 1984 91

31. D. Becirevic *et al.*, Nucl. Phys. **B 705** 2005 339

32. F. Ambrosino *et al.* [KLOE Collaboration], Phys. Lett. B **632** (2006) 76 [arXiv:hep-ex/0509045].

Frascati Physics Series Vol. XLI (2006), pp. 15-22
DISCOVERIES IN FLAVOUR PHYSICS AT e^+e^- COLLIDERS
Frascati, February 28th - March 3rd, 2006

ON THE UNIVERSALITY OF WEAK INTERACTIONS: a tribute to Paolo Franzini

Gino Isidori
INFN, Laboratori Nazionali di Frascati, I-00044 Frascati, Italy

1 Introduction

The experimental challenge posed by the theoretical relation

$$|V_{ud}|^2 + |V_{us}|^2 + |V_{ub}|^2 = 1 \ , \tag{1}$$

where $|V_{ij}|$ are the elements of the Cabibbo-Kobayashi-Maskawa matrix, [1, 2] has a long and fascinating history, in which Paolo Franzini has undoubtedly played a major role. I won't attempt a systematic recollection of all his achievements in this field and I refer to the nice talk by Nicola Cabibbo at this conference for a more detailed discussion. [3] But for the benefit of people who were still at high school in the 80's (such as myself...), I wish to recall that Paolo showed for the first time that $|V_{ub}| \ll 1$ and plays a subleading role in Eq. (1). [4] This result obtained with the CUSB experiment (see Fig. 1) –which

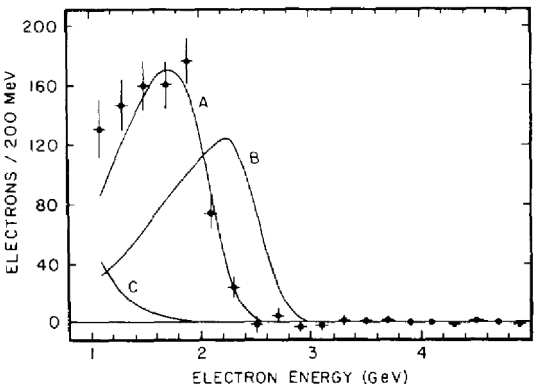

Figure 1: *The semileptonic spectrum of B decays, as observed at CUSB,* [4] *namely the first clear indication that* $|V_{ub}| \ll 1$*: (A)* $b \to ce\nu$ *hypothesis; (B)* $b \to ue\nu$ *hypothesis.*

at that time was against the common expectation of many theoreticians!– is one of the key ingredients which nowadays allows a precision of about $O(0.1\%)$ to be reached in the experiemental test of Eq. (1). [5]

As we will hear more during the rest of of this conference, Paolo played an even more important role in testing Eq. (1) during the last few years, with the precise determination of $|V_{us}|$ obtained with the KLOE experiment [6, 7] (see Fig. 2).

The interest in Eq. (1) is that this relation allows us to perform one the most significant test about the universality of weak interactions. [1] Because of the the breaking of the electroweak symmetry and the mechanism of flavor mixing, the universality of charged-current interactions is not manifest in the quark sector: it is hidden in the unitarity of the CKM matrix. When extracting the $|V_{ij}|$ from a given $u_i \to d_j \ell\nu$ process, the corresponding rate is normalised to $G_F^{(\mu)}$, or the Fermi coupling determined from the muon decay. As a result, testing the unitarity relation in Eq. (1) is equivalent to testing the universality of weak interactions between quarks and leptons.

As I will discuss in the rest of this talk, the test of Eq. (1) and other weak-current universality tests which can be performed in the kaon system are extremely interesting in view of realistic extensions of the Standard Model.

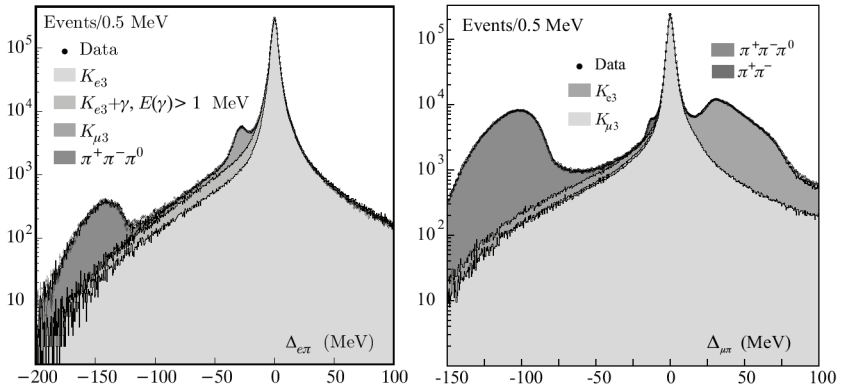

Figure 2: *Precise data on K^L_{e3} and $K^L_{\mu 3}$ spectra from KLOE.* [7]

The fascinating saga hidden behind Eq. (1) is far from over, and, with a bit of luck, the most exciting part of the story could be ahead of us.

2 Weak interactions within and beyond the SM

Despite the great phenomenological success of the Standard Model (SM), up to energy scales $\sim 10^2$ GeV, it is natural to consider this model only as the low-energy limit of a more fundamental theory. More precisely, the SM Lagrangian can be regarded as the renormalizable part of an effective field theory (EFT), valid up to some still undetermined cut-off scale Λ ($\Lambda > M_W$). Since the SM is renormalizable, we have no clear clues about the value of Λ; however, theoretical arguments based on a natural solution of the hierarchy problem suggest that Λ should not exceed a few TeV. A key experimental test of this hypothesis will soon be performed at the LHC, with the direct exploration of the TeV energy scale.

The direct search for new degrees of freedom at the TeV scale (the so called *high-energy frontier*) is not the only tool at our disposal to shed light on physics beyond the SM. A complementary and equally important source of information about the underlying theory is provided by high-precision low-energy experiments (the so called *high-intensity frontier*). The latter are particularly interesting in determining the symmetry properties of the new degrees of freedom.

Precision measurements of the effective couplings which control charged-current weak interactions of quarks and leptons are a key ingredient of the high-intensity program. As shown a long time ago by Appelquist and Carazzone, [8] heavy degrees of freedom which respect the gauge symmetry of the low-energy theory decouple at low energies. This implies that we do not expect any deviation from the SM in the leading dimension-four coupling (the gauge coupling) of the W boson to fermion fields,

$$\mathcal{L}^{\rm C.C.}_{\rm gauge} \;=\; i\frac{g}{2\sqrt{2}}\;\bar\psi^i_L\gamma^\mu\tau_+\psi^i_L\;W^+_\mu \;+\; \text{h.c.} \tag{2}$$

However, thanks to the breaking of the electroweak symmetry, what is probed in low-energy experiment is not the structure (2), but effective dimension-six operators of the type

$$\mathcal{L}^{\rm C.C.}_{\rm eff.} \;=\; G_F\;\sum C^{AB}_{ijkl}\;\bar u^i\Gamma^A d^j\;\bar\ell^k\Gamma^B\nu^l \;+\; \text{h.c.} \tag{3}$$

The values of the effective couplings C^{AB}_{ijkl} are not protected by gauge invariance and are potentially sensitive to new physics. On general grounds, one expects a power suppression of the non standard contributions of the type

$$C^{AB}_{ijkl} = \left[C^{AB}_{ijkl}\right]_{\rm SM}\left[1 + c\frac{M_W^2}{\Lambda^2}\right] \tag{4}$$

where $c \ll 1$ if the new degrees of freedom modify the effective couplings only via loop-induced amplitudes. The effects of non-standard contributions are therefore quite small, but possibly detectable by high-precision experiments.

Particularly interesting are the non-standard effects which spoil the flavor structure of the C^{AB}_{ijkl}, such as violations of lepton-flavor or quark-lepton universality. On the one hand, in principle it is straightforward to detect such effects (the deviations are seen in appropriate ratios of couplings rather in their absolute magnitude). On the other hand, these effects are particularly interesting in shedding light on the flavor structure of the new degrees of freedom.

Within the wide class of models with minimal flavor violation (MFV) with only one effective light Higgs boson, [9] the expected violations of universality (both lepton-flavor and quark-lepton universality) are quite small: in semileptonic transitions of the type $s \to u$ the effects are below the 0.1% level and thus practically undetectable. However, there are many realistic scenarios in which this is not the case. For instance, right-handed currents which are naturally present in Higgs-less models can induce $\mathcal{O}(1\%)$ violations of universality

between $K_{\mu 3}$ and K_{e3} decays. [10] Similarly, in two-Higgs doublet models with large $\tan\beta$ ($\tan\beta = \langle H_U\rangle/\langle H_D\rangle$) one expects violations of universality between $K_{\mu 2}$ and K_{e3} decays around few$\times 0.1\%$ [11]. Finally, it is worth stressing that a particularly sensitive probe of lepton-flavor violation is given by the ratio

$$R_K^{\mu/e} = \frac{\mathcal{B}(K \to \mu\nu)}{\mathcal{B}(K \to e\nu)} \ . \tag{5}$$

This observable can be predicted to 0.04% accuracy within the SM, while its deviation from the SM expectation in realistic supersymmetric frameworks can reach $\sim 1\%$. [12]

3 On the theoretical description of $K_{\ell 2}$ and $K_{\ell 3}$

The high statistics on semileptonic K decays accumulated in the last few years by KTeV [13], NA48 [14], and KLOE [7] has motivated substantial progress in the theoretical description of these processes. [5] In several observables the theoretical control is such that even the tiny deviations of lepton-flavor and/or quark-lepton universality described above (0.1%–1%) can possibly be detected.

The two master formulae for the inclusive decay rates are

$$\Gamma(K_{\ell 3[\gamma]}) = C^0_{K_{\ell 3}} I^{K\ell}(\lambda_i) \times |V_{us} \times f_+(0)|^2 \times \left[1 + 2\,\Delta^K_{SU(2)} + 2\,\Delta^{K\ell}_{\rm EM}\right] , \tag{6}$$

$$\Gamma(K_{\ell 2[\gamma]}) = C^0_{K_{\ell 2}} m_\ell^2 (m_K^2 - m_\ell^2) \times |V_{us} F_K|^2 \times \left[1 + 2\Delta^\ell_{\rm EM}\right] . \tag{7}$$

Here C^0_K are overall coefficients which can be predicted with excellent accuracy (within the SM) in terms of $G_F^{(\mu)}$ and $\alpha_{\rm em}$, while the phase-space factors $I^{K\ell}$ can be determined by experiments measuring the Dalitz plot slopes. The isospin-breaking and lepton-flavor-violating Δ's are known with errors which range from a few $\times 10^{-4}$ to a few $\times 10^{-3}$, while the dominant theoretical uncertainties ($\sim 1\%$) are confined in the two overall hadronic form factors F_K and $f_+(0)$.

The leading theoretical uncertainty of F_K and $f_+(0)$ can be eliminated in appropriate ratios of the inclusive rates. As a result, we are already able to perform tests of lepton-flavor universality at the 0.1% level, the most interesting of which is probably the $R_K^{\mu/e}$ ratio in Eq. (5). Precision tests of quark-lepton universality require better knowledge of F_K and $f_+(0)$. In this case the present theoretical error is a limiting factor, but the situation is likely to improve in the near future thanks to the new generation of lattice-QCD simulations. [17, 18, 19]

Figure 3: *The 1991-2005 selection of Paolo's "distillati".*

For these reasons, I believe that high-precision measurements of decay rates (and kinematical distributions) of $K_{\ell 3}$ and $K_{\ell 2}$ decays are –and will continue to be– a very interesting subject. These processes offer a unique tool to probe the flavor structure of physics beyond the SM.

4 More about Paolo's role

The good theoretical description of $K_{\ell 3}$ and $K_{\ell 2}$ decays is only one part of the story (the easy part...). Much more difficult is to plan and build detectors, and to set-up corresponding data analyses, such that these processes can finally be measured at the 0.1% level of accuracy. Thanks to the nice results recently obtained by KLOE, we now know this is not a dream. More important, we know that the Frascati Laboraotries can play a key role in this field in the future, improving the universality tests obtained by means of $K_{\ell 3}$ and $K_{\ell 2}$ modes. I strongly doubt this would have been possible without Paolo.

Sergio Bertolucci [20] will tell you more about the fascinating history of

the planning and the construction of the KLOE detector. Although I am not part of KLOE, I wish to add here a short –but quite important– comment about the development of the KLOE Collaboration, and especially of its young component (see Figure 3). In the last 15 years Paolo –with the help of a few senior members of KLOE– has trained a fantastic group of young physicists, which nowadays form a world-wide recognized team. If our laboratory has interesting future perspectives in the field of high-energy physics, it is mainly because of this nice group of pepole who grew up under the guidance of Paolo. The creation of this group has been a great achievement and an invaluable gift to our laboratory.

Acknowledgments

I warmly thank Paolo for all the very instructive discussions we have had in the last 10 years: it has been a pleasure and an honor for me to discuss about physics with him. More important, on behalf of many young (and less young) people of this laboratory, I wish to express very special thanks for the great role he has played (and he continues to play) in the scientific growth of LNF.

References

1. N. Cabibbo, Phys. Rev. Lett. 10 (1963) 531.
2. M. Kobayashi and T. Maskawa, Prog. Th. Phys **49** (1973) 652.
3. N. Cabibbo, these proceedings.
4. C. Klopfenstein *et al.* [CUSB Collaboration] Phys. Lett. B **130** (1983) 444.
5. An updated review can be found in E. Blucher *et al.*, *Status of the Cabibbo angle* hep-ph/0512039.
6. P. Franzini, eConf **C0406271**, SUNT05 (2004) [hep-ex/0408150].
7. F. Ambrosino *et al.* [KLOE Collaboration], Phys. Lett. B **632** (2006) 43 [hep-ex/0508027]; Phys. Lett. B **626** (2005) 15 [hep-ex/0507088]; Phys. Lett. B **636** (2006) 166 [hep-ex/0601038].
8. T. Appelquist and J. Carazzone, Phys. Rev. D **11** (1975) 2856.

9. G. D'Ambrosio, G. F. Giudice, G. Isidori and A. Strumia, Nucl. Phys. **B645** (2002) 155.

10. V. Bernard, M. Oertel, E. Passemar and J. Stern, hep-ph/0603202.

11. G. Isidori and P. Paradisi, hep-ph/0605012.

12. A. Masiero, P. Paradisi and R. Petronzio, hep-ph/0511289.

13. T. Alexopoulos *et al.* [KTeV Collaboration], Phys. Rev. Lett. **93** (2004) 181802 [hep-ex/0406001]; Phys. Rev. D **70** (2004) 092007 [hep-ex/0406003].

14. A. Lai *et al.* [NA48 Collaboration], Phys. Lett. B **602** (2004) 41 [hep-ex/0410059]; Phys. Lett. B **604** (2004) 1 [hep-ex/0410065].

15. E. Blucher *et al.*, arXiv:hep-ph/0512039.

16. H. Leutwyler and M. Roos, Z. Phys. C **25** (1984) 91.

17. D. Becirevic et al., Nucl. Phys. B **705**, 339 (2005) [hep-ph/0403217].

18. C. T. H. Davies *et al.* [HPQCD Collaboration], Phys. Rev. Lett. **92** (2004) 022001 [arXiv:hep-lat/0304004].

19. M. Okamoto, hep-lat/0510113.

20. S. Bertolucci, these proceedings.

Frascati Physics Series Vol. XLI (2006), pp. 23-32
DISCOVERIES IN FLAVOUR PHYSICS AT e^+e^- COLLIDERS
Frascati, February 28th - March 3rd, 2006

A TRIBUTE TO PAOLO FRANZINI

Ulrich Heintz
Boston University

Abstract

During the 1980's Professor Paolo Franzini shaped two experiments that contributed significantly to our understanding of particle physics, the CUSB experiment at the Cornell Electron Storage Ring and the DØ experiment at the Fermilab Tevatron. In this article I will describe his contributions to these experiments.

1 Background

I met Paolo in 1986 when I was a graduate student at the State University of New York at Stony Brook. I had just joined Juliet Lee-Franzini's group on the CUSB experiment. Over the following five years I worked on the CUSB Experiment studying the spectroscopy of the Υ system. In 1991, I joined the

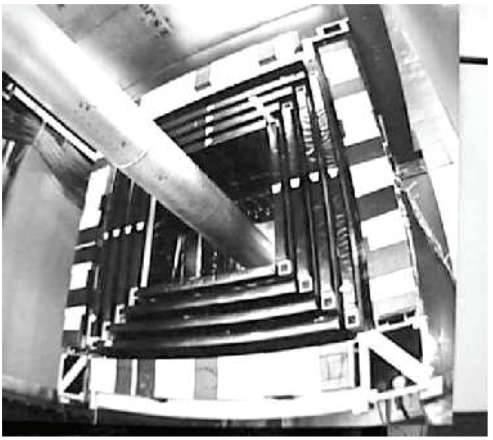

Figure 1: *Photo of the early CUSB detector with the CESR beam pipe and the four square layers of NaI crystals.*

DØ Experiment. I measured the W boson mass, participated in the discovery of the top quark and contributed to the measurement of its mass.

Paolo has shaped both these experiments. Without his contributions to these experiments, I would not have been able to carry out any of this work. But Paolo has not only shaped the experimental apparatus that I used, much more importantly, he has also shaped me as a teacher and mentor throughout these years. It is thus a great honor and privilege to express my gratitude and appreciation in this forum.

And I cannot mention Paolo without Juliet. They are a team and their dedication to science as well as to the people who they were working with, especially to their students, has been a great example for me.

2 The Columbia University Stony Brook experiment

2.1 The detector

The Columbia University Stony Brook (CUSB) detector in its first incarnation (CUSB-I) operated in the North Area of the Cornell Electron Storage Ring from 1979 to 1985. It consisted of an array of sodium iodide crystals and lead glass blocks [1)] as shown in Fig.1. The original collaboration consisted

of T. Böhringer, F. Costantini, J. Dobbins, P. Franzini, K. Han, S. W. Herb, D. M. Kaplan, L. M. Lederman, G. Mageras, D. Peterson, E. Rice, D. Son, J. K. Yoh, S. Youssef, T. Zhao from Columbia University and G. Finocchiaro, G. Gianinni, J. E. Horstkotte, D. M. J. Lovelock, C. Klopfenstein, J. Lee-Franzini, R. D. Schamberger, M. Sivertz, L. J. Spencer, P. M. Tuts from Stony Brook. From 1981 to 1984 G. Blanar, H. Dietl, G. Eigen, V. Fonseca, E. Lorenz, F. Pauss, L. Romero, H. Vogel from Max-Planck Institut in Munich and R. Imlay, G. Levman, W. Metcalf, V. Sreedhar from Louisiana State University joined the collaboration.

In 1986, a BGO crystal calorimeter (see Fig.2) and a small drift chamber — both Paolo's design — were inserted inside the sodium iodide array. As CUSB-II [2)], this detector was operated until 1991. The CUSB-II collaboration included P. Franzini, S. Kanekal, P. M. Tuts, Q. W. Wu, S. Youssef, T. Zhao from Columbia University and U. Heintz, J. E. Horstkotte, T. Kaarsberg, C. Klopfenstein, J. Lee-Franzini, D. M. J. Lovelock, M. Narain, R. D. Schamberger, S. Sontz, J. Willins, C. Yanagisawa from Stony Brook.

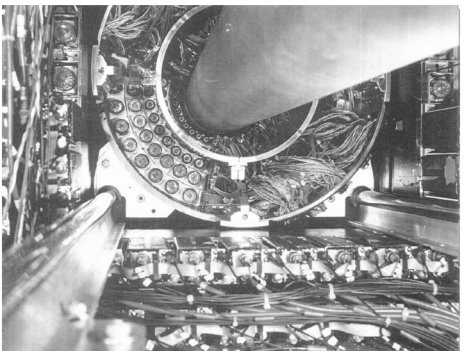

Figure 2: *Photo of the BGO array arranged in a cylinder around the CESR beam pipe. Also visible are the inner layers of the square NaI array.*

The BGO array consisted of 360 crystals arranged in five concentric cylindrical layers. The entire BGO calorimeter had a radius of about 20 cm and was 12 radiation lengths thick. It achieved excellent energy resolution for electromagnetic showers, 5% at 50 MeV and 1% at 5 GeV.

The segmentation of the calorimeter along the direction of shower develop-

ment allowed the CUSB-II detector to distinguish electromagnetic showers from hadrons and muons. With the help of the drift chamber inside the calorimeter and the muon chambers on the outside of the calorimeter, the detector could distinguish electrons/positrons, photons, muons, and hadrons. Figure 3 shows two sample events.

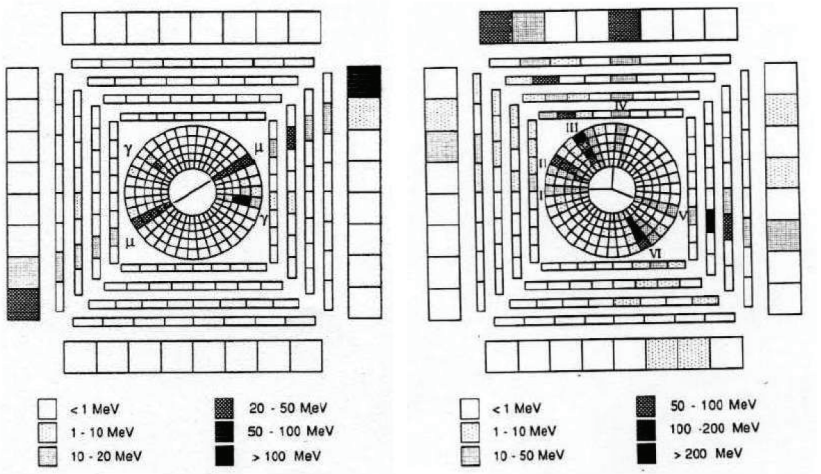

Figure 3: *Two events in the CUSB-II detector. On the left is a candidate for the decay chain* $\Upsilon(3S) \to \chi_b(2P)\gamma \to \Upsilon(2S)\gamma\gamma \to \mu^+\mu^-\gamma\gamma$ *and on the right is an event typical for hadronic decays of* $\Upsilon(3S)$.

2.2 CUSB results

The CUSB collaboration published many important results that span a wide range of topics. The main focus of the CUSB physics program was the spectroscopy of the Υ system. CUSB was the first experiment to resolve the $\Upsilon(3S)$ [1)] and to observe the $\Upsilon(4S)$ [3)]. Figure 4 shows the Υ resonances as measured by CUSB. CUSB also first observed the p-wave states $\chi_b(1P)$ [4)] and $\chi_b(2P)$ [5)] and measured their fine structure splitting [6)]. CUSB saw the first evidence of open b-flavor by observing the semileptonic decays of B mesons at the $\Upsilon(4S)$ [7)]. CUSB discovered the excited B^* meson by observing the photon line from the transition $B^* \to B + \gamma$ at the $\Upsilon(5S)$ [8)]. CUSB inferred from the

Doppler broadening of this line that there had to be a mixture of B^* and B_s^* produced at the $\Upsilon(5S)$ [9].

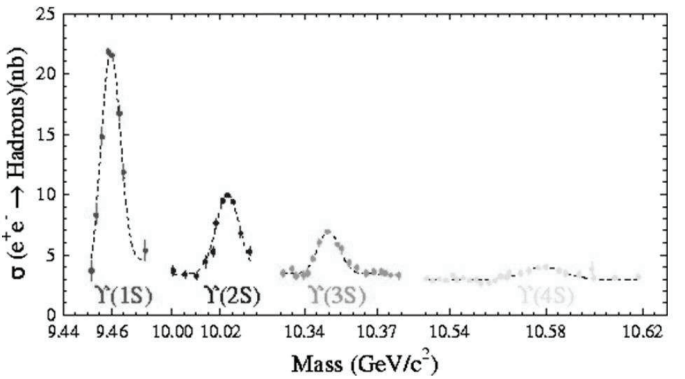

Figure 4: *The Υ resonances as measured by CUSB.*

But CUSB also made measurements and observations outside of Υ spectroscopy, such as measuring the ratio of cross sections $R = \sigma(e^+e^- \to \text{hadrons})/\sigma(e^+e^- \to \mu^+\mu-)$ and the strong coupling constant α_s from the ratio of decay rates $\Gamma(\Upsilon \to gg\gamma)/\Gamma(\Upsilon \to ggg)$ [10]. CUSB also set limits on production of axions [11], gluinos [13], and the Higgs boson [12] in Υ decays.

2.3 The CUSB experience

Although we always had the latest in computer technology at CUSB, in hindsight the tools we had at our disposal at that time seem primitive. There was no world wide web and PC's were much less powerful than today. Computer output appeared on line printers. Figures for papers were drawn by draftsmen not by graphics packages. Sometimes we slept in front of the tape drives while running through the data on huge old magnetic tapes that had to be loaded by hand.

On the other hand, CUSB data taking ran automatically without anybody on shift. It was started by the operator in the CESR control room. HV trips and other failures were reset automatically first before somebody was called in. Best of all - there were no owl shifts!

Paolo of course was the electronics wizard behind all this. I was told by another member of the group that when he was a student they were once trying to make a measurement with an oscilloscope. It didn't work and they couldn't figure out what was wrong. However whenever Paolo came by it started working. Not knowing what he had done, they started speculating: "it's his magic eyes - they tell the electrons where to go". So they took a photograph of Paolo and cut out his eyes and whenever things didn't work they held up Paolo's eyes.

Paolo and Juliet took very good care of the entire group, especially the students. Regularly we were invited to Juliet's and Paolo's house to excellent food and wonderful Italian wine.

3 The DØ experiment

3.1 A prelude

In 1981 Leon Lederman, then director of Fermilab, asked for proposals for a small, clever experiment for the DØ collision region. Paolo was part of one of these proposals, together with other physicists from Brookhaven National Laboratory, Brown University, Columbia University, Michigan State University, and SUNY Stony Brook. The proposed experiment was called "Lapdog" and it was supposed to have a calorimeter of cheap unpolished lead glass blocks.

In the course of beam tests for the "Lapdog" lead glass calorimeter, Paolo invented the H-matrix to identify electromagnetic showers. The H-matrix was defined as the inverse of the covariance matrix of the energy depositions by an electromagnetic shower of a given energy in the individual lead glass blocks. Formally

$$\left\{H^{-1}\right\}_{ij} = \frac{1}{N}\sum_{n=1}^{N}\left(E_i^{(n)} - \overline{E}_i\right)\left(E_j^{(n)} - \overline{E}_j\right),$$

where the sum is over all N electrons and the indices i and j identify calorimeter cells, so that $E_i^{(n)}$ is the energy deposited by electron n in calorimeter cell i. One can then test whether a cluster of energy depositions $E_i^{(m)}$ is consistent with the profile of an electromagnetic shower using the figure of merit

$$\zeta_m = \sum_{i,j}\left(E_i^{(m)} - \overline{E}_i\right) H_{ij}\left(E_j^{(m)} - \overline{E}_j\right)$$

which is typically small for electromagnetic showers and large for energy depositions by hadrons. In the beam tests this technique achieved hadron rejections of 10^{-3} and overlapping pions and photons were rejected at the level of 10^{-2} [14]. To this day, the H-matrix is part of the standard electron identification at DØ.

4 The birth of DØ

In 1983, all proposals for the DØ collision hall were merged into one experiment that was called DØ. Soon it became clear to the collaboration that lead glass won't do. Paolo was one of the prime pushers for a liquid argon calorimeter which was the ultimate choice. Paolo took charge of the complete design of calorimeter electronics. According to some of my DØ colleagues, Paolo "educated us all over the years", "he did it all from the early beam tests to the final product", and - being worried about coherent noise - "he was a stickler for proper grounding" and insisted on a test involving 5000 calorimeter electronics channels, about 10% of the full system. Figure 5 shows a preamplifier for the DØ calorimeter that Paolo designed.

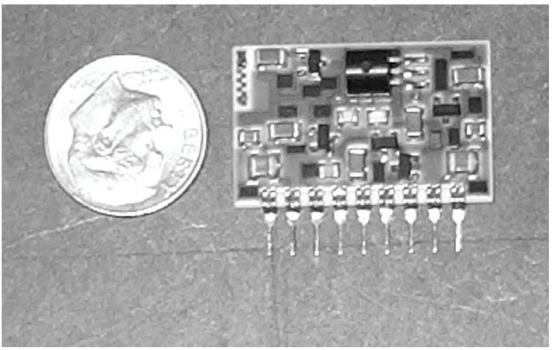

Figure 5: *A preamplifier for the DØ calorimeter readout.*

And so, in 1991 the DØ experiment [15], shaped much by Paolo's ideas, saw its first collisions. The rest is history and is documented in the over one hundred articles in peer-reviewed journals that DØ published based on the data taken from 1991-1996 [16].

5 DØ results

Among the highlights of the results that came out of DØ was the discovery of the top quark in 1995 [17]. The DØ design report had anticipated that the top quark would be found before DØ started taking data, but the top quark turned out to be much more massive than expected. Since the top quark is heavier than the W boson, it is produced mainly in top-antitop quark pairs. The top quark decays almost always into a W boson and a b quark. Thus the decay of the two W bosons from the top and antitop quark decays define the final state signatures.

The characteristics of top-antitop quark events are thus isolated, energetic leptons and missing transverse momentum from the leptonic decay of the W boson and jets with large transverse momentum from the fragmentation of the b quarks and the quarks from hadronic W boson decays. Most of these are measured with the calorimeter. The DØ liquid argon calorimeter with Paolo's electronics were essential in isolating a significant signal for top quark production.

The performance of the calorimeter was even more important for the precision measurement of the W boson mass. The crucial aspect was the stability of the calorimeter calibration over time. Over a time period of 1.5 years the response of the liquid argon never changed by more than 0.02% as monitored by α and β sources. The gains and pedestals of the electronics were also stable to a fraction of a percent.

DØ measured the mass of the W boson by reconstructing the transverse mass from the electron and the missing transverse momentum measured using the calorimeter. In 1997, DØ measured $m_W = 80.43 \pm 0.11$ GeV [18], at the time the most precise measurement of the W boson mass. This measurement relied almost entirely on the calorimeter.

Both W boson and top quark mass measurements are still topics of strong interest. These two measurements provide a crucial constraint on the mass of the standard model Higgs boson that can be compared to a direct measurement or limits on the Higgs boson mass.

6 Conclusion

As I outlined, Paolo shaped the design of the CUSB and DØ experiments, which made many important measurements and contributed very significantly to our understanding of particle physics. Paolo's contributions enabled these achievements. But there is much more to Paolo's legacy. Both Paolo and Juliet have given many students the training and education required to succeed in their careers, be it in particle physics or in another field. In doing this they have shaped our field much beyond their immediate contributions.

I would like to close with a quote from my thesis: "I should like to thank Professor Paolo Franzini whose teachings always illuminated the depth of a subject when my understanding was too superficial. [...] Juliet and Paolo cared for me as for a member of their family, providing support so far from home." Thank you, Juliet and Paolo.

Figure 6: *Paolo and Juliet in 1988.*

7 Acknowledgements

I would like to thank Paul Grannis, Juliet Lee-Franzini, Mike Marx, Meenakshi Narain, Dean Schamberger, and Mike Tuts for help in putting together this talk.

References

1. T. Böhringer et al., Phys. Rev. Lett. **44**, 1111 (1980).
2. R. D. Schamberger et al., Nucl. Instrum. Meth. **A309**, 450 (1991).
3. G. Finocchiaro et al., Phys. Rev. Lett. **45**, 222 (1980).
4. F. Pauss et al., Phys. Lett. **B130**, 439 (1983).
5. G. Eigen et al., Phys. Rev. Lett. **49**, 1616 (1982).
6. U. Heintz et al., Phys. Rev. **D46**, 1928 (1992); U. Heintz et al., Phys. Rev. Lett. **66**, 1563 (1991); M. Narain et al., Phys. Rev. Lett. **66** 3113 (1991).
7. L. J. Spencer et al., Phys. Rev. Lett. **47**, 771 (1981).
8. K. Han et al., Phys. Rev. Lett. **55**, 36 (1985).
9. J. Lee-Franzini et al., Phys. Rev. Lett. **65**, 2947 (1990).
10. R. D. Schamberger et al., Phys. Lett. **B138**, 225 (1984).
11. G. Mageras et al., Phys. Rev. Lett. **56**, 2672 (1986).
12. P. Franzini et al., Phys. Rev. **D35**, 2883 (1987).
13. P. M. Tuts et al., Phys. Lett. **B186**, 233 (1987).
14. R. Engelmann et al., Nucl. Instrum. Meth. **216**, 45 (1983).
15. S. Abachi et al., Nucl. Instrum. Meth. **A338**, 185 (1994).
16. see http://www-d0.fnal.gov/results/index.html.
17. S. Abachi et al., Phys. Rev. Lett. **74**, 2632 (1995).
18. B. Abbott et al., Phys. Rev. **D58**, 092003 (1998).

Frascati Physics Series Vol. XLI (2006), pp. 33
DISCOVERIES IN FLAVOUR PHYSICS AT e^+e^- COLLIDERS
Frascati, February 28th - March 3rd, 2006

THE MAKING OF KLOE: A RECOLLECTION

Sergio Bertolucci
Laboratori Nazionali di Frascati, Via E. Fermi 40, 00044 Frascati, Italy

Written contribution not received

Frascati Physics Series Vol. XLI (2006), pp. 35
DISCOVERIES IN FLAVOUR PHYSICS AT e^+e^- COLLIDERS
Frascati, February 28th - March 3rd, 2006

DISCOVERY POTENTIAL AND ISSUE IN KAON PHYSICS

Weiler Andreas
Physics Departments, Technische Universität München

Written contribution not received

Frascati Physics Series Vol. XLI (2006), pp. 37-46
DISCOVERIES IN FLAVOUR PHYSICS AT e^+e^- COLLIDERS
Frascati, February 28th - March 3rd, 2006

EXPERIMENTAL PERSPECTIVES IN KAON PHYSICS

Taku Yamanaka
Physics Department, Osaka University
1-1 Machikaneyama, Toyonaka, Osaka 560-0043, Japan

Abstract

Kaon experiments are now focusing on the measurements of the branching ratios of $K_L \to \pi^0 \nu\overline{\nu}$ and $K^+ \to \pi^+ \nu\overline{\nu}$ decay modes to study the CP violation and flavor physics beyond the Standard Model.

1 Introduction

Kaon experiments have been contributing to the development of elementary particle physics for many years. In the last 20 years, kaon experiments have been studying CP, T, and CPT violations, CKM matrix parameters such as $|V_{us}|$, many rare decay modes, lepton flavor violation, form factors, *etc.*. Recently, the focus is shifting more towards the CP violation and physics beyond the Standard Model.

The CP violation, as discovered in $K_L \to \pi^+\pi^-$ decay [1], is caused by an imaginary phase in the $K^0 - \bar{K}^0$ mixing amplitude. Superweak model [2] explained that the phase is introduced by a very weak $\Delta S = 2$ interaction, while Kobayashi-Maskawa explained that the phase comes in naturally in the weak mixing angles between three generations of quarks. Both theories have survived for a long time, but finally, CERN NA48 [3] and Fermilab KTeV [4] experiments rejected the Superweak Model by proving that CP is violated in $\Delta S = 1$ kaon decay process where Superweak model cannot contribute. Therefore, the currently observed CP violation is consistent with the Standard Model.

However, the CP violation effect in the standard model is not large enough to explain the matter dominance in the universe. Therefore, we have to look for CP violation in physics beyond the standard model.

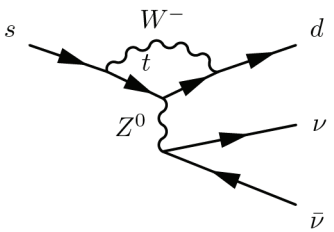

Figure 1: Penguin diagram for $\bar{K}^0 \to \pi^0\nu\overline{\nu}$.

The two rare decays modes, $K_L \to \pi^0\nu\overline{\nu}$ and $K^+ \to \pi^+\nu\overline{\nu}$, are the golden decay modes to study CP violation beyond the Standard Model. In the Standard Model, $K_L \to \pi^0\nu\overline{\nu}$ decay goes through electroweak loop diagrams, as shown in Fig. 1. The decay amplitude is directly proportional to the imaginary part of $|V_{td}|$, as:

$$< \pi^0\nu\overline{\nu}|H|K_L > \simeq < \pi^0\nu\overline{\nu}|H|K_2 > \quad (1)$$

$$\propto < \pi^0\nu\overline{\nu}|H|K^0 > - < \pi^0\nu\overline{\nu}|H|\bar{K}^0 > \quad (2)$$

$$\propto V_{td} - V_{td}^* \propto iIm(V_{td}) = i\lambda^3\eta. \quad (3)$$

The theoretical error between the amplitude and $Im(V_{td})$ is only $\sim 2\%$. On the other hand, the decay amplitude of $K^+ \to \pi^+\nu\overline{\nu}$ is roughly $|V_{td}|$ with some contamination from a c-quark contribution in the loop.

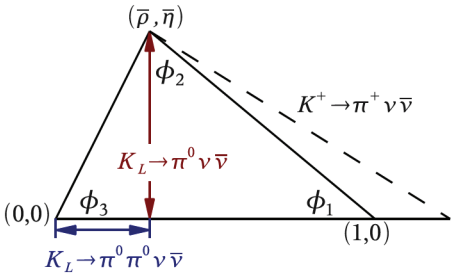

Figure 2: The unitarity triangle.

Therefore, as shown in Fig. 2, the branching ratio of $K_L \to \pi^0\nu\overline{\nu}$ directly measures the height of the unitarity triangle, while the $K^+ \to \pi^+\nu\overline{\nu}$ measures one of the sides of the triangle.

However, new physics, such as SUSY, MSSM, *etc.* can contribute to the penguin diagram in the $K \to \pi\nu\overline{\nu}$ decay, and change the branching ratios of those decays [5]. Even in this case, the small theoretical error between the amplitudes and the branching ratios still holds. On the other hand, the new physics effect is very unlikely to contribute to the tree diagram such as $B \to J/\psi K_S$ which precisely determines $\sin 2\phi_1$. Therefore, if the ρ and η are found to be inconsistent between K and B meson experiments, it will be a signature of a new physics, and give important information for sorting out various new physics scenarios.

2 $K^+ \to \pi^+\nu\overline{\nu}$

2.1 BNL E787/E949 Experiments

The decay $K^+ \to \pi^+\nu\overline{\nu}$ has been studied by BNL E787 and succeeding E949 experiments. They stopped K^+ in a target, and looked for single π^+ from the decay. The target is surrounded by spectrometer and range counters to identify π^+ using the correlation between momentum and energy. In addition, the $\pi^+ \to \mu^+ \to e^+$ decay chain was traced to further identify the π^+. In total, they have observed 3 events [6], and gave $BR(K^+ \to \pi^+\nu\overline{\nu}) = (1.47^{+1.30}_{-0.89}) \times 10^{-10}$.

2.2 CERN P326 Experiment

In order to measure the branching ratio of $K^+ \to \pi^+ \nu\overline{\nu}$ accurately, CERN P326 experiment was proposed [7]. This experiment uses K^+ decays in flight, instead of stopped kaons, to avoid having a target material in a high intensity beam. The keys of this experiment are: a) fast particle ID, high photon detection efficiency, and good missing mass resolution to remove backgrounds, and b) a high signal acceptance. Figure 3 shows the plan view of the detector and beamline of P326 experiment. After the production target, charged particles with a momentum of 75GeV/c are selected and guided through the beam line. The K^+ particles in the beam are identified with a Cerenkov counter (CEDAR). The initial direction of K^+ and its timing are accurately measured with Silicon pixel detectors (SIBES), and a set of Time Projection Chambers (FTPC). These detectors in the beam are capable of running under 800 MHz of beam mixed with π^+, K^+, and protons. The rate of K^+ is 11 MHz.

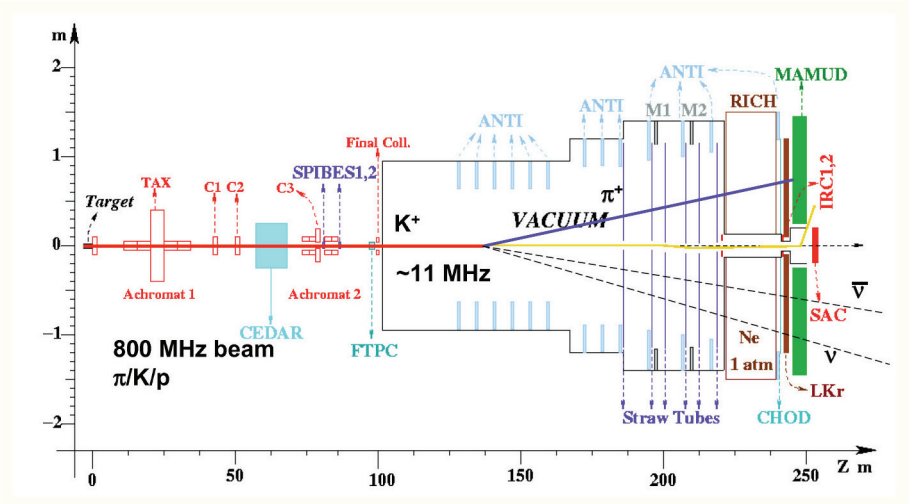

Figure 3: Plan view of the beam line and detector for CERN P326.

The momentum of π^+ from the decay is measured by six sets of straw tube chambers and two spectrometer magnets. The momentum resolution is $\sim 0.3\%$. The missing mass, M_{miss}, is calculated from the parent K^+ momentum and

the daughter π^+ momentum, as: $M^2_{miss} = P^2_K - P^2_\pi$. As shown in Fig. 4, the signal region is well isolated from the tail of $K^+ \to \pi^+\pi^0$ and $K^+ \to \mu^+\nu$ decays. In order to remove other decay modes that enter the signal region, such as $K^+ \to \pi^0 e^+\nu$, $K^+ \to \pi^0\mu^+\nu$, $K^+ \to \mu^+\nu\gamma$, $K^+ \to \pi^+\pi^0\gamma$, *etc.*, extensive particle ID and photon veto are used. The π^+ decayed from K^+ is identified by a Ring Image Cerenkov Counter (RICH) located downstream of the detector. The background decays with photons are rejected by photon veto counters surrounding the decay volume and a liquid Kr calorimeter from NA48 placed downstream of the RICH. Because of the high K^+ momentum, the energy of the photons hitting the liquid Kr calorimeter is larger than 1 GeV, and the detection inefficiency for those photons is estimated to be $10^{-4} \sim 10^{-5}$.

With one year of running, they expect to collect 65 signal events, with 9 background events.

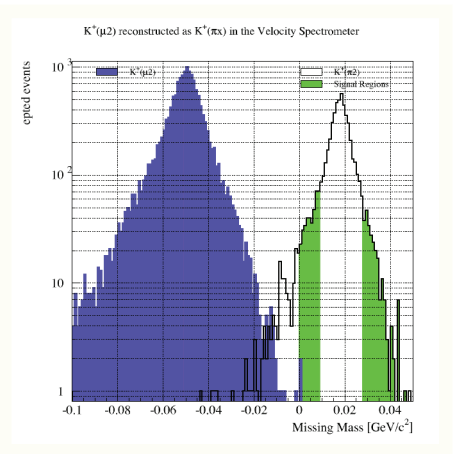

Figure 4: Missing mass spectrum for P326.

3 $K_L \to \pi^0\nu\overline{\nu}$

Currently, the best limit on the branching ratio of $K_L \to \pi^0\nu\overline{\nu}$ is given by the Fermilab KTeV experiment, $B(K_L \to \pi^0\nu\overline{\nu}) < 5.9 \times 10^{-7}$ (90% CL) [8]. This measurement used Dalitz decay, $\pi^0 \to e^+e^-\gamma$, to identify the π^0 with its invariant mass, and to reconstruct the decay vertex and the transverse

momentum of π^0. However, the Dalitz decay is not suitable for high sensitivity experiments, because of its small branching ratio (1.2%), and small acceptance due to a small opening angle between the e^+e^- pairs.

In order to measure the $K_L \to \pi^0\nu\overline{\nu}$ branching ratio, there are several issues. First, the experiment should have a high K_L flux and a high signal acceptance, because the expected branching ratios is low, $\sim 3 \times 10^{-11}$. Second, it should be able to suppress backgrounds, especially, $K_L \to \pi^0\pi^0$ decays where two of the four photons escape detection. This background should be suppressed by detecting the two extra photons with extremely low inefficiency, and by applying kinematical cuts. Third, a clean neutral beam with less neutrons, photons, and beam halo is necessary to suppress accidental hits, and π^0 production by neutron interactions.

3.1 KEK E391a Experiment

The E391a at KEK is a first dedicated experiment to study the $K_L \to \pi^0\nu\overline{\nu}$ decay. The purpose of this experiment is to test the principle of the experiment method and to prepare for the next generation of experiments. The K_L's are produced by 12 GeV protons bombarding a Pt target. Figure 5 shows the E391a detector. The energy and hit position of two photons from the decay are measured with the pure CsI calorimeter located downstream of the decay region. The decay region is covered with hermetic photon veto detector made of Pb and scintillator. The calorimeter has a beam hole at the center to let the beam go through. Another set of photon detectors are located downstream of the calorimeter to detect photons escaping through the hole. In addition, the front of the calorimeter and the surface of the photon veto are covered with scintillation counters to veto charged particles. In order to suppress π^0's produced by beam neutrons interacting with residual gas, the decay region is evacuated to 10^{-5} Pa. Most of the detector components are placed inside the vacuum tank to minimize the dead material (*e.g.*, the vacuum tank) that could absorb photons before hitting the detector.

The experiment had three data taking runs, totaling 6 months. The first run had a problem; a thin film was partially hanging in the beam, and producing π^0's. Tighter cuts were needed to remove this additional background, but with one week worth of data from the first run, E391a gave a preliminary result, $BR(K_L \to \pi^0\nu\overline{\nu}) < 2.86 \times 10^{-7}$ (90% CL) [9], based on no observed events.

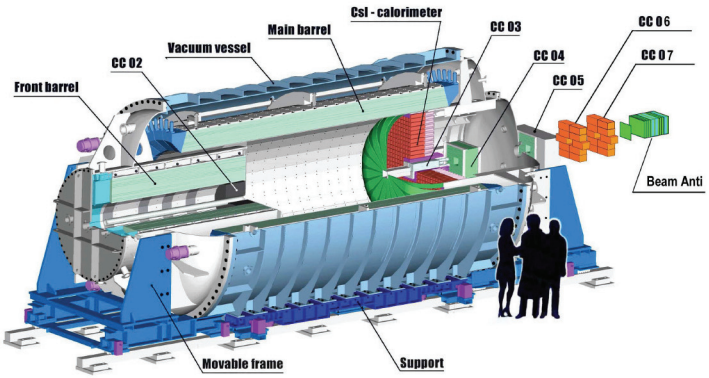

Figure 5: KEK E391a detector.

Even with one week of data, this is a factor of two improvement over the KTeV limit that was based on a half year of running. E391a expects to reach a sensitivity of $\sim O(10^{-9})$ with full data.

3.2 J-Parc Experiment

In order to observe and measure the branching ratio of $K_L \to \pi^0\nu\overline{\nu}$, E391a will first move its detector to J-Parc. The J-Parc is a high intensity proton facility with a 30∼50 GeV proton synchrotron designed to deliver 3×10^{14} protons every 3.4 s. The facility is under construction, and the beam for users is expected in 2009∼2010.

Figure 6 shows the experimental hall for a slow extraction beam line. Multiple secondary beam lines come off a common target placed in a proton beam line. The K_L beamline is extracted at 16° targeting angle, and the E391a detector will be placed at 20 m from the target.

Several modifications will be made to the detector. One is to replace the current $7 \times 7 \times 30\text{cm}^3$ CsI crystals in the calorimeter with smaller and longer $2.5 \times 2.5 \times 50\text{cm}^3$ crystals used in KTeV. This will reduce the probability of misidentifying two near-by photons as one photon (another source of missing photons), and also diminishes the probability for photons to penetrate the crystal without interaction. In addition, the photon veto in the beam will be

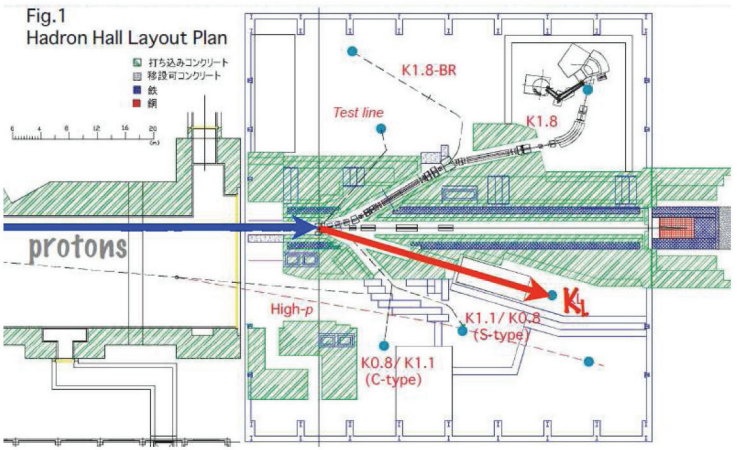

Figure 6: Beamlines at the J-Parc experimental hall.

replaced by new detector with lead and aerogel, which was originally designed for KOPIO experiment at BNL. Since this detector is sensitive to electrons produced in the forward direction, it is sensitive to photons, but insensitive to neutrons which produce hadrons in wide angles. The beam halo at E391a has already been suppressed to 10^{-5} of the beam core, but the collimators for the J-Parc beamline will be improved to further suppress beam halo neutrons.

Figure 7 shows the P_T vs. decay vertex distribution for signal and $K_L \to \pi^0\pi^0$ background Monte Carlo events. High P_T is required to reject $K_L \to \gamma\gamma$ decay background, and to reduce $K_L \to \pi^0\pi^0$ events where one photon from each π^0 is detected. With 2×10^{14} protons/spill and 3×10^7s of running time, the experiment expects to observe 3.5 Standard Model signal events with an S/N ratio of 1.4 [10].

After accumulating experience at the J-Parc high intensity environment, the experiment plans to make an optimized neutral beam line with 5° targeting angle, to get higher K_L momentum and yield. The higher K_L momentum increases the average photon energy, and thus improves the photon veto efficiency. The decay fiducial volume will be made longer, from 2 m to 13 m, and the calorimeter diameter will be increased from 2 m to 3 m. With these improvements, 130 signal events are expected in 3 Snowmass years (3×10^7s)

of running at 3×10^{14} protons/spill. The S/N ratio will also be improved to 4.8 [10].

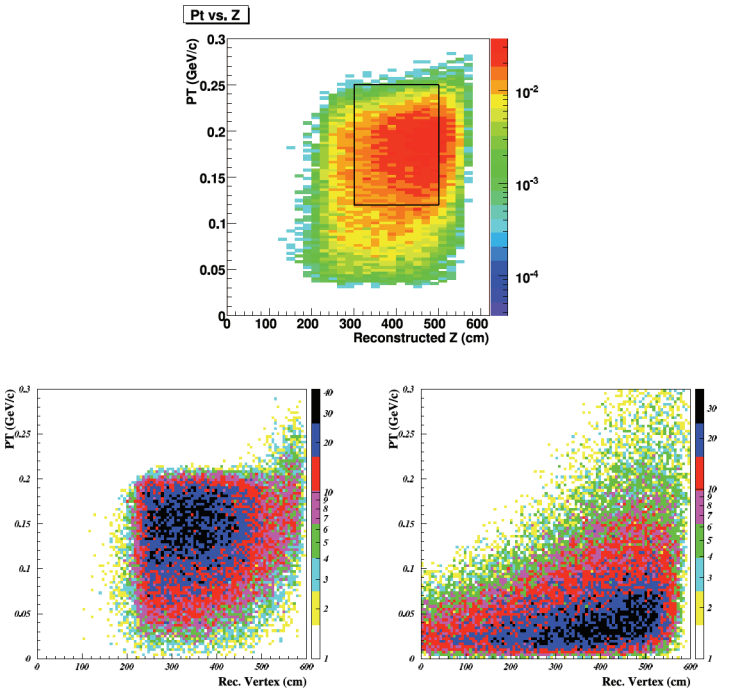

Figure 7: Top: P_T vs. reconstructed z position for left: $K_L \to \pi^0\nu\overline{\nu}$ decays. Bottom: P_T vs. z for $K_L \to \pi^0\pi^0$ background decays where two photons from the same π^0 are detected (left), and different π^0's are detected (right).

4 Conclusion

The focus of kaon experiments is now shifting towards the the study of CP violation and flavor physics beyond the Standard Model, such as SUSY. The golden decay modes, $K_L \to \pi^0\nu\overline{\nu}$ and $K^+ \to \pi^+\nu\overline{\nu}$, are precise and sensitive probes for the study, and together with precise measurements from B factories, provide information on the *flavor mixing* in the new physics scenarios. This will study the *off-diagonal* elements of the new mass matrix, and is totally

complementary to LHC experiments which will probe the *diagonal* elements of the matrix.

5 Acknowledgements

I would like to thank the organizers of the Conference for inviting me. I would also like to thank Dr. Augusto Ceccucci for supplying information on CERN P326.

References

1. J.H. Christenson *et al*, Phys. Rev. Lett. **13**, 138 (1964).
2. L. Wolfenstein, Phys. Rev. Lett. **13**, 562 (1964).
3. J.R. Batley *et al.*, Phys. Lett. **B544**, 97 (2002) .
4. A. Alavi-Harati *et al.*, Phys. Rev. **D 67**, 012005 (2003).
5. D.Bryman, A.J.Buras, G.Isidori, and L.S.Littenberg, *hep-ph/0505171*, *Int. J. Mod. Phys.* **A21**, 487 (2006), and references therein.
6. V.V. Anisimovsky *et al.*, Phys. Rev. Lett. **93**, 031801 (2004).
7. "Proposal to Measure the RareDecay $K^+ \to \pi^+ \nu\overline{\nu}$ at the CERN SPS", CERN-SPSC-2005-013 (2005), and supporting talks.
8. A. Alavi-Harati *et al.*, Phys. Rev. **D 61**, 072006 (2000).
9. K. Sakashita, presented at Kaon 2005, Evanston, Illinois, U.S.A., June, 2005.
10. J. Comfort *et al.*, "Proposal for $K_L \to \pi^0 \nu\overline{\nu}$ Experiment at J-Parc" (2006).

Frascati Physics Series Vol. XLI (2006), pp. 47-61
DISCOVERIES IN FLAVOUR PHYSICS AT e^+e^- COLLIDERS
Frascati, February 28th - March 3rd, 2006

STATUS AND PERSPECTIVES OF ϕ-FACTORIES

C. Biscari
INFN Frascati

Abstract

DAΦNE is the only ϕ *factory* presently in operation in the world. The KLOE experiment data taking is now completed, and the next term future will be dedicated to the completion of FINUDA and SIDDHARTA physics programs. The performance of the collider is described, together with the R&D programs envisaged at Frascati in the framework of the feasibility study for a higher luminosity kaon factory.

1 Introduction

When particle factory concept was first introduced in late eighties the interest to explore the ϕ resonance gave birth to several different designs of ϕ *factory* : the butterfly ring of Novosibirsk, based on round beam collisions [1)], the quasi isochronous ring of UCLA [2)], the two rings-round beam design of Mainz [3)],

and the Frascati design [4]. DAΦNE at Frascati has been the only design come to reality. It was built in the 1990s, first collisions occurred in 1998 and the first experiment, KLOE [5], was installed in 1999. Since then three experiments have shared the time and the luminosity of the collider and the DAΦNE original physics program, ranging from k-physics, to nuclear and atomic physics, will be completed well before 2010, when the three experiments, KLOE, FINUDA [6] and DEAR [7], will collect the required statistics. Interest in pursuing further these three research fields, together with a wider particle physics program, including $\gamma - \gamma$ experiments, has recently shown up [8]. The proposed experiments at the ϕ are more demanding in terms of luminosity with respect to the present DAΦNE parameters. A flexible range of energy is furthermore requested, to cover the energy span in between the ϕ and the J/ψ resonances. The design and the status of DAΦNE are here described together with the main characteristics of the proposed collider for the future.

2 DAΦNE Design and Status

DAΦNE design was based on two intersecting rings, with a large number of colliding bunches, and flat beams. The main challenges of the design, being enhanced by the low energy, have been the high currents and densities, the strong beam-beam effect together with the long damping time and the extreme sensitivity to all sources of non-linearities. On the high current side the care taken in vacuum chamber and radio-frequency, rf, system design, plus a powerful feedback system fighting bunch-by-bunch instabilities, has led the DAΦNE rings to store very high currents: 2.4 A in the electron ring, the highest so long achieved in any electron storage ring, and up to 1.5 A in the positron ring. The path towards the high currents have been paved by continuous surpasses of subsequent current thresholds, I_{th}, driven each time by a different cause: longitudinal instabilities, transverse instabilities, beam-beam limit, injection saturation, and so on. The high density at the Interaction Region, IP, for the high luminosity is another important point: the coupling correction achieved, up to values of 0.2% in the ratio between vertical and horizontal emittance, is also at the limit obtained in most storage rings, and this is more valuable considering the presence of the detector solenoid which rotates the transverse plane by almost 45°. The value of both β^* has been progressively diminished from the design value to about a factor of 2.5 less, since it has always paid in terms

Table 1: *DAΦNE main parameters for the present peak luminosity.*

		Units	DAΦNE
Date			2006
Energy (center of mass)	E_{cm}	GeV	1.02
Energy per ring	E	GeV	0.51
Number of rings			2
Circumference	C	m	97.69
Number of IPs			1
Revolution frequency	F_{rev}	MHz	3.07
Time between collisions	T_c	ns	2.7
Bunch spacing	s_b	m	0.81
Half crossing angle	$\theta/2$	mrad	15
Colliding bunches	N_b		110
Particles per bunch	N_{part}	10^{10}	2-3
Beam current (e^-e^+)	I	A	1.4/1.3
Bunch current (e^-e^+)	I_b	mA	13/12
Peak luminosity(10^{32})	L_{peak}	$cm^{-2}\ s^{-1}$	1.5
Specific luminosity/bunch(10^{28})	L_{sp}	$cm^{-2}\ s^{-1}\ mA^{-2}$	0.9
Horiz. β function at IP	H	m	2
Vert. β function at IP	V	cm	1.8
Horiz. emittance	ϵ	mm mrad	0.4
Coupling factor	κ	%	1.1
Horiz. Σ in collision	Σ_x	mm	1.26
Vert. Σ in collision	Σ_y	μm	12.6
Horiz. beam-beam tune shift	ξ_x		0.026
Vert. beam-beam tune shift	ξ_y		0.025
Bunch length (e^-e^+)	σ_L	cm	3/2
Piwinski angle*	ϕ		0.42
Momentum compaction	α_c		0.027
Synchrotron radiation integral	I_2	m^{-1}	9.5
Synchrotron radiation integral	I_3	m^{-2}	8.5
Synchrotron radiation integral	I_4	m^{-3}	0.3
Synchrotron radiation integral	I_5	m	9.6
Energy lost per turn	U_0	keV	9
Longit. damping time	τ_s	ms	17.9
rf frequency	f_{rf}	MHz	368.26
rf voltage (e^-e^+)	V_{rf}	MV	0.12/0.18
Ring impedance (e^-e^+)	Z/n	Ω	1.1/0.6
Total beam power	P_t	kW	45**
Injection energy	E_{inj}	GeV	0.51

*Piwinski angle is defined as: $\phi = \theta \cdot \sigma_L / 2\sigma_X$

** This value refers to maximum current of 5 A per beam.

of luminosity increase, always working contemporaneously in the chromaticity correction. By other hand the chromaticity correction and the dynamic aperture have been optimised mostly by acting on the higher non-linearities coming from the wiggler fields. DAΦNE is the first ring with optics based on wiggler presence, in order to shorten the damping time, and strengthen the beam against instabilities and beam-beam effect. The wigglers are used also to tune the emittance by modifying the values of the synchrotron integrals. Four wigglers per ring, with a maximum field of 1.8 T, for a total wiggler length of 8 m, halve the damping time, and allow to reach a reasonably high value of beam-beam limit. The horizontal drop-off of the vertical field introduces high order non-linearities, which have been fought by reshaping the poles with adequate shimming [9] in one of the recent shutdowns. The high stored current per bunch produce bunch lengthening, driven by the microwave longitudinal instability. This effect is more pronounced in the electron ring where the ion clearing electrodes introduce an increase in the ring impedance of about a factor of 2 with respect to the positron ring, such that the bunch length of the electron bunches is about 50% longer with respect to the positron one at the operating currents. The values of the bunch length limit the achievable vertical β^* through the hour-glass effect. The same instability produces also a transverse emittance increase, noticeable in the vertical plane and also in this case much stronger in the electron ring. Let's finally comment the choice of the working point, which is set above the integer and has progressively moved toward it, even if up to now it has not been possible moving to the values used in other factories due to the drop-off of the beam lifetime when going to very small values of the non integer part of the tunes. The DAΦNE parameters used for the peak luminosity set-up are shown in Table 1. They correspond to the last KLOE runs at the ϕ-energy. To be noticed that the peak luminosity is obtained with balanced currents, while the maximum currents stored during luminosity runs are higher for the electron ring (up to 1.8 A). Fig.1 shows the peak luminosity per day of DAΦNE during the operation years, when the three experiments have shared the collider time. Presently the collider is shutdown for the reinstallation of the FINUDA experiment and the extraction of the KLOE detector which has used the first months of 2006 for the final off-energy run.

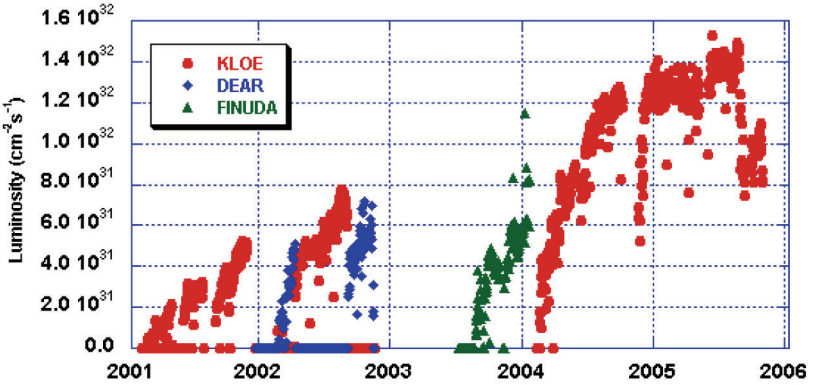

Figure 1: *DAΦNE peak luminosity history.*

3 DAΦNE Perspectives

The near future of the collider is dedicated to the run of the FINUDA and SIDDHARTA experiments. The so far achieved luminosities satisfy in principle the experiment needs. Nevertheless an extended program of R&D for the increase of the luminosity is foreseen. New kickers [10] have been designed to improve the injection efficiency, with the same parameters of the kickers for the International Linear Collider (ILC) damping rings. They have tapered strips which simultaneously reduce the impedance of the device and improve the deflecting field quality. They have a much shorter pulse (5 ns instead of 150 ns) of the present ones and the possibility of 50 Hz repetition rate. The much shorter pulse perturbs only the stored bunch corresponding to the injected one instead of about 50 bunches as in the present scheme. This should increase the positron current threshold. Reducing the impedance of the electron ring by shielding or removing the long ion-clearing-electrodes, ICEs, in the wiggler chambers will reduce the bunch lengthening and the increase of vertical emittance with the current, with a consequent net increase of luminosity, specially if accompanied by a smaller vertical β^*. The possibilities of implementing other upgrades are also being investigated: the crab cavity [11] to reduce the negative effects of the crossing angle is one of them. Another one is the very recent and exciting idea developed by Raimondi during his studies for a super B-factory project, named the crabbed waist [12], which, if confirmed, should increase by one order of magnitude the reachable luminosity.

Table 2: *DANAE luminosity and energy range*

Energy in the center of mass (GeV)	1.02	2.4
Peak luminosity (cm^{-2} s^{-1})	$\geq 10^{33}$	$\geq 10^{32}$
Total integrated luminosity (fb^{-1})	50	3

4 Physics Prospects at LNF after DAΦNE

To answer the request of the Frascati physics community for the future of the elementary particle physics after 2009, the feasibility study of an extended upgrade of DAΦNE is being realized. The e^+e^- collider design, whose range of energy and luminosity is shown in Table 2, is optimized to use DAΦNE buildings, infrastructures, injection system, and part of the ring hardware, with an overall minimization of cost and construction time. Following the Frascati tradition of applying mythological names to its accelerators, we have called it DANAE (DAfne New with Adjustable Energy). Danae, the daughter of the King of Argos, shut by her father in a tower with bronze doors, was visited by Zeus in the form of a shower of gold falling from a cloud, and from their union Perseus was born. The project excellence is assured by the application of the most recent technologies, on the basis of the DAΦNE experience and the group expertise, and by the possibility of using the next DAΦNE runs as R&D for some of the proposed new principles. DANAE design is the final step of a process in which the possibilities to upgrade DAΦNE in energy and/or luminosity have been investigated, a process which started in the workshop held in Alghero in September 2003 [13]. Let's summarize the conclusions reached so far:

- the maximum luminosity for a ϕ *factory* based on present knowledge, and involving a time-limited R&D is in the range of 10^{33} cm^{-2} s^{-1}. Luminosity higher by one order of magnitude can be envisaged if very innovative regimes are foreseen (such as the strong rf focusing [14] or the crabbed waist [12]), needing long R&D effort, and not risk free;

- the maximum energy reachable by the DAΦNE complex with the present hardware is 750 MeV per beam. By substituting dipoles, splitters and the Interaction Region, the energy of 1 GeV per beam can be reached, not yet satisfying the experimental requirements. A preliminary evaluation of the necessary

changes to reach the energy of 1.2 GeV per beam [15] has shown that the vacuum chamber and part of the magnetic elements need to be substituted. The luminosity required at the neutron-antineutron form factor threshold is in the range of 10^{32} cm^{-2} s^{-1}, and does not represent a major challenge for the design, but for the particle losses which must be kept below the allowed radiation doses, if the LNF buildings are being reused.

Summing up all above considerations we came to the design of a flexible collider, with the luminosity optimized at the ϕ production energy, and with the maximum reachable energy compatible with the present LNF infrastructures. The design is flexible enough to ensure the possibilities of future upgrades in view of further developments in the field of collider physics, but is based on well assessed principles, in order to shorten as far as possible the time necessary for its completion.

5 Basic DANAE Design Criteria

The most demanding set of DANAE parameters corresponds to the high luminosity at the ϕ-energy. The luminosity at higher energy comes almost for free once the collider hardware is correctly dimensioned. The basic DANAE design criteria are the same adopted by all factories up to now: double ring, multibunch regime, flat beams, and high collision frequency. All factories run with a single experiment in the machine: the present DAΦNE layout has two Interaction Regions (IRs), where two experiments can be installed at the same time, but only one takes data while the other one is parked. In fact the optimization of the luminosity parameters in two collision points and background shielding on both IRs has shown to be critical, and it is more effective in terms of peak and integrated luminosity to dedicate each run to a single detector. DANAE has therefore one single IR, where the experiments will be installed sequentially, thus leaving a long straight section opposite to the IR free which can be used for injection, rf systems, feedback systems. If the different experiments use a single detector, gain in shutdown and commissioning time is obtained. The DANAE design is based on the reutilization of the KLOE detector, with a tunable IR fitting different energies and detector solenoid field. Figure 2 shows a schematic layout of the DANAE rings inside the DAΦNE hall, with the new injection transfer lines, which will optimise the injection efficiency by eliminating the time needed for switching between e^+ and e^- injection configurations.

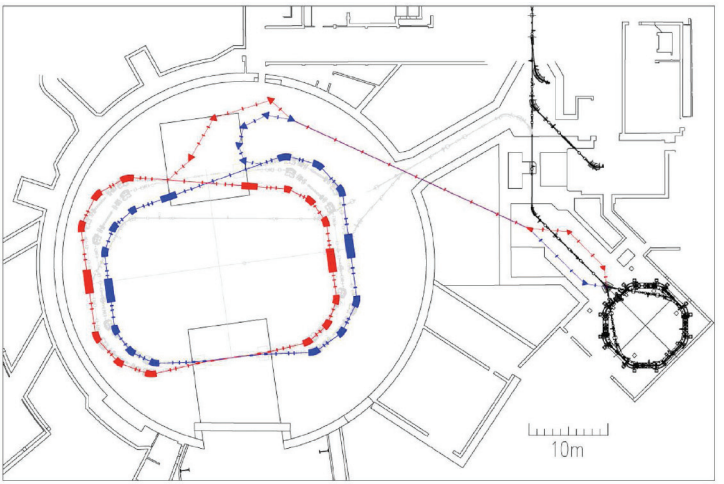

Figure 2: *Layout od DANAE inside the DAΦNE hall. Left(Right)-shifted ring corresponds to* $e^+(e^-)$

One of the main characteristics of the new collider is its flexibility. Beyond the two nominal sets of parameters, one corresponding to the high luminosity in the regime of ϕ *factory* , the second to the maximum reachable energy, the possibility of tuning the main collider parameters in a wide range is kept, with special care in the tunability of momentum compaction, emittance, and betatron tunes. All quadrupoles and sextupoles will have independent power supplies following the DAΦNE approach which has proven to be very useful during the machine commissioning, the machine study shifts and especially the operation. Table 3 contains the list of the main parameters for the two operating conditions. It can be remarked that the gain in luminosity with respect to present DAΦNE parameters is based on the increase of collision frequency thanks to the higher rf frequency, on the increase of the colliding currents, but specially on the increase of the specific luminosity. Let's recall the luminosity expression:

$$L = \frac{f_{coll}\ N^+N^-}{2\pi\ \Sigma_x^*\Sigma_y^*} \tag{1}$$

where

$$f_{coll} = N_b F_{rev} \tag{2}$$

is the collision frequency, defined by the number of bunches N_b and the revolution frequency F_{rev}; N^+ and N^- are the number of particles per bunch and

$$\Sigma^*_{x,y} = \sqrt{\sigma^{*2}_{+,x,y} \; + \; \sigma^{*2}_{-,x,y}} \tag{3}$$

are the beam cross section at the Interaction Point (IP), assuming equal beam sizes for both rings. The so called specific luminosity per bunch is defined as:

$$L_{sp} = \frac{L_{bunch}}{I_b^+ I_b^-} \tag{4}$$

Keeping the beam cross section small in collision at high currents is the key point of the high luminosity regime. Let's now mention briefly the considerations on which we base our nominal set of parameters. In a flat beam collider the beam size at the IP is minimized by the smallest achievable vertical β^* compatible with chromaticity contribution and especially with bunch length: the bunch length should be comparable or slightly longer than β^*, otherwise the luminosity decreases very fast due to the geometric "hourglass effect" and beam-beam synchro-betatron resonances. The bunch design current shouldn't exceed too much the threshold current of the longitudinal microwave instability in order to avoid the drawbacks which appear above the threshold, i.e. the bunch length and energy spread growing with the product of the bunch current and the ring impedance and the correlated vertical size blow up as observed at DAΦNE [16]. It is clear that the impedance minimization of all elements of the vacuum chamber is of extreme importance, both to increase I_{th}, and to decrease the strength of the instability. Experience in the DAΦNE vacuum chamber design, which has produced the minimum ring impedance for such short machines (0.6 Ω for the positron ring and twice as much for the electron ring, the difference being due to the presence of long ICEs) will be of great help. The longitudinal synchrotron tune Q_s should not be too high. This has been confirmed by the dedicated measurements at CESR of the luminosity versus the synchrotron tune [17] and has been also verified in numerical simulations of the beam-beam effects for DANAE. The emittance is chosen by finding the best compromise between two different effects: a high value is positive from the point of view of beam-beam tune shift, a low one is better from the point of view of parasitic crossings and small cross section at collision. The radiation damping increase is beneficial from many points of view, first of all the shorter damping time, which interferes with the beam-beam behavior and with

all instabilities with rising times in the range of ms, including the injection procedure, as shown recently in CESR-c operation at low energy [18]. A ring with wigglers which increase the synchrotron radiation integral I_3 more than I_2, will have a larger natural energy spread, and the value of I_{th} will be increased. A drawback of the wiggler presence in the rings can be the effects of non-linearities on dynamic aperture and beam-beam behavior. Wigglers placed in regions with low dispersion and low beta values are less harmful. The possibility of operating with negative momentum compaction is included in the design. Negative α_c regimes correspond to shorter bunches, but lower I_{th} [19]. The choice of emittance, horizontal and vertical β^*, and coupling factor, determines the beam-beam tune shift and through it the luminosity. We remark again the importance of maintaining the flexibility of choosing different sets of parameters in order to explore during collider operation the most effective regimes to increase the luminosity. Table 4 shows the tuning range of the most significant among them. The approach to high currents is based on a careful design of all impedance creating elements in the ring, specially the rf cavity, and on the optimization of the feedback systems, as a natural evolution of the DAΦNE experience. For the e^- ring ion trapping will be avoided by using small ICEs made of Aluminum coated with a thin layer of high resistive material distributed along the ring, with a very small impedance contribution, and by filling the ring with a gap, while Ti coating and antichambers in the positron ring will fight the electron cloud instability. The DANAE energy range goes from 0.5 to 1.2 GeV per ring. The maximum current at the maximum energy is limited to 0.5 A, in order to keep the total beam power below the reasonable limits. Injection is kept at low energy, so that the injection system does not need major modifications, and radiation shielding at injection are less demanding. Rings will be filled up to the operating current, and then ramped together up to the maximum energy.

The time needed for the technical design of all components and preparation of the calls for tenders is 18 months, and the same time is needed for the construction, although there is some overlap between the two items. If the project is approved in 2007, the first two years of the project overlap with DAΦNE operation for experiments. Once completed the DAΦNE program, the Main Ring components can be decommissioned, and at the same time the necessary building modifications for the new transfer lines can be done. The

Table 3: *DANAE design parameters, as a ϕ-factory and at the maximum energy.*

		Units	at ϕ-peak	at 1.2 GeV
Energy (center of mass)	E_{cm}	GeV	1.02	2.4
Energy per ring	E	GeV	0.51	1.2
Number of rings			2	2
Circumference	C	m	96.34	96.34
Number of IPs			1	1
Revolution frequency	F_{rev}	MHz	3.11	3.11
Time between collisions	T_c	ns	2	6
Bunch spacing	s_b	m	0.6	1.8
Half crossing angle	$\theta/2$	mrad	15	15
Colliding bunches	N_b		150	30
Particles per bunch	N_p	10^{10}	3	3.4
Beam current (e^-e^+)	I	A	2.25	0.5
Bunch current (e^-e^+)	I_b	mA	15	16.6
Peak luminosity(10^{32})	L_p	$cm^{-2}\ s^{-1}$	10	≥ 2
Specific lum./bunch	L_{sp}	$cm^{-2}s^{-1}mA^{-2}$	3 10^{28}	3 10^{28}
Horiz. β function at IP	H	m	1	1
Vert. β function at IP	V	cm	0.8	1
Horiz. emittance	ϵ	mm mrad	0.45	0.45
Coupling factor	κ	%	0.5	0.5
Horiz. Σ in collision	Σ_x	mm	0.95	0.95
Vert. Σ in collision	Σ_y	μm	6	6.7
H beam-beam tune shift	ξ_x		0.030	0.014
V beam-beam tune shift	ξ_y		0.038	0.020
Bunch length (e^-e^+)	σ_L	cm	1	1.5
Piwinski angle	ϕ		0.22	0.33
Momentum compaction	α_c		0.02	0.03
Synchr. rad. integral	I_2	m^{-1}	22.4	5.6
Synchr. rad. integral	I_3	m^{-2}	42.6	3.6
Synchr. rad. integral	I_4	m^{-3}	0.2	0.5
Synchr. rad. integral	I_5	m	23.9	1.1
Energy lost per turn	U_0	keV	21.4	165
Longit. damping time	τ_s	ms	7.6	2.2
rf frequency	f_{rf}	MHz	500	500
rf voltage (e^-e^+)	V_{rf}	MV	0.4	1.5
Ring impedance (e^-e^+)	Z/n	Ω	0.5	0.5
Total beam power	P_t	kW	48	83
Injection energy	E_{inj}	GeV	0.51	0.51

Table 4: *Range of tunability of specific parameters for ϕ operation. For each parameter the min and the max value are given, the two columns do not represent a coherent set of parameters.*

Parameter	Symbol	Units	Min	Max
Emittance	ϵ_x	mrad	0.2	0.5
Momentum compaction	α_c		-0.03	0.05
Horizontal β^*	β_x^*	m	0.5	1.5
Vertical β^*	β_y^*	mm	5	10
Coupling	κ	%	0.3	1
Half horiz. crossing angle	θ_{cross}	mrad	10	20
Particles/bunch	N	10^{10}	2.8	4
Bunch current	I_{bunch}	mA	13.8	20
Total current	I_{tot}	A	2	3
rf voltage	V	MV	0.4	1.5
Bunch length	σ_L	mm	8	15
Beam-beam tune shift	$\xi_{x,y}^*$		0.025	0.06
Synchrotron tune	Q_s		0.02	0.1

decommissioning time has been estimated as 3 months, considering that only the components inside the DAΦNE hall must be disentailed. One year is estimated for the two rings installation, and nine months for commissioning. The total time from the project approval to the collisions for the first experiment is therefore 4 years.

6 Further DANAE Upgrades

The basic DANAE design is based on already well assessed principles, on the present knowledge in collider physics, and especially on the DAΦNE experience. It includes nevertheless the possibility of adding new features, in order to open in the future other possibility for increasing the luminosity. One of this is the installation of crab cavities which are beneficial for improving the beam-beam behavior. The long straight section opposite to the IR has available space for such a device, and the flexibility of the optics allows the tuning of the lattice for such a regime. Let's recall that the effectiveness of such devices will be tested in few months by the KEKB team on their B-factory, with the foreseen installation

of one crab cavity per ring [20]. Also the Strong rf focusing regime [14] could be implemented: the modulation of the bunch length in order to allow values of the vertical betatron function at the IP in the range of very few mm can be obtained with a regime with high rf voltage derivative and large dispersion in the dipoles, producing drifting of the longitudinal phase plane along the orbit. The regime in which the drifting changes sign in the two arcs of the ring, corresponding to a small momentum compaction, can be applied to DANAE, with the high voltage cavity placed in a zone near the IR, in order to have the minimum bunch length at the IP. The necessary space for the harmonic cavity which gives the rf focusing is in fact foreseen in the ring layout. And of course also the crabbed waist [12] regime will be investigated as a possibility for the new collider, with the advantage of having the flexibility of optimising the overall collider parameters in order to take advantage of all the possibilities for the maximum increase of the reachable luminosity.

References

1. A.N Skrinsky *et al.*, *Novosibirsk Project of ϕ-Meson Factory*, Proceedings of the Workshop on Physics and Detectors for DAFNE, Frascati, 9-12 April 1991, p.67

2. C. Pellegrini, *The UCLA ϕ-Factory Project*, Proceedings of the Workshop on Physics and Detectors for DAFNE, Frascati, 9-12 April 1991, p.83

3. A. Streun, *ϕ-Factory Design Studies at Mainz*, Proceedings of the Workshop on Physics and Detectors for DAFNE, Frascati, 9-12 April 1991, p.99

4. G. Vignola *et al.*, *DAΦNE Design Criteria and Project Overview*, Proceedings of the Workshop on Physics and Detectors for DAFNE, Frascati, 9-12 April 1991, p.11

5. Kloe Collaboration, *KLOE: A General Purpose Detector for DAFNE*, Laboratori Nazionali di Frascati-INFN, LNF-92/019 (IR), (1992)

6. FINUDA Collaboration, *Finuda Technical Report*, Laboratori Nazionali di Frascati-INFN, LNF-95/024 (IR), (1995)

7. DEAR Collaboration, *DAFNE Exotic Atom Research - DEAR Proposal*, Laboratori Nazionali di Frascati-INFN, LNF-95/055 (IR), (1995)

8. *Expression of Interest for the continuation of the KLOE physics program at DAFNE upgraded in luminosity and in energy*, http://www.lnf.infn.it/lnfadmin/direzione/KLOE2-LoI.pdf, April 2006
Measurement of the nucleon form factor in the time-like region at DAFNE2, http://www.lnf.infn.it/conference/nucleon05/FF/loi_06.pdf, 11 April 2006
LoI for the study of deeply bound kaonic nuclear states at DAFNE2, http://www.lnf.infn.it/lnfadmin/direzione/LOI_MARCH_AMADEUS. April 2006
F. Ambrosino *et al.*, *Prospects for e+e- physics at Frascati between the ϕ and the Y*, in preparation

9. S. Guiducci *et al.*, *The modified DAFNE wigglers*, Proceedings of EPAC04, p.1678

10. D. Alesini *et al.*, *Design and Tests of New Fast Kickers for the DAFNE Collider and the ILC Damping Rings*, presented at EPAC06, to be published

11. A. Gallo *et al.*, *Preliminary Study of a Crab Crossing System for DAFNE*, presented at EPAC06, to be published

12. P. Raimondi, *Recent optimization in collider parameters*, presented at SuperB Meeting, Frascati, March 2006

13. *Workshop on e^+e^- in the 1-GeV to 2-GeV Range: Physics and Accelerator Prospects* - ICFA Mini-workshop - Working Group on High Luminosity e^+e^- Colliders, Alghero, Sardinia, Italy, 10-13 September 2003,http://www.lnf.infn.it/conference/d2/

14. A. Gallo, P. Raimondi and M. Zobov, *Strong RF Focusing for Luminosity Increase: Short Bunches at IP*, e-Print Archive: physics/0404020;
C. Biscari, *Bunch Length Modulation in Highly Dispersive Storage Rings*, Phys. Rev. ST Accel. Beams 8: 091001, 2005.

15. D. Alesini *et al.*, *Preliminary Considerations on Machine Requirements for a Neutron-Antineutron Form Factor Experiment at Frascati*, LNF-DAFNE Technical Note, G-63, 15/7/2005,

http://www.lnf.infn.it/acceleratori/dafne/NOTEDAFNE/G/G-63.pdf

16. DAFNE Machine Development Shift on 13/04/2005, http://www.lnf.infn.it/acceleratori/dafne/report/High_momentumCompaction.pdf

17. A. Temnykh, *Effect of High Synchrotron Tune on Beam-Beam Interaction: Simulation and Experiment*, Talk presented at ICFA Mini-Workshop on Frontiers of Short Bunches in Storage Rings, 7-8 November 2005, 2005, Frascati, Italy, http://www.lnf.infn.it/conference/sbsr05/TALKS/temnikh.ppt

18. A. Temnykh, *CESRc Wiggler Magnets*, ICFA Mini-workshop Working Group on High Luminosity e^+e^- Colliders, 10-13 September 2003, Alghero, Italy, http://www.lnf.infn.it/conference/d2/TALKS/Temnykh2.pdf

19. M. Zobov, *Negative Momentum Compaction at DAFNE*, Talk presented at the Workshop on e^+e^- in the 1-2 GeV Range: Physics and Accelerator Prospects, 10-13 September 2003, Alghero, Italy, http://www.lnf.infn.it/conference/d2/TALKS/zobov1.pdf

20. K. Hosoyama, K. Hara, A. Kabe, Y. Kojima, Y. Morita, H. NakaiI, Li Shao Peng, K. Ohkubo, H. Hattori and M. Inoue, *Superconducting Crab Cavity for KEKB*, Proceedingsof the 1998 APAC, Tsukuba.

Frascati Physics Series Vol. XLI (2006), pp. 63-68
DISCOVERIES IN FLAVOUR PHYSICS AT e^+e^- COLLIDERS
Frascati, February 28th - March 3rd, 2006

RECENT MEASUREMENTS OF V_{us}

S. Glazov
DESY, Notkestrasse 85, Hamburg, Germany 22607

Abstract

Several recent measurements of the CKM matrix element $|V_{us}|$ have found a value deviating significantly from the previous PDG average. Self-consistency of the old and new results is discussed. An average of the recent measurements of $|V_{us}|$ is in agreement with CKM matrix unitarity.

1 Introduction

The Cabibbo-Kobayashi-Maskawa (CKM) matrix [1, 2] describes the charged current couplings of the up-type u, c and t quarks to the down-type d, s and b quarks. The matrix defines the transformation form the quark mass eigenstates to the quark weak eigenstates. The unitarity of this transformation is an exact prediction of the Standard Model (SM). The most stringent test of the unitarity is based on the elements of the first row of the matrix. Measurements of the

CKM matrix element $|V_{us}|$ performed before 2004 [3], $|V_{us}| = 0.2196 \pm 0.0023$, lead to a deviation from unitarity at 2.2σ level:

$$\delta \equiv 1 - \left(|V_{ud}|^2 + |V_{us}|^2 + |V_{ub}|^2\right) = 0.0043 \pm 0.0019. \quad (1)$$

The value of $|V_{us}|$ has been determined based on a measurement of the kaon semileptonic decay width, a method which gives the best experimental precision. In SM, the $K \to \pi\ell\nu$ decay rate is given by

$$\Gamma_{K\ell 3} = \frac{G_F^2 M_K^5}{192\pi^3} S_{EW}(1 + \delta_K^\ell) C^2 \, |V_{us}|^2 \, |f_+(0)|^2 \, I_K^\ell, \quad (2)$$

where G_F is the Fermi constant, M_K is the kaon mass, S_{EW} are the universal short distance and δ_K^ℓ are the mode dependent long distance radiative corrections, $C = 1$ for K_L decays and $C = 1/2$ for $K^\pm$ decays, $|f_+(0)|$ is the decay form factor value for zero four momentum transfer squared $t = 0$, and I_K^ℓ are the decay mode and form factor dependent dimensionless phase space integrals. The experimental inputs are the semileptonic decay widths and phase space integrals while radiative corrections and $|f_+(0)|$ are calculated theoretically.

Starting from the original determination [4], only K_{Le3} and $K_{e3}^\pm$ decay modes have been used to extract the value of $|V_{us}|$. This has been motivated by contradictory experimental data [5] on the slope of the scalar form factor λ_0 which is needed to calculate I_K^μ. On the other hand, if instead of the controversial experimental value of λ_0 a theoretical calculation is used [6], the value of $|V_{us}|$ obtained using old PDG [3] width of $K_L \to \pi^\pm\mu^\mp\nu$ decay mode is about 3σ larger than that obtained using $K_L \to \pi^\pm e^\mp\nu$, taking into account correlated uncertainties. This apparent inconsistency of the determinations based on pre-2004 K_{Le3} and $K_{L\mu 3}$ data has been overlooked until recently.

2 Recent Measurements

Recently several experiments have reported measurements of kaon semileptonic decay widths and form factor slopes. The first new results have been reported by the E865 experiment at Brookhaven [7]. E865 measures the branching fraction of $K^+ \to \pi^0 e^+\nu$ decay mode normalized to $K^+ \to \pi^+\pi^0$, $K^+ \to \pi^0\mu^+\nu$ and $K^+ \to \pi^+\pi^0\pi^0$. For $K^+ \to \pi^0 e^+\nu$ decay, π^0 is detected using Dalitz $\pi^0 \to e^+e^-\gamma$ decay mode. E865 finds $|V_{us}| = 0.2272 \pm 0.0030$, which is significantly larger than the PDG evaluation and consistent with CKM matrix

unitarity. This observation triggered new analyses by KTeV, NA48 and KLOE collaborations.

KTeV reports measurements of the K_L semileptonic decay widths [8] and form factor slopes [9] which are combined together to extract $|V_{us}|$ [10]. The branching fractions are determined by measuring the six largest K_L decay modes in terms of five ratios of the partial decay widths. The six decay modes account for more than 99.9% of the total decay rate thus these ratios may be converted into the branching fractions for the six decay modes.

KTeV measures $f_+(t)$ form factor slopes for both $K_L \to \pi^\pm e^\mp \nu$ and $K_L \to \pi^\pm \mu^\mp \nu$ decay modes and also $f_0(t)$ for the $K_L \to \pi^\pm \mu^\mp \nu$ decay mode. In this determination, KTeV uses partial reconstruction of event kinematics employing only the transverse momentum of the particles. This approach allows to reduce systematic uncertainties caused by unknown momentum of the decaying kaon while leading to only small increase of the statistical error.

NA48 presents measurements of the $K_L \to \pi^\pm e^\mp \nu$ decay width [11] and $f_+(t)$ form factor slope [12]. The measurement of the $K_L \to \pi^\pm e^\mp \nu$ decay branching fraction is based on the measurement of the $K_L \to \pi^\pm e^\mp \nu$ decay rate normalized to all decays with two charged particles in the final state, $R = \Gamma_{Ke3}/\Gamma(K_L \to all\ 2-track)$. This ratio R is combined with the $K_L \to \pi^0\pi^0\pi^0$ decay branching fraction to determine the K_{e3} decay branching fraction.

Several new results are also reported by KLOE collaboration [13]. In particular, KLOE measures the four largest K_L branching fractions [14], K_L lifetime [15] and $f_+(t)$ form factor slopes [16].

The experimental results on K_L branching fractions are represented in Figure 1 which also shows an average of the recent measurements calculated taking into account reported correlations. Using the fitted values of the branching fractions and τ_L, we determine $\Gamma(K_L \to \pi^\pm e^\mp \nu) = (0.7911 \pm 0.0032) \times 10^7 s^{-1}$ and $\Gamma(K_L \to \pi^\pm \mu^\mp \nu) = (0.5276 \pm 0.0023) \times 10^7 s^{-1}$.

The new results strongly disagree with the old PDG average for $K_L \to \pi^\pm e^\mp \nu$ and $K_L \to 3\pi^0$ decay modes while the new data are in fair agreement. There is about 3σ tension between KTeV and KLOE measurements of the $K_L \to \pi^\pm e^\mp \nu$ decay branching fraction. On the other hand, for the $K_L \to \pi^\pm \mu^\mp \nu$ decay mode all experimental data are consistent. Therefore the consistency of the $|V_{us}|$ determination using the two semileptonic decay modes provides an important experimental cross check. This consistency check can be

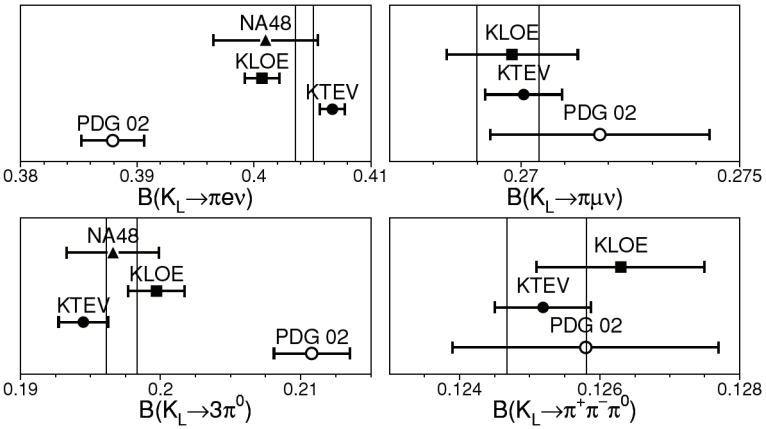

Figure 1: *Four largest K_L branching fractions measured by NA48* [11] *(triangles), KLOE* [14] *(boxes), KTeV* [8] *(closed circles) and from PDG-2002* [3] *(open circles). The vertical lines indicate the $\pm 1\sigma$ limits from the average of the recent measurements (from KTeV, NA48 and KLOE).*

performed by comparing G_F for the two decay modes taking the ratio of eq.2 for $K_L \to \pi^{\pm} e^{\mp} \nu$ and $K_L \to \pi^{\pm} \mu^{\mp} \nu$:

$$\left(\frac{G_F^{\mu}}{G_F^{e}}\right)^2 = \left[\frac{\Gamma(K_L \to \pi^{\pm}\mu^{\mp}\nu)}{\Gamma(K_L \to \pi^{\pm}e^{\mp}\nu)}\right] \Big/ \left(\frac{1+\delta_{K_{\mu 3}}}{1+\delta_{K_{e3}}} \cdot \frac{I_K^{\mu}}{I_K^{e}}\right). \tag{3}$$

Many common uncertainties cancel in this ratio. The ratio of the radiative corrections is calculated to be $(1+\delta_K^{\mu})/(1+\delta_K^{e}) = 1.0058 \pm 0.0010$ [17]. The ratio of the phase space integrals, calculated using the KTeV result for the semileptonic form factors is $I_K^{\mu}/I_K^{e} = 0.6622 \pm 0.0018$, the uncertainty in this ratio depends mostly on the uncertainty in $f_0(t)$ form factor. Using the average value for the semileptonic widths, the ratio of the couplings squared is

$$(G_F^{\mu}/G_F^{e})^2 = 1.0014 \pm 0.0045, \tag{4}$$

which is in perfect agreement with lepton universality.

The $f_+(t)$ form factor slopes measured by KTeV, NA48 and KLOE are in very good agreement for the one parameter linear and pole parameterizations but show discrepancy for the quadratic parameterization: KTeV observes large

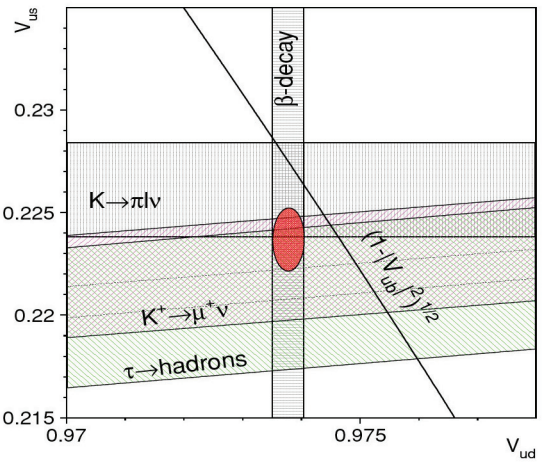

Figure 2: *Determinations of $|V_{ud}|$ from super-allowed β decays* [21] *(vertical band) and $|V_{us}|$ from $K \to \pi\ell\nu$ decays (horizontal band) compared to allowed regions from $K^+ \to \mu^+\nu$* [19] *and τ-lepton hadronic decays* [20] *(two inclined bands). The line represents the prediction from unitarity calculated as $\sqrt{1-|V_{ub}|^2}$, where $|V_{ub}| = (3.6 \pm 0.7) \times 10^{-3}$ (the width of the line is larger than uncertainty arising from uncertainty in $|V_{ub}|$). The ellipse corresponds to the $\Delta\chi^2 = 1$ contour for the average of all experimental results.*

second order term, NA48 does not observe it while KLOE result is in between. For the determination of $|V_{us}|$, KTeV values of I_K^ℓ obtained using second order fit are used including the parameterization uncertainty which corresponds to the difference between quadratic and pole model fits. Numerically this uncertainty is about equal to the difference between KTeV and KLOE results.

Combining all recent experimental results based on semileptonic kaon decays including those obtained with K^+ and K_S, and using $|f_+(0)| = 0.960 \pm 0.009$ from the lattice QCD calculation [18] we determine

$$|V_{us}| = 0.2261 \pm 0.0009_{\text{exp}} \pm 0.0021_{\text{th.}} = 0.2261 \pm 0.0023. \qquad (5)$$

Figure 2 shows this result together with other determinations of $|V_{us}|$ [19, 20] and a determination of $|V_{ud}|$ [21] and compares the allowed region with the CKM unitarity prediction. Based on these data, $\delta = 0.0017 \pm 0.0009$ which is consistent with no-deviation from unitarity at 2.0σ level.

References

1. N. Cabibbo, Phys. Rev. Lett. **10**, 531 (1963).
2. M. Kobayashi and T. Maskawa, Prog. Theor. Phys. **49**, 652 (1973).
3. Particle Data Group, Phys. Rev. D. **66**, 1 (2002).
4. H. Leutwyler and M. Roos, Z. Phys. **C25**, 91 (1984).
5. Particle Data Group, Phys. Lett, **111B**, 73 (1982).
6. J. Bijnens, G. Colangelo, G. Ecker, and J. Gasser, Semileptonic kaon decays, in:DAΦNE Physics Handbook (eds L. Maiani, G. Pancheri and N. Paver) (1994), hep-ph/9411311.
7. BNL E865, A. Sher *et al*, Phys. Rev. Lett. **91**, 261802 (2003).
8. KTeV, A. Alavi-Harati *et al*, Phys. Rev. D. **70**, 092006 (2004).
9. KTeV, A. Alavi-Harati *et al*, Phys. Rev. D. **70**, 092007 (2004).
10. KTeV, A. Alavi-Harati *et al*, Phys. Rev. Lett. **93**, 181802 (2004).
11. NA48, A. Lai *et al*, Phys. Lett. B. **602**, 41 (2004).
12. NA48, A. Lai *et al*, Phys. Lett. B. **604**, 1 (2004).
13. B. Sciascia, Experimental status and perspectives on $|V_{us}|$, this proceedings.
14. KLOE, F. Ambrosino *et al*, Phys.Lett. B. **632** 43 (2006).
15. KLOE, F. Ambrosino *et al*, Phys. Lett. B. **626**, 15 (2005).
16. KLOE, F. Ambrosino *et al* , Submitted to Phys. Lett. B., (2006) hep-ex/0601038
17. T. Andre (2004), hep-ph/0406006.
18. D. Becirevic *et al*, Nucl. Phys. B **705**, 339 (2005).
19. W. Marciano, Phys. Rev. Lett. **93**, 231803 (2004).
20. E. Gamiz *et al*, Phys. Rev. Lett. **94**, 011803 (2005).
21. J.C. Hardy and I.S. Towner, Phys. Rev Lett. **94**, 092502 (2005).

Frascati Physics Series Vol. XLI (2006), pp. 69-68
DISCOVERIES IN FLAVOUR PHYSICS AT e^+e^- COLLIDERS
Frascati, February 28th - March 3rd, 2006

KLOE EXTRACTION OF V_{us} FROM KAON DECAYS AND LIFETIMES

presented by B. Sciascia,
INFN Frascati, for the KLOE collaboration

Abstract

The most precise determination of $V_{\rm us}$ comes from semileptonic kaon decays. The KLOE experiment at DAΦNE, the Frascati ϕ *factory* , has measured all the experimental inputs to $V_{\rm us}$ for both neutral and charged kaons. Preliminary results for $BR(K^\pm \to \pi^0 e^\pm \nu)$ and $BR(K^\pm \to \pi^0 \mu^\pm \nu)$, and for $\tau_\pm$ are presented, together with the measurements of the $K_L e3$ and $K_L \mu 3$ branching ratios (BR), the $K_S e3$ BR, the K_L lifetime τ_L, and the $K_L e3$ form factors. From our results for the 5 branching ratios and τ_L we find $V_{\rm us}$=0.2254±0.0020. We have also measured the fully inclusive $K^+_{\mu 2}(\gamma)$ absolute branching ratio for which we obtain BR($K^+ \to \mu\nu(\gamma)$)=0.6366±0.0017. Combining this value with recent lattice results for f_K/f_π gives $V_{\rm us}$=0.2246±0.0016.

1 DAΦNE and KLOE

The most precise verification of the unitarity of the CKM mixing matrix is obtained today from the V_{us} and V_{ud} values, neglecting $|V_{ub}|^2 \sim 0.00002$. With the KLOE detector [1] we can measure all experimental inputs to V_{us}: branching ratios, lifetimes, and form factors.

In the DAΦNE e^+e^- collider, beams collide at a center-of-mass energy $W \sim M(\phi)$. Since 2001, KLOE has collected an integrated luminosity of $\sim$2.5 fb^{-1}. Results presented below are based on 2001-02 data for $\sim$450 pb^{-1}. The KLOE detector consists of a large cylindrical drift chamber surrounded by a lead/scintillating-fiber electromagnetic calorimeter. A superconducting coil around the calorimeter provides a 0.52 T field. The drift chamber, Ref. [1)], is 4 m in diameter and 3.3 m long. The momentum resolution is $\sigma(p_T)/p_T \sim 0.4\%$. Two track vertices are reconstructed with a spatial resolution of ~ 3 mm. The calorimeter, Ref. [2)], composed of a barrel and two endcaps, covers 98% of the solid angle. Energy and time resolution are $\sigma(E)/E = 5.7\%/\sqrt{E(\mathrm{GeV})}$ and $\sigma(t) = 57 \text{ ps}/\sqrt{E(\mathrm{GeV})} \oplus 100$ ps. The KLOE trigger, Ref. [3)], uses calorimeter and drift chamber information. For the present analysis only the calorimeter signals are used. Two energy deposits above threshold, $E > 50$ MeV for the barrel and $E > 150$ MeV for the endcaps, are required.

[1]KLOE collaboration: F. Ambrosino, A. Antonelli, M. Antonelli, C. Bacci, P. Beltrame, G. Bencivenni, S. Bertolucci, C. Bini, C. Bloise, V. Bocci, F. Bossi, D. Bowring, P. Branchini, R. Caloi, P. Campana, G. Capon, T. Capussela, F. Ceradini, S. Chi, G. Chiefari, P. Ciambrone, S. Conetti, E. De Lucia, A. De Santis, P. De Simone, G. De Zorzi, S. Dell'Agnello, A. Denig, A. Di Domenico, C. Di Donato, S. Di Falco, B. Di Micco, A. Doria, M. Dreucci, G. Felici, A. Ferrari, M. L. Ferrer, G. Finocchiaro, S. Fiore, C. Forti, P. Franzini, C. Gatti, P. Gauzzi, S. Giovannella, E. Gorini, E. Graziani, M. Incagli, W. Kluge, V. Kulikov, F. Lacava, G. Lanfranchi, J. Lee-Franzini, D. Leone, M. Martini, P. Massarotti, W. Mei, L. Meola, S. Miscetti, M. Moulson, S. Müller, F. Murtas, M. Napolitano, F. Nguyen, M. Palutan, E. Pasqualucci, A. Passeri, V. Patera, F. Perfetto, L. Pontecorvo, M. Primavera, P. Santangelo, E. Santovetti, G. Saracino, B. Sciascia, A. Sciubba, F. Scuri, I. Sfiligoi, A. Sibidanov, T. Spadaro, M. Testa, L. Tortora, P. Valente, B. Valeriani, G. Venanzoni, S. Veneziano, A. Ventura, R. Versaci, G. Xu.

2 Kaon tagging

The ϕ meson decays mainly into kaons: 49% to K^+K^- and 34% to K_L-K_S pairs. We can thus tag K_L, K_S, K^+, and K^- beams by detecting respectively K_S, K_L, K^-, and K^+ decays. Tagging allows measurements of absolute branching ratios. A K_S beam is tagged using events with a K_L interaction in the calorimeter (K_L-crash). K_L-mesons are tagged detecting $K_S \to \pi^+\pi^-$ decays. Charged kaons are tagged using two-body decays, $K^\pm \to \mu^\pm\nu$ and $K^\pm \to \pi^\pm\pi^0$. Perfect tagging requires that the detection efficiency of the tagging mode be independent of the decay mode of the tagged kaon. In reality, some dependency of the tagging efficiency on the decay mode of the signal kaon exists. This dependence is carefully measured using Monte Carlo (MC) and data control samples for each BR measurement.

3 Semileptonic $K^\pm$ decays

The measurement of the branching ratios for the $K^\pm$ semileptonic decays is performed using four data samples defined by different decay modes for the tagging kaon: $K^+_{\mu 2}$, $K^+_{\pi 2}$, $K^-_{\mu 2}$, and $K^-_{\pi 2}$. This redundancy allows the systematic effects due to the tag selection to be kept under control. Kaons are identified as tracks with momentum $70 < p < 130$ MeV, originating from the collision point. The kaon decay vertex must be within a fiducial volume (FV) defined as a cylinder of radius $40 < r < 150$ cm, centered at the collision point, coaxial with the beams. The decay track, extrapolated to the calorimeter, must point to an appropriate energy deposit. $K_{\mu 2}$ ($K_{\pi 2}$) decays are selected by applying a 3σ cuts around the muon (pion) momentum calculated in the kaon rest frame, according to the proper mass hypothesis. For the $K^\pm_{\pi 2}$ tag, identification of the π^0 from the vertex is also required. Finally, to reduce the dependency of the tag selection efficiency on the decay mode of the signal kaon, the tagging decay is required to satisfy the calorimeter trigger. In the analyzed data set about 60 million tag decays were identified and divided into the four tag samples. To select a semileptonic decay on the signal side, a one-prong kaon decay vertex must be reconstructed in the FV. The daughter track has to reach the calorimeter and to overlap an energy deposit; two-body decays are rejected by requiring that its momentum in the kaon frame, computed assuming the pion mass, is less than 195 MeV. The lepton mass is obtained

from the velocity of the lepton computed from the time of flight. The number of K_{e3} and $K_{\mu 3}$ decays is then obtained by fitting the m^2_{lept} distribution to a sum of MC distributions for the signals and various background sources, each multiplied by a free scale factor. An example of the lepton mass distribution is shown in fig. 1.

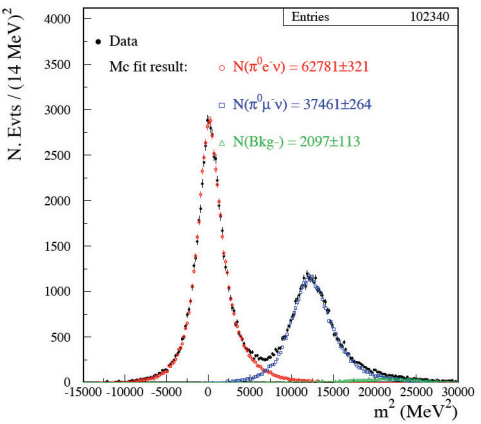

Figure 1: *Lepton mass distribution of the K^-_{13} sample tagged by $K^+_{\mu 2}$ events.*

The BR is evaluated separately for each tag sample, dividing by the number of tag counts and correcting for acceptances. The latter are obtained from MC simulations. Corrections are applied to account for data-MC differences in tracking and clustering. About 190 000 $K^\pm_{e3}$ and 100 000 $K^\pm_{\mu 3}$ decays are selected. The resulting BR's are:

$$BR(K^\pm_{e3}) = (5.047 \pm 0.046_{Stat+Tag} \pm 0.080_{Syst})\%$$

$$BR(K^\pm_{\mu 3}) = (3.310 \pm 0.040_{Stat+Tag} \pm 0.070_{Syst})\%.$$

These values are averages over the four different tag samples for each channel, and have been calculated with correlations carefully taken into account. The error is dominated by the error on data/MC efficiency corrections and the systematic error from the signal selection efficiency is still preliminary.

4 $K^{\pm}$ lifetime

The $K^{\pm}$ lifetime is an experimental input to the determination of $V_{\rm us}$. The present fractional uncertainty is about 0.2%, corresponding to an uncertainty of 0.1% for $V_{\rm us}$. However, see Ref. [4], there are large discrepancies between results of different experiments. The value of $\tau_{\pm}$ also affects the geometrical acceptance in BR measurements. KLOE is close to complete a new, high-statistics $\tau_{\pm}$ measurement using two different methods: one based on the measurement of the decay length and the other on the decay time of the kaons. Comparison between the two methods allows a consistency check. The preliminary result which uses the decay length of the $K^{\pm}$ is $\tau_{\pm} = 12.336 \pm 0.044_{Stat} \pm 0.065_{Syst}$ ns.

5 $K_S \to \pi e \nu$ decay

The KLOE analysis of $K_S \to \pi e \nu$ proceeds from the K_L-crash tagged sample and exploits the excellent timing performance of the EmC to identify signal events by TOF and to assign the charge of the lepton in the final state. Figure 2 shows the distribution in $E_{\rm miss} - p_{\rm miss}$ for $K_S \to \pi^- e^+ \nu$ event candidates for one state of lepton charge. This quantity is similar to the missing mass and is zero for signal events. The signal peak is prominent and cleanly separated from the background. Using 410 pb^{-1} of data from 2001 and 2002, KLOE has

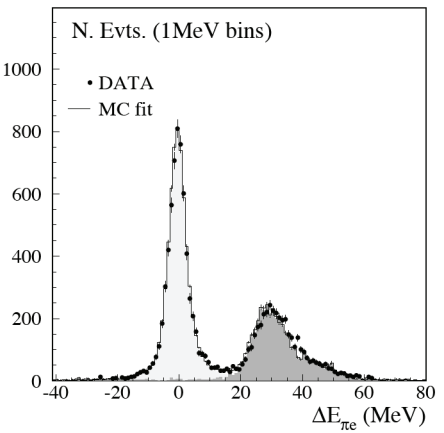

Figure 2: *Distribution in $E_{\rm miss} - p_{\rm miss}$ for candidate $K_S \to \pi^- e^+ \nu$ events in the 2002 data set.*

obtained the results $\mathrm{BR}(\pi^- e^+ \nu) = (3.528 \pm 0.057 \pm 0.027) \times 10^{-4}$, $\mathrm{BR}(\pi^+ e^- \bar{\nu}) = (3.517 \pm 0.050 \pm 0.029) \times 10^{-4}$, and $\mathrm{BR}(\pi e \nu) = (7.046 \pm 0.076 \pm 0.051) \times 10^{-4}$ [5]. The value of the combined BR for both charge states is in good agreement both with the previous KLOE result, and with the KLOE (see below) and KTeV [6] values for $\mathrm{BR}(K_L \to \pi e \nu)$, assuming $\Delta S = \Delta Q$ and using the KLOE average value for τ_L (the K_L lifetime) discussed below. The small number of $K_S \to \pi e \nu$ events doesn't allow to measure the parameters of the semileptonic form factor with an accuracy comparable with that obtained with K_L decays. However, it is worth doing this measurement with the K_S since nobody has ever done it before and since it can only be done at a *ϕ factory* . We obtain for the linear slope of the K_S semileptonic form factor $\lambda_+ = (33.9 \pm 4.1) \times 10^{-3}$. This result is in agreement with the corresponding value from linear fit of K_L semileptonic form factor. A_S is found to be $(1.5 \pm 9.6 \pm 2.9) \times 10^{-3}$. With the full 2.5 fb^{-1} from all running, KLOE can measure A_S with an uncertainty of $\sim 3 \times 10^{-3}$, about equal to the expected value of this parameter. Measurement of $\mathrm{BR}(K_S \to \pi \mu \nu)$ is more difficult, as the similarity of the π and μ masses complicates TOF PID, and background from $K_S \to \pi^+ \pi^-$ decays with $\pi \to \mu \nu$ is harder to eliminate. Nevertheless, a preliminary analysis has been performed on the 2001–2002 data, and yields $\mathrm{BR}(K_S \to \pi \mu \nu)$ with a 3% statistical error.

6 K_L decays

The BR's for K_L decays to $\pi e \nu$ and $\pi \mu \nu$ give access to V_{us}. Heretofore, these BR's were known only through various measurements of the ratios of the K_L BR's for dominant decays (i.e., decays to $3\pi^0$ and $\pi^+ \pi^- \pi^0$, in addition to the above). Using the $K_S \to \pi^+ \pi^-$ decay as a tag, KLOE has measured the absolute BR's for all four dominant decays with uncertainties of 0.5–1% [7]. The analysis is based on 328 pb^{-1} of 2001–2002 data. Decays to $\pi e \nu$, $\pi \mu \nu$, and $\pi^+ \pi^- \pi^0$ are reconstructed in the DC with PID from the decay kinematics. Decays to $3\pi^0$ are reconstructed in the EmC as TOF-localized vertices of three or more photons. The errors on the absolute BR's are dominated by the uncertainty on the value of τ_L, which enters into the calculation of the geometrical efficiency. This source of uncertainty can be all but removed (at the cost of correlating the errors among the BR measurements) by applying the constraint that the K_L BR's sum to unity. The sum of the four KLOE BR measurements plus the PDG BR values for K_L decays to $\pi^+ \pi^-$, $\pi^0 \pi^0$, and $\gamma\gamma$ is $1.0104 \pm$

0.0076. Applying the constraint gives $\mathrm{BR}(\pi e\nu(\gamma)) = 0.4007 \pm 0.0006 \pm 0.0014$, $\mathrm{BR}(\pi\mu\nu(\gamma)) = 0.2698 \pm 0.0006 \pm 0.0014$, $\mathrm{BR}(3\pi^0) = 0.1997 \pm 0.0005 \pm 0.0019$, and $\mathrm{BR}(\pi^+\pi^-\pi^0(\gamma)) = 0.1263 \pm 0.0005 \pm 0.0011$, as well as a value for the K_L lifetime, $\tau_L = 50.72 \pm 0.17 \pm 0.33$ ns.

KLOE has also measured τ_L directly, using 10^7 $K_L \to 3\pi^0$ events from 400 pb^{-1} of 2001–2002 data [8]. $K_L \to \pi^+\pi^-\pi^0$ decays, for which the track and photon vertices can be independently reconstructed, provide a control sample for checking the EmC time scale, and demonstrate that the efficiency for reconstructing a vertex of three or more photons is uniformly greater than 99% inside the fiducial volume ($0.37\lambda_L$). The result, $\tau_L = 50.92 \pm 0.17 \pm 0.25$ ns, is consistent with the value obtained from the sum of the K_L BR's. These are two independent measurements; their average gives the KLOE value, $\tau_L = 50.84 \pm 0.23$ ns. For comparison, the best previous measurement is $\tau_L = 51.54 \pm 0.44$ ns [9].

The form-factor slopes for semileptonic kaon decays are another important input for the determination of V_{us}. Using a sample of 328 pb^{-1} of 2001–2002 data, KLOE has obtained the distribution in $t \equiv (p_K - p_\pi)^2/m^2_{\pi^+}$ for 2×10^6 $K_L \to \pi e\nu$ decays. The data are divided into subsamples by run period and lepton charge, and the t distributions are fit with the forms $f_+(t) = f_+(0)[1 + \lambda_+ t]$, $f_+(0)[1 + \lambda'_+ t + \lambda''_+ t^2/2]$, and the pole model $f_+(t) = M_V^2/(M_V^2 - t)$. The linear fit gives $\lambda_+ = (28.6 \pm 0.5 \pm 0.8) \times 10^{-3}$ with $\chi^2/N_{\mathrm{dof}} = 330/363$, while the quadratic fit gives $\lambda'_+ = (25.5 \pm 1.5 \pm 1.9) \times 10^{-3}$ and $\lambda''_+ = (1.4 \pm 0.7 \pm 0.7) \times 10^{-3}$, with correlation coefficient $\rho(\lambda'_+, \lambda''_+) = -0.95$ and $\chi^2/N_{\mathrm{dof}} = 325/362$ [10]. The fit with the pole model gives $M_V = (870 \pm 7)$MeV. The phase space integrals, needed for the $|V_{\mathrm{us}} f_+(0)|$ measurement, calculated in the pole-model or in the quadratic parametrization have a difference of 0.5 per mil if the KLOE results are used (see also figure 3), while it is as high as 6 per mil in the case of the KTeV measurements. The additional statistics from 2004–2005 running should help in gauging the significance of the quadratic term, as well as with the measurement of the form-factor slopes for $K_L \to \pi\mu\nu$ decays.

7 Determination of V_{us}

The BR's of the semileptonic K_L decays, together with the result $BR(K_S \to \pi e\nu(\gamma)) = (7.09 \pm 0.09) \times 10^{-4}$ and the preliminary results on the semileptonic $K^\pm$ decays, allow five independent determinations of the observable $|V_{\mathrm{us}} f_+(0)|$,

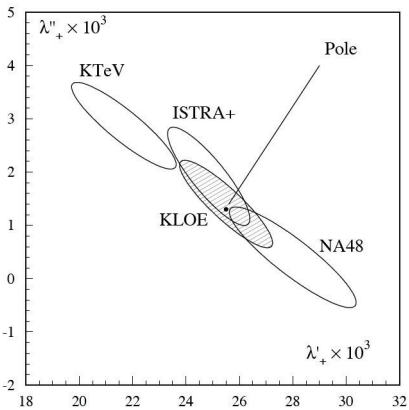

Figure 3: *Comparison of recent measurements of K_L form factor.*

as shown in Fig. 4, in which the new KLOE value of τ_L has been used to convert K_L BR's to partial widths. Averaging the five KLOE values gives $|V_{\rm us} f_+(0)|$ $= 0.2166 \pm 0.0005$, with $\chi^2/{\rm DoF} = 1.9/4$. The fractional uncertainty is about 0.25%. A precise estimate of $f_+(0)$, 0.961 ± 0.008, was first given in 1984 [11].

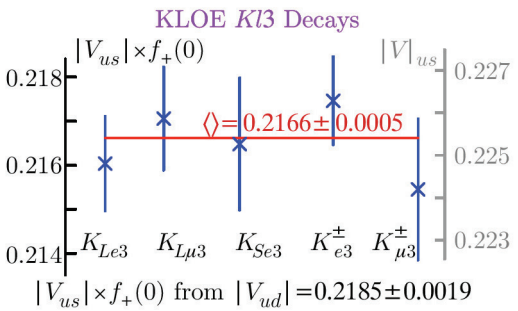

Figure 4: $|V_{\rm us} f_+(0)|$ *measurements. For K_L BR the KLOE τ_L has been used.*

Recent lattice calculations [12] give $f_+(0) = 0.960 \pm 0.009$, in agreement with Ref. [11]. Using the value from [11] and the average of our results for $|V_{\rm us} f_+(0)|$ we find $V_{\rm us} = 0.2254 \pm 0.0020$.

8 $V_{\rm us}$ from $BR(K^+ \to \mu^+\nu(\gamma))$

KLOE has also measured the radiation inclusive, absolute $K^+_{\mu 2}$ branching ratio. From about 9×10^5 $K^+_{\mu 2}$ decays obtained from a sample of about 250 pb^{-1} KLOE obtains $BR(K^+ \to \mu^+\nu(\gamma))$=0.6366±0.0009$_{Stat}$ ±0.0015$_{Syst}$ [13], for an overall fractional error of 0.27%. Using recent lattice results on the decay constants of pseudoscalar mesons [14], we find $V_{\rm us}$= 0.2246±0.0016 (see figure 5). The fractional error of about 1% is dominated by the uncertainty in the f_K/f_π computation.

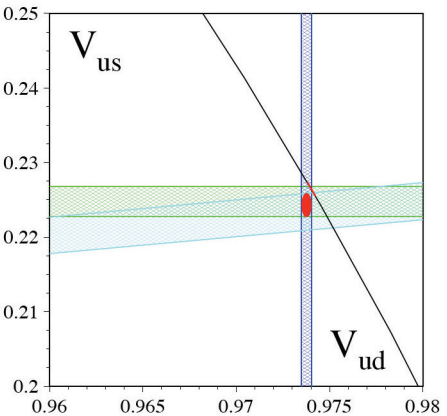

Figure 5: *Pictorial view of* $V_{\rm us}$, $V_{\rm ud}$ *and* $V_{\rm us}/V_{\rm ud}$ *measurements in the* $V_{\rm us}$ *vs* $V_{\rm ud}$ *plane. The small ellipse represents the fit result for* $V_{\rm us}$ *and* $V_{\rm ud}$. *Also the Unitarity line is shown.*

References

1. M. Adinolfi *et al.*, [KLOE Collaboration], *The tracking detector of the KLOE experiment*, *Nucl. Instrum. Meth* **A 488** 2002 51

2. M. Adinolfi *et al.*, [KLOE Collaboration], *The KLOE electomagnetic calorimeter*, *Nucl. Instrum. Meth* **A 482** 2002 364

3. M. Adinolfi *et al.*, [KLOE Collaboration], *The trigger system of the KLOE experiment*, *Nucl. Instrum. Meth* **A 492** 2002 134

4. S. Eidelman *et al.*, Particle Data Group, *Phys. Lett.* **B 592** 2004 1

5. KLOE Collaboration, F. Ambrosino *et al.*, *Phys. Lett.* **B**, in press [hep-ex/0601026].

6. KTeV Collaboration, T. Alexopoulos *et al.*, *Phys. Rev.* **D 70** (2004) 092006.

7. KLOE Collaboration, F. Ambrosino *et al.*, *Phys. Lett.* **B**, in press [hep-ex/0508027].

8. KLOE Collaboration, F. Ambrosino *et al.*, *Phys. Lett.* **B 626** (2005) 15.

9. K.G. Vosburgh *et al.*, *Phys. Rev.* **D 6** (1972) 1834.

10. KLOE Collaboration, F. Ambrosino *et al.*, *Phys. Lett.* **B**, in press [hep-ex/0601038].

11. H. Leutwyler and M. Roos, *Z. Phys.* **C 25** 1984 91

12. D. Becirevic *et al.*, *Nucl. Phys.* **B 705** 2005 339

13. F. Ambrosino *et al.*, [KLOE Collaboration], *Phys. Lett.* **B**, in print, hep-ex/0509045

14. C. Aubin *et al.*, MILC Collaboration, *Phys. Rev.* **D 70** 2004 114501
W.J. Marciano, *Phys. Rev. Lett.* **96** 2006 032002

Frascati Physics Series Vol. XLI (2006), pp. 79-85
DISCOVERIES IN FLAVOUR PHYSICS AT e^+e^- COLLIDERS
Frascati, February 28th - March 3rd, 2006

STATUS AND PERSPECTIVES OF CP AND CPT TESTS WITH NEUTRAL KAONS AT KLOE

KLOE Collaboration[1]
presented by
A. Di Domenico
Dipartimento di fisica, Universitá di Roma "La Sapienza"
& INFN Sezione di Roma, Rome, Italy

Abstract

The results of CP and CPT tests with neutral kaons based on the analysis of a sample of ~ 400 pb^{-1} collected by the KLOE experiment are presented. Perspectives for the full data sample analysis of 2.5 fb^{-1} are also briefly discussed.

KLOE[1] completed the data taking in March 2006 with a total integrated luminosity of ~ 2.5 fb^{-1}. The results presented in the following refer to the data

[1]KLOE collaboration: F. Ambrosino, A. Antonelli, M. Antonelli, C. Bacci, P. Beltrame, G. Bencivenni, S. Bertolucci, C. Bini, C. Bloise, V. Bocci, F. Bossi, D. Bowring, P. Branchini, R. Caloi, P. Campana, G. Capon, T. Capussela, F. Ceradini, S. Chi, G. Chiefari, P. Ciambrone, S. Conetti, E. De Lucia, A. De Santis, P. De Simone, G. De Zorzi, S. Dell'Agnello, A. Denig, A. Di Domenico, C. Di Donato, S. Di Falco, B. Di Micco, A. Doria, M. Dreucci, G. Felici, A. Ferrari, M. L. Ferrer, G. Finocchiaro, S. Fiore, C. Forti, P. Franzini, C. Gatti, P. Gauzzi, S. Giovannella, E. Gorini, E. Graziani, M. Incagli,

sample collected during years 2001 and 2002, corresponding to an integrated luminosity of about 400 pb^{-1}.

1 Search for the CP Violating $K_S \to 3\pi^0$ Decay

The $K_S \to 3\pi^0$ decay would signal a pure CP violation in mixing and/or decay. The Standard Model prediction is BR($K_S \to 3\pi^0$)$\sim 2 \times 10^{-9}$. At KLOE neutral kaon pairs are produced in $\phi \to K_S K_L$ decay, and a K_S is tagged by identifying the interaction of the K_L in the calorimeter (K_L-crash). A direct search of $K_S \to 3\pi^0$ requires a K_L-crash and six photons coming from the IP. In order to get the BR, final event counting is normalized to the $K_S \to 2\pi^0$ rate. Since the decay $K_S \to 3\pi^0$ has 6 photons in the final state, the major expected background is the much more abundant CP-even $K_S \to 2\pi^0$ decay in addition with two fake photons coming from shower fragments, machine background overlapping in time the event, or both. A kinematic fit procedure in the $2\pi^0$ and $3\pi^0$ hypothesis is able to reject the background to an affordable level. At the end 2 candidate signal events are found with an expected background of $3.13 \pm 0.82_{\rm stat} \pm 0.37_{\rm syst}$ events. This result leads to the best upper limit on the BR up to date [1]:

$$BR(K_S \to 3\pi^0) < 1.2 \times 10^{-7}$$

at 90% c.l., improving the previous best limit by NA48 [2] by a factor six. This limit translates into a limit on

$$|\eta_{000}| = \left| \frac{A(K_S \to 3\pi^0)}{A(K_L \to 3\pi^0)} \right| = \sqrt{\frac{\tau_L}{\tau_S} \frac{\mathrm{BR}(K_S \to 3\pi^0)}{\mathrm{BR}(K_L \to 3\pi^0)}} < 0.018$$

at 90% c.l., using τ_L and BR($K_L \to 3\pi^0$) from KLOE measurements [3, 4], and τ_S from PDG [5]; as a consequence $|\eta_{000}|$ does not constitute anymore the limiting factor in the CPT test from unitarity, as discussed below.

W. Kluge, V. Kulikov, F. Lacava, G. Lanfranchi, J. Lee-Franzini, D. Leone, M. Martini, P. Massarotti, W. Mei, S. Meola, S. Miscetti, M. Moulson, S. Müller, F. Murtas, M. Napolitano, F. Nguyen, M. Palutan, E. Pasqualucci, A. Passeri, V. Patera, F. Perfetto, L. Pontecorvo, M. Primavera, P. Santangelo, E. Santovetti, G. Saracino, B. Sciascia, A. Sciubba, F. Scuri, I. Sfiligoi, T. Spadaro, M. Testa, L. Tortora, P. Valente, B. Valeriani, G. Venanzoni, S. Veneziano, A. Ventura, R.Versaci, G. Xu

An improvement on the upper limit of the BR of a factor 5-10 is expected from the analysis of the full KLOE data sample of 2.5 fb^{-1}.

2 Measurement of CP Violation in $K_L \to \pi^+\pi^-$ Decay

A $K_L \to \pi^+\pi^-$ decay sample is selected requiring a K_S tag, i.e. two charged tracks with opposite curvature close to the IP forming a vertex recognized as a $K_S \to \pi^+\pi^-$ decay. The K_L line of flight is then reconstructed, and the K_L charged decay is identified requiring two charged tracks of opposite curvature with a small distance of closest approach to the line of flight, and forming a vertex. The $K_L \to \pi^+\pi^-$ decays are easily recognized exploiting the clean separation between them and the other charged K_L decays in the distribution of the $\sqrt{E^2_{miss} + P^2_{miss}}$ variable, where P_{miss} and E_{miss} are the missing momentum and the missing energy at the decay vertex, in the hypothesis of $K_L \to \pi^+\pi^-$ decay. The signal events are normalized to $K_{\mu 3}$ events. Using the KLOE measurements for $K_{\mu 3}$, we obtain the following result:

$$BR(K_L \to \pi^+\pi^-) = (1.963 \pm 0.012_{\rm stat} \pm 0.017_{\rm stat}) \times 10^{-3}$$

that is fully inclusive with respect to final-state radiation, in good agreement with the measurement from KTeV [6] $(1.975 \pm 0.012) \times 10^{-3}$, and in strong disagreement with the value reported by the PDG $(2.090 \pm 0.025) \times 10^{-3}$. Using KLOE results for $BR(K_S \to \pi^+\pi^-)$ and τ_L, PDG values for τ_S and ϵ'/ϵ, and subtracting the CP conserving direct photon-emission contribution [7], we obtain $|\epsilon| = (2.216 \pm 0.013) \times 10^{-3}$.

3 CPT and $\Delta S = \Delta Q$ Tests with $K_S \to \pi e \nu$ Decays

The K_{e3} decays of K_S are selected requiring a K_L-crash and two tracks forming a vertex close to the IP, and associated with two energy deposits in the calorimeter. Pions and electrons are recognized using the time-of-flight technique. The number of signal events is normalized to the number of $K_S \to \pi^+\pi^-$ in the same data set. The result of the branching ratio separated for the two charge states is [8]:

$$\begin{aligned}
{\rm BR}(K_S \to \pi^- e^+ \nu) &= (3.528 \pm 0.062) \times 10^{-4} \\
{\rm BR}(K_S \to \pi^+ e^- \bar{\nu}) &= (3.517 \pm 0.058) \times 10^{-4} \\
{\rm BR}(K_S \to \pi e \nu) &= (7.046 \pm 0.091) \times 10^{-4}
\end{aligned}$$

The result on the semileptonic asymmetry of K_S, measured for the first time, is:

$$\begin{aligned} A_S &= \frac{\Gamma(K_S \to \pi^- e^+ \nu) - \Gamma(K_S \to \pi^+ e^- \bar{\nu})}{\Gamma(K_S \to \pi^- e^+ \nu) + \Gamma(K_S \to \pi^+ e^- \bar{\nu})} \\ &= (1.5 \pm 9.6_{\text{stat}} \pm 2.9_{\text{syst}}) \times 10^{-3} \end{aligned}$$

The uncertainty on A_S can be reduced at the level of $\approx 3 \times 10^{-3}$ with the analysis of the full data sample of 2.5 fb^{-1}.

¿From the total BR and using τ_L and BR($K_L \to \pi e \nu$) from KLOE measurements [3, 4], and τ_S from PDG [5], we measure the real part of the $\Delta S = \Delta Q$ violating, CPT conserving parameter x_+ in semileptonic decay amplitudes:

$$\Re x_+ = \frac{1}{4}\left(\frac{BR(K_S \to \pi e \nu)\tau_L}{BR(K_L \to \pi e \nu)\tau_S} - 1\right) = (-1.2 \pm 3.6) \times 10^{-3}$$

The error on this value represents an improvement by almost a factor of two with respect to the most precise previous measurement from CPLEAR [9].

From the sum and the difference of the K_L and K_S semileptonic charge asymmetries one can test CPT conservation. Using the values of A_L from KTeV [12], $\Re\delta$ from CPLEAR [10], and $\Re\epsilon$ from PDG we measure the real part of the CPT and $\Delta S = \Delta Q$ violating parameter x_- in semileptonic decay amplitudes:

$$\Re x_- = \frac{A_S - A_L}{4} - \Re\delta = (-0.8 \pm 2.5) \times 10^{-3}$$

improving by a factor five the previous best measurement by CPLEAR [10], and the real part of the CPT violating, $\Delta S = \Delta Q$ conserving parameter y in semileptonic decay amplitudes:

$$\Re y = \Re\epsilon - \frac{A_S + A_L}{4} = (0.4 \pm 2.5) \times 10^{-3}$$

with a precision comparable to that obtained by CPLEAR from unitarity relation [11].

4 CPT Test from Bell-Steinberger Relation

The unitarity relation can be used to test the CPT symmetry:

$$(1 + i \tan\phi_{SW})[\Re\epsilon - i\Im\delta] = \frac{1}{\Gamma_S}\sum_f A^*(K_S \to f)A(K_L \to f) = \sum_f \alpha_f$$

after having provided all the α_i and ϕ_{SW} as inputs. Using KLOE measurements, PDG values, and a combined fit of KLOE and CPLEAR data in order to improve the precision on $\Im x_+$, we obtain:

$$\Re\epsilon = (160.2 \pm 1.3) \times 10^{-5} \,, \qquad \Im\delta = (1.2 \pm 1.9) \times 10^{-5}$$

improving by almost a factor three the previous best result on $\Im\delta$ from CPLEAR [11]. The limiting factor of the present result is the uncertainty on ϕ_{+-} entering in α_{+-}. In fact, using the KLOE upper limit on $BR(K_S \to 3\pi^0)$ and the A_S measurement, α_{000} and $\alpha_{\pi l\nu}$ do not limit anymore the test sensitivity.

5 Decoherence and CPT Tests Using Kaon Interferometry

The quantum interference between the two kaon decays in the CP violating channel $\phi \to K_S K_L \to \pi^+\pi^-\pi^+\pi^-$ has been observed for the first time by KLOE. The selection of the sample requires two vertices, each with two opposite curvature tracks inside the drift chamber, with an invariant mass and total momentum compatible with the two neutral kaon decays. The experimental resolution on the time difference Δt in the case of $\pi^+\pi^-$ decays can be improved exploiting the good momentum resolution of the KLOE detector and the closed kinematics of the event. After a kinematic fit, a resolution $\sigma_{\Delta t} \sim 0.9\tau_S$ is obtained. The measured $|\Delta t|$ distribution can be fitted with the expression:

$$I(\pi^+\pi^-,\pi^+\pi^-;|\Delta t|) \propto e^{-\Gamma_L|\Delta t|} + e^{-\Gamma_S|\Delta t|} - 2(1-\zeta_{SL}) e^{-\frac{(\Gamma_S+\Gamma_L)}{2}|\Delta t|} \cos(\Delta m \Delta t)$$

where the quantum mechanical expression in the $\{K_S, K_L\}$ basis has been modified with the introduction of a decoherence parameter ζ_{SL}, and a factor $(1 - \zeta_{SL})$ multiplying the interference term. Analogously, a ζ_{00} parameter can be defined in the $\{K^0, \bar{K^0}\}$ basis [13]. After having included resolution and detection efficiency effects, the background due to coherent and incoherent K_S-regeneration on the beam pipe wall, and keeping fixed in the fit Δm, Γ_S and Γ_L to the PDG values, the preliminary KLOE results are:

$$\begin{aligned} \zeta_{SL} &= 0.043 \pm 0.037_{\text{stat}} \pm 0.008_{\text{syst}} \\ \zeta_{00} &= (0.24 \pm 0.20_{\text{stat}} \pm 0.02_{\text{syst}}) \times 10^{-5} \end{aligned}$$

compatible with the quantum mechanics prediction, i.e. $\zeta_{SL} = \zeta_{00} = 0$, and no decoherence effects. These results improve of five orders of magnitude in the

case of ζ_{00} the previous ones obtained by Bertlmann and co-workers [13] in a re-analysis of CPLEAR data.

Another analysis based on the same data constrains the CPT violation parameters α, β and γ related to decoherence induced by quantum gravity effects [14, 15, 16]. The KLOE preliminary results are:

$$\begin{aligned}
\alpha &= \left(-10^{+41}_{-31}\text{stat} \pm 9_{\text{syst}}\right) \times 10^{-17}\,\text{GeV} \\
\beta &= \left(3.7^{+6.9}_{-9.2}\text{stat} \pm 1.8_{\text{syst}}\right) \times 10^{-19}\,\text{GeV} \\
\gamma &= \left(-0.5^{+5.8}_{-5.1}\text{stat} \pm 1.2_{\text{syst}}\right) \times 10^{-21}\,\text{GeV}
\end{aligned}$$

The uncertainties of the results on β and γ are of the same order of magnitude of the ones obtained by CPLEAR studying single neutral kaon decays to $\pi^+\pi^-$ and $\pi e\nu$ final states [17], and are approaching the interesting Planck's scale region, i.e. $\mathcal{O}(m_K^2/M_{Planck}) \sim 2 \times 10^{-20}\,\text{GeV}$.

The uncertainties on the ζ_{SL}, ζ_{00}, α, β, and γ parameters should improve by about a factor of 2.2 with the analysis of the full data sample.

References

1. KLOE coll., F. Ambrosino et al., Phys. Lett. **B619** (2005) 61.
2. NA48 coll., A. Lai et al., Phys. Lett. **B610** (2005) 165.
3. KLOE coll., F. Ambrosino et al., Phys. Lett. **B632** (2006) 43.
4. KLOE coll., F. Ambrosino et al., Phys. Lett. **B626** (2005) 15.
5. Particle Data Group, S. Eidelman et al., Physics Letters **B592**, 1 (2004).
6. KTeV coll., T. Alexopoulos et al., Phys. Rev. **D70** (2004) 092006.
7. E. Ramberg et al., Phys. Rev. Lett. **D70** (1993) 2525.
8. KLOE coll., F. Ambrosino et al., Phys. Lett. **B636** (2006) 173.
9. CPLEAR coll., A. Angelopoulos et al., Phys. Lett. **B444** (1998) 38.
10. CPLEAR coll., A. Angelopoulos et al., Phys. Lett. **B444** (1998) 52.
11. CPLEAR coll., A. Apostolakis et al., Phys. Lett. **B456** (1999) 297.

12. KTeV coll., A. Alavi-Harati et al., Phys. Rev. Lett. **88** (2002) 181601.

13. R. A. Bertlmann, W. Grimus, B. C. Hiesmayr, Phys. Rev. **D60** (1999) 114032

14. J. Ellis, J. L. Lopez, N. .E. Mavromatos, D. V. Nanopoulos, Phys. Rev. **D53** (1996) 3846.

15. P. Huet, M. Peskin, Nucl. Phys. **B434** (1995) 3

16. F. Benatti, R. Floreanini, Nucl. Phys. **B511** (1998) 550.

17. CPLEAR coll., R. Adler et al., Phys. Lett. **B364** (1995) 239.

Frascati Physics Series Vol. XLI (2006), pp. 87-97
DISCOVERIES IN FLAVOUR PHYSICS AT e^+e^- COLLIDERS
Frascati, February 28th - March 3rd, 2006

LEPTON UNIVERSALITY AND RARE KAON DECAYS: A WINDOW TOWARDS NEW PHYSICS

PARIDE PARADISI

Dipartimento di Fisica, Universit di Roma, "Tor Vergata", via della Ricerca Scientifica, Roma, Italy

INFN, Sezione di Roma II, via della Ricerca Scientifica, Roma, Italy

Abstract

We discuss theoretical virtues of the K physics and emphasize the unique role of rare and elicity suppressed K decays in probing the nature of physics beyond the Standard Model (SM). The important role played by the lepton universality to probe new physics within Supersymmetric (SUSY) extensions of the SM are discussed in the light of the recent NA48/2 improvement on $R_K = \Gamma(K \to e\nu)/\Gamma(K \to \mu\nu)$. Within SUSY $\mu - e$ non-universal contributions can arise from lepton flavor violating (LFV) sources. We show that $\mu - e$ non-universality in K_{l2} can reach the per-cent level compatible with the bounds coming from LFV τ decays. Moreover, the impact of SUSY LFV effects on $B \to \ell\nu$ (with $\ell = e, \mu, \tau$) is also discussed. Finally, we emphasize also the great chance provided by the rare kaon $K \to \pi\nu\bar{\nu}$ decays to probe possible new sources of flavour symmetry breaking and of CP violation.

1 Introduction

High precision electroweak tests represent a powerful tool to probe the SM and, hence, to constrain or obtain indirect hints of new physics beyond it. Kaon and pion physics are obvious grounds where to perform such tests, for instance in the well studied π_{l2} ($\pi \to l\nu_l$) and K_{l2} ($K \to l\nu_l$) decays, where $l = e$ or μ. Unfortunately, the relevance of these single decay channels in probing the SM is severely hindered by our theoretical uncertainties on non perturbative quantities like f_π and f_K, which still remain at the percent level. On the other hand, in the ratios $R_\pi = \Gamma(\pi \to e\nu)/\Gamma(\pi \to \mu\nu)$ and $R_K = \Gamma(K \to e\nu)/\Gamma(K \to \mu\nu)$ of the electronic and muonic modes, the hadronic uncertainties cancel to a very large extent. As a result, the SM predictions of R_π and R_K are known with excellent accuracy [1)] and this makes possible to fully exploit the great experimental resolutions on R_π [2)] and R_K [2, 3)] to constrain new physics effects. Given our limited predictive power on f_π and f_K, deviations from the $\mu - e$ universality represent the best hope we have at the moment to detect new physics effects in π_{l2} and K_{l2}. The most recent NA48/2 result on R_K:

$$R_K^{exp.} = (2.416 \pm 0.043_{stat.} \pm 0.024_{syst.}) \cdot 10^{-5} \quad \text{NA48/2}$$

which will further improve with current analysis, significantly improves on the previous PDG value, $R_K^{exp.} = (2.44 \pm 0.11) \cdot 10^{-5}$. This is to be compared with the SM prediction which reads:

$$R_K^{SM} = (2.472 \pm 0.001) \cdot 10^{-5}.$$

Denoting by $\Delta r_{NP}^{e-\mu}$ the deviation from $\mu - e$ universality in R_K due to new physics, i.e.:

$$R_K = \frac{\Gamma_{SM}^{K \to e\nu_e}}{\Gamma_{SM}^{K \to \mu\nu_\mu}} \left(1 + \Delta r_{NP}^{e-\mu}\right), \tag{1}$$

the NA48/2 result requires (at the 2σ level):

$$-0.063 \leq \Delta r_{NP}^{e-\mu} \leq 0.017 \quad \text{NA48/2}. \tag{2}$$

In the following, we consider low-energy supersymmetric extensions of the SM (with R parity) as the source of new physics to be tested by R_K. The question we intend to address is whether SUSY can cause deviations from $\mu - e$ universality in K_{l2} at a level which can be probed with the present attained

experimental sensitivity, namely at the percent level. We will show that i) it is indeed possible for regions of the minimal supersymmetric standard model (MSSM) to obtain $\Delta r_{NP}^{e-\mu}$ of $\mathcal{O}(10^{-2})$ and ii) such large contributions to K_{l2} do not arise from SUSY lepton flavor conserving (LFC) effects, but, rather, from lepton flavor violating (LFV) ones. Finally, being the NA48/2 R_K central value below the SM prediction, one may wonder whether SUSY contributions could have the correct sign to account for such an effect. We will show that there exist regions of the SUSY parameter space where the total R_K arising from all such SM and SUSY terms is indeed lower than R_K^{SM}.

2 $\mu - e$ universality in $\pi \to l\nu$ and $K \to l\nu$ decays

The SM contributions to π_{l2} and K_{l2} are helicity suppressed; hence, these processes are very sensitive to non-SM effects. In particular, charged Higgs bosons ($H^{\pm}$) appearing in any model with two Higgs doublets (including the SUSY case) can contribute at tree level to the above processes inducing the following effects [5]:

$$\frac{\Gamma(M \to l\nu)}{\Gamma_{SM}(M \to l\nu)} = r_H = \left[1 - \left(\frac{m_d}{m_d + m_u}\right)^2 \tan^2\beta \frac{m_M^2}{m_H^2}\right]^2 \tag{3}$$

where m_u is the mass of the up quark while $m_{s,d}$ stands for the down-type quark mass of the M meson ($M = K, \pi$). From Eq. (3) it is evident that such tree level contributions do not introduce any lepton flavour dependent correction. The first SUSY contributions violating the $\mu - e$ universality in $M \to l\nu$ decays arise at the one-loop level with various diagrams involving exchanges of (charged and neutral) Higgs scalars, charginos, neutralinos and sleptons. For our purpose, it is relevant to divide all such contributions into two classes: i) LFC contributions where the charged meson M decays without FCNC in the leptonic sector, i.e. $M \to l\nu_l$; ii) LFV contributions $M \to l_i\nu_k$, with $i \neq k$ (in particular, the interesting case will be for $i = e, \mu$, and $k = \tau$). A typical contribution of the first class is of order

$$\Delta r_{SUSY}^{e-\mu} \sim \frac{\alpha_2}{4\pi}\left(\frac{m_\mu^2 - m_e^2}{m_H^2}\right)\tan^2\beta\,, \tag{4}$$

where H denotes a heavy Higgs circulating in the loop. Then, even if we assume particularly favorable circumstances like $\tan\beta = 50$, we end up with

$\Delta r^{e-\mu}_{SUSY} \leq 10^{-6}$ much below the percent level of experimental sensitivity. One could naively think that contributions of the second class (LFV contributions) are further suppressed with respect to the LFC ones. On the contrary, we show that charged Higgs mediated SUSY LFV contributions, in particular in the kaon decays into an electron and a tau neutrino, can be strongly enhanced. The quantity which now accounts for the deviation from the $\mu - e$ universality is $R^{LFV}_{\pi,K} = \sum_i \Gamma(\pi(K) \to e\nu_i) / \sum_i \Gamma(\pi(K) \to \mu\nu_i)$ (with $i = e, \mu, \tau$) with the sum extended over all (anti)neutrino flavors (experimentally one determines only the charged lepton flavor in the decay products). The dominant SUSY contributions to $R^{LFV}_{\pi,K}$ arise from the charged Higgs exchange. The effective LFV Yukawa couplings we consider are:

$$l H^{\pm} \nu_\tau \to \frac{g_2}{\sqrt{2}} \frac{m_\tau}{M_W} \Delta^{3l}_R \tan^2\beta \qquad l = e, \mu. \tag{5}$$

The Δ^{3l}_R terms are induced at one loop level by non holomorphic corrections through the exchange of gauginos and sleptons, provided LFV mixing among the sleptons (for phenomenological applications, see [4]). Since the Yukawa operator is of dimension four, the quantities Δ^{3l}_R depend only on ratios of SUSY masses, hence avoiding SUSY decoupling. Δ^{3l}_R is proportional to the off-diagonal flavor changing entries of the slepton mass matrix $\delta^{3j}_{RR} = (\tilde{m}^2_\ell)_{3Rj R} / \langle \tilde{m}^2_\ell \rangle$. Following the thorough analysis in [6], it turns out that $\Delta^{3l}_R \leq 10^{-3}$. Making use of the LFV Yukawa coupling in Eq. (5), it turns out that the dominant contribution to $\Delta r^{e-\mu}_{NP}$ reads [7]:

$$R^{LFV}_K \simeq R^{SM}_K \left[1 + \left(\frac{m^4_K}{M^4_H} \right) \left(\frac{m^2_\tau}{m^2_e} \right) |\Delta^{31}_R|^2 \tan^6\beta \right]. \tag{6}$$

Taking $\Delta^{31}_R \simeq 5 \cdot 10^{-4}$ accordingly to what said above, $\tan\beta = 40$ and $M_H = 500 GeV$ we end up with $R^{LFV}_K \simeq R^{SM}_K (1 + 0.013)$. Turning to pion physics, one could wonder whether the analogous quantity $\Delta r^{e-\mu}_{\pi\, SUSY}$ is able to constrain SUSY LFV. However, the correlation $\Delta r^{e-\mu}_{\pi\, SUSY} \leq (m^4_\pi / m^4_k) \Delta r^{e-\mu}_{K\, SUSY} < 10^{-4}$ clearly shows that the constraints on $\Delta r^{e-\mu}_{K\, susy}$ force $\Delta r^{e-\mu}_{\pi\, susy}$ to be much below its actual experimental upper bound. LFV effects to $\Delta r^{e-\mu}_{K\, SUSY}$ at the per cent level are allowed by the experimental bounds on LFV tau decays ($Br(\tau \to l_j X) \leq 10^{-7}$, with $X = \gamma, \eta, \mu\mu$). In fact, $\Delta r^{e-\mu}_{K\, SUSY}$ at the percent level corresponds to $Br(\tau \to eX) \leq 10^{-10}$ [9]. The above SUSY dominant contribution to $\Delta r^{e-\mu}_{NP}$ increases the value of R_K with respect to the SM expectation. On the other hand, the recent NA48/2 result exhibits a central value

lower than R_K^{SM}. One may wonder whether SUSY could account for such a lower R_K. Obviously, the only way it can is through terms which, contributing to the LFC $K \to l\nu_l$ channels, can interfere (destructively) with the SM contribution. One can envisage the possibility of making use of the large LFV contributions to give rise to LFC ones through double LFV mass insertions in the scalar lepton propagators. The corrections to the LFC $H^{\pm} l \nu_l$ vertices induced by LFV effects are:

$$l H^{\pm} \nu_l \to \frac{g_2}{\sqrt{2}} \frac{m_l}{M_W} \tan\beta \left(1 + \frac{m_\tau}{m_l} \Delta_{RL}^{ll} \tan\beta\right) \quad l = e, \mu \tag{7}$$

where the second term is generated by a double LFV source that, as a final effect, preserves the flavour. Indeed Δ_{RL}^{ll} is proportional to $\delta_{RR}^{l3} \delta_{LL}^{3l}$. In the large slepton mixing case, Δ_{RL}^{ll} terms are of the same order of Δ_R^{3l}. These new effects modify the previous R_K^{LFV} expression in the following way:

$$R_K^{LFV} \simeq R_K^{SM} \left[\left| 1 - \frac{m_K^2}{M_H^2} \frac{m_\tau}{m_e} \Delta_{RL}^{11} \tan^3\beta \right|^2 + \left(\frac{m_K^4}{M_H^4}\right)\left(\frac{m_\tau^2}{m_e^2}\right) |\Delta_R^{31}|^2 \tan^6\beta \right]. \tag{8}$$

Setting the parameters as in the example of the above section and if $\Delta_{RL}^{11} = 10^{-4}$ we get $R_K^{LFV} \simeq R_K^{SM}(1 - 0.032)$.

3 $\tau - e(\mu)$ universality in $B \to \ell\nu$ decays

The results of the above section can be easily applied also to the case of charged B mesons, namely to the $B \to \ell\nu$ (with $\ell = e, \mu, \tau$) processes. Defining a total decay rate including LFV channels $\Gamma_{LFV}^{(B\to\ell\nu)} = \sum_i \Gamma(B \to \ell\nu_i)$ (with $i, \ell = e, \mu, \tau$), we obtain the following expressions [11]:

$$\frac{\Gamma_{LFV}^{(B\to l\nu_i)}}{\Gamma_{SM}^{B\to l\nu_l}} \simeq \left[r_H + \left(\frac{m_B^4}{M_{H^\pm}^4}\right)\left(\frac{m_\tau^2}{m_l^2}\right) |\Delta_R^{3l}|^2 \tan^6\beta \right] \qquad \frac{\Gamma_{LFV}^{(B\to\tau\nu_i)}}{\Gamma_{SM}^{B\to\tau\nu_\tau}} \simeq r_H. \tag{9}$$

$B \to \tau\nu$ can not receive sizable LFV contributions due to the absence of any Yukawa enhancement. In the most favorable scenarios, taking into account the constraints from LFV τ decays [9, 10], spectacular order-of-magnitude enhancements for the e channel and $O(1)$ deviations from the SM in the μ channel can be expected:

$$\Gamma_{LFV}^{B\to\mu\nu_\tau} \leq 0.5 \cdot \Gamma_{SM}^{B\to\mu\nu_\mu}, \qquad \Gamma_{LFV}^{B\to e\nu_\tau} \leq 2 \cdot 10^4 \cdot \Gamma_{SM}^{B\to e\nu_e}. \tag{10}$$

On the other hand, it turns out that there exists a strict correlation between $B \to e\nu_\tau$ and $\Delta r^{e-\mu}_{K\,Susy}$ so that:

$$\frac{\Gamma^{(B\to e\nu_\tau)}_{LFV}}{\Gamma^{B\to e\nu_e}_{SM}} \simeq \left[r_H + \frac{m_B^4}{m_K^4} \Delta r^{e-\mu}_{K\,Susy} \right] \leq 2 \cdot 10^2, \tag{11}$$

As shown, $\Delta r^{e-\mu}_{K\,Susy}$ is much more effective to constrain $\Gamma(B \to e\nu_\tau)$ than LFV tau decay processes. If the experimental resolution on $\Gamma(B \to e\nu)$ will be increased and if a signal will be observed beyond SM prediction then, this would be clear evidence that some new processes are generating the $B \to e\nu$ decay, with Higgs mediation being a leading candidate. Moreover, it is noteworthy that we would be enforced to conclude that only LFV effects may concur to that enhancement. At the same time, we do not expect so large LFV effects in $B \to \mu\nu$. However, given that $B \to \tau\nu$ is not affected by sizable LFV effects, it is convenient to define the $R^{\ell/\tau}_{LFV} = \Gamma^{(B\to\ell\nu)}_{LFV}/\Gamma^{(B\to\tau\nu)}_{LFV}$ (with $\ell = e, \mu$) ratio that takes into account the deviation from the $\ell - \tau$ lepton universality without loosing information about LFV effects. In this way, both the decay coupling constant f_B and the matrix element V_{ub} (the major source of uncertainty within the SM prediction) cancel in $R^{\ell/\tau}_{LFV}$ so that $R^{\ell/\tau}_{LFV}$ represents the most powerful tool to disentangle new physics effects in the above processes. Finally, we remark that a key ingredient of all the effects discussed in the present work are large $\tan\beta$ values so, it is legitimate to ask how natural is this framework. The regime of large $\tan\beta$ [$\tan\beta = (m_t/m_b)$] has an intrinsic theoretical interest since it allows the unification of top and bottom Yukawa couplings, as predicted in well-motivated grand-unified models. Moreover, as recently discussed in [11], this scenario is particularly appealing also from a phenomenological point of view. In fact, in this framework, one could naturally accommodate the present (non-standard) central values of both $BR(B \to \tau\nu)$ and $(g-2)_\mu$, explain why the lightest Higgs boson has not been observed yet, and why no signal of new physics has been observed in $BR(B \to X_s\gamma)$ and ΔM_{B_s} without requiring any fine tuning. So, one of the virtues of the large $\tan\beta$ regime of the MSSM is its naturalness in flavor physics and in precise electroweak tests.

4 Rare K decays: $K \to \pi\nu\bar{\nu}$

The strong suppression within the Standard Model (SM) and the high sensitivity to physics beyond the SM of the two $K \to \pi\nu\overline{\nu}$ rates, signal the unique

possibilities offered by these rare processes in probing the underlying mechanism of flavour mixing. This statement has been reinforced by the recent theoretical progress in the evaluation of NNLO [12] and power-suppressed [14] contributions to $K^+ \to \pi^+ \nu\overline{\nu}$. These allow to obtain predictions for the corresponding branching ratio of high accuracy ($\sim 6\%$), not far from the exceptional level of precision ($\sim 2\%$) already reached in the $K_L \to \pi^0 \nu\overline{\nu}$ case [15, 16].

Within the MSSM, sizable non-standard contributions to $K \to \pi\nu\overline{\nu}$ decays can be generated only going beyond the so-called Minimal Flavour Violation (MFV) hypothesis [17] and are mediated or by the exchange of chargino/up-squark loops [18] or by charged Higgs/top-quark loops [19]. In the first case, large effects are generated only if the left-right mixing of the up squarks has a flavour structure substantially different from the MFV hypothesis. In the second case, deviations from the SM expectations are induced by the presence of off-diagonal mixing terms in the right-right down squark sector (with sizable effects even for tiny, CKM-type, mixing) but only for large values of $\tan\beta$.

The dimension-six effective Hamiltonian relevant for $K^+ \to \pi^+ \nu\bar{\nu}$ and $K_{\rm L} \to \pi^0 \nu\bar{\nu}$ decays in the general MSSM can be written as:

$$\mathcal{H}_{\rm eff} = \frac{G_{\rm F}}{\sqrt{2}} \frac{\alpha}{2\pi} \sin^2\theta_{\rm w} \left[\mathcal{H}_{\rm eff}^{(c)} + \mathcal{H}_{\rm eff}^{(s.d.)} \right] \; + \; \text{h.c.} \tag{12}$$

where $\mathcal{H}_{\rm eff}^{(c)}$ denotes the operators which encode physics below the electroweak scale (in particular charm quark loops) and are fully dominated by SM contributions [12], while

$$\mathcal{H}_{\rm eff}^{(s.d.)} = \sum_{l=e,\mu,\tau} V_{ts}^* V_{td} \left[X_L (\bar{s}d)_{V-A} (\bar{\nu}_l \nu_l)_{V-A} + X_R (\bar{s}d)_{V+A} (\bar{\nu}_l \nu_l)_{V-A} \right] \tag{13}$$

denotes the part of the effective Hamiltonian sensitive to short-distance dynamics.

Within the Standard Model $X_R = 0$ and X_L is a real function (thanks to the normalization with the CKM factor $V_{ts}^* V_{td} \equiv \lambda_t$) [15, 12]:

$$X_L^{\rm SM} = 1.464 \pm 0.041 \; . \tag{14}$$

Within the MSSM, in general both X_R and X_L are not vanishing, and the misalignment between quark and squark flavour structures implies that are both complex quantities. Since the $K \to \pi$ matrix elements of $(\bar{s}d)_{V-A}$ and

$(\bar{s}d)_{V+A}$ are equal, the following combination

$$X = X_L + X_R \tag{15}$$

allows us to describe all the short-distance contributions to $K \to \pi\nu\overline{\nu}$ decays. In terms of this quantity the two branching ratios can be written as:

$$\mathcal{B}(K^+ \to \pi^+\nu\bar{\nu}) = \kappa_+ \left[\left(\frac{\mathrm{Im}(\lambda_t X)}{\lambda^5} \right)^2 + \left(P_{(u,c)} + \frac{\mathrm{Re}(\lambda_t X)}{\lambda^5} \right)^2 \right] , \tag{16}$$

$$\mathcal{B}(K_{\mathrm{L}} \to \pi^0\nu\bar{\nu}) = \kappa_L \left(\frac{\mathrm{Im}(\lambda_t X)}{\lambda^5} \right)^2 , \tag{17}$$

where $\lambda = |V_{us}| = 0.225$, the κ-factors are $\kappa_+ = (4.84 \pm 0.06) \times 10^{-11}$ and $\kappa_L = (2.12 \pm 0.03) \times 10^{-10}$ [15], and the contribution arising from charm and light-quark loops is $P_{(u,c)} = 0.41 \pm 0.04$ [12, 14].

In the limit of almost degenerate superpartners, the chargino/up-squarks contribution is given by the following expression [18]:

$$\left(X_{\mathrm{eff}}^{\chi^\pm} \right)_L = \frac{1}{96} \left[\frac{(\delta^{up}_{LR})_{23} (\delta^{up}_{RL})_{31}}{\lambda_t} \right] \tag{18}$$

while the charged Higgs/top-quark exchange leads to [19]:

$$\left(X_{\mathrm{eff}}^{H^\pm} \right)_R \simeq \left[\frac{(\delta^d_{RR})_{31} (\delta^d_{RR})_{32}}{\lambda_t} \right] \left(\frac{m_b^2 \tan^2\beta}{2M_W^2} \right) \left(\frac{\alpha_s}{9\pi} \right)^2 \frac{\tan^2\beta}{(1 \pm \frac{\alpha_s}{3\pi} \tan\beta)^4} \frac{y_{tH}}{4} \log(y_{tH}) \tag{19}$$

where the above expression is obtained in the limit where $y_{tH} = m_t^2/M^2_{H^\pm} \ll 1$ and the $\pm$ sign in Eq. (19) refers to $\pm\mu$, μ being the Higgs mixing mass term. The effects of the above contributions are examined separately in Fig. (1) where

Table 1: Basic choice of the flavour-conserving parameters used in Fig. 1.

Charginos:	$\mu = 500 \pm 10$ GeV	$M_2 = 300 \pm 10$ GeV	$\tan\beta = 2$–4
Up-squarks:	$M_{\tilde{u}_R} = 600 \pm 20$ GeV	$M_{\tilde{q}_L} = 800 \pm 20$ GeV	$A_0 = 1$ TeV
Other mass terms:	$M_1 = 500$ GeV	$M_{\tilde{d}_R} = M_{\tilde{l}} = M_3 = M_{H^+} = 2$ TeV	

the constraints of B physics observables (that are sensitive to same SUSY parameters) are also reported. In case of chargino induced contributions, we choice the parameters reported in Tab.1.

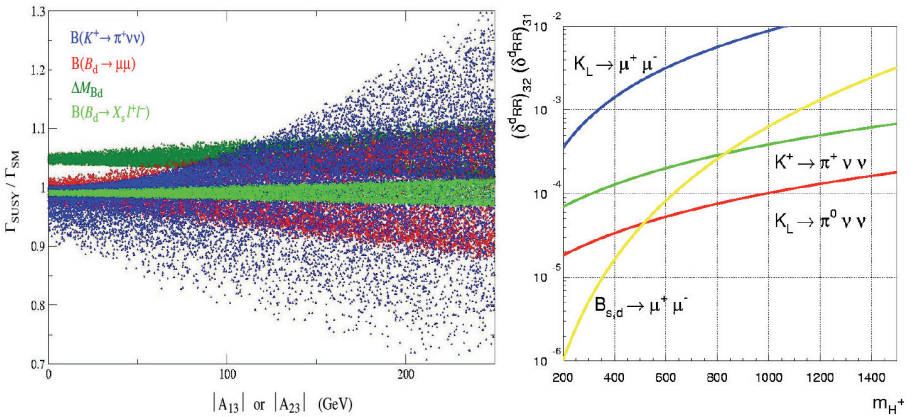

Figure 1: On the left it is shown the dependence of various FCNC observables (normalized to their SM value) on the up-type trilinear terms A_{13} and A_{23} imposing $A_{ij} \leq \lambda A_0$. The flavour-conserving parameters of the model are fixed as specified in Table 1. On the right it is shown the sensitivity to $(\delta^d_{RR})_{23}(\delta^d_{RR})_{31}$ of various rare K and B decays as a function of the charged-Higgs boson mass setting $\tan\beta = 50$, $\mu < 0$ and assuming almost degenerate superparteners. The bounds from the two $K \to \pi\nu\bar{\nu}$ modes are obtained under the assumption of 10% error in the measurement of their branching ratios while the $B_{s,d} \to \mu^+\mu^-$ bounds refer to the latest experimental limits [20].

As shown in Fig. (1), large departures from the SM expectations are allowed in both of the examined scenarios.

5 Conclusions

In this work, we have first discussed the important role played by the study of the lepton universality to probe new physics. In particular, a precise measurement of the flavor conserving K_{l2} decays may shed light on the size of LFV in new physics. Moreover, as a future perspective, we have also discussed the possibility to observe large violations of lepton universality in the B physics, namely in the ratios $BR(B \to \mu\nu)/BR(B \to \tau\nu)$ and $BR(B \to e\nu)/BR(B \to \tau\nu)$ as a particularly interesting tool to find non standard effects. Finally, we have outlined the main SUSY contributions to $K \to \pi\nu\bar{\nu}$ pointing out that large departures from the SM expectations are possible in two different scenarios beyond the Minimal Flavour Violation (MFV) hypothesis.

Acknowledgments

I thank G. Isidori and F. Mescia for useful discussions.

References

1. W.J. Marciano and A. Sirlin, Phys.Rev.Lett. 71 3629 (1993); M.Finkemeier, Phys.Lett. B 387 391 (1996).
2. S.Eidelman et al. (Particle Data Group), Phys. Lett. B 592, 1 (2004).
3. L.Fiorini, for the NA48/2 Collaboration at ICHEP 2005.
4. K.S. Babu and C. Kolda, Phys.Rev.Lett.**89**, 241802 (2002).
5. W.S.Hou, Phys. Rev. D 48, 2342 (1992).
6. A. Brignole and A. Rossi, Phys. Lett. B 566, 217 (2003); A. Brignole and A. Rossi, Nucl. Phys. **B 701**, 3 (2004).
7. A. Masiero, P. Paradisi and R. Petronzio, [arXiv:hep-ph/0511289].

8. M. Sher, Phys. Rev. D 66, 057301 (2002); R. Kitano, M. Koike, S. Komine and Y. Okada, Phys. Lett. B 575, 300 (2003); A. Dedes, J. R. Ellis and M. Raidal, Phys. Lett. **B 549**, 159 (2002); E. Arganda, A. M. Curiel, M. J. Herrero and D. Temes, Phys. Rev. D 71, 035011 (2005).

9. P. Paradisi, JHEP **0602**, 050 (2006); P. Paradisi, [arXiv:hep-ph/0601100].

10. P. Paradisi, JHEP **0510** (2005) 006.

11. G. Isidori and P. Paradisi, arXiv:hep-ph/0605012.

12. A. J. Buras, M. Gorbahn, U. Haisch and U. Nierste, hep-ph/0508165; hep-ph/0603079.

13. G. Buchalla and A. J. Buras, Nucl. Phys. **B548** (1999) 309; M. Misiak and J. Urban, Phys. Lett. **B451** (1999) 161.

14. G. Isidori, F. Mescia and C. Smith, Nucl. Phys. **B718** (2005) 319.

15. A. J. Buras, F. Schwab and S. Uhlig, hep-ph/0405132; D. Bryman, A. J. Buras, G. Isidori, L. Littenberg, Int. J. Mod. Phys. A **21** (2006) 487.

16. G. Buchalla and G. Isidori, Phys. Lett. **B440** (1998) 170.

17. L. J. Hall and L. Randall, Phys. Rev. Lett. **65** (1990) 2939; G. D'Ambrosio, G. F. Giudice, G. Isidori and A. Strumia, Nucl. Phys. **B645** (2002) 155.

18. G. Colangelo and G. Isidori, JHEP **09** (1998) 009; G. Isidori, F. Mescia, P. Paradisi, C. Smith and S. Trine, [arXiv:hep-ph/0604074].

19. G. Isidori and P. Paradisi, Phys. Rev. D **73**, 055017 (2006).

20. R. Bernhard *et al.* [CDF Collaboration], hep-ex/0508058.

OPENING REMARKS

Frascati Physics Series Vol. XLI (2006), pp. 101-108
DISCOVERIES IN FLAVOUR PHYSICS AT e^+e^- COLLIDERS
Frascati, February 28th - March 3rd, 2006

THE BATTLE OF ALBUERA, THE FC LIVERPOOL AND THE STANDARD MODEL

Ikaros I. Bigi
Physics Dept., University of Notre Dame du Lac, Notre Dame, IN 46556, U.S.A.
email: ibigi@nd.edu

Abstract

The Standard Model despite its well-known short comings is unlikely to yield without offering stubborn resistance. There are compelling arguments that New Physics lurks around the TeV scale. Continuing comprehensive studies of beauty, τ and charm transitions can be instrumentalized to reveal it and shed light on it. They are thus complementary to findings obtained at the LHC and presumably essential in clarifying the true nature of that New Physics. A Super-B facility seems to provide the cleanest environment for pursuing such an ambitious program. I list desirable features of such a setup as well as challenges for the accelerator and detector designs and for the theoretical analysis.

1 The Verdict on the SM

After losing the battle of Albuera in 1811 Marechal Soult declared: "I had beaten the British – it was just they did not know when they were beaten."

Soult was actually one of Napoleon's best generals, and experts agree he was right on both counts. For those with a much shorter memory span one can point to a similar experience just last year: at halftime in the finals of the European Champions League AC Milano was leading FC Liverpool 3:0 with truly gorgeous play, yet the pesky Brits while still being outplayed in the second half – except for those magic eight minutes – refused to concede.

This is the story as well with the Standard Model (SM): We all know how to design an extension to the SM that is greatly superior to it – now we have to overcome the SM's refusal to concede defeat.

Even in the last few years since the turn of the millenium the SM has scored unprecedented successes in flavour physics: CKM dynamics describe a vast array of very diverse phenomena culminating in **CP** violation as observed in particle decays as CKM's signature achievement. Yet we are in search of a 'New **CP** Paradigm': for we know that CKM dynamics is grossly inadequate for baryogenesis, which posits the observed baryon number of the Universe as a *dynamically generated* quantity rather than an *initial input value*. There are further shortcomings of the SM as revealed mostly by heavenly data: (a) ν oscillations; (b) 'dark matter'; (c) 'dark energy'.

In addition there are serious explanatory deficits of a general nature (I am even not including the so far unresolved 'Strong **CP** Problem'):

(i) *Electroweak Symmetry Breaking and the Gauge Hierarchy*: What are the dynamics driving the electroweak symmetry breaking of $SU(2)_L \times U(1) \to U(1)_{QED}$? How can we tame the instability of Higgs dynamics with its quadratic mass divergence? I find the arguments compelling that point to New Physics at the ~ 1 TeV scale – like low-energy SUSY; therefore I call it the 'confidently predicted' New Physics or **cpNP**.

(ii) *Quantization of electric charge*: While electric charge quantization $Q_e = 3Q_d = -\frac{3}{2}Q_u$ is an essential ingredient of the SM – it allows to vitiate the Adler-Bell-Jackiw or triangle anomaly – it does not offer any understanding. It would naturally be explained through Grand Unification at very high energy scales implemented through, e.g., $SO(10)$ gauge dynamics, where leptons and quarks are placed in the same multiplet. I call this the 'guaranteed New Physics' or **gNP**.

(iii) *Family Replication and CKM Structure*: We infer from the observed width of Z^0 decays that there are three (light) neutrino species. The hierar-

chical pattern of CKM parameters as revealed by the data is so peculiar as to suggest that some other dynamical layer has to underlie it. I refer to it as 'strongly suspected New Physics' or **ssNP**. We are quite in the dark about its relevant scales. Saying we pin our hopes for explaining the family replication on Super-String or M theory is a scholarly way of saying we have hardly a clue what that **ssNP** is.

2 On Finding What Drives the Electroweak Symmetry Breaking

The next big challenge to which we have to rise is to find *and identify* the **cpNP**. It has provided the justification for the LHC and drives the motivation for the ILC – an excellent one in my view.

Let me make two judgment calls. While I have reflected on them, I understand that reasonable people can honourably disagree.

- Any future facility has to be justified by its ability *to find New Physics and identify its salient features* – learning new lessons on QCD will no longer suffice. This applies also to a new τ-charm factory *beyond* BESIII.
- Heavy flavour studies *might* provide insights into questions **(ii)** & **(iii)** listed above – but we cannot *count* on it. Therefore we can*not* justify a new facility with such a hope.

Instead I advocate *instrumentalizing* studies of flavour dynamics as expressed below through five statements:

1. *Comprehensive and detailed* heavy flavour studies will be *crucial in identifying* the **cpNP**.
2. I remain skeptical that studies in hadroproduction can be fully competitive with those at e^+e^- machines in τ, charm and even beauty transitions as far as precision and comprehensiveness are concerned.

   In this context I want to emphasize that B_d and B_s decays represent truly different, yet complementary chapters in 'Nature's Book on Fundamental Dynamics'.
3. A Super-B factory allows comprehensive precision studies of B, τ and charm decays. A very detailed plan for such a project has been developed by the KEKB team [1)].

4. To be competitive in τ & charm studies a *future* τ-charm factory has to be of the Super-τ/charm variety, i.e. with a luminosity of at least $10^{34} cm^{-2} s^{-1}$.

5. I am convinced that a compelling justification for a Super-B facility can be given – yet one cannot merely follow the lines of argument given originally in favour of a B factory. There

   - one had so-called 'killer-applications', namely **CP** violation in $B_d \to \psi K_S$, $\pi^+\pi^-$ and $K\pi$
   - with predictions of reasonable accuracy
   - requiring a luminosity in the $(10^{33} - 10^{34}) cm^{-2} s^{-1}$ range.

   While history repeats itself, it never does so in an identical fashion. For a Super-B project we face a fundamentally different 'landscape':

   - We can*not count* on killer applications.
   - We can*not count* on a *numerically* massive intervention by New Physics.
   - 'Merely' finding New Physics is *not* enough – we must identify its salient features.
   - There is no clear benchmark for the needed luminosity.
   - Thus our guidance has to come from what – rather unkindly – has been referred to as the 'Wall Street mantra of greed': "Lots is good, more is better, aim for the sky!"

   There are basically two kinds of research:

- One has a more or less well-developed theoretical framework, where one has at least clarified the categories of relevant questions. Answering those (with the help of experiment) can be called '*hypothesis-driven*' research. In that case one has always something to show for one's efforts. Not surprisingly such projects are most popular with funding agencies.

- Alternatively one has a situation that is unsatisfactory in a conceptual or even phenomenological way, yet with no compelling theory candidate to

fill the gap. Without such guidance one performs '*hypothesis-generating*' research in the hope that more analyses will point to a new paradigm. Such work thus has the potential to lead to a revolution – alas funding agencies display markedly less enthusiasm for it.

The program at the B factories has *primarily* been of the *hypothesis-driven* variety – and a most successful one at that. Yet at a Super-B factory (with τ and charm) we have to conduct *hypothesis-generating* research with one of the goals being the search for the 'New **CP** Paradigm'.

3 Challenges for a Super-B Facility

Precision in acquiring and interpreting data is essential if we want to draw the desired lessons from heavy flavour studies. The 'conditio sine qua non' is to have huge statistics of comprehensive high quality data. A large body of well measured transitions is more important than a few rates determined with infinite precision.

There is the (in)famous challenge from Sanda: "We need a luminosity of $10^{43} cm^{-2} s^{-1}$!" While it is certainly 'tongue-in-cheek', it is not just frivolous; it has more than a kernel of truth, in particular when combined by Sanda's empirical conjecture that every second '3 sigma' effect goes away.

Yet, as already stated, statistics is not all. For the goal of a Super-B facility has to go beyond 'doing more of the same'. We need not only more data, but also data of a different and higher quality. New observables have to be opened up to detailed study. This requires a hermetic detector operating in a low background environment with superb μvertex resolution. This would allow to study transitions like $B \to \tau\nu$, $\tau^+\tau^-$l, $\tau\nu X$, $\nu\bar{\nu}X$ and $B \to \gamma X_s$ vs. γX_d.

Also energy flexibility would be very desirable, i.e. to study $\Upsilon(5S) \to B_s\bar{B}_s$ and even $\psi(3770) \to D\bar{D}$ etc. in addition to $\Upsilon(4S) \to B\bar{B}$.

Finally it would be quite desirable to have a *polarized* electron beam available. It would lead to the production of polarized τ leptons and probably also of polarized charm baryons. This polarization would be a powerful tool to enhance the sensitivity to **CP** violation in the decays of those states; at the same time it would help to control systematics.

The area around Rome has an ancient history of superbly engineered and

Figure 1: *A prominent linear machine near Rome.*

long lasting linear structures, see Fig.1. The stated aim for an 'ILC inspired' Super-B facility [2] is to achieve a luminosity of $10^{36} cm^{-2} s^{-1}$ (or more) with tiny beams and a hermetic detector, maybe even with a polarized beam, 'soon' and 'here', i.e. near Rome.

Life teaches us all too often that if something is too good to be true – it usually is. Is it in this case? Keep in mind we cannot afford failure.

4 Questions and Challenges

Let me pose to you some questions that I would like to see addressed – or better still answered – at the workshop or in the near future.

- What integrated luminosity can be achieved at a Super-B factory by 2016, i.e after mature data taking has taken place at the LHC, and by 2020, when a realistic optimist can hope for the ILC to begin running?
- How and when can the feasibility of the linear Super-B concept be established?
- What will be the quality of the $e^{\pm}$ beams, and how hermetic can the detector be?

Figure 2: *An allegory on HEP's future landscape.*

- What kind of integrated luminosity can be achieved in, say, a two year run at the $\Upsilon(5S)$ run?
- How many *precision* measurements can be made by (an upgraded) LHCb?
- Can (an upgraded) LHCb do competitive **CP** studies in charm transitions?
- How feasible is a Super-τ-Charm factory with $(10^{34} - 10^{35})cm^{-2}s^{-1}$, and what is its price tag? Would it be competitive with respect to **CP** searches in τ decays?
- While the items listed so far mainly concern experimental and technical issues, there is a lot to be done by interested theorists as well: to identify the features of the conjectured New Physics one has to state the required
  - benchmark observables [1];
  - benchmark accuracy and
  - validation checks for establishing control over theoretical uncertainties.

  It is also crucial to interpret findings from the LHC – including 'no-shows'.

and hopefully the ILC; those landmarks are represented by the two rocks on the picture. I believe there is still some pathway left between them for dedicated studies at a Super-Flavour facility as indicated by the gap between the two rocks. Heavy flavour studies thus resemble a passage between Scylla and Charybdis. It requires a crew and a skipper that combine experience with some daring to navigate through this strait – where can we find them?

References

1. See Letter of Intent at http://belle.kek.jp/superb/.
2. See INFN Roadmap Report at http://arxiv.org/abs/physics/0512235.

Frascati Physics Series Vol. XLI (2006), pp. 109-118
DISCOVERIES IN FLAVOUR PHYSICS AT e^+e^- COLLIDERS
Frascati, February 28th - March 3rd, 2006

THE ROLE OF THE LHC IN THE FLAVOUR ERA

Michelangelo L. Mangano
Physics Department, Theoretical Physics, CERN

Abstract

I shall give a brief and selective overview of the LHC discovery potential, concentrating on two possible direct probes of BSM phenomena of relevance to flavour: the top quark, and supersymmetry.

1 Introduction

In the Summer 2007 the Large Hadron Collider (LHC) will start colliding protons at $\sqrt{S} = 14$ TeV. There is great and fully justified expectation that the data provided by the LHC will significantly improve our understanding of Nature. Exposing the mechanism of electroweak symmetry breaking (EWSB), and identifying the Higgs boson or its alternatives, will be the first and most important goal. The Standard Model (SM), which has been tested very accurately in the recent years, defines without ambiguity the mechanism which

brings the Higgs boson to existence. There are nevertheless good reasons for theorists to suspect that physics *beyond* the SM (BSM) should play a key role in the dynamics of EWSB [1]. If that is the case, one expects that the findings of the LHC will help physicists move towards an understanding of the next layer of fundamental questions in high-energy physics:

- What is Dark Matter (DM)?
- What is the orgin of the family structure of the SM and of their properties (mass spectra, mixing patterns)?
- What is the origin of neutrino masses, and why are they so small compared to those of the other known particles?
- What is the origin of the baryon asymmetry of the universe (BAU)?
- Why $SU(3) \otimes SU(2) \otimes U(1)$?
- ...

We tend to associate today the origin of the SM with the gauge principle and the consolidation of Yang-Mills interactions as unitary and renormalizable quantum field theories. We often forget that flavour phenomena have contributed as much as the gauge principle, if not more, in shaping the overall structure of the SM. It is the existence of flavours (both in the lepton and quark sector) which gives the SM its family and generation structure. Assembling quarks in EW doublets is a result of the suppression of flavour-changing neutral currents (FCNCs), which led to the GIM mechanism and to the prediction of the charm quark. Kaon decays led to the observation of CP violation, and to the CKM model. B_d mixing, similarly to the role played by $K^0 - \bar{K}^0$ mixing in getting the mass range for charm, was the first experimental phenomenon which correctly anticipated the large value of the top quark mass. And, last but not least, the observation of neutrino masses provides the first concrete and uncontroversial evidence that the SM is incomplete: most modestly, we need to introduce degrees of freedom for sterile right-handed neutrinos; more ambitiously, neutrino masses are a window on physics at the grand unification scale!

It is remarkable that most of the questions listed above have flavour at their core, and it is therefore reasonable to expect that flavour physics will continue playing a crucial role in the progress of HEP. In particular, there

are several elements which directly associate the phenomena related to EWSB with flavour issues. The most obvious link is that it is precisely EWSB which exposes flavour phenomena: in absence of EWSB, all fermions would be degenerate, and no flavour effect would be manifest. Secondly, flavour properties provide important constraints on building models of EWSB beyond the SM: technicolour theories are strongly constrained by their typically large rates of FCNC; extra-dimensional models for EWSB link the fermionic mass spectrum to properties of the extra dimensions; little-Higgs theories require the existence of new fermions, like a massive partner of the top quark; in supersymmetric theories EWSB can be generated dynamically thanks to the large value of the top quark mass, making EWSB, in some sense, a flavour-driven phenomenon. The numerical coincidence of the top mass value with the scale of EWSB, which leads to a value of the top Yukawa coupling equal to 1 within a few percent, is yet another misterious hint of a possible direct connection between EWSB and flavour. And, last but not least, at least two of the three outstanding experimental evidences for BSM physics (DM, the BAU and neutrino masses), have an explicit connection with flavour.

In the SM, flavour physics deals with the fermionic sector. All flavour phenomena are encoded in the fermion Yukawa matrices. Beyond the SM, flavour phenomena may cover a much wider landscape: FCNCs can be mediated, for example, by gauge-sector particles, like charged Higgs bosons, gauginos, new gauge bosons, or by scalar supersymmetric partners of the SM fermions. In addition, new flavours can be expected in the form of new generations, exotic particles of standard quarks (e.g. Kaluza-Klein excitations), etc. The role of the LHC, therefore, will be to provide evidence for such new states, and to trigger and motivate further measurements to be performed with the more standard experimental tools for flavour physics: the e^+e^- factories discussed at this Workshop, fixed-target high-intesity kaon studies, $\mu \to e\gamma$ searches, electric dipole moment searches, neutrino mass and mixing measurements, etc. The coincidence of several independent inputs from all these facilities will most likely be the necessary ingredient for a deeper understanding of the key questions of HEP. In this presentation, I shall give a brief and selective overview of the LHC discovery potential, concentrating on two possible direct probes of BSM phenomena of relevance to flavour: the top quark, and supersymmetry.

Table 1: *Expected sensitivity to anomalous top couplings at the LHC.*

1-σ limits	min	max
V_R	-0.10	0.16
g_L	-0.08	0.05
g_R	-0.02	0.02

2 Top quark properties

The top quark has been discovered already since more than 10 years, but its properties have not yet been studied in much detail. The small cross-section for $t\bar{t}$ production at the Tevatron has allowed so far only collecting of the order of few hundred events. Large backgrounds, and the difficulty in reconstructing uniquely the overall kinematics of the event, limit the ability to determine with good accuracy its EW couplings [2]. The absolute strength of the tbW coupling can only be probed through single top production, a process which has still not been observed [3]. In view of the key role played by the 3rd generation in flavour physics, a more thorough examination of top properties will be one of the first goals of the LHC. The production rate will be over 100 times larger than at the Tevatron, and the S/B ratio will significantly improve, both because of a reduced relative rate of W+jets events, and because of the possibility to set much harder selection cuts. The study of angular distributions in the top decay will then allow to set interesting limits (see Table 1) to the existence of possible anomalous contributions to the tbW vertex, which can be parametereized in general as:

$$\begin{aligned} \mathcal{L} \;=\; & -\frac{g}{\sqrt{2}}\bar{b}\gamma^{\mu}\left(V_L P_L + V_R P_R\right) t\, W^{-}_{\mu} \\ & -\frac{g}{\sqrt{2}}\,\bar{b}\,\frac{i\sigma^{\mu\nu}\,q_{\nu}}{M_W}\left(g_L P_L + g_R P_R\right) t\, W^{-}_{\mu} + \text{h.c.}\,, \end{aligned} \tag{1}$$

where $P_{L,R} = (1 \mp \gamma_5)/2$. The impact of these limits on various BSM models is under study.

The large production rates will allow probing rare FCNC decays at a level consistent with what predicted by some BSM models, as shown in Table 2.

While the Tevatron experiments are expected to soon detect single top production, accurate studies will have to wait the LHC. An example of the LHC potential to explore or constrain BSM models is given in fig. 1, where

Table 2: *Expected sensitivity to FCNC top decays at the LHC, with the expected SM rates, the current limits, and the rates allowed in some BSM models (2-Higgs doublet models, SUSY with R-parity violation, exotic quarks).*

BR	SM	2HDM	RPV	exotic Q	Today	LHC
$t \to qZ$	10^{-13}	$\leq 10^{-6}$	$\leq 10^{-4}$	$\leq 10^{-2}$	≤ 0.08 (LEP)	$\leq 6.5 \times 10^{-5}$
$t \to q\gamma$	10^{-13}	$\leq 10^{-7}$	$\leq 10^{-5}$	$\leq 10^{-5}$	≤ 0.003 (HERA)	$\leq 1.8 \times 10^{-5}$
$t \to qg$	10^{-11}	$\leq 10^{-5}$	$\leq 10^{-3}$	$\leq 10^{-4}$	≤ 0.29 (CDF)	$\leq 4.3 \times 10^{-4}$

the SM value of the s- and t-channel cross-sections, and the accuracy of the respective LHC measurements, are compared with the expectations in some exotic models [4].

3 Supersymmetry searches

Supersymmetry (SUSY) is the most compelling scenario for physics BSM. Its discovery, should it exists, represents the single most important goal of the LHC after the detection of the Higgs boson. The existence of SUSY may have dramatic consequences for flavour physics. The new scalar partners of quarks and leptons will come with their own mass matrices and mixings, leading to a full range of new flavour-mixing phenomena [5]. The extended Higgs sector of SUSY may contribute with new sources of CP violation. The flavour and CP consequences of SUSY could be probed, via virtual effects, by the next generation of flavour factories: e^+e^- collisions and K and μ facilities. The observation of new flavour phenomena, however, could also be detected at the LHC through the direct observation and study of the new particles. It is in this domain that the complementarity and synergy of the LHC and flavour factories might emerge as a driving theme of HEP in the next decade. A complete review of the LHC potential in this area is being explored in the course of a dedicated 1-year long Workshop, dedicated to the role of "Flavour in the LHC era" [6]. A preliminary assessment, based on material already available from several years of study by the LHC collaborations, was reviewed at the Workshop by Polesello [7]. Because of the limited space available, I shall limt myself here to few examples taken from the study of slepton searches.

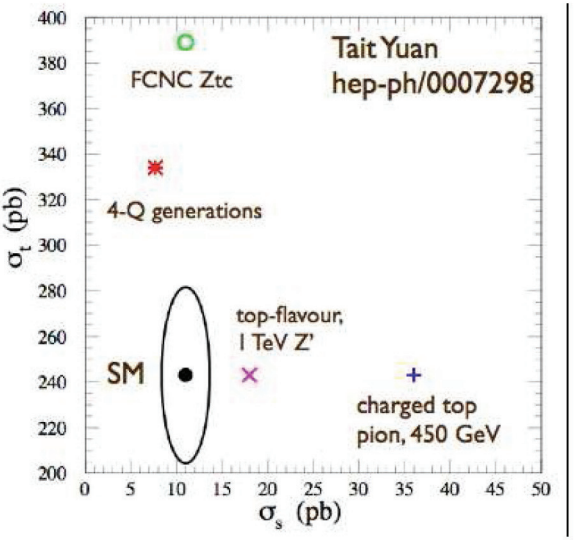

Figure 1: *Experimental accuracy in the determination of the s-channel (σ_s) and t-channel (σ_t) single top production rates, compared with the predictions of some exotic models.*

3.1 Slepton reconstruction

The observation of neutrino masses and mixings indicates that the leptonic sector of the SM hides a potentially rather interesting and surprising phenomenology. The large mixing between 2nd and 3rd generation is at odds with the mixing patterns observed in the quark sector. In the context of SUSY models, the scalar neutrinos could inherit some of the features of their light partners, and share them with the scalar charged leptons [8].

The properties of scalar leptons in SUSY theories are therefore a potential source of very interesting flavour phenomenology. They are produced directly via the DY mechanism, $pp \to Z^* \to \tilde{\ell}^+\tilde{\ell}^-$, and decay primarily as $\tilde{\ell} \to \chi_1^0 \ell$, leading to final states with two leptons and $\not\!\!E_T$. The backgrounds from WW production, however, are usually too large.

Since scalar leptons are typically lighter than scalar quarks, chain decays like the ones shown in Fig. 2 offer larger rates, and comparably smaller backgrounds. The comparison between the rates of different flavours is a direct determination of the relative BR($\chi_2^0 \to \tilde{\ell}^{\pm}\,\ell^{\mp}$), and therefore a possible probe

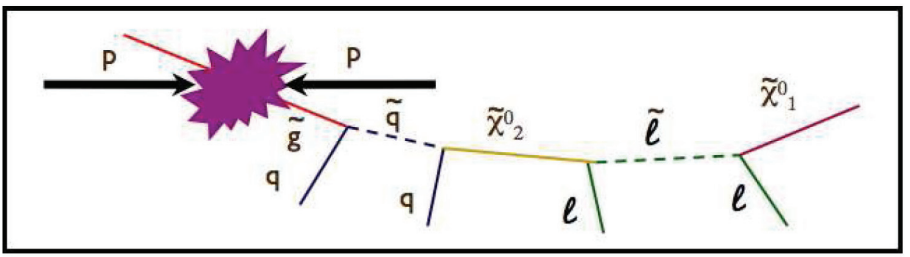

Figure 2: *Chain decay of a gluino, leading to dilepton final states.*

of the mass differences between sleptons. The invariant mass distribution of the dilepton pair exhibits also a sharp kinematical threshold, given by:

$$\max\left(m(\ell^+\ell^-)\right) \;=\; m(\chi_2)\,\sqrt{\frac{m^2(\chi_2)-m^2(\tilde{\ell})}{m^2(\chi_2)}}\,\sqrt{\frac{m^2(\tilde{\ell})-m^2(\chi_1)}{m^2(\ell)}} \qquad (2)$$

and shown for a specific example in Fig. 3. The range of mSUGRA parameter space where the dilepton endpoints are observable is shown, for two different integrated luminosities, in Fig. 4.

3.2 Lepton flavour violation in SUSY decays

As mentioned above, a large mixing between the τ and μ scalar leptons, $\delta = M^2_{\mu\tau}/M^2_L = \mathcal{O}(1)$, is a natural consequence, in grand-unified SUSY models, of the observed, large, $\nu_\mu - \nu_\tau$ mixing. This mixing could lead to observable lepton-flavour violation (LFV) processes [8]. The canonical signature, $\tau \to \mu\gamma$, is already being explored by B factories [9], and will be studied as well by the LHC using $W \to \tau\nu$ events. At the LHC, in addition, one could also observe LVF couplings directly in neutralino decays such as:

$$\chi_2^0 \to \tilde{\ell_2}^{\pm}\,\ell_3^{\mp} \to \chi_1^0\ell_2^+\ell_3^- \qquad (3)$$

The LHC potential for these decays has been studied by ATLAS in the context of minimal SUGRA models. For a specific point in parameter space (m_0=100 GeV, $m_{1/2}$=300 GeV, A_0=300 GeV, $\tan\beta$=10, $\mu > 0$), the 5σ limit on BR($\tilde{\chi}_2^0 \to \tau\mu\ \tilde{\chi}_1^0$) achievable with 30fb^{-1} is 2.3% ($\delta \sim 0.1$). This sensitivity to $\tilde{\tau}$-$\tilde{\mu}$ mixing is better than what could be obtained from a direct measurement of BR($\tau \to \mu\gamma$).

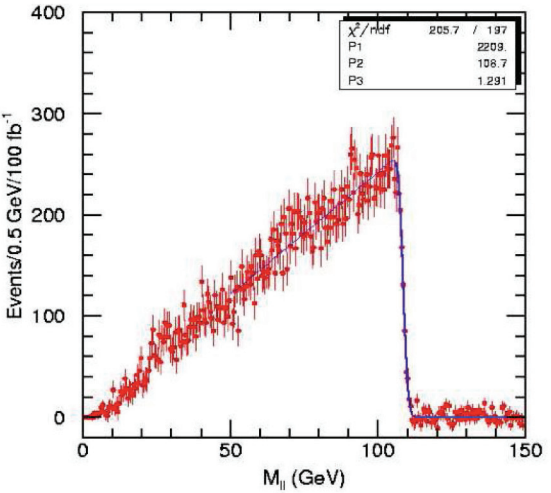

Figure 3: *Example of dilepton endpoint.*

4 CONCLUSIONS

Whether or not new physics is seen at the LHC, maintaining diversity in the experimental programme is our best investment for HEP. If new physics (especially SUSY) is discovered at the LHC, additional justification will be added to the development of a global flavour physics programme (CP and FCNC in both the quark and charged lepton sectors), mandatory to explore the nature of the new BSM framework (e.g. to identify the SUSY breaking scenario). Both the high-energy and the low-energy, high-intensity paths will eventually bring essential input to the understanding of new physics. The pursuit of the high-energy and of the high-intensity frontiers should therefore be seen as complementary and ancillary components of the same exploration, and as such they should both be pursued and supported in our quest for the ultimate laws of physics. High-intensity e^+e^- colliders, scanning the energy range between the ϕ and the $\Upsilon(4S)$ will be a crucial element in this scientific enterprise.

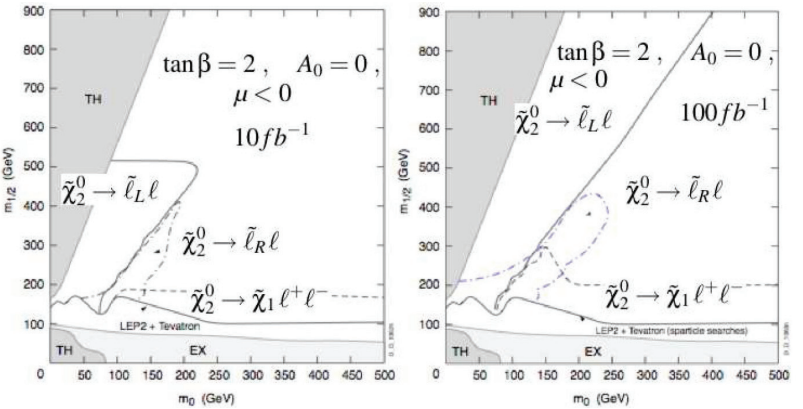

Figure 4: *Range of mSUGRA parameter space where the dilepton endpoints are observable.*

References

1. R. Barbieri, arXiv:hep-ph/0410223.

2. E. W. Varnes [CDF Collaboration], FERMILAB-CONF-06-078-E *Presented at TOP 2006: International Workshop on Top Quark Physics, Coimbra, Portugal, 12-15 Jan 2006*

3. V. M. Abazov *et al.* [D0 Collaboration], arXiv:hep-ex/0604020. A. Taffard [CDF and D0 Collaborations], FERMILAB-CONF-05-494-E *Presented at Hadron Collider Physics Symposium 2005, Les Diablerets, Switzerland, 4-9 Jul 2005*

4. T. Tait and C. P. Yuan, Phys. Rev. D **63**, 014018 (2001) [arXiv:hep-ph/0007298].

5. A. J. Buras, arXiv:hep-ph/0505175.

6. `http://cern.ch/flavlhc`

7. See e.g. G. Polesello, plenary talk at the 1st meeting of the "Flavour in the era of the LHC" Workshop, CERN, Nov 7-10 2005, http://agenda.cern.ch/fullAgenda.php?ida=a052129.

8. See e.g. A. Masiero, S. Vempati, O. Vives, arXiv:hep-ph/0405017.

9. B. Aubert *et al.* [BABAR Collaboration], arXiv:hep-ex/0508012. K. Hayasaka [Belle Collaboration], Nucl. Phys. Proc. Suppl. **144** (2005) 149.

CHARM-QUARK PHYSICS

Frascati Physics Series Vol. XLI (2006), pp. 121-134
DISCOVERIES IN FLAVOUR PHYSICS AT e^+e^- COLLIDERS
Frascati, February 28th - March 3rd, 2006

THE SYBILS' ADVICE ON CHARM (AND τ LEPTONS)

Ikaros I. Bigi
Physics Dept., University of Notre Dame du Lac, Notre Dame, IN 46556, U.S.A.
email: ibigi@nd.edu

Abstract

The importance of future studies of charm and τ decays is emphasized as probes of New Physics: the most powerful tools are **CP** asymmetries in charm and τ decays both in partial widths and final state distributions. While these searches for **CP** violation are instrumentalized in the search for and hopefully future analysis of New Physics, they might also shed light on the **CP** breaking dynamics required to implement baryogenesis. e^+e^- Super-Flavour Factories are optimally suited for the challenge, in many aspects even uniquely so.

1 Executive Summary

Talking about charm near Rome is particularly pleasant to me: For many of the allegories I have used over the years concerning charm have an obvious connection to Rome.

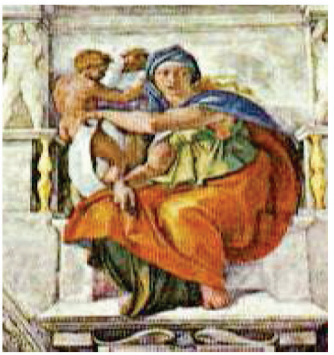

Figure 1: *My IAC: La Delfica, left, and La Tiburtina, right.*

- My intention: "I have come to praise C., not bury it."
- My judgment:"Charm – Come Botticelli nella Sistina"
- My IAC: The Sybils – "La Delfica" aka "Pythia" and the local one from Tivoli, "La Tiburtina", see Fig. 1.

While the meaning of the first item is obvious, the other two need some elucidation. While Botticelli – charm physics – can match neither Michelangelo – beauty physics – nor Raffaello – kaon physics – and therefore is often overlooked vis-a-vie the masterworks by Michelangelo in the Sistine chapel and by Raffaello nearby through an adverse 'genius loci', he is still Botticelli, i.e. a world class artist.

My visionary advisors emphasize four items:

- After having found that **CP** violating phases in the quark sector can be truly large, we need to uncover **CP** violation in leptodynamics. The three most promising (or should I say least discouraging) areas are:
  - neutrino oscillations;
  - electron electric dipole moments (EDM's);
  - τ decays.

- Baryogenesis implies the need for a 'New Paradigm of **CP** Violation' – possibly or even probably in leptodynamics.
- New Physics most likely induces flavour changing neutral currents: those could be (much) less suppressed for *up*- than *down*-type quarks.
- Charm is the only *up*-type quark allowing a full range of probes for New Physics:
  - Since top quarks do not hadronize [1)], there can be no $T^0 - \bar{T}^0$ oscillations. More generally, hadronization, while hard to bring under theoretical control, enhances the observability of **CP** violation.
  - As far as u quarks are concerned, π^0, η and η' decays electromagnetically, not weakly. They are their own antiparticles and thus cannot oscillate. **CP** asymmetries are mostly ruled out by **CPT** invariance.

In my view the justification for a Super-B factory can be and has to be based on three goals:

1. A comprehensive and detailed analysis of B (and B_s) transitions must be the first and foremost goal.
2. Analyzing τ decays represent a superb second goal, since their most profound lessons might still be waiting to be learnt, and no other machine can be competitive.
3. Probing charm processes constitute a still excellent third goal when one considers the envisioned luminosity $L \sim 10^{36}$ cm^{-2} s^{-1} [2)] and energy flexibility coupled with the ability to study final state distributions with neutrals that is unmatched by any other set-up.

Thus I find it most appropriate to speak of a Super-Flavour factory.

I would like to emphasize the following design considerations for the detector.

- A very hermetic detector coupled with low backgrounds will be most helpful or even essential to control systematics in B, τ and charm studies, like $B \to \tau\tau/\tau\nu/\tau\nu X_c/\tau\nu D$, $\tau \to l\nu\bar{\nu}$.

- The resolution of the microvertex detector should be driven by the presumably more demanding requirements of charm physics, in particular concerning $D^0 - \bar{D}^0$ oscillations and **CP** violation there. This should benefit also searches for **CP** violation in τ decays and in B_s transitions on the $\Upsilon(5S)$ with the latter driven by $\Delta\Gamma$ effects.

- A *polarized* electron beam would be most helpful for **CP** studies in τ and Λ_c decays to enhance sensitivity and control systematics.

There are several excellent reviews that the committed reader can consult to find out about details and further support for the statements on charm decays in this overview [3].

Future studies of τ and charm transitions constitutes 'hypothesis *generating*' rather than 'hypothesis *driven*' research. Antiquity's paradigm of 'hypothesis generating' analysis is represented by Delphi and its Pythia – and by the nearby Tivoli with La Tiburtina.

2 τ Decays – the Next Hero Candidate

The study of τ decays, which has taught us valuable lessons on QCD, can still reveal the intervention of New Physics through *lepton flavour violating* (LFV) transitions [4, 5, 6] and **CP** *asymmetries*.

With respect to LFV there are three classes of modes, namely (i) $\tau \to l\gamma$, (ii) $\tau \to l_1 l_2 l_3$ and (iii) $\tau \to l\nu_1\nu_2$. While typically rates for type (i) channels exceed those for type (ii), there are notable exceptions. Furthermore type (iii) can be probed through careful checks of lepton universality in τ decays [7]. Since all these types are forbidden in the SM, the observable rate is *quadratic* in the New Physics amplitude.

2.1 **CP** Violation

As already mentioned to implement baryogenesis we need a new source of **CP** violation, and that might well be in leptodynamics driving leptogenesis as the primary effect. τ leptons provide one of the more promising areas to search for such effects:

- The τ spin provides an important tool to enhance the experimental sensitivity.

- **CPT** constraints are less restrictive than in μ decays.
- Non-minimal Higgs dynamics, which can provide a source of **CP** violation, enjoy enhanced couplings in τ decays, in particular for $\tau \to \nu K\pi$, which is Cabibbo suppressed in the SM.

Two general remarks might be of use here: (a) The sought-after **CP** asymmetry is *linear* in the New Physics amplitude, since the SM provides the other amplitude. (b) One can search for **CP** violation in the production of τ leptons through their EDM. Yet there one is competing against *electromagnetic* forces, in marked contrast to the situation with *weak* decays. Therefore the chances for an observable effect are better in the latter case.

In principle one can perform a comprehensive 'Fetscher-type' analysis of $\tau \to l\nu\bar{\nu}$ as for $\mu \to e\nu\bar{\nu}$ [8]. Yet I view the channels $\tau^{\pm} \to \nu K^{\pm}\pi^0/K^0\pi^{\pm}$ as more promising also for the observable features of its final state: such a three-body final state can exhibit **CP** violation also through asymmetries in the final state as discussed in general terms in Refs. [9], namely Dalitz plot asymmetries and/or **T** odd distributions. It is quite possible – actually likely – that asymmetries in differential distributions are significantly larger than in integrated rates. Furthermore they would yield more information on the underlying transition operator and allow consistency checks to control systematics.

T odd moments – correlations that change sign under time reversal **T** – allow to make efficient use of limited statistics. A **T** odd and **CP** violating correlation has been found in $K_L \to \pi^+\pi^- e^+e^-$ between the di-pion and di-lepton planes. It has been searched for in $K^+ \to \mu^+\nu\pi^0$: $\langle \vec{s}_\mu \cdot (\vec{p}_\mu \times \vec{p}_\pi)\rangle$. In close analogy to the latter one can form a **T** odd moment in $\tau \to \nu K\pi$, if the τ spin can be exploited:

$$O_T \equiv \langle \vec{s}_\tau \cdot (\vec{p}_K \times \vec{p}_\pi)\rangle \stackrel{\mathbf{T}}{\Longrightarrow} -O_T \tag{1}$$

This would be possible most efficiently if one had the e^- beam *longitudinally polarized*, since it would lead to the τ being produced polarized. Alternatively one can rely on a special property of $e^+e^- \to \gamma^* \to \tau^+\tau^-$, namely that the τ pair is 'spin-aligned': the polarization of one τ can be tagged by the decay of the other [10]. Final state interactions can induce a non-zero **T** odd correlation even with the dynamics **T** conserving. Yet in $e^+e^- \to \tau^+\tau^-$ one can compare **CP** conjugate moments and thus isolate genuine **CP** violation.

The aim should be to probe the 10^{-3} level; the question is whether systematic uncertainties can be pushed below the 1% level without polarized beams.

The often heard statement that practically no **CP** violation in τ decays is expected within the SM is not quite correct in a subtle way. As pointed out recently the 'known' **CP** impurity in the K_L wave function, which implies a corresponding impurity for K_S based on **CPT** symmetry induces a reliably predicted asymmetry in the absence of New Physics [11]:

$$\frac{\Gamma(\tau^+ \to \bar{\nu} K_S \pi^+) - \Gamma(\tau^- \to \nu K_S \pi^-)}{\Gamma(\tau^+ \to \bar{\nu} K_S \pi^+) + \Gamma(\tau^- \to \nu K_S \pi^-)} \simeq 2\mathrm{Re}\epsilon_K \simeq (3.27 \pm 0.12) \cdot 10^{-3} \quad (2)$$

The intervention of New Physics in τ decay would then modify this value. Such an effect does of course not exist for the similar mode $\tau^+ \to \bar{\nu} K^+ \pi^0$. Comparing the findings in those two modes would thus provide a useful cross check on possible detector biases.

3 Inconclusive $D^0 - \bar{D}^0$ oscillations

$D^0 - \bar{D}^0$ oscillations are a fascinating quantum mechanical phenomenon, and they form an important ingredient when searching for manifestations of New Physics, yet by themselves they represent only an ambiguous probe of New Physics.

Oscillations can be characterized by two quantities, namely $x_D = \frac{\Delta M_D}{\Gamma_D}$ and $y_D = \frac{\Delta \Gamma_D}{2\Gamma_D}$. Oscillations are slowed down in the SM due to GIM suppression and $SU(3)_{fl}$ symmetry. Comparing a *conservative* SM bound with the present data

$$x_D(SM), y_D(SM) < \mathcal{O}(0.01) \;\; vs. \;\; x_D|_{exp} < 0.03\,, \;\; y_D|_{exp} = 0.01 \pm 0.005 \quad (3)$$

we conclude that the search has just now begun. There exists a considerable literature – yet typically with several ad-hoc assumptions concerning the nonperturbative dynamics. It is widely understood that the usual quark box diagram is utterly irrelevant due to its untypically severe GIM suppression $(m_s/m_c)^4$. A systematic analysis based on an OPE has been given in Ref. [12] in terms of powers of $1/m_c$ and m_s. Contributions from higher-dimensional operators with a much softer GIM reduction of $(m_s/\mu_{had})^2$ due to 'condensate' terms in the OPE yield

$$x_D(SM)|_{OPE}\,, \;\; y_D(SM)|_{OPE} \sim \mathcal{O}(10^{-3})\,. \quad (4)$$

Ref. [13] finds very similar numbers, albeit in a quite different approach. When evaluating the predictions in Eq.4 one has to distinguish carefully between two similar sounding questions:

- "What are the *most likely* values for x_D and y_D within the SM?"
  My answer as given above: For both $\sim \mathcal{O}(10^{-3})$.
- "How large could x_D and y_D *conceivably* be within the SM?"
  My answer: One cannot rule out 10^{-2}.

While one predicts similar numbers for $x_D(SM)$ and $y_D(SM)$, one should keep further in mind that they arise in very different dynamical environments. ΔM_D is generated from *off*-shell intermediate states and thus is sensitive to New Physics, which could produce $x_D \sim \mathcal{O}(10^{-2})$. $\Delta\Gamma_D$ on the other hand is shaped by *on*-shell intermediate states; while it is hardly sensitive to New Physics, it involves much less averaging or 'smearing' than ΔM_D making it thus much more vulnerable to violations of quark-hadron duality. *A similar concern applies to* $\Delta\Gamma(B_s)$. Observing $y_D \sim 10^{-3}$ together with $x_D \sim 0.01$ would provide intriguing, though not conclusive evidence for New Physics, while $y_D \sim 0.01 \sim x_D$ would pose a true conundrum for its interpretation.

This skepticism does not mean one should not make the utmost efforts to probe $D^0 - \bar{D}^0$ oscillations down to the x_D, $y_D \sim 10^{-3}$ level. For one we might be only one theory breakthrough away from making a precise prediction. Yet more importantly this challenge provides an important experimental validation check. A superb resolution for the μvertex detector is presumably essential here.

4 CP Violation with & without Oscillations

Most – though not all – factors favour dedicated searches for **CP** violation in charm transitions:

$\oplus$ Since baryogenesis implies the existence of New Physics in **CP** violating dynamics, it would be unwise not to undertake dedicated searches for **CP** asymmetries in charm decays, where the 'background' from known physics is between absent and small: for within the SM the effective weak phase is highly diluted, namely $\sim \mathcal{O}(\lambda^4)$, and it can arise only in *singly Cabibbo suppressed* transitions, where one expects asymmetries to reach the $\mathcal{O}(0.1\%)$ level; significantly larger

values would signal New Physics. *Any* asymmetry in *Cabibbo allowed or doubly suppressed* channels requires the intervention of New Physics – except for $D^{\pm} \to K_S \pi^{\pm}$ [14], where the **CP** impurity in K_S induces an asymmetry of $3.3 \cdot 10^{-3}$. One should keep in mind that in going from Cabibbo allowed to Cabibbo singly and doubly suppressed channels, the SM rate is *suppressed* by factors of about twenty and four hundred, respectively:

$$\Gamma_{SM}(H_c \to [S=-1]) : \Gamma_{SM}(H_c \to [S=0]) : \Gamma_{SM}(H_c \to [S=+1]) \simeq$$
$$1 : 1/20 : 1/400 \tag{5}$$

$\oplus$ Strong phase shifts required for *direct* **CP** violation to emerge in partial widths are in general large as are the branching ratios into relevant modes; while large final state interactions complicate the interpretation of an observed signal in terms of the microscopic parameters of the underlying dynamics, it enhances the observability of a signal.

$\oplus$ **CP** asymmetries can be linear in New Physics amplitudes thus increasing sensitivity to the latter.

$\oplus$ Decays to final states of *more than* two pseudoscalar or one pseudoscalar and one vector meson contain more dynamical information than given by their widths; their distributions as described by Dalitz plots or **T** odd moments can exhibit **CP** asymmetries that can be considerably larger than those for the width. Final state interactions while not necessary for the emergence of such effects, can fake a signal; yet that can be disentangled by comparing **T** odd moments for **CP** conjugate modes:

$$O_T(D \to f) \neq -O_T(\bar{D} \to \bar{f}) \quad \Longrightarrow \quad \textbf{CP} \text{ violation} \tag{6}$$

I view this as a very promising avenue, where we still have to develop the most effective analysis tools for small asymmetries.

$\oplus$ The distinctive channel $D^{\pm *} \to D\pi^{\pm}$ provides a powerful tag on the flavour identity of the neutral D meson.

$\ominus$ The 'fly in the ointment' is that $D^0 - \bar{D}^0$ oscillations are on the slow side.

$\oplus$ Nevertheless one should take on this challenge. For **CP** violation involving $D^0 - \bar{D}^0$ oscillations is a reliable probe of New Physics: the asymmetry is controlled by $\sin \Delta m_D t \cdot \mathrm{Im}(q/p)\bar{\rho}(D \to f)$. Within the SM both factors are small, namely $\sim \mathcal{O}(10^{-3})$, making such an asymmetry unobservably tiny –

unless there is New Physics; for a recent New Physics model see Ref. [15]. One should note that this observable is *linear* in x_D rather than quadratic as for **CP** insensitive quantities like $D^0(t) \to l^- X$. $D^0 - \bar{D}^0$ oscillations, **CP** violation and New Physics might thus be discovered simultaneously in a transition. Such effects can be searched for in final states common to D^0 and $\bar{D}^0$ decays like **CP** eigenstates – $D^0 \to K_S\phi$, K^+K^-, $\pi^+\pi^-$ – or doubly Cabibbo suppressed modes – $D^0 \to K^+\pi^-$. In the end it might turn out that the corresponding three-body final states – $D^0 \to K_S\pi^+\pi^-$, $D^0 \to K^+K^-\pi^0/\pi^+\pi^-\pi^0$ and $D^0 \to K^+\pi^-\pi^0$ – allow searches with higher sensitivity. Undertaking *time-dependent* Dalitz plot studies requires a higher initial overhead, yet in the long run this should pay handy dividends exactly since Dalitz analyses can invoke many internal correlations that in turn serve to control systematic uncertainties. [1]

$\oplus$ It is all too often overlooked that **CPT** invariance can provide nontrivial constraints on **CP** asymmetries. For it imposes equality not only on the masses and total widths of particles and antiparticles, but also on the widths for 'disjoint' subsets of channels. 'Disjoint' subsets are the decays to final states that can*not* rescatter into each other. Examples are semileptonic vs. nonleptonic modes with the latter subdivided further into those with strangeness $S = -1, 0. + 1$. Observing a **CP** asymmetry in one channel one can then infer in which other channels the 'compensating' asymmetries have to arise.

4.1 A Potential New Star: Λ_c (& Ξ_c) Decays

With the electron beam longitudinally polarized charm quarks and antiquarks would be produced polarized. At least some of this polarization should emerge, when those charm quarks hadronize into charm baryons, and it can be revealed through their weak decays. This would provide a powerful probe of **CP** violation and **T** odd moments similar to what can happen in τ decays as described above.

[1] Pythagoras' dictum "There is no royal way to mathematics" applies to fundamental physics as well.

4.2 Experimental Status & Future Benchmarks

So far only time integrated **CP** asymmetries have been analyzed where sensitivities of order 1% [several %] have been achieved for Cabibbo allowed and once suppressed modes with two [three] body final states [16]. Time *dependent* **CP** asymmetries (i.e. those involving $D^0 - \bar{D}^0$ oscillations) still form completely 'terra incognita'. Considering the charm production rates achieved at the B factories in particular and at FNAL I suspect the main limitation has been a lack of manpower rather than statistics.

Since the primary goal is to establish the intervention of New Physics, one 'merely' needs a sensitivity level above the reach of the SM; 'merely' does not mean it can easily be achieved. As far as *direct* **CP** violation is concerned – in partial width as well as in final state distributions – this means asymmetries down to the 10^{-3} or even 10^{-4} level in Cabibbo allowed channels and 1% level or better in twice Cabibbo suppressed modes; in Cabibbo once suppressed decays one wants to reach the 10^{-3} range although CKM dynamics can produce effects of that order because future advances might sharpen the SM predictions – and one will get it along the other channels. For *time dependent* asymmetries in $D^0 \to K_S\pi^+\pi^-$, K^+K^-, $\pi^+\pi^-$ etc. and in $D^0 \to K^+\pi^-$ one should strive for the $\mathcal{O}(10^{-4})$ and $\mathcal{O}(10^{-3})$ levels, respectively.

Statisticswise these are not utopian goals considering that LHCb expects to record about $5 \cdot 10^7$ *tagged* $D^* \to D + \pi \to K^+K^- + \pi$ events in a nominal year of 10^7 s [17].

When going after asymmetries below the 1% or so one has to struggle against systematic uncertainties, in particular since detectors are made from matter. I can see three powerful weapons in this struggle:

- Resolving the time evolution of asymmetries that are controlled by x_D and y_D, which requires excellent microvertex detectors;
- Dalitz plot consistency checks;
- quantum statistics constraints on distributions, **T** odd moments etc.

5 Conclusions

Two aspects of τ decays deserve, actually require even more determined scrutiny than has been brought to bear up to now: lepton flavour violation (LFV) and

CP violation.

The observation of neutrino oscillations tells us that LFV does exist in nature. There are intriguing (SUSY) GUT scenarios connecting the observed $b \to s\gamma$ with $\tau \to \mu\gamma$ transitions and suggesting the latter to occur possibly at levels close to existing bounds and in any case probably within one or two orders of magnitude of them. The phenomenology of LFV in τ decays is complementary to that in muon decays and actually richer. While most models predict higher rates for $\tau \to l\gamma$ than for decays into three leptons [4, 7] one should search also for the latter with vigour. The more experimental sensitivity can be achieved, the better. Finally τ production in e^+e^- annihilation has no practical competition from any other production process.

We should keep in mind that we need a new **CP** paradigm to realize baryogenesis and that quite possibly leptogenesis might be the primary effect. This provides a more specific motivation to the general goal to probe **CP** violation in leptodynamics. Again τ decays constitute a much richer and more fertile laboratory than muon decays. Having polarized electron beams leading to the production of polarized τ pairs would provide a very powerful though presumably not mandatory tool. It appears unlikely at present that one could have too much experimental sensitivity. No other setup can realistically compete with $e^+e^- \to \tau^+\tau^-$ concerning **CP** studies.

Charm is often viewed as a 'has-been' quantum number: after a few absolute branching ratios have been measured accurately to provide validation opportunities to lattice QCD, there is nothing of substance to be learnt from them. This view overlooks that charm hadrons keep amazing us with features that had not been anticipated as demonstrated recently by the discovery of the D_s^{**}, $X(3872)$, $X(3940)$ and $Y(4260)$ resonances [16]. Those findings have led to a re-analysis of our understanding – or lack thereof – of hadronic spectroscopy [18, 19, 20].

Yet even beyond that weak charm decays might teach us important, possibly even unique lessons on New Physics. While it is possible to construct New Physics models that lead to **CP** asymmetries not far below present bounds and well above SM predictions, they are neither compelling nor particularly intriguing. Yet it behooves us to be aware of our ignorance: "We know so much about the flavour structure, yet understand so little." It is quite conceivable that flavour changing neutral currents are considerably stronger for

up-type than for down-type quarks. Charm is the only up-type quark allowing for a full range of probes of New Physics through **CP** studies with and without oscillations. Charm thus might, just might provide essential support for the emerging New SM.

Charm studies can benefit from many experimental and phenomenological advantages. They suffer from the drawback that charm decays in contrast to K and B decays are not KM suppressed and that oscillations proceed at best at slow speed. Yet even on the theoretical side there are some advantages, namely the 'dullness' of the SM electroweak phenomenology and the reasonable expectation that hadronization effects of charm can be brought mostly under theoretical control due to the comprehensive data sets accumulated by the CLEO-c and BESIII collaborations.

We should also keep in mind that we have only recently entered a territory in charm studies, where one could reasonably hope to uncover New Physics – and there are still two to three orders of magnitude in sensitivity waiting for the enterprising 'treasure hunter'.

One last brief comment on experimental considerations: Doing truly superb studies of B decays has to be the paramount objective of a Super-Flavour factory. Yet it can also do superb and even unique τ and charm studies. One should seriously study how one can maximize the latter without in any way jeopardizing the former. One item might be to 'overdesign' the μvertex detector beyond the needs of $B_{u,d}$ studies to enhance its usefulness for charm and probably also τ physics as well as for $\Delta\Gamma$ effects in $\Upsilon(5S) \to B_s^{(*)}\overline{B}_s^{(*)}$.

6 Epilogue

Finding any signal of New Physics in high $p_\perp$ studies at the LHC will provide a great boost substantially as well as morally. Among other things it would make it mandatory to analyze the impact of that New Physics in heavy flavour studies. The first working hypothesis though would have to be that B and K decays being CKM suppressed provide the highest sensitivity to the New Physics – unless one finds something rather exotic like a neutral boson decaying into, say, two jets of which only one contains charm.

My message has been as specific as could be expected when coming from the Pythia on the right in Fig.2 rather the one on the left, with whom high energy physicists are more familiar, and when communicated by a mere mortal

Figure 2: *Two very distinct visions of Pythia.*

like me, who is not even a priest.

Acknowledgments

It always is a most gratifying experience to come to the Rome area for discussing nature's puzzles with colleagues. This was also true this time, and I am thankful for the organizers of this workshop for creating this opportunity. This work was supported by the NSF under grant PHY03-55098.

References

1. I.I. Bigi, Y. Dokshitzer, V. Khoze, J. Kühn, P. Zerwas, *Phys. Lett.* **B181** (1986) 157.

2. M. Biagini, these Proceedings.

3. G. Burdman *et al.*, "Rare Charm Decays in the SM and Beyond", *Phys.Rev.***D66** 47; S. Bianco *et al.*, "A Cicerone for the Physics of Charm", *La Rivista del Nuovo Cim.* **26** (2003) # 7-8; G. Burdman, I. Shipsey, "$D^0 - \bar{D}^0$ Mixing and Rare Charm Decays", *Ann.Rev.Nucl.Part.Sci.* **53** (2003); I.I. Bigi, hep-ph/0412041, to appear in 'Proceed. of FPCP04', Daegu, Korea, 2004.

4. J. Hisano, these Proceedings.

5. M. Roney, these Proceedings.

8. W. Fetscher, *http* : *//www.panic*05.*lanl.gov/abstracts*/361/*fetscher*361*panic*2005.*pdf*

9. J.H. Kühn, E. Mirkes, *Phys.Lett.* **B398** (1997) 407.

10. Y.-S. Tsai, *Phys.Rev.* **D4** (1971) 2821; S.Y. Pi, A.I. Sanda, *Ann.Phys.(N.Y.)* **106** (1977) 171; J.H. Kühn, *Phys.Rev.* **D52** (1995) 3128; C.A. Nelson, *Phys.Rev.* **D53** (1996) 5001.

11. I.I. Bigi, A.I. Sanda, *Phys.Lett.* **B625** (2005) 47.

12. I.I. Bigi, N.G. Uraltsev, *Nucl.Phys.***B592** (2001) 92.

13. A. Falk *et al.*, *Phys.Rev.* **D65** (2002) 054034.

14. I.I. Bigi, H. Yamamoto, *Phys.Lett.* **B349** (1995) 363; S. Bianco *et al.*, "A Cicerone for the Physics of Charm", *La Rivista del Nuovo Cim.* **26** (2003) # 7-8.

15. K. Agashe, G. Perez, A. Soni, *Phys.Rev.* **D71** (2005) 016002.

16. I. Shipsey, these Proceedings.

17. T. Nakada, these Proceedings.

18. N.A. Törnqvist, *Phys. Lett.* **B590**, 209 (2004); E. Braaten, M. Kusunoki, *Phys. Rev.* **D69**, 074005 (2004); E.S. Swanson, *Phys. Lett.* **B588**, 189 (2004); M. Voloshin, *Phys. Lett.* **B604**, 69 (2004).

19. E. Kou, O. Pene, [arXiv:hep-ph/0507119]; F.E. Close, P.R. Page, [arXiv:hep-ph/0507199]; Shi-Lin Zhu, *Phys. Lett.* **B625**, 212 (2005).

20. L. Maiani, F. Piccinini, A.D. Polosa, V. Riquer, *Phys. Rev.* **D71**, 014028 (2005); *Phys. Rev.* **D72**, 031502 (2005).

Frascati Physics Series Vol. XLI (2006), pp. 135-168
DISCOVERIES IN FLAVOUR PHYSICS AT e^+e^- COLLIDERS
Frascati, February 28th - March 3rd, 2006

STATUS OF CHARM FLAVOR PHYSICS

I. Shipsey
Department of Physics, Purdue University, West Lafayette, IN 47907, U.S.A.

Abstract

The role of charm in testing the Standard Model description of quark mixing and CP violation through measurements of lifetimes, decay constants and semileptonic form factors is reviewed. Together with Lattice QCD, charm has the potential this decade to maximize the sensitivity of the entire flavor physics program to new physics. and pave the way for understanding physics beyond the Standard Model at the LHC in the coming decade. The status of indirect searches for physics beyond the Standard Model through charm mixing, CP-violation and rare decays is also reported.

1 Introduction

Charm plays a dual role in flavor physics. First it provides important supporting measurements for studies of CP-violation in B physics. These measurements test QCD technologies such as Lattice QCD, QCD sum rules and

chiral theory. The first of these theoretical approaches is the most promising for very precise calculations of decay constants and form factors which are the most relevant supporting measurements for B physics. Second, charm provides unique opportunities for indirect searches for physics beyond the SM.

2 Big Questions in Flavor Physics

The big questions in quark flavor physics are: (1) "What is the dynamics of flavor?" The gauge forces of the standard model (SM) do not distinguish between fermions in different generations. The electron, muon and tau all have the same electric charge, quarks of different generations have the same color charge. Why generations? Why three? (2) "What is the origin of baryogenesis?" Sakharov gave three criteria, one is CP-violation [1]. There are only three known examples of CP-violation: the Universe, and the beauty and kaon sectors. However, SM CP-violation is too small, by many orders of magnitude, to give rise to the baryon asymmetry of the Universe. Additional sources of CP-violation are needed. (3) "What is the connection between flavor physics and electroweak symmetry breaking?" Extensions of the SM, for example supersymmetry, contain flavor and CP-violating couplings that should show up at some level in flavor physics but precision measurements and precision theory are required to detect the new physics.

3 Charm in CKM physics

This is the decade of precision flavor physics. The goal is to over-constrain the CKM matrix with a range of measurements in the quark flavor changing sector of the SM at the per cent level. If inconsistencies are found between, for example, measurements of the sides and angles of the B_d unitarity triangle, it will be evidence for new physics. Many experiments will contribute including BaBar and Belle, CDF, D0 at Fermilab, ATLAS, CMS, and LHC-b at the LHC, BESIII, CLEO-c, and experiments studying rare kaon decays.

However, the study of weak interaction phenomena, and the extraction of quark mixing matrix parameters remain limited by our capacity to deal with non-perturbative strong interaction dynamics. Current constraints on the CKM matrix are shown in Fig. 1(a). The widths of the constraints, except that of $\sin 2\beta$, are dominated by the error bars on the calculation of hadronic

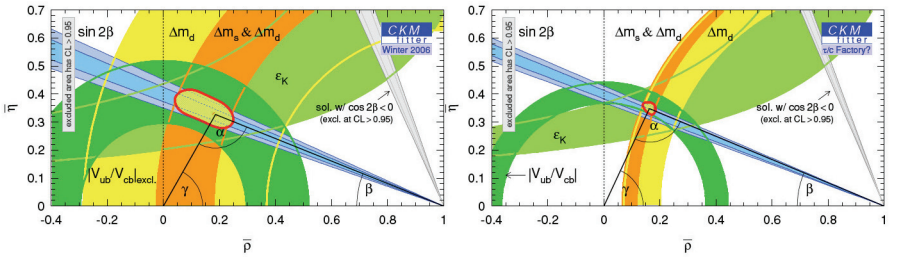

Figure 1: *Lattice impact on the B_d unitarity triangle from B_d and B_s mixing, $|V_{ub}|/|V_{cb}|$, ϵ_K, and $\sin 2\beta$. (a) Winter 2006 status of the constraints including the recent observation of B_s mixing. (b) Prospects under the assumption that LQCD calculations of B system decay constants and semileptonic form factors achieve the the precision projected in Table 9.*

matrix elements. Recent advances in LQCD have produced calculations of non-perturbative quantities such as f_π, f_K, and heavy quarkonia mass splittings that agree with experiment [2]. Several per cent precision in charm and beauty decay constants and form factors is hoped for, but the path to higher precision is hampered by the absence of accurate charm data against which to test lattice techniques. This is beginning to change with the BES II run at the $\psi(3770)$, and the start of data taking at the charm and QCD factory CESR-c/CLEO-c [3]. Later in the decade BES III at the new double ring accelerator BEPC-II will also turn on [4]. CLEO-c is in the process of obtaining charm data samples one to two orders of magnitude larger than any previous experiment, and the BES III data set is expected to be $\sim \times 20$ larger than CLEO-c. These data sets have the potential to provide unique and crucial tests of LQCD, and other QCD technologies such as QCD sum rules and chiral theory, with accuracies of 1-2%.

If LQCD passes the charm factory tests, we will have much greater confidence in lattice calculations of decay constants and semileptonic form factors in B physics. When these calculations are combined with 500 fb^{-1} of B factory data, and improvement in the direct measurement of $|V_{tb}|$ at the Tevatron [5], they will allow a significant reduction in the size of the errors on $|V_{ub}|, |V_{cb}|, |V_{td}|$ and $|V_{ts}|$, quantitatively and qualitatively transforming knowledge of the B_d unitarity triangle, see Fig. 1(b), and thereby maximizing the sensitivity of heavy quark physics to new physics.

Equally important, LQCD combined with charm data allows a significant advance in understanding and control over strongly-coupled, non-perturbative quantum field theories in general. Field theory is generic, weak coupling is not. Two of the three known interactions are strongly coupled: QCD and gravity (string theory). Understanding strongly coupled theories may be a crucial to interpret new phenomena at the high energy frontier.

3.1 Decay Constants

The B_d (B_s) meson mixing probability can be used to determine $|V_{td}|$ ($|V_{ts}|$).

$$\Delta m_d \propto |V_{tb}V_{td}|^2 f_{B_d}^2 B_{B_d} \tag{1}$$

The B_d mixing rate is measured with exquisite precision (1%) [6] but the decay constant is calculated with a precision of about 10-15%. If theoretical precision could be improved to 3%, the error on $|V_{td}|$ would be about 5%.

Since LQCD hopes to predict f_B/f_{D^+} with a small error, measuring f_{D^+} would allow a precision prediction for f_B. Hence a precision extraction of $|V_{td}|$ from the B_d mixing rate becomes possible. Similar considerations apply to B_s mixing now it has been observed i.e. a precise determination of $f_{D_s^+}$ would allow a precision prediction for f_{B_s} and consequently a precision measurement of $|V_{ts}|$. Finally the ratio of the two neutral B meson mixing rates determines $|V_{td}|/|V_{ts}|$, but $|V_{ts}| = |V_{cb}|$ by unitarity and $|V_{cb}|$ is known to a few per cent, and so the ratio again determines V_{td}. Which method of determining $|V_{td}|$ will have the greater utility depends on which combination of hadronic matrix elements have the smallest error.

Charm leptonic decays measure the charm decay constants $f_{D_s^+}$ and f_{D^+} because $|V_{cs}|$ and $|V_{cd}|$ are known from unitarity to 0.1% and 1% respectively.

$$\frac{\mathcal{B}(D^+ \to \mu\nu_\mu)}{\tau_{D^+}} = (\text{const.}) f_{D^+}^2 |V_{cd}|^2 \tag{2}$$

(Charge conjugation is implied throughout this paper.) The measurements are also a precision test of the LQCD. At the start of 2004 f_{D^+} was experimentally undetermined and $f_{D_s^+}$ was known to 33%.

3.2 Semileptonic form factors

$|V_{ub}|$ is determined from beauty semileptonic decay

$$\frac{d\Gamma(B \to \pi e^- \bar{\nu}_e)}{dq^2} = (\text{const.})|V_{ub}|^2 f_+^{B\pi}(q^2)^2 \tag{3}$$

The differential rate depends on a form factor, $f_+(q^2)$ that parameterizes the strong interaction non-perturbative effects. A representative value of $|V_{ub}|$ determined from $B \to \pi \ell^- \bar{\nu_e}$ is [7]:

$$|V_{ub}| = (3.76 \pm 0.16^{+0.87}_{-0.51}) \times 10^{-3} \tag{4}$$

where the uncertainties are experimental statistical and systematic, and from the LQCD calculation of the form factor, respectively. The experimental errors are expected to be reduced to 5% with B factory data samples of 500 fb^{-1} each, and the theory error will dominate.

Again, because the charm CKM matrix elements are known from unitarity, the differential charm semileptonic rate

$$\frac{d\Gamma(D \to \pi e^+ \nu_e)}{dq^2} = (\text{const.})|V_{cd}|^2 f_+^{D\pi}(q^2)^2 \tag{5}$$

tests calculations of charm semileptonic form factors. Thus, a precision measurement tests the LQCD calculation of the $D \to \pi$ form factor. As the form factors governing $B \to \pi e^- \bar{\nu_e}$ and $D \to \pi e^+ \nu_e$ are related by heavy quark symmetry, the charm test gives confidence in the accuracy of the $B \to \pi$ calculation. The B factories can then use a tested LQCD prediction of the $B \to \pi$ form factor to extract a precise value of $|V_{ub}|$. At the start of 2004, $\mathcal{B}(D \to \pi e^+ \nu_e)$ had been determined to 45% [6, 8], and the absolute value of the $D \to \pi$ form factor had not been measured.

Lifetimes of the charm mesons are interpreted within the framework of the Operator Product Expansion. Within OPE the total decay width can be expressed as a series in $1/m_c$ [9].

$$\begin{aligned} \Gamma(H_c) &= \Gamma_c + \mathcal{O}(1/m_c^2) \\ &+ \Gamma_{\text{PI,WA,WS}}(H_c) + \mathcal{O}(1/m_c^4) \end{aligned} \tag{6}$$

Mechanisms in which light quarks in the $c-$hadron are involved: Pauli Interference (PI), Weak Annihilation (WA) and Weak Scattering (WS), are $O(1/m_c^3)$

Table 1: *Charm lifetime world averages in fs.*

Particle	Lifetime (fs)
D^+	1040 ± 7
D_s^+	504 ± 4
D^0	410.3 ± 1.5
Ξ_c^+	442 ± 26
Λ_c^+	200 ± 6
Ξ_c^+	112^{+13}_{-10}
Ω_c^+	69 ± 12

but phase space enhanced. The charm lifetimes are in Table 1. The PDG2004 lifetimes are dominated by the exquisitely precise FOCUS measurements from 2002. The D^+ and D^0 lifetimes are known to 7 and 4 per mille, which is as precise as kaon lifetimes are known. PDG2004 does not include the D_s lifetime measurement from FOCUS and so we have averaged it with the PDG value in Table 1. The lifetimes can be explained within OPE [9]. To gain a deeper understanding absolute inclusive semileptonic branching ratios of $c-$hadrons, especially the D_s^+ and charm baryons, which are currently not well known, need to be measured. For charm CKM physics, the most important point to note is that errors on lifetimes are not a limiting factor in the measurement of absolute rates.

4 Absolute Charm Branching Ratios

We reviewed above the importance of absolute charm leptonic and semileptonic branching ratios. The absolute hadronic branching ratios $\mathcal{B}(D^+ \to K^-\pi^+\pi^+)$, $\mathcal{B}(D^0 \to K^-\pi^+)$, and $\mathcal{B}(D_s^+ \to \phi\pi^+)$ are also important as, currently, all other D^+, D^0 and D_s^+ branching ratios are determined from ratios to one or the other of these branching fractions [6]. In consequence, nearly all branching fractions in the B and D sectors depend on these reference modes.

Absolute charm branching ratios are poorly known, see Table 2. The reason is that charm produced at B factories and at the Tevatron or at dedicated fixed target facilities allows relative rate measurements but absolute rate measurements are hard because backgrounds are sizeable, and, crucially, the number of D mesons produced is not easily determined.

Table 2: Status of important charm branching ratios circa 2004.

Mode	$\mathcal{B}$ (%)	$\delta\mathcal{B}/\mathcal{B}$
$D^+ \to \mu^+\nu_\mu$	$0.08^{+0.17}_{-0.05}$	100
$D_s^+ \to \mu^+\nu_\mu$	0.60 ± 0.14	24
$D^0 \to \pi^- e^+ \nu_e$	$0.30^{+0.23}_{-0.12}$	45
$D^0 \to K^-\pi^+$	3.80 ± 0.09	2.4
$D^+ \to K^-\pi^+\pi^+$	9.2 ± 0.6	6.5
$D_s^+ \to \phi\pi^+$	3.6 ± 0.9	25
$\Lambda_c^+ \to pK^-\pi^+$	5.0 ± 1.3	26
$J/\psi \to \mu^+\mu^-$	5.88 ± 0.10	1.7

To illustrate one way around this problem consider the clever measurement of $\mathcal{B}(D_s^+ \to \phi\pi^+)$ from the BABAR collaboration [10]. The first stage in the analysis is to produce a beam of D_s^+. This is achieved by partially reconstructing $B^0 \to D_s^{*+}D^{*-}$, where the D^{*+} and the photon in the decay $D_s^{*+} \to D_s^+\gamma$ are reconstructed but the D_s^+ is not observed. BABAR find

$$\mathcal{B}(B^0 \to D_S^{*+}D^{*-}) = (1.88 \pm 0.09 \pm 0.17)\% \tag{7}$$

In the second step $B^0 \to D_S^{*+}D^{*-}$ is fully reconstructed

$$\begin{aligned}\mathcal{B}(B^0 \to D_s^{*+}D^{*-})\mathcal{B}(D_s \to \phi\pi) \\ = (8.81 \pm 0.86) \times 10^{-4}\end{aligned} \tag{8}$$

Dividing these

$$\mathcal{B}(D_s \to \phi\pi) = (4.81 \pm 0.52 \pm 0.38)\% \tag{9}$$

The total error of 12.5%, of which 7.5% is systematic, represents a dramatic improvement on the 25% precision of the PDG value. Further improvement in the measurement of this important quantity is expected at the B factories, although it will be challenging to reduce the systematic error significantly. In principle, a several per cent measurement of $\mathcal{B}(D_s \to \phi\pi)$ is achievable at a charm factory.

5 BES II and CLEO-c at the $\psi(3770)$

In 2003 the venerable BES II detector accumulated an integrated luminosity of 33 pb^{-1} at and around the $\psi(3770)$, a factor three greater than the previous

Storage Ring (CESR) has been upgraded to CESR-c with the installation of 12 wiggler magnets to increase damping at low energies. The CLEO-c detector is a minimal modification of the well understood CLEO III detector. It is the first modern detector to operate at charm threshold. In 2003 a CLEO-c pilot run accumulated 56 pb^{-1} at the $\psi(3770)$ ($360,000 D\bar{D}$ pairs) and this was followed by the first full run accumulating a further 225 pb^{-1} for a total of 281 pb^{-1}at the $\psi(3770)$ ($1.8\times10^6 D\bar{D}$ pairs) CLEO-c has also accumulated about 200 pb^{-1} at $\sqrt{s} \sim 4170$ MeV for D_s physics. These $\psi(3770)$ datasets exceeds those of the BESII (Mark III) experiments by factors of 30 (15). CLEO-c expects to take data until April 2008 and will approximately triple each data set by that time,

In the very near future the BEPCII Project will be commissioned, This is a two ring machine with 93 bunches in each beam. Luminosity is expected to be $10^{33}\text{cm}^{-2}\text{s}^{-1}$ at 1.89 GeV $6\times10^{32}\text{cm}^{-2}\text{s}^{-1}$ at 1.55 GeV and $6\times10^{32}\text{cm}^{-2}\text{s}^{-1}$ at 2.1 GeV. The linac was installed in 2005. The ring is to be installed this year (2006) and the BESIII detector will be in place and commissioned in 2007 with data taking beginning of 2008, with early running at the J/psi. Although the detailed run plan has not been decided: an example is given here. At 5/fb/yr or 15/fb/3yrs, there will be $90\times10^6 D\bar{D}$ pairs or a factor 20 greater than the full CLEO-c data sample. Three years at 4170 MeV would produce $2\times10^6 D_s\bar{D}_s$ pairs in three years again a factor 20 greater than the full CLEO-c data set.

In the longer term proposed Super B Factories at KEK or SuperB or a dedicated charm factory would produce an abundance of charm. For example the SuperB machine at $10^{36}\text{cm}^{-2}\text{s}^{-1}$ will produce $10^{10} e^+e^- \rightarrow c\bar{c}$ pairs/10^7s. Due to the "Linear Collider design" there is an option to lower the energy to 4 GeV with a modest luminosity penalty of a factor 10. In this mode of operation the super B Factory becomes a super flavour factory. When discussing charm factory results from CLEO-c I will extrapolate to BEPCII/BESIII (my estimates, not official ones) and to super flavour. For the latter I will assume 1×10^{35} for 10^7 s which is ($6.4\times10^9 D\bar{D}$ pairs) at the $\psi(3770)$ exceeding the BEPCII and CESR-c data samples by a factor of 70 and 1,000 respectively.

5.1 Analysis Technique

There are decisive advantages to running at charm threshold. As $\psi \to D\bar{D}$, the technique is to fully reconstruct one D meson in a hadronic final state, the tag, and then to analyze the decay of the second D meson in the event to extract inclusive or exclusive properties.

As $E_{\rm beam} = E_D$, the candidate is required to have energy close to the beam energy, and the beam-constrained candidate mass, $M_D{=}\sqrt{E^2_{\rm beam} - p^2_{\rm cand}}$, is computed. Charm mesons have many large branching ratios to low multiplicity final states, and so the tagging efficiency is very high, about 25%, compared to much less than 1% for B tagging at a B factory.

Tagging creates a single D meson beam of known momentum. The beam constrained mass for events in which the second D meson is also reconstructed are shown in Fig. 2. These double tag events, which are key to making absolute branching fraction measurements, are pristine. The absolute branching fraction is given by:

$$\mathcal{B}(D^+ \to K^-\pi^+\pi^+) = \frac{N(K^-\pi^+\pi^+)}{\epsilon(K^-\pi^+\pi^+) \times N(D^-)} \tag{10}$$

where $N(K^-\pi^+\pi^+)$ is the number of $D^+ \to K^-\pi^+\pi^+$ observed in tagged events, $\epsilon(K^-\pi^+\pi^+)$ is the reconstruction efficiency and $N(D^-)$ is the number of tagged events.

In a method similar to that pioneered by Mark III [11, 12], CLEO fits to the observed single tag and double tag yields for six D^+ and three D^0 modes [13]. I will only consider the two most important branching fractions here. For $D^0 \to K^-\pi^+$ the total errors are comparable to previous measurements, see Table 3. But the true improvement is that the previous most precise measurements from ALEPH [14] and CLEO [15] were based on comparing $D^{*+} \to D^0\pi_s, D^0 \to K^-\pi^+$ with and without explicitly reconstructing the D^0. The latter measurement relies on a correlation between the momentum of the slow pion from the D^* and the thrust axis of the $e^+e^- \to q\bar{q}$ event. Consequently, these early measurements had poor signal to noise whereas the CLEO-c measurement has a signal to noise of about 60/1.

This is the most precise measurement of $\mathcal{B}(D^+ \to K^-\pi^+\pi^+)$ to date, see Table 4 but the improvement is again much more than statistics. The previous most precise measurement, which was from CLEO [16], bootstrapped

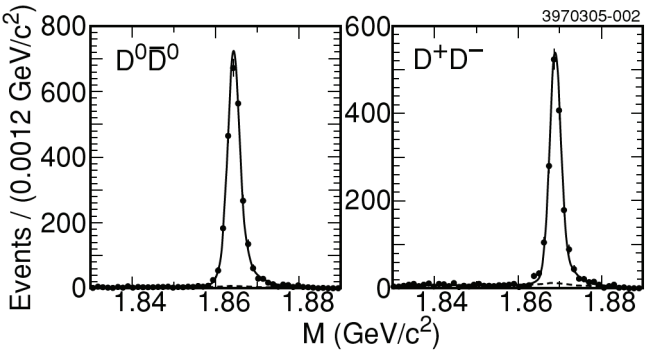

Figure 2: *Beam constrained mass of D mesons in CLEO-c events in which both D mesons have been fully reconstructed.*

Table 3: The $D^0 \to K^-\pi^+$ absolute charm branching ratio.

$\mathcal{B}(\%)$	Error (Source)
$3.82 \pm 0.07 \pm 0.12$	3.6% (CLEO [15])
$3.90 \pm 0.09 \pm 0.12$	3.8% (ALEPH [14])
3.80 ± 0.09	2.4% (PDG)
$3.91 \pm 0.08 \pm 0.09$	3.1 % (CLEO-c [13])

on $D^0 \to K^-\pi^+$ through a measurement of

$$\frac{\mathcal{B}(D^{*+} \to D^0\pi^+)\mathcal{B}(D^0 \to K^-\pi^+)}{\mathcal{B}(D^{*0} \to D^+\pi^0)\mathcal{B}(D^+ \to K^-\pi^+\pi^+)} \tag{11}$$

so it was not independent of $\mathcal{B}(D^0 \to K^-\pi^+)$, while the new measurement has no dependence on $\mathcal{B}(D^0 \to K^-\pi^+)$ a much more satisfactory situation.

BES II has performed a similar analysis. These recent measurements are in remarkably good agreement with the PDG averages, indicating that the charm, and hence beauty, decay scales, are approximately correct and are now, finally, on a solid foundation.

The CLEO-c $\psi(3770)$ integrated luminosity goal of 0.75 fb^{-1} may sound small compared to the more than 500 fb^{-1} collected by Belle, and the slightly

Table 4: The $D^+ \to K^-\pi^+\pi^+$ absolute charm branching ratio.

$\mathcal{B}(\%)$	Error (Source)
$9.3 \pm 0.6 \pm 0.8$	10.8% (CLEO [16])
$9.1 \pm 1.3 \pm 0.4$	14.9% (MKIII [17])
9.1 ± 0.7	7.7% (PDG)
$9.52 \pm 0.25 \pm 0.27$	3.9 % (CLEO-c [13])

Table 5: Charm factory hadronic branching ratio measurement expected precision with 0.75fb^{-1} data samples at the $\psi(3770)$ and above $D_s\bar{D}_s$ threshold. The first uncertainty is statistical and the second systematic.

Mode	$\delta\mathcal{B}/\mathcal{B}$ (%)	
	PDG2004	0.75fb^{-1}
$D^0 \to K^-\pi^+$	2.4%	0.6% , 1.1%
$D^+ \to K^-\pi^+\pi^+$	7.7%	0.7% , 1.2%
$D_s^+ \to \phi\pi$	12.5% [10]	4.0%

smaller sample by BABAR. However, the ability to perform a tagged analysis is comparable at the two types of factory because the tagging efficiency is at least 25 times larger at a charm factory than at a B factory, and the cross section is about six times larger. Hence,

$$\frac{N(B \text{ tags at a } B \text{ factory})}{N(D \text{ tags at a charm factory})} \sim 1. \tag{12}$$

In consequence the number of events in 100pb^{-1} with two D mesons reconstructed is about the same as the number of events at 10 GeV with 500fb^{-1} with two B mesons reconstructed. Projections for the expected precision with which the reference hadronic branching ratios will be measured with a 0.75fb^{-1} data set are given in Table 5. CLEO-c and, later BES III, will set the scale for all heavy quark measurements.

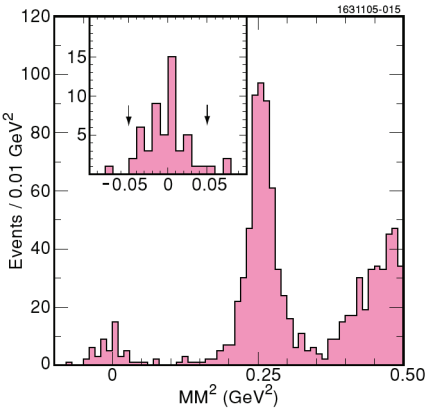

Figure 3: *The MM^2 distribution in events with D^- tag, a single charged track of the correct sign, and no additional (energetic) showers. The insert shows the signal region for $D^+ \to \mu\nu_\mu$. A $\pm 2\sigma$ range is indicated by the arrows.*

5.2 Charm Decay Constant

The measurement of the leptonic decay $D^+ \to \mu^+\nu_\mu$ benefits from the fully tagged D^- at the $\psi(3770)$. One observes a single charged track recoiling against the tag that is consistent with a muon of the correct sign. Energetic electromagnetic showers un-associated with the tag are not allowed. The missing mass $MM^2 = m_\nu^2$ is computed; it peaks at zero for a decay where only a neutrino is unobserved. Fig. 3 shows the MM^2 distribution from CLEO-c [18].

There are 50 candidate signal events, and $2.81 \pm 0.3^{+0.84}_{-0.22}$ background events. After correcting for efficiency, CLEO-c finds

$$\mathcal{B}(D^+ \to \mu^+\nu_\mu) = (4.40 \pm 0.66^{+0.09}_{-0.12}) \times 10^{-4}, \tag{13}$$

where the uncertainties are statistical and systematic, respectively. Under the assumption of three generation unitarity, and using the precisely known D^+ lifetime, CLEO-c obtains

$$f_{D^+} = (222.6 \pm 16.7^{+2.8}_{-3.4}) \text{ MeV}. \tag{14}$$

This is the most precise measurement of f_{D^+} [18]. The result appeared at Lepton-Photon 2005 just two days after the first unquenched lattice QCD cal-

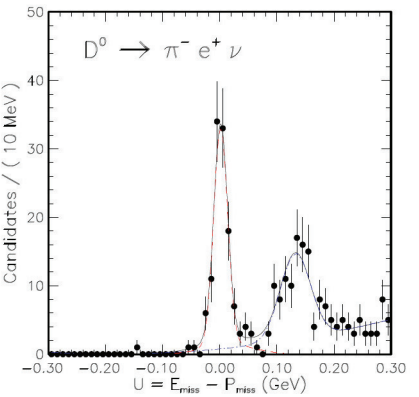

Figure 4: *The $U = E_{miss} - P_{miss}$ distribution in events with a $\bar{D}^0$ tag, a positron, and a single charged track of the correct sign. The peaks at zero and 0.13 GeV correspond to $D^0 \rightarrow \pi^- e^+ \nu_e$ and $D^0 \rightarrow K^- e^+ \nu_e$ (preliminary.)*

culation [19] had predicted:

$$f_{D^+} = (201 \pm 3 \pm 17) \text{ MeV}. \tag{15}$$

The combined experimental error is 8% while the LQCD error is also 8% [19]. The results are in good agreement but errors are still large. The only other positive observation of this decay is by BES II who found three candidate events with a background of 0.25 events in their 33pb^{-1} data sample. They find a branching ratio of $(0.122^{+0.111}_{-0.053} \pm 0.010)\%$ corresponding to $f_{D^+} = (371^{+129}_{-119} \pm 25)$ MeV [20]. The CLEO value is considerably smaller and in better agreement with expectations from the lattice and other theoretical approaches. With 0.75 fb^{-1} a 4.5% error for f_{D^+} is expected. Similar precision is expected for $f_{D_s^+}$ at $\sqrt{s} = 4160$ MeV. BES III will make even more precise measurements achieving a precision of several per cent for both f_{D^+} and $f_{D_s^+}$ which is well matched to the ultimate precision of the LQCD calculations.

5.3 Measurement of the Charm Semileptonic Form Factors

The measurement of semileptonic decay absolute branching ratios and absolute form factors is also based on the use of tagged events. The analysis procedure,

Table 6: Selected CLEO-c charm semileptonic branching ratio measurements in % and a comparison to the PDG.

Mode	PDG	CLEO-c
$D^0 \to \pi^- e^+ \nu_e$	0.36 ± 0.06	$0.26 \pm 0.03 \pm 0.1$
$D^0 \to K^- e^+ \nu_e$	3.58 ± 0.18	$3.44 \pm 0.10 \pm 0.1$
$D^+ \to \pi^0 e^+ \nu_e$	0.31 ± 0.05	$0.44 \pm 0.06 \pm 0.01$
$D^+ \to \overline{K}^0 e^+ \nu_e$	6.7 ± 0.9	$8.71 \pm 0.38 \pm 0.37$

using $D^0 \to \pi^- e^+ \nu_e$ as an example is as follows. A positron and a hadronic track are identified recoiling against the tag. The quantity $U = E_{miss} - P_{miss}$ is calculated, where E_{miss} and P_{miss} are the missing energy and missing momentum in the event. For a tagged event with a semileptonic decay E_{miss} and P_{miss} are the components of the four-momentum of the neutrino. U peaks at zero if only a neutrino is missing. The U distribution in 56 pb$^-$1 of CLEO-c data is shown in Fig. 4 where a clean signal of about 100 events is observed for $D \to \pi e^+ \nu_e$ with S/N 20/1 [21]. In previous analyses at B Factories and fixed target experiments the background was usally larger than the signal see for example [22].

The kinematic power of running at threshold also allows previously unobserved modes such as $D^0 \to \rho^- e^+ \nu_e$ to be easily identified [21]. BES II have performed similar analyses [23] [24] and results are in good agreement with CLEO-c. Selected CLEO-c absolute semileptonic branching ratio measurements are compared to PDG values in Table 6.

This modest data sample has already produced several important measurements. The ratio of $\Gamma(D^0 \to K^- e^+ \nu_e)/\Gamma(D^+ \to \overline{K}^0 e^+ \nu_e)$ is expected to be unity by isospin. The PDG value is 1.35 ± 0.19 [6]. Using the measured branching fractions for the decays of $D^0 \to K^- e^+ \nu_e$ and $D^+ \to \overline{K}^0 e^+ \nu_e$ and the lifetimes of the D^0 and D^+ [6] CLEO-c obtains the ratio of the decay widths

$$\frac{\Gamma(D^0 \to K^- e^+ \nu_e)}{\Gamma(D^+ \to \overline{K}^0 e^+ \nu_e)} = 1.00 \pm 0.05 \pm 0.04 \qquad (16)$$

where the first error is statistical and the second systematic. The CLEO0-c result, and a less precise result from BES II, are consistent with unity thereby

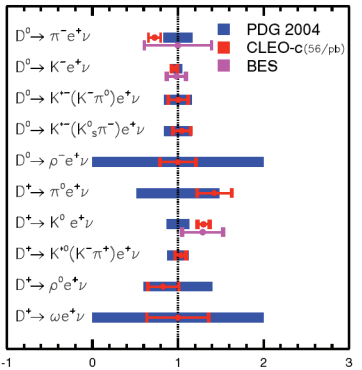

Figure 5: *CLEO-c, BES II and the PDG values for a range of charm meson semileptonic branching ratios. Results are normalized to PDG values for ease of display.*

solving a long standing puzzle.

As the charm CKM matrix elements are known from unitarity, the absolute differential charm semileptonic rate

$$\frac{d\Gamma(D \to \pi e^+ \nu_e)}{dq^2} = (\text{const.})|V_{cd}|^2 f_+(q^2)^2 \tag{17}$$

tests calculations of charm semileptonic form factor q^2 dependence and form factor magnitude. A precision absolute branching fraction measurement also tests the magnitude of the form factor if an assumption is made about the functional form of the q^2 dependence. Recently there have been several beautiful measurements of the form factor shape in $D \to K\ell^+\nu_\ell$ and $D \to \pi\ell^+\nu_\ell$ by CLEO, FOCUS, Belle, and BABAR. By reconstructing two D mesons in $e^+e^- \to c\bar{c}$ events at 10 GeV Belle are able to make an absolute measurement and so a determination of the form factor magnitude as well. CLEO-c promise results soon.

In a pseudoscalar to pseudoscalar transition the differential rate is proportional to the third power of the daughter hadron momentum due to the P-wave nature of the decay. The p^3 term dominates the differential rate. The form factor parameterizes the additional q^2 dependence of the semileptonic amplitude arising from non-perturbative QCD. The form factor is largest at

$q^2 = q^2_{max}$ where the daughter hadron is stationary in the rest frame of the D meson and decreases by about a factor of two at $q^2 = 0$. Since most of the rate is at $q^2 = 0$ it is traditional to normalize the form factor at $q^2 = 0$, however it is simpler to calculate the form factor at $q^2 = q^2_{\rm max}$ where the rate vanishes as we at the edge of phase space.

Several choices for the functional form of $f_+(q^2)$ have been proposed. The simple pole model is a form predicted by vector meson dominance also called nearest pole dominance [25], in which exchange is dominated by the lowest lying vector meson (the spectroscopic pole) with the quantum numbers of the $c \to s$ transition.

$$f_+(q^2) = \frac{f_+(q^2 = 0)}{1 - \frac{q^2}{m^2_{pole}}} \tag{18}$$

Where $m_{pole} = M_{D^*}$ for $D \to \pi\ell\nu_\ell$ and $m_{pole} = M_{D^*_s}$ for $D \to K\ell\nu_\ell$. At lower values of q^2 the spectrum has contributions from higher poles, and to account for this the modified pole or BK parametrization was proposed [26]

$$f_+(q^2) = \frac{f_+(q^2 = 0)}{(1 - \frac{q^2}{m^2_{pole}})(1 - \frac{\alpha q^2}{m^2_{pole}})} \tag{19}$$

Here α parameterizes the contributions of all additional poles combined, and m_{pole} remains the spectroscopic pole. The q^2 spectrum in $D \to K\ell\nu_\ell$ can be described by the pole model within experimental resolution, but the pole mass needed to do so is far from the spectroscopic pole. The B-K parametrization describes the data for $D \to K\ell\nu_\ell$ within the experimental precision and also provides a way to parameterize the lattice calculations. A comparison of a lattice prediction for α to data is shown for FOCUS and BABAR data in Figure 6. The precision of the prediction and the measurements are at the 10% level. Agreement is good, although the errors are still large.

The FOCUS, BABAR and Belle measurements check the shape of the form factor. The normalization can be checked by either fitting to the differential rate to obtain $f^+(0)V_{cx}$ or from the absolute branching fraction, in both cases using unitarity and the D meson lifetime. A comparison of absolute branching fraction measurements and the LQCD prediction is shown in Figure 7. Here while the measurement has recently become much more precise, the precision of the prediction lags experiment significantly. Agreement is reasonable, although the theory errors are in urgent need of being reduced.

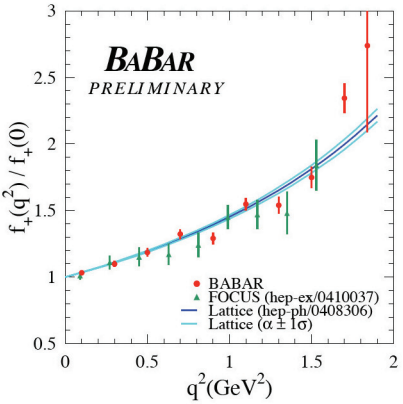

Figure 6: *The differential rate, normalized to the rate at $q^2 = 0$ for the decay $D^0 \to K^-\ell\nu_\ell$ after removal of phase space factors, compared to the LQCD prediction.*

Table 7: Experimental measurements and theoretical predictions of shape parameters in $D \to K$ semileptonic decay.

Measurement	α	m_{pole} GeV
E691 1989 [27]	–	$2.1^{+0.4}_{-0.2} \pm 0.2$
CLEO 1991 [28]	–	$2.0^{+0.4+0.3}_{-0.2-0.2}$
MARKIII 1991 [29]	–	$1.8^{+0.5+0.3}_{-0.2-0.2}$
CLEOII 1993 [30]	–	$2.00 \pm 0.12 \pm 0.18$
E687 1995 [31]	–	$1.87^{+0.11+0.07}_{-0.08-0.06}$
CLEOIII 2005 [22]	$0.36 \pm 0.10^{+0.03}_{-0.07}$	$1.89 \pm 0.05^{+0.04}_{-0.03}$
FOCUS 2005 [32]	$0.28 \pm 0.08 \pm 0.07$	$1.93 \pm 0.05 \pm 0.03$
Belle 2006 [33]	$0.52 \pm 0.08 \pm 0.06$	–
BABAR 2006 [34]	$0.43 \pm 0.03 \pm 0.04$	$1.854 \pm 0.016 \pm 0.020$
LQCD [35]	$0.50 \pm 0.06 \pm 0.07$	–
LCSR [36]	$-0.07^{+0.15}_{-0.07}$	–
CQM [37]	0.24	–

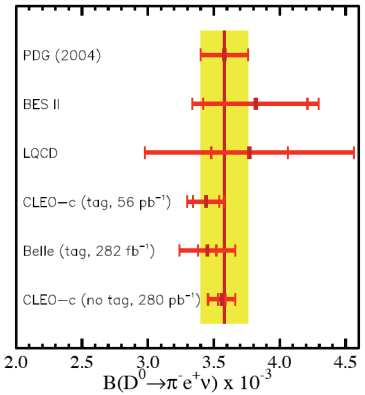

Figure 7: *Measurements of the absolute branching fraction for* $D \to \pi e^+ \nu_e$ *and comparison to LQCD. A preliminary result from an untagged measurement from CLEO-c has also been included.*

The q^2 resolution at a charm factory is about 0.025 GeV^2, which is more than a factor of 10 better than CLEO III which achieved a resolution of 0.4 GeV^2 [22]. This huge improvement is due to the kinematics at the $\psi(3770)$ resonance, i.e. that the D meson momentum is known. (Belle have recently achieved similar q^2 resolution by using a charm tagging technique at 10 GeV.) The combination of large statistics, and excellent kinematics will enable the absolute magnitudes and shapes of the form factors in every charm semileptonic decay to be measured, in many cases to a precision of a few per cent. This is a stringent test of LQCD.

By taking ratios of semileptonic and leptonic rates, CKM factors can be eliminated. Two such ratios are

$$\begin{aligned} &\Gamma(D^+ \to \pi^0 e^+ \nu_e)/\Gamma(D^+ \to \mu\nu_\mu) \\ &\Gamma(D_s^+ \to (\eta \text{ or } \phi) e^+ \nu_e)/\Gamma(D_s^+ \to \mu\nu_\mu) \end{aligned} \qquad (20)$$

These ratios depend purely on hadronic matrix elements and can be determined to 8% and so will test amplitudes at the 4% level. This is an exceptionally stringent test of LQCD.

If LQCD passes the experimental tests outlined above it will be possible to use the LQCD calculation of the $B \to \pi$ form factor with increased confidence

Table 8: Experimental measurements and theoretical predictions of shape parameters in $D \to \pi$ semileptonic decay.

Measurement	α	m_{pole} GeV
CLEOIII 2005 [22]	$0.37^{+0.20}_{-0.31} \pm 0.15$	$1.86^{+0.10+0.10}_{-0.09-0.03}$
FOCUS 2005 [32]	–	$1.91^{+0.03}_{-0.15} \pm 0.07$
Belle 2006 [33]	$0.10 \pm 0.21 \pm 0.10$	–
LQCD [35]	$0.44 \pm 0.06 \pm 0.07$	–
LCSR [36]	$0.01^{+0.11}_{-0.07}$	–
CQM [37]	0.30	–

at the B factories to extract a precision V_{ub} from $B \to \pi e^- \bar{\nu}_e$. BaBar and Belle will also be able to compare the LQCD prediction of the shape of the $B \to \pi$ form factor to data as an additional cross check.

Successfully passing the experimental tests allows the charm factories to use LQCD calculations of the charm semileptonic form factors to directly measure $|V_{cd}|$ and $|V_{cs}|$. Using the isospin averaged semileptonic widths $\Gamma(D \to Ke^+\nu_e)$ and $\Gamma(D \to \pi e^+ \nu_e)$ [21] and the LQCD prediction of the semileptonic partial width [35] I obtain

$$\begin{aligned} V_{cs} &= 0.957 \pm 0.017 \pm 0.093 \\ V_{cd} &= 0.213 \pm 0.008 \pm 0.029 \end{aligned} \tag{21}$$

where the uncertainties are experimental statistical, experimental systematic and from LQCD. The results are consistent with the unitarity values

$$\begin{aligned} V_{cs} &= 0.9745 \pm 0.0008 \\ V_{cd} &= 0.2238 \pm 0.012 \end{aligned} \tag{22}$$

V_{cd} has previously been determined from neutrino production of di-muons off of nucleons, and V_{cs} has been determined from $W \to cs$ transitions at LEP to be [6]

$$\begin{aligned} |V_{cs}| &= 0.976 \pm 0.014 \\ |V_{cd}| &= 0.224 \pm 0.012 \end{aligned} \tag{23}$$

Table 9: LQCD impact (in per cent) on the precision of CKM matrix elements. A charm factory data set of 3/fb and a B factory data set of 500/fb is assumed.

	V_{cd}	V_{cs}	V_{cb}	V_{ub}	V_{td}	V_{ts}
2004	7	11	4	15	36	39
LQCD	2	2	3	5	5	5

Due to the large theoretical uncertainties in the CLEO-c numbers the extracted values of V_{cs} and V_{cd} should be considered as tests of LQCD. Nonetheless, they are the single most precise determinations of V_{cs} and V_{cd} to date. With 0.75fb^{-1} of data the CLEO-c precision is expected to be respectively:

$$\begin{aligned} |V_{cs}| &= \sqrt{0.8\% \oplus \delta\Gamma/2\Gamma} \\ |V_{cd}| &= \sqrt{1.6\% \oplus \delta\Gamma/2\Gamma} \end{aligned} \tag{24}$$

Where $\delta\Gamma/\Gamma$ is the uncertainty in the partial rate from theory. This in turn allows new unitarity tests of the CKM matrix. For example, the second row of the CKM matrix can be tested at the few % level. With the current measurements I find:

$$1 - (|V_{cs}|^2 + |V_{cd}|^2 + |V_{cb}|^2) = 0.037 \pm 0.181 \tag{25}$$

which is consistent with unitarity, with an uncertainty dominated by the LQCD charm semileptonic form factor magnitude The measurements also allow the first column of the CKM matrix to be tested with similar precision to the first row (which is currently the most stringent test of CKM unitarity); finally, the ratio of the long sides of the *uc* unitarity triangle will be tested to a few percent.

Table 9 provides a summary of projections for the precision with which the CKM matrix elements will be determined if LQCD passes the charm factory tests in the D system. In the tabulation the current precision of the CKM matrix elements is obtained by considering methods applicable to LQCD, for example the determination of $|V_{cb}|$ and $|V_{ub}|$ from inclusive decays and OPE is not included. The projections are made assuming B factory data samples of 500 fb^{-1} and improvement in the direct measurement of $|V_{tb}|$ expected from the Tevatron experiments [5].

5.4 The bottom line

How can we be sure that if LQCD works for D mesons it will work for B mesons? Or, equivalently, is charm factory data sufficient to demonstrate that lattice systematic errors are under control? There are a number of reasons to answer this question in the affirmative. (1) There are two independent effective field theories: NRQCD and the Fermilab method. (2) The CLEO-c, and later BESIII, data provide many independent tests in the D system; leptonic decay rates, and semileptonic modes with rate and shape information. (3) The B factory data provide additional independent cross checks such as $d\Gamma(B \to \pi\ell\nu)/dp_\pi$. (4) Unlike models, methods used for the D/B system can be tested in heavy onia with measurements of masses, and mass splittings, Γ_{ee} and electromagnetic transitions. (5) The main systematic errors limiting accuracy in the D/B systems are: chiral extrapolations in $m$light, perturbation theory, and finite lattice spacing. These are similar for charm and beauty quarks. In my opinion a combination of CLEO-c and BES III data in the D systems and onia, plus information on the light quark hadron spectrum, can clearly establish whether or not lattice systematic errors are under control.

While this picture is encouraging, experimentalists also have concerns. The lattice technique is all encompassing but LQCD practitioners are very conservative about what can be calculated. For example when there was a hint that $\sin 2\beta(\psi K_S^0) \neq \sin 2\beta(\phi K_S^0)$, and when CP violation was observed in $B \to K\pi$ [38] the lattice was not able to contribute. There is a pressing need to move beyond the limited set of easy to calculate quantities in the next few years: for example resonances such as ρ, ϕ and K^* may be difficult to treat on the lattice, but they feature in many important D semileptonic decays which will be well measured by the charm factories. There is also a need to be able to calculate for states near threshold such as $\psi(2S)$ and $D_s(0)^+$, and hadronic weak decays in the B and D systems as well.

6 New physics searches with charm

In the early part of the 20th Century table top nuclear β decay experiments conducted at the MeV mass scale probed the W at the 100 GeV mass scale. In an analogous way can we find violations of the Standard Model by studying low energy processes? The existence of multiple fermion generations appears to

originate at very high mass scales and so can only be studied indirectly. Mixing, CP violation, and rare decays may investigate the new physics at these scales through intermediate particles entering loops. Why is charm a good place to look? In the charm sector, the SM contributions to these effects are small, in other words, a background free search for new physics is possible (see caveats below). Typically $D^0 - \bar{D}^0$ mixing $\mathcal{O}(< 10^{-2})$, CP asymmetry $\mathcal{O}(< 10^{-3})$ and rare decays $\mathcal{O}(< 10^{-6})$. In addition, charm is a unique probe of the up-type quark sector (down quarks in the loop). The sensitivity of searches for new physics in charm depends on high statistics rather than high energy.

6.1 Charm Mixing

Mixing has been a fertile ground for discoveries. The neutral kaon mixing amplitude occurs at the same order as the kaon decay width $\propto |V_{us}|^2$ and so the mixing rate is of order unity. The mixing rate, which vanishes in the SU(4) symmetry limit, was measured in 1958, was used to bound the charm quark mass, 16 years before the discovery of charm. The CP violating part of $K^0\bar{K}^0$ mixing, ϵ_K, first measured in 1964 was a crucial clue that the top quark existed, thirty years before its discovery. In the $B^0\bar{B}^0$ system the top quark dominates the mixing amplitude, the B decay width is Cabibbo suppressed $\propto |V_{cb}|^2$ and mixing is also Cabibbo suppressed $\propto |V_{td}|^2$. The mixing rate is again of order unity, which was an early indication that $m_{\rm top}$ was large. In $D^0\bar{D}^0$ mixing the amplitude is proportional to $\sin^2\theta_c \sim 0.05$ but the decay width is not Cabibbo suppressed ($V_{cs} \sim 1$). There is additional GIM suppression of order $(m_s^2 - m_d^2)/m_W^2 = 0$ in the SU(3) limit, and so the rate for D mixing in the SM is the product of Cabibbo suppression and an SU(3) breaking term, the latter being extremely difficult to estimate [39]

$$\text{mixing} \sim \sin^2\theta_c \times [SU(3)\text{ breaking}]^2 \tag{26}$$

In consequence, SM predictions span the range bounded by the experimental upper limit of 1% and the short distance box diagram rate of $\mathcal{O}(10^{-8})$ [40] and the di-penguin rate $\mathcal{O}(10^{-10})$ [41]. New physics predictions span the same large range [42], implying that the observation of D mixing alone is not a clear indication of new physics. However, the current experimental bounds $\mathcal{O}(10^{-2})$ [43, 44, 45] already constrain new physics models.

Table 10: Summary of measurements of y_{CP}

		%
Belle	2003	$1.15 \pm 0.69 \pm 0.38$
BABAR	2003	$0.8 \pm 0.4^{+0.5}_{-0.4}$
CLEO	2001	$-1.1 \pm 2.5 \pm 1.4$
Belle	2001	$-0.5 \pm 1.0^{+0.7}_{-0.8}$
FOCUS	2000	$3.4 \pm 1.4 \pm 0.7$
E791	1996	$0.8 \pm 2.9 \pm 1.0$

Neutral meson mixing is characterized by two dimensionless parameters

$$x = \Delta M/\Gamma, y = \Delta\Gamma/2\Gamma \tag{27}$$

where $\Delta m = m_1 - m_2$ is the mass difference and $\Delta\Gamma = \Gamma_1 - \Gamma_2$ is the width difference between the two neutral D meson CP eigenstates, and Γ is the average width. If mixing occurs either x or y or both are non-zero.

The lifetime difference y is constructed from the decays of a D into physical states, and so it is expected to be dominated by SM contributions. In addition to the tiny SM contribution, the mass difference, x, is sensitive to new particles in the box diagram loop. Thus, new physics can significantly modify x, leading to $x >> y$. This signature for new physics is lost, however, if a relatively large y of $\mathcal{O}(1\%)$ is observed [46]. As CP violating effects in mixing in the SM must involve the third quark generation, and since the bottom quark contribution to the box diagram is highly suppressed, $\propto V_{cb}V_{ub}^*$, the observation of CP violating effects in D mixing would be an unambiguous signal of new physics.

Mixing, and CP-violation in mixing, can be searched for in a variety of ways. Measurements of y are summarized in Table 10 and are reviewed in [44] [43] [45]. The world average is

$$y_{CP} = (0.9 \pm 0.4)\% \tag{28}$$

In the limit of CP-conservation $y_{CP} = y$. The 95% C.L. range of y is the horizontal band in Figure 8.

Searching for D mixing in semileptonic decays is straightforward as there

Table 11: Summary of searches for D^0 mixing with semileptonic decays. (Limits are 90% C.L.)

	R_M	U. L. $\times 10^{-3}$
Belle	2005	1.0
CLEO	2005	7.8
BABAR	2004	4.2
FOCUS	2002	1.01
E791	1996	5.0

is an unambiguous signal that mixing has occurred:

$$D^{*+} \to D^0\pi^+_{\rm tag}, D^0 \to K^- e^+ \nu_e \text{ unmixed} \tag{29}$$

$$D^{*+} \to D^0\pi^+_{\rm tag}, D^0 \to \overline{D^0} \to K^+ e^- \overline{\nu_e} \text{ mixed} \tag{30}$$

The flavor of the D meson at birth is tagged by the sign of the pion from the D^*, the flavor at decay is tagged by the sign of the lepton. The time evolution of a neutral D meson depends on the type of state into which it decays, and it is particularly straightforward for semileptonic final states.

$$\Gamma_{\rm unmix} \propto e^{-t/\tau} \tag{31}$$

$$\Gamma_{\rm mix} \cong e^{-t/\tau}(t/\tau)^2 \frac{1}{4}(x^2 + y^2) \tag{32}$$

where t is the proper time of the D^0 decay, and the approximation is valid in the limit of small mixing rates. The time integrated mixing rate relative to the unmixed rate is

$$R_{\rm mix} = \frac{1}{2}(x^2 + y^2) \tag{33}$$

The rate depends quadratically on x and y and does not provide a way to differentiate between them. Table 11 is a compilation of results. The 95% CL limit on $R_{\rm mix}$, a circular region centered on $(x = 0, y = 0)$ is displayed in Figure 8.

Another way to search for D mixing is in the hadronic decay $D^0 \to K^-\pi^+$. This method is sensitive to a linear function of x^2 and y, and can differentiate between them. The most restrictive mixing constraints come from this mode.

Table 12: Mixing searches using $D^0 \to K^+\pi^-$. Comparison of the 95% C.L. limits in per cent for the fit output parameters when CP conservation is assumed in the fit. The FOCUS entries are one dimensional limits.

	R_D $[\times 10^{-3}]$	y' [%]	$x'^2/2$ [%]
2006 Belle [47]	$3.77 \pm 0.08 \pm 0.05$	(-2.8, 2.1)	< 0.036
2005 FOCUS [48]	$4.29 \pm 0.63 \pm 0.28$	(-11.0, 6.6)	< 0.385
2003 BABAR [49]	$3.57 \pm 0.22 \pm 0.27$	(-5.6, 3.9)	< 0.11
2000 CLEO [50]	$3.32^{+0.63}_{-0.65} \pm 0.40$	(-5.8, 1.0)	< 0.041

The unmixed signal is the Cabibbo favored (CF) $D^0 \to K^-\pi^+$. The mixed signal is $D^0 \to \bar{D^0} \to K^+\pi^-$ but it has a background from doubly Cabibbo suppressed (DCS) decays $D^0 \to K^+\pi^-$. Interference between the CF and DCS decays, which is linear in y', gives rise to the power of the method. The proper decay time distribution is fit to distinguish between DCS and the mixing signal. For $|x|, |y| \ll 1$ and negligible CP-violation, the decay time distribution for $D^0 \to K^+\pi^-$ is

$$\frac{dN}{dt} = [R_D + \sqrt{R_D} y' \Gamma t + 1/4(x'^2 + y'^2)(\Gamma t)^2] e^{-\Gamma t} \tag{34}$$

where R_D is the ratio of DCS to CF decay rates. In principle, there is a strong phase difference, $\delta_{K\pi}$, between the CF and DCS amplitudes which rotates x and y to x' and y'. To search for CP-violation one determines R_D, x' and y' separately for D^0 and $\bar{D^0}$. Most recent analyses have been made both with and without requiring CP conservation. Table 12 is a compilation of results. Figure 8 shows: (a) That the Belle recent analysis is an impressive step forward in sensitivity. (b) There remains no statistically significant evidence for D meson mixing although the situation is becoming increasingly tantalizing.

At a charm factory as $\psi(3770) \to D\overline{D}$ and $C = -1$ quantum coherence guarantees that the mixing signature $D^0 \to K^-\pi^+$, $\overline{D^0} \to D^0 \to K^-\pi^+$, cannot be mimicked by one D undergoing a DCS decay. Combining with semileptonic decays to increase sensitivity, a 0.75/fb (15/fb) sample reaches $x < 1.7\%$ $(x < 0.4\%)$. A more sophisticated approach: The Quantum Correlated Analysis (TQCA) makes a combined fit to single and double flavor and CP tag yields, which are a function of $\mathcal{B}_i, x^2, y, \delta_i$. TQCA is estimated to achieve a sensitivity for 0.75/fb (10/fb, 1,000/fb) of $x < 2.4\%$ $(x < 1.3\%, x < 0.1\%)$ and

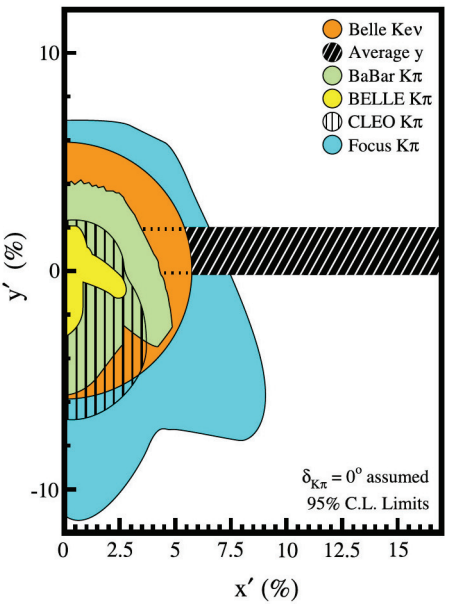

Figure 8: *The status of searches for D meson mixing at the 95% C.L. The semicircle $x^2 + y^2$ is the most restrictive limit from semileptonic decays. For $D^0 \to K^+\pi^-$, $x - y$ contours are shown separately for Belle, BABAR, CLEO, and FOCUS. For the former three, the limits allow for CP violation in the decay amplitude, the mixing amplitude, and the interference between these two processes. To place y $\delta_{k\pi} = 0$ is assumed. The world average allowed range for y is the horizontal band. If $\delta_{k\pi} \neq 0$ the allowed y region would rotate clockwise about the origin by an angle $\delta_{k\pi}$.*

$y < 1.2\%$ ($y < 0.3\%, y < 0.03\%$). Purohit showed at this workshop that a B Factory with 10/ab in a $D(t) \to K^-\pi^+$ analysis reaches $x < 1\%$ and Nakada showed that at LHC-b in one year an analysis of $D(t) \to K^0\pi\pi$ reaches a sensitivity of $x < 0.4\%$.

6.2 Measurement of the hadronic phase

At the $\psi(3770)$ if a D^0 is observed to decay to a CP eigenstate which is CP even: then in the limit of CP conservation, the state recoiling against the tag has a definite CP as well and it must be of opposite sign, in this case CP odd. Consider the situation where the second D decays to a flavor mode:

which defines two triangles from which $\cos\delta_{K\pi}$ can be determined. Determining $\delta_{K\pi}$ is necessary to rotate x' and y' measured in $D(t) \to K\pi^-$ to x and y. The method is limited by the number of CP tags, but can be extended to many modes simultaneously in the TQCA where the sensitivity for 0.75/fb (10 /fb) is $\cos\delta_{K\pi} \pm 0.13$ (± 0.05).

6.3 Charm contributions to ϕ_3/Γ

The phase of V_{ub}, ϕ_3/Γ can be determined by the interference between $b \to u$ and $b \to c$ decays where the D decays to a CP eigenstate or a flavor mode. In the first the D mixing parameters are needed and in the second knowledge of $\cos\delta_{K\pi}$. Both methods require very large integrated luminosity. A third method, the Dalitz method, is currently the most accessible method experimentally. Here $B \to DK^+, D \to K^0_S\pi\pi$ With this approach the B factories have measured $\phi_3 = 68 \pm 14 \pm 13 \pm 11^\circ$ [51], and $\gamma = 67 \pm 28 \pm 13 \pm 11$ [52], where the third uncertainty is from the D decay model and can be reduced by analyzing CP tagged Dalitz plots for $D \to K^0_S\pi\pi$ at charm factories. A study by Bondar [53] estimates statistical uncertainty on ϕ_3/γ at a B-Factory from $B \to DK^+$ to be ($\pm 6^\circ$ for 1/ab and $\pm 2^\circ$ for 10/ab. The integrated luminosity needed to provide the number of CP tagged $D \to K^0_S\pi\pi$ to match the statistical uncertainty from the super B factory for $\pm 6^\circ$ is 0.75/fb and $\pm 2^\circ$ for 10/fb. The latter is a good match to the capabilities of BES III. CLEO-c sensitivity (281/pb) is consistent with Bondar's prediction

6.4 Charm CP Violation

Three types of CP violation are possible. (1) CP violation in the $D^0 - \bar{D}^0$ mixing matrix. As D mixing is very small, CP-violation in D mixing, commonly parameterized by $A_{\rm m}$, is negligible both in the SM and many of its extensions. Experiments are not yet statistically sensitive to it, and so we will not consider it. (2) CP violation in the interference between mixing and decay. It is time dependent, since mixing is involved but it is also small since D mixing is suppressed. It is a good place to search for new physics, but experiment is only now becoming sensitive enough. (3) Direct CP violation. This occurs when the absolute value of the D decay amplitude to a final state f is not equal to the CP-conjugate amplitude

For direct CP-violation to occur, two amplitudes with different weak

phases and different strong phases must contribute to the decay process. The expression for the CP asymmetry A_{CP} is

$$A_{\rm CP} = \frac{\Gamma(D^0 \to f) - \Gamma(\bar{D^0} \to f)}{\Gamma(D^0 \to f) + \Gamma(\bar{D^0} \to f)}$$
$$= \frac{2ImA_1A_2\sin(\delta_1 - \delta_2)}{|A_1|^2 + |A_2|^2 + 2ReA_1A_2^*\cos(\delta_1 - \delta_2)} \quad (36)$$

where A_i, δ_1 and δ_2 are the moduli of the amplitudes, the weak phase difference and the strong phase differences, respectively.

In the SM, direct CP violation in the D meson system occurs for singly Cabibbo suppressed decays such as $D^0 \to \pi^+\pi^-/K^+K^-/K^+K^-\pi^+$, because for these decays there are several candidates for the second weak amplitude including penguin graphs, WA diagrams for D_s^+ decays, and channels with a K_S^0 54).

Predictions for A_{CP} are difficult due to the unknown strong phase. In the SM $A_{CP} < 10^{-3}$. New physics can produce $A_{CP} \approx 1\%$. However, if an asymmetry at the 1% level was observed, one could not rule out a hadronic enhancement of the SM. Therefore it is necessary to analyze many channels to elucidate the source of CP violation. Selected measurements of $A_{\rm CP}$ are shown in Figure 9. Sensitivity approaches 1%.

At the $\psi(3770)$ CP violating asymmetries can be measured by searching for events with two CP odd or two CP even final states. For $D \to K^+K^-$ charm factory sensitivity for (0.75/fb , 10/fb, 1,000/fb) is ($A_{CP} < 0.08, < 4 \times 10^{-3}, < 6 \times 10^{-5}$) at 90% C.L. Nakada has shown that in one year at LHC-b the sensitivity is $A_{CP} < 1.4 \times 10^{-4}$. An alternative is to search for CP violation in $D \to f, D_{CP} \to$ flavor mode. The sensitivities at charm factories are ($A_{CP} < 0.025, < 6 \times 10^{-3}, < 7 \times 10^{-4}$) at 90% C.L. respectively.

Alternative search strategies include Dalitz plot analyses that are particularly sensitive since they probe CP-violating phases in the amplitude rather than in the rate, are beginning to be attempted. These can be performed at charm threshold exploiting the quantum coherence and at higher energies.

6.5 Rare Decays

In the SM flavor changing neutral currents are suppressed by the GIM mechanism. The dilepton decay proceeds by penguin annihilation or a box diagram. SM expected branching ratios are $\mathcal{B}(D^0 \to e^+e^-) \sim 10^{-23}$, $\mathcal{B}(D^0 \to$

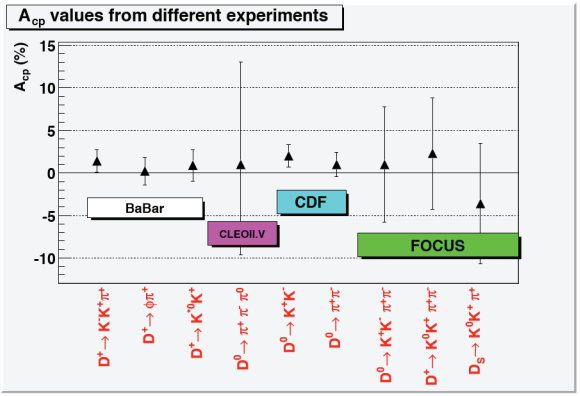

Figure 9: *Selected searches for direct CP violation in D decay.*

$\mu^+\mu^-) \sim 3 \times 10^{-13}$. The lepton flavor violating mode $D^0 \to e^\pm\mu^\mp$ is strictly forbidden. New physics may enhance these processes. For example R-parity violating SUSY predicts $\mathcal{B}(D^0 \to e^+e^-) \leq 10^{-10}$, $\mathcal{B}(D^0 \to \mu^+\mu^-) \leq 10^{-6}$ and $D^0 \to e^\pm\mu^\mp \leq 10^{-6}$ [55]. The result of a BABAR search which significantly improved upon previous upper limits [56], is shown in Figure 10 and Table 13 respectively. BES III will reach a sensitivity of few $\times 10^{-7}$ a super flavour factory at 10 GeV with 50/ab will achieve afew $\times 10^{-9}$ and if operated at the $\psi(3770)$ also afew $\times 10^{-9}$. However the 10 GeV measurement is likely to be compromised by large backgrounds while the $\psi(3770)$ measurement will have little background and so the latter will be far superior, although still four orders of magnitude above the SM rate.

If new physics is present in rare D decays it is likely to be more experimentally accessible in the modes $D \to X\ell^+\ell^-$. In the SM the $\mathcal{B}(D^+ \to \pi e^+e^-) = 2.0 \times 10^{-6}$. In R-parity violating SUSY the integrated rate increases by only 20%, however the differential dilepton mass distribution is significantly modified compared to the SM at low and high dilepton masses well away from the $\rho/\omega/\phi$ SM contributions. Several experiments have recently made searches, see Table 13. If $D^+ \to \pi e^+e^-$ is at the SM level, only 1 evt/fb will be produced at the $\psi(3770)$ implying BESIII will observe 24 events (including a factor of

Table 13: Selected recent searches for rare D decays.

Mode	Upper Limit $\times 10^{-6}$	
e^+e^-	BABAR	1.2
$\mu^+\mu^-$	BABAR	1.3
$e^\pm\mu^\mp$	BABAR	0.81
πe^+e^-	CLEO-c	7.4
Ke^+e^-	BABAR	3.6

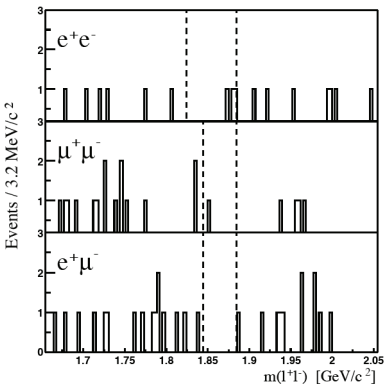

Figure 10: *The di-lepton invariant mass distribution for* $D^0 \to e^+e^-$, $D^0 \to \mu^+\mu^-$ *and* $D^0 \to e^\pm\mu^\mp$. *The dashed lines indicate the signal mass region.*

two for $D^+ \to \pi\mu^+\mu^-$.) While this sounds modest, just imagine if these event are clustered at low or high dilepton mass well away from SM contributions, it would be clear evidence for new physics!

In summary the experimental sensitivity for both D^0 and D^+ rare decays is in the range $10^{-5} - 10^{-6}$. For some modes, notably $D \to \pi^+\ell^+\ell^-$, measurements are beginning to confront models of new physics. In other cases, measurements are far above the SM prediction. The outlook for rare charm decays is promising. CDF, the B Factories, the charm factories, ATLAS/CMS and LHC-b will all contribute. For selected projections see [44].

7 SUMMARY

New physics searches in the charm sector involving mixing, $CP-$violation and rare decays have become considerably more sensitive in the past several years, however, all results are null.

In charm's role as a natural testing ground for QCD techniques, there has been solid progress. Data at the $\psi(3770)$ from BESII and CLEO-c, and later BESIII, is finally producing a new era of precision absolute charm branching ratios. This is well-matched to developments in theory, especially the lattice, which has a goal to calculate to a few percent precision in the $D, B, \Upsilon,$ and ψ systems. CLEO-c, and later BES III, will provide few per cent precision tests of lattice calculations in the D system and in heavy onia, which will quantify the accuracy for the application of LQCD to the B system. If all goes to plan, BABAR, Belle, CDF, D0, CMS, ATLAS, and LHC-b data, in combination with LQCD will produce a few per cent determinations of $|V_{ub}|, |V_{cb}|, |V_{td}|$, and $|V_{ts}|$ thereby maximizing the sensitivity of the flavor physics program to new physics beyond the SM this decade and aid understanding beyond the SM physics at the LHC in the coming decade.

8 Acknowledgements

I thank my colleagues on BABAR, Belle, BES II, CDF, CLEO, D0, FOCUS and LHC-b for many valuable discussions. Bo Xin is thanked for technical assistance. I am particularly grateful to Stefano Bianco for organizing a superb meeting in Frascati and for his patience while I completed this manuscript.

References

1. A.D. Sakharov, JETP Lett. **6** 24 (1967).
2. C.T.H. Davies *et al.* Phys. Rev. Lett. **92** 022001 (2004).
3. CLEO-c/CESR-c Taskforces and CLEO Collaboration, Cornell LEPP Preprint CLNS 01/1742 (2001).
4. A decription of the BES III physics program and detector, and the design of the BEPCII accelerator may be found at the http://bes.ihep.ac.cn/conference/wksp04

5. J. Swain and I. Taylor, Phys. Rev. **D58** 093006 (1998).

6. S. Eidelman *et al.* Phys Lett. **B593** (2004) 1.

7. The Heavy Flavours Averaging Group (HFAG) summer 2005.

8. The PDG reports $\mathcal{B}(D \to \pi e^+ \nu_e)$ with an error of 20%, but the sole measurement, by the Mark III experiment, reports an error of 45%.

9. G. Bellini, I.I. Bigi and P.J. Dornan, Phys. Rep. **289** 1 (1997).

10. BaBar Collaboration, B. Aubert *et al.* Phys. Rev. D **71** 091104 (2005).

11. MARK III Collaboration, R.M. Baltrusaitis *et al.*, Phys. Rev. Lett. **56** 2140 (1986).

12. MARK III Collaboration, J. Adler *et al.*, Phys. Rev. Lett. **60** 89 (1988).

13. CLEO Collaboration, Q. He *et al.*, Phys. Rev. Lett. **95** 121801 (2005).

14. ALEPH Collaboration R. Barate *et al.* Phys. Lett. B **405** 191 (1997).

15. The CLEO measurement of $\mathcal{B}(D^0 \to K^-\pi^+)$ is obtained by combining CLEO Collaboration, D.S. Akerib *et al.*, Phys. Rev. Lett. 71 3070 (1993) and CLEO Collaboartion M. Artuso *et al.,* Phys. Rev. Lett. **80** 3193 (1998).

16. The CLEO measurement is obtined using [15] and CLEO Collaboration R. Balest *et al.,* Phys. Rev. Lett. **72** 2328 (1994).

17. MARK III Collaboratiion, J. Adler *et al.,* Phys. Rev. Lett. **60** 89 (1988).

18. CLEO Collaboration, M. Artuso *et al.*, arXiv:hep-ex/050857.

19. (MILC Collaboration) C. Aubin *et al.* hep-lat/0506030 (2005).

20. The BES II Collaboration M. Abilikim *et al.* Phys. Lett. B 610, 183 (2005).

21. CLEO Collaboration, G.S. Huang *et al.,* Phys. Rev. Lett. **95** 1818101 (2005). CLEO Collaboration T.E. Coan *et al.*, Phys. Rev. Lett. **95** 181802 (2005).

22. CLEO Collaboration, G.S. Huang *et al.*, Phys. Rev. Lett.**94** 011802 (2005).

23. BES Collaboration, M. Ablikim *et al.* hep-ex/0410030 submitted to Phys. Lett. (2004).

24. BES Collaboration, M. Ablikim *et al.* Phys. Lett. **B597** 39 (2004).

25. J.D. Richman and P. R. Burchat Rev. Mod. Phys. **67** 893 (1995).

26. D. Becirevic and A.B. Kaidelov, Phys. Lett. **B478**, 417 (2000).

27. E691 Collaboration J.C. Anjos *et al.,* Phys. Rev. Lett. **62** 1587 (1989).

28. CLEO Collaboration, G. Crawford *et al.,* Phys. Rev. D **44**, 3394 (1991).

29. MARK III Collaboration, A. Bai *et al.,* Phys. Rev. Lett. **66**, 1011 (1991).

30. CLEO Collaboration, A. Bean *et al.,* Phys. Lett. B **317**, 647 (1993).

31. E687 Collaboration, P.L. Fabretti *et al.,* Phys. Lett. B **317**, 647 (1995).

32. FOCUS Collaboration, J.M. Link *et al.,* Phys. Let. B**697**, 233 (2005).

33. Belle Collaboration, L. Widhalm *et al.,* hep-ex/0604049.

34. BABAR Collaboration, J.D. Jackson talk at Charm2006 Beijing, China (2006).

35. C.Aubin *et al.,* Phys. Rev. Lett. **94** 011601 (2005).

36. A. Khodjamirian *et al.,* Phys. Rev. D**62**, 014002 (2000).

37. D. Melikhov and B. Stech, Phys. Rev. D **62**, 014006 (2000).

38. BABAR Collaboration, B. Aubert *et al.*, Phys. Rev. Lett. **93** 131801 (2004).

39. A.F. Falk, Y. Grossman, Z. Ligeti and A.A. Petrov, Phys. Rev. D **65** 05034 (2002); A.F. Falk, Y. Grossman, Z. Ligeti, Y, Nir and A.A. Petrov, Phys. Rev. D **69** 114021 (2004).

40. A. Datta and D. Kumbhakar, Z. Phys. **C27**, 515 (1985).

41. A.A. Petrov, Phys. Rev **D56**, 1685 (1997), hep-ph/9703335.

42. A. A. Petrov hep-ph/0311371.

43. S. Bianco, F.L. Fabbri, D. Benson and I. Bigi, Riv. Nuovo Cim. **26N7-8**, 1 (2003). hep-ex/0309021.

44. G. Burdman and I. Shipsey, Ann. Rev. Nucl. Part. Sci., (2003). hep-ph/0310076.

45. D. Asner $D^0\overline{D^0}$ Mixing Review to appear in PDG 2006.

46. S. Bergmann, Y. Grossmann, Z. Ligeti, Y. Nir, A. Petrov, Phys. Lett. **B486**, 418 (2000).

47. Belle Collaboration L. M. Zhang *et al.* arXiv:hep-ex/060124 submitted to Phys. Rev. Lett.

48. FOCUS Collaboration, J.M. Link *et al.* Phys. Lett. B **618** 23 (2005).

49. BABAR Collaboration, Aubert B, *et al.* Phys. Rev. Lett. **91** 171801 (2003).

50. CLEO Collaboration, R. Godang, *et al.* Phys. Rev. Lett. **84** 5038 (2000).

51. Belle Collaboration Phys. Rev D **70** 072003 (2004).

52. BABAR Collaboration hep-ex/0507101.

53. A. Bondar hep-ph/0510246.

54. I.I. Bigi and A.I. Sanda, Phys. Lett. **B171** 320 (1986).

55. G. Burdman *et al.,* Phys. Rev. **D66** 014009 (2002).

56. BABAR Collaboration, B. Aubert *et al.* Phys. Rev. Lett. **93** 101801 (2005).

Frascati Physics Series Vol. XLI (2006), pp. 169-176
DISCOVERIES IN FLAVOUR PHYSICS AT e^+e^- COLLIDERS
Frascati, February 28th - March 3rd, 2006

OBSERVATION OF X(1835) AND MULTIQUARK CANDIDATES AT BESII

Shan JIN for the BES Collaboration
Institute of High Energy Physics, CAS, Beijing 100049, China
jins@ihep.ac.cn

Abstract

In this talk, I would review the new observation of X(1835), which has properties inconsistent with any know mesons, but consistent with expectations for the state that produces the strong $p\bar{p}$ mass threshold enhancement observed in the $J/\psi \to \gamma p\bar{p}$ process at BESII. I will also talk about some other multiquark candidates which are indicated by $p\overline{\Lambda}$ and $K^-\overline{\Lambda}$ mass threshold enhancements.

1 Observation of X(1835) in $J/\psi \to \gamma\pi^+\pi^-\eta'$ at BESII

An anomalous enhancement near the mass threshold in the $p\overline{p}$ invariant mass spectrum from $J/\psi \to \gamma p\overline{p}$ decays was reported by the BES II experiment [1]. This enhancement was fitted with a sub-threshold S-wave Breit-Wigner resonance function with a mass $M = 1859^{+\ 3+\ 5}_{-10-25}$ MeV/c^2, a width $\Gamma < 30$ MeV/c^2 (at the 90% C.L.) and a product branching fraction (BF) $B(J/\psi \to \gamma X) \cdot$

$B(X \to p\overline{p}) = (7.0 \pm 0.4(stat)^{+1.9}_{-0.8}(syst)) \times 10^{-5}$. This surprising experimental observation has stimulated a number of theoretical speculations [2, 3, 4, 5, 6, 7] and motivated further investigations on baryon-antibaryon mass threshold structures, which led to the subsequent experimental observation of a strong $p\overline{\Lambda}$ mass threshold enhancement in $J/\psi \to pK^-\overline{\Lambda}$ decay [8]. Among various theoretical interpretations of the $p\overline{p}$ mass threshold enhancement, the most intriguing one is that of a $p\overline{p}$ bound state, sometimes called *baryonium* [2, 5, 9], which has been the subject of many experimental searches [10]. The baryonium interpretation of the $p\overline{p}$ mass enhancement requires a new resonance with a mass around 1.85 GeV/c^2 and it would be supported by the observation of the resonance in other decay channels. Possible decay modes for a $p\overline{p}$ bound state, suggested in Ref. [4, 5], include $\pi^+\pi^-\eta'$.

The results reported here are based on a sample of 5.8×10^7 J/ψ decays detected with the upgraded Beijing Spectrometer (BESII) at the Beijing Electron-Positron Collider (BEPC). The analysis is described in detail in Ref. [11]. For the $J/\psi \to \gamma\pi^+\pi^-\eta'(\eta' \to \pi^+\pi^-\eta, \eta \to \gamma\gamma)$ channel, Figure 1(b) shows the $\pi^+\pi^-\eta$ invariant mass distribution , where a clear η' signal is visible. The $\pi^+\pi^-\eta'$ invariant mass spectrum for the selected events is shown in Fig. 1(c), where a peak at a mass around 1835 MeV/c^2 is observed. For the $J/\psi \to \gamma\pi^+\pi^-\eta'(\eta' \to \gamma\rho)$ channel, the $\gamma\pi^+\pi^-$ invariant mass distribution shows an η' signal (Fig. 2(b)). For this channel there is also a distinct peak near 1835 MeV/c^2 in the $\pi^+\pi^-\eta'$ invariant mass spectrum (Fig. 2(c)).

The combined spectrum (the sum of the histograms in Figs. 1(c) and 2(c))) is fitted with a Breit-Wigner (BW) function convolved with a Gaussian mass resolution function (with $\sigma = 13$ MeV/c^2) to represent the $X(1835)$ signal plus a smooth polynomial background function. The mass and width obtained from the fit (shown in the bottom panel of Fig. 3) are $M = 1833.7 \pm 6.1$ MeV/c^2 and $\Gamma = 67.7 \pm 20.3$ MeV/c^2. The signal yield from the fit is 264 ± 54 events with a confidence level 45.5% ($\chi^2/d.o.f. = 57.6/57$) and $-2\ln L = 58.4$. A fit to the mass spectrum without a BW signal function returns $-2\ln L = 126.5$. The change in $-2\ln L$ with $\Delta(d.o.f.) = 3$ corresponds to a statistical significance of 7.7 σ for the signal.

Using MC-determined selection efficiencies of 3.72% and 4.85% for the $\eta' \to \pi^+\pi^-\eta$ and $\eta' \to \gamma\rho$ modes, respectively, we determine a product BF of

$$B(J/\psi \to \gamma X(1835)) \cdot B(X(1835) \to \pi^+\pi^-\eta') = (2.2 \pm 0.4) \times 10^{-4}.$$

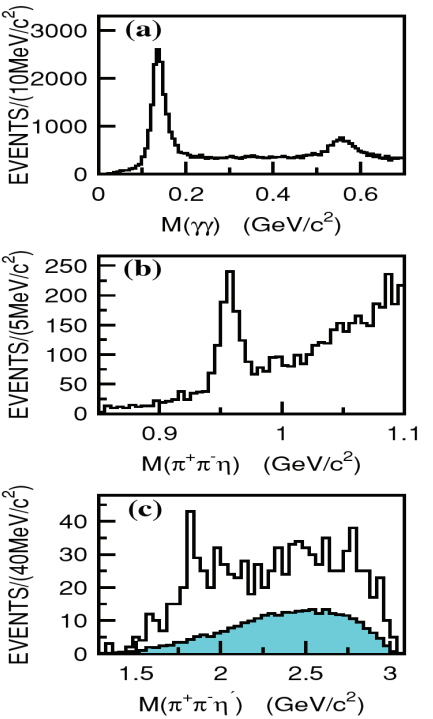

Figure 1: *Invariant mass distributions for selected* $J/\psi \to \gamma\pi^+\pi^-\eta'(\eta' \to \pi^+\pi^-\eta, \eta \to \gamma\gamma)$ *candidate events. (a) The invariant mass distribution of* $\gamma\gamma$ *pairs. (b) The* $\pi^+\pi^-\eta$ *invariant mass distribution. (c) The* $\pi^+\pi^-\eta'$ *invariant mass distributions; the open histogram is data and the shaded histogram is* $J/\psi \to \gamma\pi^+\pi^-\eta'$ *phase-space MC events (with arbitrary normalization).*

The mass and width of the $X(1835)$ are not compatible with any known meson resonance [12]. We examined the possibility that the $X(1835)$ is responsible for the $p\bar{p}$ mass threshold enhancement observed in radiative $J/\psi \to \gamma p\bar{p}$ decays [1]. It has been pointed out that the S-wave BW function used for the fit in Ref. [1] should be modified to include the effect of final-state-interactions (FSI) on the shape of the $p\bar{p}$ mass spectrum [6, 7]. Redoing the S-wave BW fit to the $p\bar{p}$ invariant mass spectrum of Ref. [1] including the zero Isospin, S-wave FSI factor of Ref. [7], yields a mass $M = 1831 \pm 7$ MeV/c^2 and a width $\Gamma < 153$ MeV/c^2 (at the 90% C.L.); these values are in good agreement with the mass and width of $X(1835)$ reported here. Moreover, according to Ref. [5], the $\pi\pi\eta'$ decay mode is expected to be strong for a $p\bar{p}$ bound state.

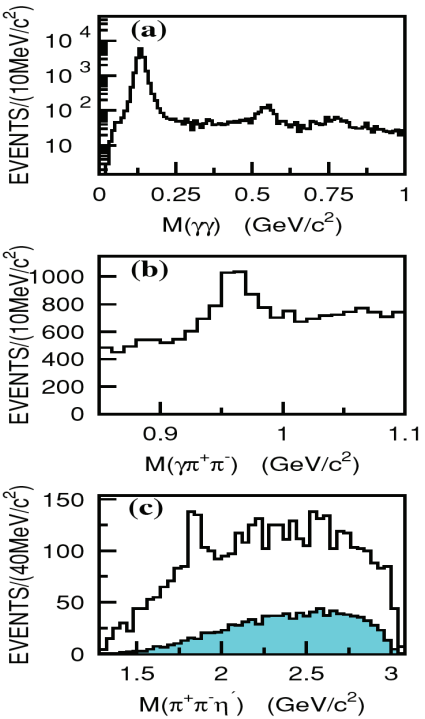

Figure 2: *Invariant mass distributions for the selected* $J/\psi \to \pi^+\pi^-\eta'(\eta' \to \gamma\rho)$ *candidate events, (a) The invariant mass distribution for* $\gamma\gamma$ *pairs. (b) The* $\gamma\pi^+\pi^-$ *invariant mass distribution. (c) The* $\pi^+\pi^-\eta'$ *invariant mass distributions: the open histogram is data and the shaded histogram is from* $J/\psi \to \gamma\pi^+\pi^-\eta'$ *phase-space MC events (with arbitrary normalization).*

Thus, the $X(1835)$ resonance is a prime candidate for the source of the $p\bar{p}$ mass threshold enhancement in $J/\psi \to \gamma p\bar{p}$ process. In this case, the J^{PC} and I^G of the $X(1835)$ could only be 0^{-+} and 0^+, which can be tested in future experiments. Also in this context, the relative $p\overline{p}$ decay strength is quite strong: $B(X \to p\overline{p})/B(X \to \pi^+\pi^-\eta') \sim 1/3$ [The product BF determined from the fit that includes FSI effects on the $p\bar{p}$ mass spectrum is within the systematic errors of the result reported in Ref. [1)].]. Since decays to $p\overline{p}$ are kinematically allowed only for a small portion of the high-mass tail of the resonance and have very limited phase space, the large $p\overline{p}$ branching fraction implies an unusually strong coupling to $p\overline{p}$, as expected for a $p\overline{p}$ bound state [9, 13)]. However, other possible interpretations of the $X(1835)$ that have no relation to the $p\overline{p}$ mass

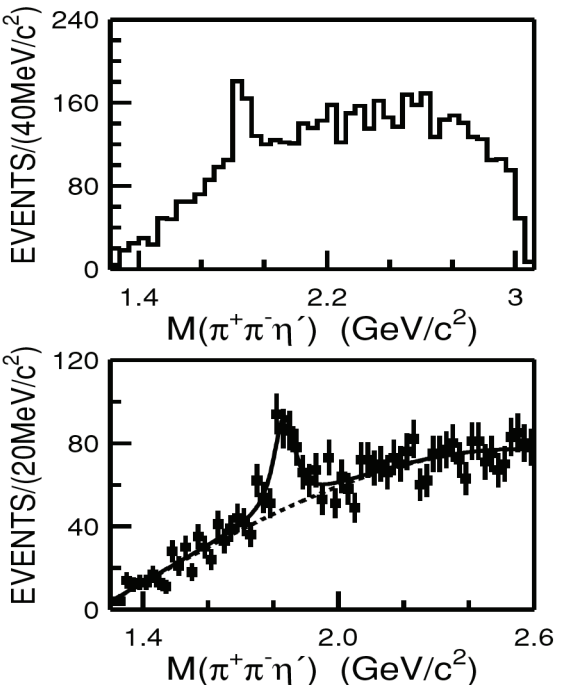

Figure 3: *The $\pi^+\pi^-\eta'$ invariant mass distribution for selected events from both the $J/\psi \to \gamma\pi^+\pi^-\eta'(\eta' \to \pi^+\pi^-\eta, \eta \to \gamma\gamma)$ and $J/\psi \to \gamma\pi^+\pi^-\eta'(\eta' \to \gamma\rho)$ analyses. The bottom panel shows the fit (solid curve) to the data (points with error bars); the dashed curve indicates the background function.*

threshold enhancement are not excluded.

2 Observation of $p\overline{\Lambda}$ mass threshold enhancement in $J/\psi \to pK^-\overline{\Lambda}$

The detailed analysis is described in Ref. [8]. The $p\overline{\Lambda}$ invariant mass spectrum for the selected events is shown in Fig. 4(a), where an enhancement is evident near the mass threshold. No corresponding structure is seen in a sample of $J/\psi \to pK^-\overline{\Lambda}$ MC events generated with a uniform phase space distribution. The $pK^-\overline{\Lambda}$ Dalitz plot is shown in Fig. 4(b). In addition to bands for the well established $\Lambda^*(1520)$ and $\Lambda^*(1690)$, there is a significant N^* band near the $K^-\overline{\Lambda}$ mass threshold, and a $p\overline{\Lambda}$ mass enhancement, isolated from the Λ^* and N^* bands, in the right-upper part of the Dalitz plot.

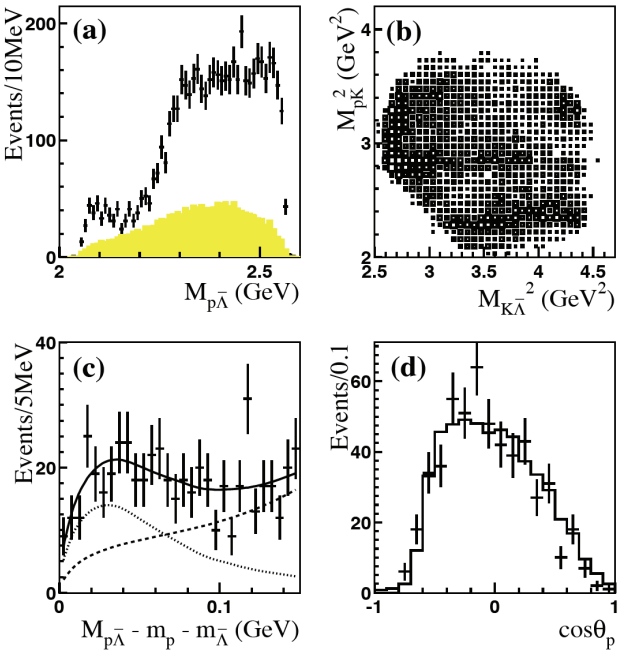

Figure 4: *(a) The points with error bars indicate the measured $p\overline{\Lambda}$ mass spectrum; the shaded histogram indicates phase space MC events (arbitrary normalization). (b) The Dalitz plot for the selected event sample. (c) A fit (solid line) to the data. The dotted curve indicates the Breit-Wigner signal and the dashed curve the phase space 'background'. (d) The $\cos\theta_p$ distribution under the enhancement, the points are data and the histogram is the MC (normalized to data)*

This enhancement can be fit with an acceptance weighted S-wave Breit-Wigner function, together with a function describing the phase space contribution, as shown in Fig. 4(c). The fit gives a peak mass of $m = 2075 \pm 12$ MeV and a width $\Gamma = 90 \pm 35$ MeV. The enhancement deviates from the shape of the phase space contribution with a statistical significance of about 7σ.

The fit yields $N_{res} = 238 \pm 57$ signal events, corresponding to a branching ratio

$$BR(J/\psi \to K^- X) BR(X \to p\overline{\Lambda}) = (5.9 \pm 1.4) \times 10^{-5}.$$

Searching for the same enhancement in $K\pi$ and $K\pi\pi$ modes in the $J/\psi, \psi'$ – $KK\pi, KK\pi\pi$ processes would help to confirm the presence of this anomalous

peak and understand its nature, and in particular distinguish whether it is from a conventional K^* meson, a possible multi-quark state, or a resonance in the baryon-antibaryon interaction. If its decay widths to $K\pi$ and $K\pi\pi$ modes are much smaller than to $p\overline{\Lambda}$ modes, the interpretation as conventional K^* meson would be disfavored.

3 Observation of $K^-\overline{\Lambda}$ mass threshold enhancement in $J/\psi \to pK^-\overline{\Lambda}$

In the above Dalitz plot (Fig. 4(b)), a clear band, is observed near the $K^-\overline{\Lambda}$ mass threshold. We have performed very preliminary partial wave analysis (PWA) and obtained: the mass of this threshold structure N_X^* is in the range of 1500 MeV to 1650 MeV, the width is about 70 MeV to 110 MeV and its spin-parity favors $1/2^-$. In particular, it has a branching ratio $B(J/\psi \to \overline{p}N_X^*)B(N_X^* \to K^+\Lambda)$ larger than 2×10^{-4}.

Considering that the mass of N_X^* is below or very close to $K^-\overline{\Lambda}$ threshold, i.e., the phase space producing $K^-\overline{\Lambda}$ final state is very small, the large branching ratio to $K^-\overline{\Lambda}$ indicates that N_X^* has very strong coupling to $K^-\overline{\Lambda}$, suggesting that it could be the $K^-\overline{\Lambda}$ resonant state predicted by chiral SU(3) quark model [14].

4 Acknowledgements

This work is supported in part by the National Natural Science Foundation of China under contracts No. 10425523, the 100 Talents Program of CAS under Contract No. U-24, and the Knowledge Innovation Project of CAS under Contract No. KJCX2-SW-N10.

References

1. BES Collaboration, J.Z. Bai *et al.*, Phys. Rev. Lett. **91**, 022001 (2003).

2. A. Datta, P.J. O'Donnell, Phys. Lett. **B567**, 273 (2003); M.L. Yan *et al.*, hep-ph/0405087; B. Loiseau, S. Wycech, hep-ph/0502127.

3. J. Ellis, Y. Frishman and M. Karliner, Phys. Lett. **B566**, 201 (2003); J.L. Rosner, Phys. Rev. D **68**, 014004 (2003).

4. C.S. Gao and S.L. Zhu, Commun. Theor. Phys. 42, 844 (2004), hep-ph/0308205.

5. G.J. Ding and M.L. Yan, Phys. Rev. C **72**, 015208 (2005).

6. B.S. Zou and H.C. Chiang, Phys. Rev. D **69**, 034004 (2003).

7. A. Sibirtsev *et al.*, Phys. Rev. D **71**, 054010 (2005).

8. BES Collaboration, M. Ablikim *et al.*, Phys. Rev. Lett. **93**, 112002 (2004).

9. I.S. Shapiro, Phys. Rept. **35**, 129 (1978); C.B. Dover, M. Goldhaber, Phys. Rev. D **15**, 1997 (1977).

10. For recent reviews of this subject, see E. Klempt *et al.*, Phys. Rep. **368**, 119 (2002) and J-M. Richard, Nucl. Phys. Proc. Suppl. **86**, 361 (2000).

11. BES Collaboration, M. Ablikim *et al.*, Phys. Rev. Lett. **95**, 262001 (2005).

12. Particle Data Group, S. Eidelman *et al.*, Phys. Lett. **B592**, 1 (2004).

13. S.L. Zhu and C.S. Gao, hep-ph/0507050.

14. F. Huang and Z.Y. Zhang, Phys.Rev C **72**, 024003 (2005), nucl-th/0507025.

Frascati Physics Series Vol. XLI (2006), pp. 177-188
DISCOVERIES IN FLAVOUR PHYSICS AT e^+e^- COLLIDERS
Frascati, February 28th - March 3rd, 2006

FUTURE PERSPECTIVES FOR CHARM PHYSICS AT A SUPER B-FACTORY

Milind V. Purohit
Univ. of South Carolina, Columbia, SC 29212, USA

Abstract

We review the current status of charm physics and speculate on what topics might still be interesting in six years or so and what a Super B-factory could aim to do. Extrapolations are based mainly on recent results from BaBar and Belle, although results from E791, FOCUS and CLEO are also cited.

1 Introduction

The questions that are examined here are:

- What charm physics can be done with $\sim 10\ ab^{-1}$ per year?
- What charm physics will still be interesting in $\sim$2012?

- How does charm at a B-factory compare to charm physics from hadronic machines? This last one is largely rhetorical and will likely be answered by other speakers at this workshop.

Disclaimer: In the interest of taking an overview and making extrapolations, 2σ, 90% CL and 95% CL limits have been used interchangeably.

This talk focuses on:

- The discovery aspects of charm physics;
- What will be interesting in the future;
- The reach of a Super-B factory.

Conclusions drawn here are based on extrapolations mainly from BaBar and Belle, and also from CLEO, E791 and FOCUS.

2 Topics in Charm Physics

Charm physics covers many topics, including:

- $D^0 - \overline{D}^0$ mixing
- Rare and forbidden charm decays;
- CP violation searches;
- T violation searches;
- Semileptonic Decays;
- Charm Spectroscopy;
- Low Energy Hadron Physics;
- Many other topics.

Here we focus on the first few, which are most likely to still be interesting in a few years, but comment on the last few as well.

3 The Search for $D^0 - \overline{D}^0$ mixing

For decays of neutral D^0 mesons, the mixing rate can be defined as

$$R_{mix} \equiv \frac{\Gamma(D^0 \to \overline{D}^0 \to \overline{f})}{\Gamma(D^0 \to f)}$$

where f is a final state and $\overline{f}$ is its CP-conjugate. Short distance calculations in the standard model predict a low rate of $R_{mix} \sim 10^{-7}$ for the box diagram which goes up to possibly as high as $\sim 10^{-3}$ when long distance effects are included; nevertheless we would like to observe mixing as a first step. Parameters that describe mixing are $x \equiv \Delta M/\Gamma$, $y \equiv \Delta\Gamma/2\Gamma$, where the time-integrated $R_{mix} = (x^2 + y^2)/2$. Strong phases can rotate $(x, y) \to (x', y')$. y can also be measured by using the difference in the D^0 lifetime measured in two decay modes, such as $K^-\pi^+$ and K^-K^+.

New physics effects can easily produce $R_{mix} > 10^{-7}$, and are the only way we can get CP violation in mixing. [1, 2, 3] These new physics effects will enhance the mass difference parameter x, but not $\Delta\Gamma$, or y.

3.1 Strategies for Charm Mixing Searches

The usual strategy is to tag the flavor at birth using the slow pion in $D^{*+} \to D^0\pi^+$ decays and tag the flavor at decay time using the lepton (for leptonic decay such as $Ke\nu$) or kaon (for hadronic decays such as $K\pi$). Of course, charm factory experiments such as CLEO-c and BES can use the coherent production and evolution of neutral D-pairs instead.

3.2 FOCUS $D^0 - \overline{D}^0$ mixing

Results from the FOCUS experiment can be described best using a contour rather than by a single number such as R_{mix}. This is shown in figure 1 for the decay mode $K^{\pm}\pi^{\mp}$.

3.3 BaBar 2004 result for semileptonic mixing

Using a data sample of 80 fb^{-1} on resonance and 7.1 fb^{-1} off-resonance, the BaBar experiment employed a neural network event selector and a neural network for $p^*(D^0)$ reconstruction, where p^* is the c.m. momentum of the D^0

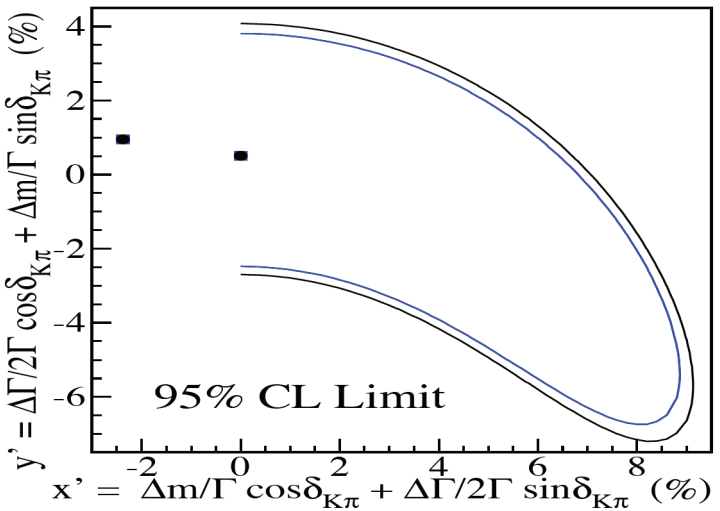

Figure 1: *95% CL contour in (x', y') space from the FOCUS experiment.*

reconstructed in the semi-muonic decay mode. An unbinned extended maximum likelihood fit using ΔM and transverse lifetime was then done, where $\Delta M \equiv m(\pi D^0) - m(D^0)$. First, a fit to the high-statistics right-sign (RS) sample yielded $N_{unmixed} = 49620 \pm 324$ events. Subsequently a fit to wrong-sign (WS) sample for N(mix) gave $N_{mix} = 114 \pm 61$ wrong sign signal events. In the semileptonic case, we can define R_{mix} simply by

$$R_{mix} \equiv N_{mix}/N_{unmixed}$$

Systematics in this analysis when evaluated as fraction of statistical error are listed in the table below.

The final result is $R_{mix} = 0.0023 \pm 0.0012 \pm 0.0004$. [5)] At the 90% CL this corresponds to the limit $R_{mix} < 0.0042$. The limiting systematic clearly comes from pdfs which should improve with statistics.

3.4 BaBar Hadronic $D^0 - \overline{D}^0$ mixing results

To date, the best BaBar result for $D^0 - \overline{D}^0$ mixing comes from the analysis of $K^+\pi^-$ decays of the D^0 meson. Using 57 fb^{-1}, the result is $R_{mix} < 1.3 \times 10^{-3}$

Table 1: Systematic errors for the BaBar semileptonic mixing result as fraction of statistical error.

Type of Systematic Error	Error (%)
Mixed ΔM PDF	0.27
Mixed decay time PDF	0.06
Combinatoric ΔM PDF	0.13
Bkg D^0 decay model	0.13
Bkg D^+ decay model	0.10
Total systematic	0.35
Total stat. + syst.	1.06

at the 95% CL. [6] Limits on y and Δy have also been determined by the BaBar experiment. [7]

3.5 Belle Semileptonic $D^0 - \overline{D}^0$ mixing result

Using 253 fb^{-1} of data the Belle experiment recently found $R_{mix} < 1.0 \times 10^{-3}$ at the 90% CL. [8] The major systematic uncertainties come from the wrong-sign background description and binning. Once again, their result should scale to a higher statistics sample. [8]

3.6 Belle Hadronic $D^0 - \overline{D}^0$ mixing result

Using 400 fb^{-1} of data, we can approximate the recent Belle result [9] in the charged $K\pi$ mode as $R_{mix} < 4.0 \times 10^{-4}$ at the 90% CL. Once again, the major systematic error comes from variation in cuts and in particular, from variation of the $p^*(D^*)$ cut. Therefore, this result should also scale with statistics.

3.7 $D^0 - \overline{D}^0$ mixing: R_{mix} Projection

Finally, we can project the R_{mix} results above to the year $\sim$ 2012 when a Super B-factory might be ready by simply scaling according to $1/\sqrt{N}$. The projection is based on a 1-year sample of 10 ab^{-1} and is shown in the figure 2 below.

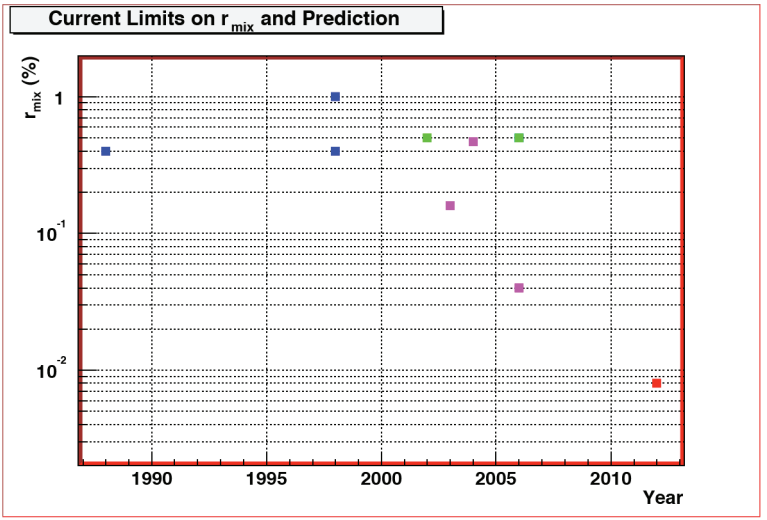

Figure 2: *Existing measurements and projection for R_{mix} limits from Super B-factories of the future.*

4 Searches for CP-violation

CP violation in charm is expected to first manifest itself in Singly Cabibbo-suppressed (SCS) decays. Within the Standard Model, one expects CP violation asymmetries in SCS Decays of the order of 10^{-3}, while New Physics may give CP violation asymmetries as large as $\sim 10^{-2}$. [1, 2)]

4.1 Standard Model interfering amplitudes

In the Wolfenstein parameterization, the CKM matrix (below) clearly gives only a small CP violating asymmetry.

$$V = \begin{pmatrix} V_{ud} & V_{us} & V_{ub} \\ V_{cd} & V_{cs} & V_{cb} \\ V_{td} & V_{ts} & V_{tb} \end{pmatrix}, \quad \begin{pmatrix} \text{where } \lambda \sim 0.22, \\ \text{and } A \sim 0.86 \end{pmatrix}$$
$$= \begin{pmatrix} 1-\lambda^2/2 & \lambda & A\lambda^3(\rho - i\eta) \\ -\lambda & 1-\lambda^2/2 & A\lambda^2 \\ A\lambda^3(1-\rho-i\eta) & -A\lambda^2 & 1 \end{pmatrix}$$

4.2 BaBar Search for CP violation in SCS charm decays

Pre-BaBar limits were $\sim (2-5) \times 10^{-2}$ leaving a considerable window for new physics discovery. Based on ~43,000 $D^+ \to K^- K^+ \pi^+$ decays from ~80 fb^{-1} we measure the asymmetry

$$A_{CP} \equiv \frac{\frac{\mathcal{B}(D^+ \to K^+ K^- \pi^+)}{\mathcal{B}(D_s^+ \to K^+ K^- \pi^+)} - \frac{\mathcal{B}(D^- \to K^+ K^- \pi^-)}{\mathcal{B}(D_s^- \to K^+ K^- \pi^-)}}{\frac{\mathcal{B}(D^+ \to K^+ K^- \pi^+)}{\mathcal{B}(D_s^+ \to K^+ K^- \pi^+)} + \frac{\mathcal{B}(D^- \to K^+ K^- \pi^-)}{\mathcal{B}(D_s^- \to K^+ K^- \pi^-)}}$$

where

$$\mathcal{B}(D^+ \to K^+ K^- \pi^+) \propto \frac{\Gamma(D^+ \to K^+ K^- \pi^+)}{\epsilon(D^+ \to K^+ K^- \pi^+)}.$$

We find that $A_{CP} = +0.014 \pm 0.010 \pm 0.008$ for the inclusive events, that $A_{CP} = +0.002 \pm 0.015 \pm 0.006$ for decays into $\phi\pi$ and that $A_{CP} = +0.009 \pm 0.017 \pm 0.007$ for decays into $K^* K$.

Table 2: $KK\pi$ Yields

$D^+_{(s)}$ yield	$D^-_{(s)}$ yield
21632 ± 228 D^+ events	20940 ± 226 D^- events
23066 ± 217 D_s^+ events	22928 ± 214 D_s^- events

The systematic errors on A_{CP} are listed in the table below. It is clear that all these errors should scale with luminosity. Finally, there are recent results from Belle using 281 fb^{-1} in the $K^- \pi^+ \pi^0$ and $K^- \pi^+ \pi^+ \pi^-$ modes, giving 2σ limits of 10.6% and 8.8% respectively in these two modes. [10)]

Table 3: Systematic errors for the BaBar CP violation result in %.

Source	$KK\pi$	ϕ_π	$K^{*0}K$
MC simulation	0.06	0.06	0.06
Background estimate	0.63	0.32	0.49
Event Selection	0.51	0.56	0.54
Total	0.81	0.65	0.73

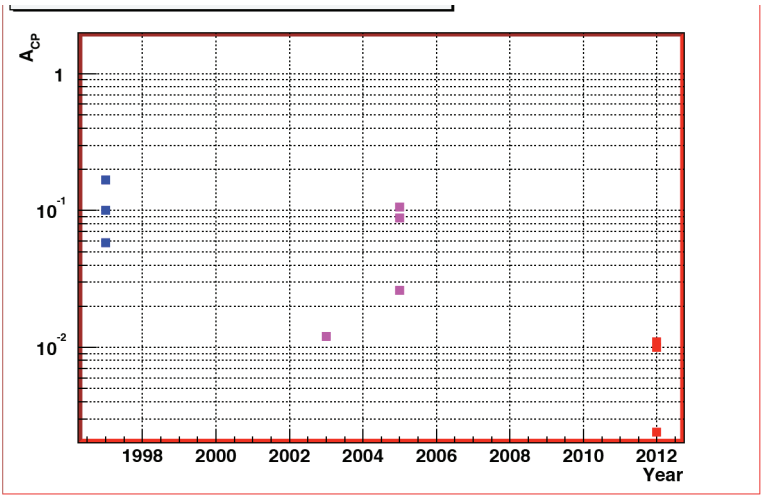

Figure 3: *Existing measurements and projection for CPV limits in SCS decays from Super B-factories of the future.*

4.3 CP Violation Limits Projection

Again, we can project the A_{CP} results above to the year ~ 2012 when a Super B-factory might be ready by simply scaling according to $1/\sqrt{N}$. The projection is based on a 1-year sample of 10 ab^{-1} and is shown in the figure 3 below.

5 Searches for T-violation

For some time now, theorists have urged us to look at 4-body (and higher) charm decay modes for evidence of T-violation using the triple product of momenta. For example, in the $D^0 \to K^-K^+\pi^+\pi^-$ mode, one can examine the quantity

$$C_T = \vec{p}_{K^-} \cdot (\vec{p}_{\pi^+} \times \vec{p}_{\pi^-})$$

The idea is to look for the asymmetry

$$A_C \equiv \frac{(C_T > 0) - (C_T < 0)}{(C_T > 0) + (C_T < 0)}$$

Although A_C can be non-zero just due to a strong phase, the asymmetry A_T formed by comparing A_C from D^0 decays with the similar asymmetry $\overline{A}_C$ from

D^0 decays is non-zero only if there is a CP-violating weak phase, where

$$A_T \equiv \frac{A_C - \overline{A}_C}{2} \qquad \text{or} \qquad \frac{A_C - \overline{A}_C}{A_C + \overline{A}_C}$$

5.1 Current Status of T-violation searches

FOCUS has done this search in a few modes [11] and no positive signal is seen. Results are listed in the table below. (CLEO-c is also searching in these modes and in the decay mode $D^+ \to K^+ K^{*-} e^+ e^-$).

Table 4: FOCUS results for A_T.

Decay Mode	A_T
$D^0 \to K^- K^+ \pi^+ \pi^-$	$0.010 \pm 0.057 \pm 0.037$
$D^+ \to K^0_S K^+ \pi^+ \pi^-$	$0.023 \pm 0.062 \pm 0.022$
$D^+ \to K^0_S K^+ \pi^+ \pi^-$	$-0.036 \pm 0.067 \pm 0.023$

It is much harder to extrapolate to a Super B-factory starting from a fixed-target experiment. Using a rule-of-thumb, one gets 1σ errors for 10 ab^{-1} of roughly 0.3%. Of course, this number will vary by mode. It is even harder to project a systematic error, but note that FOCUS systematics were dominated by selection criteria. Similarly, CLEO-c's systematics are reportedly dominated by knowledge of background shape and selection criteria, so a simple statistics-based projection should be roughly valid.

6 Rare and Forbidden Charm Decays

Leptonic decay modes such as $D^0 \to e^+ e^-$, $\mu^+ \mu^-$ have very low rates [1] in the SM: from $\sim 10^{-15}$ to 3×10^{-11}, depending on long-distance contributions. Some new physics models can give larger rates, perhaps as high as 0.6×10^{-10}. Will a Super B-factory be able to see the standard model rates? Probably not, but the good news here is that with particle ID improvements, it may get closer than predicted! E791 studied a large number of modes, [12, 13, 14] as did the FOCUS [15] and CLEO experiments. [16, 17, 18] Similarly, from BaBar [19] the 90% CL limits for the $D^0 \to e^+ e^-$, $\mu^+ \mu^-$, $e^\pm \mu^\mp$ modes are 1.2×10^{-6}, 1.3×10^{-6} and 0.81×10^{-6} respectively.

6.1 Projection for Rare Decay BF's

The BaBar limits on $D^0 \to \ell^+\ell^-$ BF's extrapolate to $\sim 10^{-7}$ at a Super B-factory. With improvements in particle ID, one can imagine reaching the level of a few $\times 10^{-8}$. While future hadronic experiments should be good at two-body modes, there are dozens of other rare modes that require study, most likely by a Super-B factory.

Another interesting point about the πe^+e^- and ρe^+e^- decay modes of the D mesons [1)] is that the SM rate in certain regions of the e^+e^- mass has very small theoretical uncertainty. A Super-B factory should take advantage of this to look for new physics.

7 Semileptonic Form Factors: $D^0 \to K^*$ and other transitions.

Presently q^2 distributions measured by E791, [21, 22, 23)] FOCUS [24, 25)] and CLEO [26, 27)] are based on $\sim 10\sigma$ (D^0) - $100\sigma(D^+)$ signals. In these analyses, truly 4-dimensional fits run out of statistics. CLEO-c will get signals $\sim \times 5$ larger in significance, while BaBar / Belle have at least an order of magnitude higher statistics compared to CLEO. A 10 ab^{-1} Super B-factory could get signal yields that are $\sim \times 50$-100 larger in significance than present B factories. This should allow for excellent model-independent studies in full 4-dimensional glory. Resolution should not be a problem because none of the distributions of decay variables has sharp peaks.

8 Other comments

By definition, it is hard to predict pleasant surprises in spectroscopy. Judging from recent experience however, a Super B-factory is a super place for such discoveries! Further, there is a wealth of charm data to be studied: the masses, widths, BF's of D mesons, excited D's, charm baryons and excited baryons are some examples. A Super B-factory is a clean environment that allows almost all such particles to be studied efficiently. Recent work has shown that charm mesons are a wonderful source of low-energy scattering data. [28, 29)] We need to understand the existence and behaviour of a large number of resonances, and establish the validity or limitations of connecting to other measurements of scattering amplitudes. [30)] Studies of charm baryons should similarly be useful. Finally, a complete understanding of charm should include production studies

and again, a Super B-factory may be the best place to study correlations in charm particle production and in their fragmentation.

References

1. G. Burdman & I. Shipsey, Ann. Rev. Nucl. Part. Sci., 2003, also available as hep-ph/0310076.
2. S. Bianco, F. L. Fabbri, D. Benson & I. Bigi, hep-ex/0309021.
3. A. Petrov, "Charm physics: theoretical review", hep-ph/0311371.
4. K. Stenson, "$D^0 - \overline{D}^0$ hadronic mixing and DCS decays from FOCUS", hep-ex/0501006.
5. B. Aubert *et al.*, Phys. Rev. **D70** 091102 (2004).
6. B. Aubert *et al.*, Phys. Rev. Lett. **91** 171801 (2003).
7. B. Aubert *et al.*, Phys. Rev. Lett. **91** 121801 (2003).
8. K. Abe *et al.*, Phys. Rev. **D72** 071101 (2005).
9. K. Abe *et al.*, Phys. Rev. Lett. **94** 071801 (2005).
10. K. Abe *et al.*, Phys. Rev. Lett. **95** 231801 (2005).
11. J. M. Link *et al.*, Phys. Lett. **B622** 239 (2005).
12. E. M. Aitala *et al.*, Phys. Rev. Lett. **86** 3969 (2001).
13. E. M. Aitala *et al.*, Phys. Lett. **B462** 401 (1999).
14. E. M. Aitala *et al.*, Phys. Rev. Lett. **76** 364 (1996).
15. J. M. Link *et al.*, Phys. Lett. **B572** 21 (2003).
16. T. E. Coan *et al.*, Phys. Rev. Lett. **90** 101801 (2003).
17. T. E. Freyberger *et al.*, Phys. Rev. Lett. **76** 3065 (1996) Erratum-ibid. **77** 2147 (1996).
18. Q. He *et al.*, Phys. Rev. Lett. **95** 221802 (2005).

19. B. Aubert *et al.*, Phys. Rev. Lett. **93** 191801 (2004).

20. S. Fajfer and J. Kamenik, Phys. Rev. **D72** 034029 (2005).

21. E. M. Aitala *et al.*, Phys. Lett. **B450** 294 (1999).

22. E. M. Aitala *et al.*, Phys. Lett. **B440** 435 (1998).

23. E. M. Aitala *et al.*, Phys. Rev. Lett. **80** 1393 (1998).

24. J. M. Link *et al.*, **B607** 67 (2005).

25. J. M. Link *et al.*, **B607** 233 (2005).

26. G. S. Huang *et al.*, Phys. Rev. Lett. **94** 011802 (2005).

27. A. Bean *et al.*, Phys. Lett. **B317** 647 (1993).

28. E. M. Aitala *et al.*, Phys. Rev. **D73** 032004 (2006).

29. J. M. Link *et al.*, **B585** 200 (2004).

30. D. Aston *et al.*, Nucl. Phys. **B296** 493 (1988).

Frascati Physics Series Vol. XLI (2006), pp. 189-194
DISCOVERIES IN FLAVOUR PHYSICS AT – e- e+ COLLIDERS
Frascati, February 28th - March3rd, 2006

FUTURE OF CHARM PHYSICS AT HADRONIC MACHINES

Sandro De Cecco
Istituto Nazionale di Fisica Nucleare, sezione di Roma
Piazzale Aldo Moro 5, 00185 Roma, Italy

Abstract

We present a selection of topics in charm physics as production cross section and search for CPV and D^0 mixing, that can be studied at colliders. We describe relevant results from the Tevatron run II and give some perspectives for the LHC experiments contribution to this field.

1 Introduction

In the past, charm physics has been mainly studied at e^+e^- machines and at fixed target experiments. In recent years many world class results in this field came from hadron collider experiments such CDF and D0 at the Tevatron. Exploiting the large charm production cross section and the high Luminosity of the Tevatron proton-anti-proton collider as well as the enhanced detector

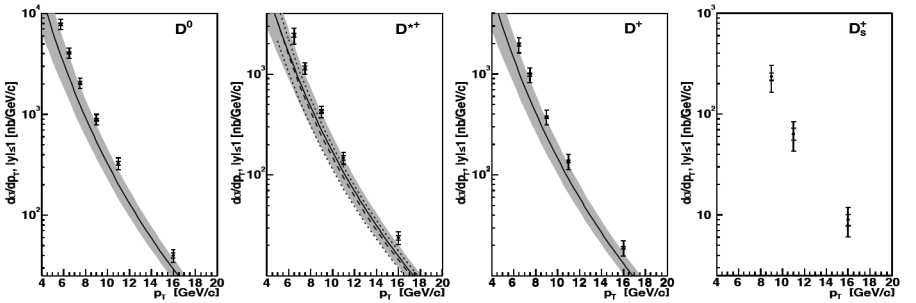

Figure 1: *Charm meson differential cross sections for* D^0,$D^{*\pm}$,$D^{\pm}$ *and* D_s.

capabilities in selecting and reconstructing heavy flavour signals, D0 and particularly CDF demonstrated that high precision measurements in charm physics are possible at hadronic machines. In this contribution we present a selection of relevant topics in the charm sector that can be studied at colliders describing the results coming from the Tevatron run II and giving some perspectives for the Large Hadron Collider experiments contribution to this field. In section 2 we will focus on charm production related topics while section 3 is dedicated to searches for CP Violation in charmed mesons and D^0 mixing.

2 Charm production at hadronic colliders

For the first time at an hadronic collider the prompt charm meson production cross section as been measured by the CDF experiment thanks to its detector and trigger upgrades especially designed for heavy flavour physics. In particular CDF implemented a new level 1 trigger XFT based on drift chamber fast tracking and level 2 trigger Silicon Vertex Trigger SVT [1)] based on precise impact parameter measurement with silicon detector. This upgrade gives direct access to hadronic decays of D and B mesons and allow the collection of large charm signal yields. Different species of charm mesons has been reconstructed in the following final states: $D^0 \to K^-\pi^+$, $D^{*+} \to D^0\pi^+$, $D^0 \to K^-\pi^+$, $D^+ \to K^-\pi^+\pi^+$, $D_s^+ \to \Phi\pi^+$ with $\Phi \to K^+K^-$. The data used for this measurement correspond to a luminosity of only $5.8 \pm 0.3 pb^{-1}$ integrated in the very first months of Tevatron run II. The impact parameter of reconstructed charm mesons is used to distinguish directly produced charm from secondary charm, originating from B decay. Due to the transverse kick

in the decay of B hadrons, secondary charm mesons may not point back to the primary vertex. The direct charm meson efficiencies are then calculated using a parametrized detector and trigger Monte Carlo simulation. The integrated production cross sections (for $|y| < 1$) were found to be: $\sigma(D0, p_T \geq 5.5GeV) = 13.3 \pm 0.2 \pm 1.5\mu b, \sigma(D^{*+}, p_T \geq 6.0GeV) = 5.2 \pm 0.1 \pm 0.8\mu b, \sigma(D^+, p_T \geq 6.0GeV) = 4.3 \pm 0.1 \pm 0.7\mu b, \sigma(D_s, p_T \geq 8.0GeV) = 0.75 \pm 0.05 \pm 0.22\mu b$. As a comparison the bottom meson cross section, measured in the $B^+ \to J/\Psi K^+$ mode by CDF in Run I [2] is $\sigma(B^+, p_T \geq 6.0GeV, |y| < 1) = 3.6 \pm 0.6\mu b$. Differential prompt charm x-sections are plotted in Fig.1 with the superimposed band of FONLL [4] theoretical prediction corresponding to the maximum variation of renormalization and factorization scales between 0.5 and 2.0 $\times\sqrt{p_T^2 + m^2}$; where D fragmentation function was taken from Aleph measurement [5]. Measured x-sections are around a factor 1.5 higher than calculations which is consistent with the case of $b\bar{b}$ x-section. The CDF measurement of $c\bar{c}$ x-section is hence a major input to QCD calculations of HF production processes and to hadronization models. Further inputs to theoretical calculation of heavy flavour production could come from the study of angular correlations of $c\bar{c}$ pairs from which information on the relative strength of production mechanisms can be extracted. Moreover CDF and D0 performed accurate measurements of the masses and widths of $D_{1,2}$ excited D^{**} charm states, studies of charmonium production, of charmed barions and of X(3872) properties. The last topics are not discussed here.

3 CP Violation and D^0 mixing searches

Standard Model predictions for CP asymmetries and mixing parameters x and y in the charm sector are all in the range between 0.1% and 1%. Measuring asymmetries above the percent level will be strong indication for physics beyond SM. In particular direct CP asymmetries are predicted at 10^{-3} level in D^0 Cabibbo suppressed decays while almost null in Cabibbo allowed decays. Measuring asymmetries above the percent level will be strong indication for physics beyond SM. With an integrated luminosity of $123 \pm 7pb^{-1}$, CDF measured Cabibbo suppressed branching fractions for $D^0 \to \pi^+\pi^-, K^+K^-$ relative to the allowed mode $D^0 \to K\pi$ and direct CP asymmetries $A_{CP}(D^0 \to \pi^+\pi^-, K^+K^-)$ for $D^0(\bar{D^0})$. About 93k $D^0 \to K^-\pi^+$, 8.2k $D^0 \to K^-K^+$ and 3.7k $D^0 \to \pi^-\pi^+$ decays were reconstructed (see Fig.2) as well as for the C.C. $\bar{D^0}$ with simi-

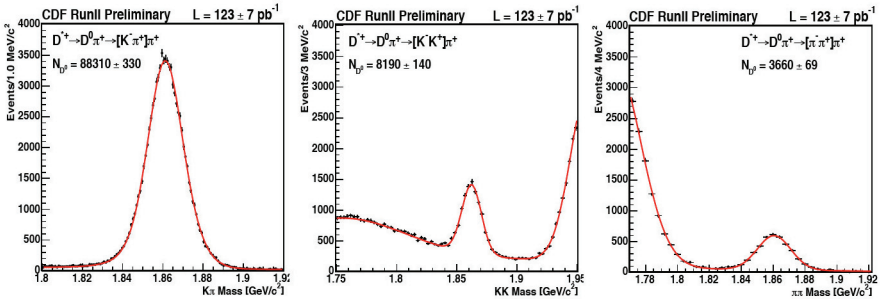

Figure 2: *CDF* $D^{*+} \to D^0\pi^+$ *signals with* $D^0 \to K^-\pi^+$,K^+K^-,$\pi^+\pi^-$.

lar yields. The $D^0(\bar{D}^0)$ mesons were selected requiring they originate from a $D^{*+}(D^{*-})$ decay: $D^{*\pm} \to D^0(\bar{D}^0)\pi^\pm$. This request gives an excellent signal purity and initial $D^0(\bar{D}^0)$ flavour tag through the charge of the bachelor pion from the strong (CP-conserving)$D^{*\pm}$ decay. Since charm quarks are produced in $c\bar{c}$ pairs at collider $D^{*\pm}$ flavour tagging is unbiased. The raw CP asymmetries, has been corrected for the intrinsic charge asymmetry of the CDF detector which is the main systematic effect but still can be controlled at the few per mille level. Detector charge asymmetry has been measured on un-biased track samples; residual corrections were evaluated on $D^0 \to K\pi$ sample where no CP-asymmetry is expected. The results [6] for A_{CP} are: $A_{CP}(D^0 \to KK) = 2.0 \pm 1.7 \pm 0.6\%$ and $A_{CP}(D^0 \to \pi\pi) = 3.0 \pm 1.9 \pm 0.6\%$. This result has the world best precision on this quantity and will be updated with the full statistics collected at the Tevatron. CDF expects to collect around 2 Millions of $D^{*\pm} \to D^0\pi^\pm$ with $D^0 \to K\pi$ per fb^{-1} and achieve a $\sigma(A_{CP})$ 10^{-3}. Similarly in the D^+ sector decays like the $D^\pm \to \pi^\mp\pi^\pm\pi^\pm$ can be used at Tevatron to search for CP violation in the Dalitz structure analysis. The D^0 meson mixing receives contribution from both $x = \Delta M/\Gamma$ and $y = \Delta\Gamma/2\Gamma$ and SM predictions are in the range between 10^{-4} and 10^{-2}. New Physics could enhance x through internal loops in mixing box diagrams. There are two main strategies to measure D^0 mixing. One consists in the extraction of y measuring the lifetime difference $\Delta\Gamma$ between CP eigenstates $D^0 \to KK, \pi\pi$ and CP mixed state $D^0 \to K\pi$. In this case $y_{CP} = \tau_{K\pi}/\tau_{KK} - 1$ and one has to measure the lifetimes of the two modes. Current precision at the B factories is $\sigma(y_{CP})$ 0.006 and CDF expect to have comparable errors. Most sensitive

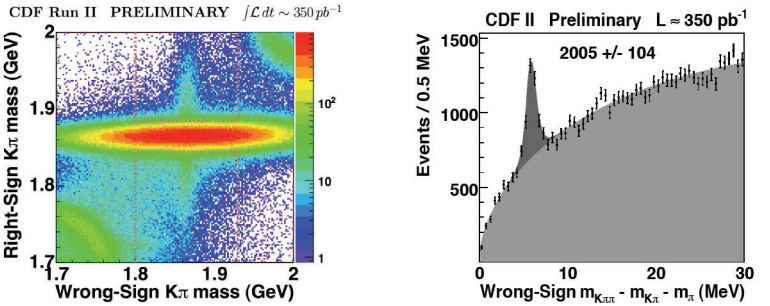

Figure 3: *Right sign vs wrong sign $K\pi$ masses (left), wrong sign signal mass difference $m_{K\pi\pi} - m_{K\pi} - m_{\pi}$ (right)*

way is to search for "wrong sign" $K\pi$ pairs in D^0 decays. These can occur through mixing or directly through doubly Cabibbo suppressed decays or with the interference of the two processes. A D^0 time dependent tagged analysis can deconvolve these components in the wrong sign time structure which is $r(t) = [R_{DCS} + \sqrt{R_{DCS}}y't + 1/4(x'^2 + y'^2)t^2]e^{-t}$, where R_{DCS} is the doubly Cabibbo suppressed rate. B factories has set limits in the x, y plane with this method but they are not yet sensitive to SM values for mixing parameters. CDF has measured, with an integrated Luminosity of 350 pb^{-1}, the time integrated value of the wrong sign to right sign ratio to be $4.05 \pm 0.21(stat) \pm 0.12(syst)$ which compares well in precision with Babar and Belle. The expectations from CDF time dependent analysis are similar to B factories: the CDF higher wrong sign D^0 yield (see fig.3, right), counterbalances limited particle identification capabilities to separate kaons from pions, therefore the separation mainly relies on kinematics (see fig.3, left) exploiting excellent momentum resolution.

4 Charm physics at LHC and complementarity with H.F. factories

The outcome of e^+e^- machine experiments (Babar, Belle and especially CLEO-c) for charm physics is extensively reported in [7]. Producing charm at Ψ resonances make possible for instance to measure absolute B.R. as well as charm mesons decay factors (f_D, f_{D_s}) which are of fundamental importance to check HQET calculations for beauty and charm physics. Coherent $D\bar{D}$ production can also be exploited for mixing and CP violation searches in a relatively clean environment. On the other side the $D\bar{D}$ production cross section is around 5

nb which has to be compared to 10-100μb at Tevatron and LHC. As we discussed in the previous sections the CDF experiment at Tevatron demonstrates that with adequate trigger strategies to select charmed mesons, high precision measurements in some first choice charm physics topics are possible like in the search for D^0 mixing and CP violation.

At the LHC the LHC-b experiment will implement an high level trigger stream dedicated to the selection of $D* \rightarrow D^0\pi$ with two body $D^0 \rightarrow hh'$ decays. For this purpose the ability to trigger on displaced vertexes will be exploited in a similar way to what CDF does and a bandwidth of 250Hz should be dedicated. LHC-b expect to have around 25% charm fraction in the trigger composition which in one year of operations at nominal LHC Luminosity of $2 \cdot 10^{32} cm^{-2} s^{-1}$ will lead to a yield of 250-500 Million $D* \rightarrow D^0\pi$ decays selected in the $D^0 \rightarrow K\pi$ mode [8]; this yield is almost two orders of magnitude more than what CDF expects to collect with the full Tevatron statistics. Very preliminary estimates based on signal statistics only for LHC-b potential in CP violation and mixing give $\sigma(A_{CP})$ 10^{-4} in the KK channel and $\sigma(y_{CP})$ 10^{-4}. The time dependent wrong sign D^0 analysis in LHC-b will certainly benefit from great PID capability. Detailed studies are on going but we could conclude that LHC-b will possibly be sensitive in SM range for A_{CP} and x, y mixing quantities and will definitely take over what CDF started in charm physics at hadronic machines.

References

1. A.Bardi et al. N.I.M. A **485**, 178-182 (2002)
2. D.Acosta et al.[CDF coll.], Phys. Rev. D **65**, 052005 (2002)
3. D.Acosta *et al*[CDF coll.],Phys. Rev. Lett. **91**, 241804 (2003)
4. M.Cacciari and P.Nason, arXiv:hep-ph/0306212
5. R. Barate et al.[Aleph], Eur. Phys. J. **C16**, 597-611 (2000)
6. D.Acosta *et al*[CDF coll.],Phys. Rev. Lett. **94**, 122001 (2005)
7. I.Shipsey, in these proceedings.
8. T.Nakada, in these proceedings.

BOTTOM-QUARK PHYSICS I

R.N. Cahn	The B-Factory Legacy
S. Malvezzi	CPV in Three-Body Decays: The Power of the Dalitz-Plot Analysis
A.J. Schwartz	Searches for D^0– $\overline{D}^0$ Mixing: Finding the (Small) Crack in the Standard Model
F. Lehner	Rare Charm and Bottom Decays at TeVatron
D. Becirevic	Flavour Physics From Lattice QCD
G. Rong	Search for Non–Ddbar decays of $\psi(3770)$ and Measurement of the Partial Widths
D. Asner	Constraints on Charm Mixing, Strong Phases and Doubly-Cabibbo-Suppressed Decays from CLEO-c
S. Fajfer	Search for Effects of Littlest Higgs Model $D^+ \to \pi^+ \ell^+ \ell^-$ and $D^0 \to \rho^0 \ell^+ \ell^-$ Decays

Frascati Physics Series Vol. XLI (2006), pp. 197-206
DISCOVERIES IN FLAVOUR PHYSICS AT e^+e^- COLLIDERS
Frascati, February 28th - March 3rd, 2006

THE B-FACTORY LEGACY

Robert N. Cahn
Lawrence Berkeley National Laboratory, Berkeley, CA, USA

Abstract

Kaon physics was the foundation for much of what we know of the Standard Model, from the existence of strangeness (and thus quarks), particle oscillations ($K_L - K_S$), parity violation ($\tau - \theta$ puzzle), and CP violation to the absence of flavor-changing neutral currents. The full significance of these discoveries became clear only much later. B physics is likely in the same way to play a key role in decoding the discoveries at LHC. Whatever new physics is found there, strong constraints on its interpretation will come from flavor-changing neutral currents. The results now emerging from the Belle and BaBar experiments are thus likely to be of increasing importance, even after these experiments conclude data-taking. How far will these experiments be able to go in establishing precision results that will constrain our interpretation of LHC discoveries? We estimate this by extrapolating from the latest Belle and BaBar results.

1 K Physics Taught Us Most of What We Know

The discovery[1] by Rochester and Butler of "vee" particles revealed that particles produced in strong interactions might not be able to decay strongly. Gell-Mann's additive quantum number, strangeness, explained this and presaged his invention of SU(3) and the quark model. The proposal of Gell-Mann and Pais suggested that in addition to the short-lived neutral K meson, there was another, long-lived one. The discovery of the K_L at Brookhaven in 1956 exposed the phenomenon of particle oscillation, which was to play a recurring role over the next half century.

The $\tau - \theta$ puzzle, the existence of decays to $\pi^+\pi^0(\tau)$ and to $\pi^+\pi^+\pi^-(\theta)$, the first having natural spin-parity and the latter, as evidenced in the Dalitz plot, having $J^P = 0^-, 2^-...$, but with apparently the same mass, revealed parity violation. Eight years after the fall of parity, Cronin, Fitch, Turlay and collaborators found the equally surprising CP violation in the neutral K sector.

Less dramatic, but ultimately of great importance was the absence of decays that seemed to violate no fundamental conservation law. Strangeness was clearly violated in weak decays like $K_L \to \pi^+\pi^-\pi^0$, so what prevented $K_L \to \mu^+\mu^-$, which occurs at a rate 10 million times slower? The absence of flavor-changing neutral currents is now a central feature of the Standard Model of particle physics and a powerful constraint on any additions to it.

2 Will B Mesons Be the K Mesons of the 21st Century?

B mesons are analogous to K mesons in that they have decays that are CKM-suppressed relative to, say, D mesons, which decay through a diagonal element of the CKM matrix. This feature makes mixing relevant and allows detailed examination of decays that occur only through virtual-particle loops. In the "box" diagram of mixing and the box-like diagram of penguin decays – both gluonic and electromagnetic – particles beyond the Standard Model can make their appearance. Indeed, they will make their appearance and the question is: how are their effects suppressed? In the Standard Model, effects are suppressed by $\Delta m^2/m_W^2$, that is, by the ratio of the difference of squares of quark masses over the square of the W mass.

[1]For history, see *Experimental Foundations of Particle Physics*, Robert N. Cahn and Gerson Goldhaber, Cambridge Press, 1989.

The "boxes" that contain the new physics can be studied in B physics and at the LHC. At the LHC with ATLAS and CMS, we will cut open the box to reveal the new particles as real. In B physics we can only shake the "box" and listen for sounds that are circumstantial evidence of the particles inside. Clearly, the advantage is to LHC, but there is still room for B physics to come to the fore. Most likely, not every new particle will be seen at LHC, either because some are too massive or because some are hard to produce or to identify. Yet these still may make their contribution to mixing and rare decays. In addition, B physics is sensitive not just to masses but to couplings and mixing. These may be less accessible at the LHC.

A critical issue for the new particles will be how they manage to avoid large flavor-changing neutral currents. Here B mesons can play a crucial role. Not only they do provide the opportunity to observe the flavor-changing neutral currents in nonleptonic decays, but whether or not deviations are found from the expectations of the Standard Model, these measurements will be essential constraints on theories attempting to explain the new particles found at the LHC. It is particularly important to stress that what is most important here is the precision achieved by the B factories, not whether deviations are found. The absence of deviations could be especially powerful in eliminating some possible models proposed in response to LHC data.

3 The Real Power of B-Factories Comes in the Long Run

Much has been made of some discrepancies between Standard Model predictions and results from the B factories, especially in the measurement of $\sin 2\beta$, where results from the $b \to c\bar{c}s$ decays give a larger value than those from the penguin decays, $b \to sg$. While this particular discrepancy has persisted when all penguin decays are combined, the weight of the discrepancy has shifted from time to time, from one decay to another. Never has the discrepancy reached 5σ. Such a high standard is appropriate, especially when there are so many decays to be examined.

Once there are results from LHC pointed to specific channels for large discrepancies (or for no discrepancies), the significance of the B-factory measurements will be much enhanced. Evidence at the three-σ level showing a predicted pattern would be a lot more persuasive than the random discrepancies we find today. For this reason, the data being collected and analyzed by

Belle and BaBar will not fade in interest but will rather increase.

Projections from BaBar indicate that by the end of running in 2008 approximately 1.0 ab^{-1} will have been collected, while the figure for Belle is approximately 1.5 ab^{-1}.

4 Time-Dependent CP Violation Measurements

The CKM matrix is a central feature of the Standard Model. It encapsulates the basic facts: there are three and only three generations; the weak eigenstates are not the mass eigenstates. This requires that the CKM matrix be unitary. Redefining the phases of the quark states enables us to specify the CKM matrix by four real parameters. One unitarity relation leads to the famous unitarity triangle, whose angles are α, β, and γ or ϕ_2, ϕ_1, and ϕ_3.

Measurements of the time dependence of decays affected by B^0-$\overline{B}^0$ mixing provide directly the quantities S_f and C_f defined by

$$\frac{\Gamma(\overline{B}^0 \to f) - \Gamma(B^0 \to f)}{\Gamma(\overline{B}^0 \to f) + \Gamma(B^0 \to f)} = S_f \sin \Delta m t - C_f \cos \Delta m t \qquad (1)$$

In the simplest case, f is a CP eigenstate and the decay has contributions only with a single weak phase. Then $C_f = 0$ and S_f is simply related to an angle of the unitarity triangle. This is so for $f = J/\psi K_S$, which occurs through $b \to c\bar{c}s$ and then $S = \sin 2\beta$. It should also hold for "penguin" decays through $b \to s\bar{s}s$. The penguin decays involve virtual particles and particles outside the Standard Model can contribute, too. Thus discrepancies between $\sin 2\beta$ measured in different channels would signal contributions from outside the Standard Model, provided they are larger than those anticipated from small contributions from within the Standard Model.

4.1 β

The classic measurement of $\sin 2\beta$ is in $B \to J/\psi K_S$, but other charmonium states and other K's and K^*'s contribute similarly. After some years of convergence the results from Belle [1] ($0.652 \pm 0.039 \pm 0.020$) and BaBar [2] ($0.722 \pm 0.040 \pm 0.023$) differ a bit more than they had recently. The subject of intense interest, $\sin 2\beta$ measured in the penguin modes $b \to sg$, continues to tantalize. The discrepancy with the result in $b \to c\bar{c}s$ varies from one penguin mode to another, leaving a still uncertain picture. See Table 1. What is

important is that the enormous increase in data expected by the end of 2008 will leave very small statistical uncertainties in a number of modes. Whether $\sin 2\beta$ in these modes agree or disagree with the value found in the "golden" mode, these precision measurements will provide a crucial test of how the new physics uncovered at the LHC is reconciled with the absence of flavor-changing neutral currents.

	Belle				BaBar				Both
Mode	S 2005	$\pm$ 2005	lum fb^{-1}	$\pm$ 2008	S 2005	$\pm$ 2005	lum fb^{-1}	$\pm$ 2008	200
ϕK_S	0.44	0.27	357	0.132	0.50	0.25	205	0.113	0.08
$\eta' K_S$	0.62	0.12	357	0.059	0.36	0.13	205	0.059	0.04
KKK_S	0.60	0.18	357	0.088	0.41	0.17	205	0.077	0.05
$K_S K_S K_S$	0.58	0.36	357	0.176	0.63	0.30	205	0.136	0.10
$f_0 K_S$	0.47	0.36	357	0.176	0.95	0.32	192	0.140	0.11
$\pi^0 K_S$	0.22	0.47	357	0.229	0.35	0.30	205	0.136	0.11
$c\bar{c}K_S$	0.65	0.04	357	0.019	0.72	0.04	205	0.018	0.01
$\pi^+\pi^-$	-0.67	0.16	253	0.066	-0.30	0.17	205	0.077	0.05
$\rho^+\pi^-$ S	-0.28	0.23	140	0.070	-0.10	0.14	192	0.061	0.04
$\rho^+\pi^-$ A^{+-}	-0.02	0.16	140	0.049	-0.21	0.11	192	0.048	0.03
$\rho^+\pi^-$ A^{-+}	-0.53	0.29	140	0.089	-0.47	0.14	192	0.061	0.05
$\rho^+\rho^-$ S	0.09	0.42	253	0.172	-0.33	0.24	205	0.109	0.09

Table 1: Projections for statistical uncertainties for $\sin 2\beta$ and $\sin 2\alpha$ and related quantities. Current values are given and projections through 2008, for Belle and BaBar separately and for the two combined in 2008.

4.2 α

The story of α is one of the most surprising of all those to come from the B factories. The channel $B \to \pi^+\pi^-$ was second only to $B \to J/\psi K_S$ in the attention it was given at the outset. Some argued that penguins would be a big problem and that $B \to \rho\pi$ offered enough channels two separate the penguins from the trees. Instead, it is $B \to \rho\rho$ that has emerged as the most telling channel. The reason, again, is penguins. Penguins are important in $B \to \pi\pi$. To overcome penguins, you need to measure, in addition to the time dependence of $B^0 \to \pi^+\pi^-$, the branching fractions for $B^+ \to \pi^+\pi^0$,

$B^0 \to \pi^+\pi^-$, $\overline{B}^{\upsilon} \to \pi^+\pi^-$, $B^0 \to \pi^0\pi^0$, and $\overline{B}^{\upsilon} \to \pi^0\pi^0$. Some recent results are shown in Table 2.

	BaBar	$\int \mathcal{L}dt$	Belle	$\int \mathcal{L}dt$
BF($\pi^+\pi^0$)	$5.8 \pm 0.6 \pm 0.4$ [3]	205	$5.0 \pm 1.2 \pm 0.5$ [4]	78
BF($\pi^+\pi^-$)	$5.5 \pm 0.4 \pm 0.3$ [5]	205	$4.4 \pm 0.6 \pm 0.3$ [4]	78
BF($\pi^0\pi^0$)	$1.17 \pm 0.32 \pm 0.10$ [6]	205	$2.3^{+0.4\ +0.2}_{-0.5\ -0.3}$ [7]	253

Table 2: Recent branching fractions in units of 10^{-6} for various $B \to \pi\pi$ channels. Integrated luminosities for each channel are given in fb^{-1}.

To correct for the penguin contribution, we need to form the "isospin" triangles with sides equal to the magnitudes of the decay amplitudes for $B \to \pi\pi$ and $\overline{B} \to \pi\pi$. The correction is either the difference or the sum of the angles opposite the side for $\pi^0\pi^0$. We see that the $\pi^0\pi^0$ decays are not much suppressed relative to the other channels and thus all the angles of the triangles are fairly large. As a consequence the penguin corrections is potentially large and poorly known. We don't know whether the two isospin triangles are to be oriented so that the angle that gives the correction is the sum or the difference of the two angles opposite the $\pi^0\pi^0$ sides. As a result, the bound on the correction is 35^o at 90% CL.

The situation for $\rho\rho$, in contrast, is entirely serendipitous. An obvious potential issue is that since the ρ has spin one, there are three partial waves. However, measurements show that only the longitudinal polarization contributes and this has pure CP even. In addition, contrary to the $\pi\pi$ cse, the neutral-neutral final state has a much suppressed branching fraction. In fact, we have only a limit on the branching fraction. See Table 3.

We see that the angles opposite the $\rho^0\rho^0$ side must be small and thus the uncertainty in the correction for penguins is also small. Quantitatively, it is $\pm 11^o$.

4.3 γ

The measurement of γ is achieved through interference between $b \to c\overline{u}s$ and $b \to u\overline{c}s$. Interference is possible only for a final state that can be reached through both c and $\overline{c}$: (Cabibbo-suppressed) decays of D^0 and $\overline{D}^0$ to common final states. Consider, in particular $B^- \to D^0 K^-$ and $B^- \to \overline{D}^0 K^-$ and write

$$\frac{A(B^- \to D^0 K^-)}{A(B^- \to \overline{D}^0 K^-)} = r_B e^{i(\delta_B - \gamma)} \tag{2}$$

so δ_B comes from the strong phase and γ comes from the CKM matrix element. It has been found that a particularly effective channel is $D^0 \to K_S \pi^+ \pi^-$, which obviously is accessible to $\overline{D}^0$ as well. Of course, in the D^0 decay it is $\overline{K}^0$ that is produced while from $\overline{D}^0$ we get K^0. Thus the decay amplitudes for the D^0 and the $\overline{D}^0$ are the same except that the π^+ and π^- need to be interchanged. The Dalitz plot itself can be studied with very high statistics and the underlying amplitude described by a sum of many resonances. This yields decay amplitudes with well determined phases. Then, the fit to this particular channel will be very sensitive to relative phases and thus to γ. The current values [13] from BaBar ($67 \pm 28(\text{stat}) \pm 13(\text{syst}) \pm 11(\text{model})$ and Belle ($53^{+15}_{-18}(\text{stat}) \pm 3(\text{syst}) \pm 9(\text{model})$) are similar.

5 Sides of the Unitarity Triangle

Precision in the measurement of the sides of the unitarity triangle has reached better than 2% for $|V_{cb}|$ where a value near $(41.7 \pm 0.7) \times 10^{-3}$ is anticipated. About V_{ub} there remains much more uncertainty. The Heavy Flavor Averaging

	BaBar	(fb^{-1})	Belle	(fb^{-1})
BF($\rho^+\rho^0$)	$17.2 \pm 2.5 \pm 2.8$ [8]	205	$31.7 \pm 7.1^{+3.8}_{-6.7}$ [9]	78
BF($\rho^+\rho^-$)	$30 \pm 4 \pm 5$ [10]	82	$22.8 \pm 3.8^{+2.3}_{-2.6}$ [11]	253
BF($\rho^0\rho^0$)	< 1.1 [12]	205		

Table 3: Recent branching fractions in units of 10^{-6} for various $B \to \rho\rho$ channels. Integrated luminosities for each channel are given in fb^{-1}.

Group gives [14] results of $(4.45 \pm 0.20 \pm 0.26) \times 10^{-3}$ and $(4.41 \pm 0.20 \pm 0.20) \times 10^{-3}$, depending on the scheme used. With somewhat lower value of $\sin 2\beta$ arising from the latest Belle measurement, there is potential for a modest conflict in the unitarity triangle. As always, only time will tell.

6 Radiative Penguins

The decay $b \to s\gamma$ has a special place in B physics because it is sensitive to new physics contributions at the loop level, while the Standard Model process itself also occurs at the one-loop level. Unfortunately, it is the inclusive process, $B \to X_s\gamma$ that is theoretically attractive, while experimentally it is $B \to K^*\gamma$ and the like that we prefer to measure. For the inclusive process, we may proceed by adding up many channels (semi-inclusive) or by indeed just measuring the photon (fully inclusive). Representative results from BaBar are for the semi-inclusive $(327 \pm 18^{+55}_{-40}{}^{+4}_{-9}) \times 10^{-6}$ [15] and $(367 \pm 29 \pm 34 \pm 29) \times 10^{-6}$ [16] for the fully inclusive. In the long run, the model dependence of the semi-inclusive method will cause it to lose out in the race with the fully inclusive technique.

7 Theory: Limits and Advances

As the precision of measurements increases, the demands on theory will increase accordingly. Both lattice gauge theory and QCD phenomenology must make advances if B physics is to reach the potential available with 2 ab^{-1}. This is particularly so for V_{ub}, V_{cb}, and radiative penguins, but similar demands will come for all high precision measurements, like $\sin 2\beta$. Particularly in the LHC era, the full utility of B physics measurements will require greatly improved understanding of the influence of QCD.

8 The 2008 Scorecard

Combining current results and projections to anticipated integrated luminosities at Belle and BaBar we venture to make predictions for the uncertainties we will have at the end of 2008: $\sigma(\sin 2\beta; b \to c\bar{c}s) = 0.020$, $\sigma(\sin 2\beta; b \to sg) = 0.040 - 010$, $\sigma(\alpha) = 8^o$, $\sigma(\gamma) = 10^o$, $\sigma(V_{ub}) = 6\%$, $\sigma(b \to s\gamma) = 5\%$, $\sigma(A_{SL}) = 2 \times 10^{-3}$.

A similar picture is provided by a prospective CKM triangle for the end of 2008.

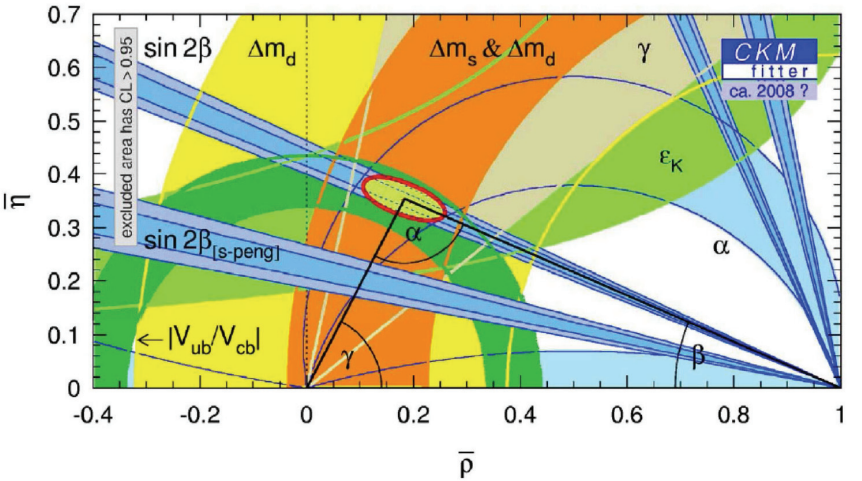

Figure 1: *A projection of the unitarity triangle in 2008, with the assumptions* $\sigma(V_{ub}) = 6.5\%$, $\sigma(\Delta m_s) = 5\%$, $\sigma(\sin 2\beta) = 0.019$, $\sigma(\alpha) = 8^o$, $\sigma(\gamma) = 10^o$. *Figure courtesy Andreas Hoecker.*

9 The Legacy

The B factories today are challenging the Standard Model as did LEP in its day. The results of the B factories will not decline in importance in the coming years, but rather will increase since they will provide a major constraint on models proposed to explain the new physics found at the LHC. Whether the results from BaBar and Belle agree with the Standard Model or contradict it, they will complement the LHC results. The higher the precision obtained by BaBar and Belle, the more powerful will be their message. Just as K physics has stood as a bedrock for particle physics for five decades, B physics will be a lasting legacy for fundamental physics.

Acknowledgment I am grateful to Zoltan Ligeti for his advice and explanations.

References

1. Belle Collaboration, K. Abe, *et al.*, hep-ex/0507037.
2. BaBar Collaboration, B. Aubert *et al.*, *Phys. Rev. Lett.* **94**, 161803 (2005).
3. BaBar Collaboration, B. Aubert *et al.*, *Phys. Rev. Lett.* **94**, 181802 (2005).

4. Belle Collaboration, Y. Chao, *et al.*, *Phys. Rev.* **D69**, 111102 (2004).

5. BaBar Collaboration, B. Aubert *et al.*, hep-ex/0508046.

6. BaBar Collaboration, B. Aubert *et al.*, *Phys. Rev.* **D73**, 071102 (2005).

7. Belle Collaboration, Y. Chao, *et al.*, *Phys. Rev.* **D71**, 091106 (2004).

8. BaBar Collaboration, G. Schott *et al.*, Preliminary result, Rencontre de Moriond Electroweak, March 2006.

9. Belle Collaboration, J. Zhang, *et al.*, *Phys. Rev. Lett.* **91**, 221801 (2003).

10. BaBar Collaboration, B. Aubert *et al.*, *Phys. Rev. Lett.* **93**, 231801 (2004).

11. Belle Collaboration, A. Somov, *et al.*, hep-ex/0601024.

12. BaBar Collaboration, B. Aubert *et al.*, *Phys. Rev. Lett.* **94**, 131801 (2005).

13. Heavy Flavor Averaging Group, http://www.slac.stanford.edu/xorg/hfag /triangle/moriond2006/index.shtml#gamma_D0K

14. Heavy Flavor Averaging Group, http://www.slac.stanford.edu/xorg/hfag /semi/winter06/winter06.shtml

15. BaBar Collaboration, B. Aubert *et al.*, *Phys. Rev.* **D72**, 052004 (2005).

16. BaBar Collaboration, B. Aubert *et al.*, hep-ex/0507001.

Frascati Physics Series Vol. XLI (2006), pp. 207-216
DISCOVERIES IN FLAVOUR PHYSICS AT e^+e^- COLLIDERS
Frascati, February 28th - March 3rd, 2006

CPV IN THREE-BODY DECAYS: THE POWER OF THE DALITZ-PLOT ANALYSIS

Sandra Malvezzi
INFN Sezione di Milano, Via Celoria 16, 20133 Milano–Italy

Abstract

Over the last few years we have seen a resurrection of the Dalitz-plot technique in the analysis of modern, heavy-flavour experiments. I shall briefly present and discuss the power of this analysis technique, some preliminary results from pilot studies in the beauty sector and possible benefits available from the charm-field expertise.

1 Introduction – The Dalitz-plot revenge

Over the last decade Dalitz-plot analysis has spread widely through the heavy flavour community and has now become quite a standard technique for CPV investigation in the beauty sector: I like to call it the Dalitz-plot revenge. This non-trivial analysis tool allows for the determination of a complete set

of decay parameters, i.e., amplitudes and phases. CP is a peculiar phase phenomenon: exploiting interference and making use of a formalism with explicit CKM phases, it is possible to measure the Unitarity Triangle angles, as is the case for α in the $B \to \rho\pi$ decay and γ in the $B \to D^{(*)}K^{(*)}$ decay. The Dalitz-plot approach has to be considered complementary to other measurements: independent determinations, to over-constrain the Unitarity Triangle, provide a non-trivial test of the Standard Model. Comparing results in various channels and via different analysis techniques will allow us to find possible SM inconsistency and the way to New Physics.

2 Pilot studies in the beauty sector

2.1 $B \to \rho\pi$

A theoretically clean way to extract α is via a time-dependent Dalitz plot analysis of $B \to \rho\pi$. The formalism has been suggested and completely developed by theorists [1]. The experimental analysis of $B \to \pi^+\pi^-\pi^0$ implies, from the operative point of view, disentangling the $\rho\pi$ intermediate states from the other $(\pi\pi)\pi$ resonant and non-resonant components. Data are progressively becoming available, along with a few tentative analyses. A full Dalitz analysis has been performed by BaBar, providing a preliminary measurement of $\alpha = (113^{+27}_{-17} \pm 6)^\circ$ [2]. A partial Dalitz analysis has been carried out by Belle too, just selecting distinct bands in the two-pion mass combinations and disregarding residual interference. The measured value is $\alpha = (102 \pm 11 \pm 15)^\circ$ [3].

2.2 $B \to \rho\rho$

The $B \to \rho\pi$ channel has been somewhat obscured by the greater attention recently paid to the $B \to \rho\rho$ decay, owing to the relatively small penguin pollution. Its analysis is, however, potentially complicated, with three possible helicity states in the decay: helicity 0 states are CP even, helicity ± 1 states are not CP eigenstates. Nature seems to be kind to us and gives almost full longitudinal polarization for this mode [4, 5], highly simplifying the measurement, avoiding the need of complete angular analysis and of much higher statistics. BaBar and Belle have published α values of $(100 \pm 13)^\circ$ and $(88 \pm 17)^\circ$ respectively.

2.3 Some complications for α extraction

Both the $B \to \rho\pi$ Dalitz-plot analysis and the $B \to \rho\rho$ (non-Dalitz plot) analysis share some analogous complications. Indeed, the road to go from three pions to $\rho\pi$ or from four pions to $\rho\rho$ can be rather insidious and requires selecting and filtering the desired intermediate states among the possible $\sigma\pi$, $f_0(980)\pi$, $\sigma\sigma$, $\sigma\pi\pi$ etc. This poses the problem of how to deal with strong-dynamics effects, in particular those regarding the scalar mesons. The $\pi\pi$ S-wave is characterized by broad, overlapping states: unitarity is not explicitly guaranteed by a simple sum of Breit–Wigner functions. In addition, independently of the nature of the σ (genuine resonance or a strong dynamics structure), it is not a simple Breit–Wigner; the $f_0(980)$ is a Flatté-like function, and its lineshape parametrization needs a precise determination of KK and $\pi\pi$ couplings.

2.4 $B \to DK$

The possibility of observing CP violation in the $B \to DK$ channel is based on two key facts: namely, B can produce neutral D mesons of both flavours and D^0, $\bar{D}^0$ can decay into a common final state. The two amplitudes interfere with a phase that is the sum of strong and weak interaction phases: $\theta_+ = \delta + \gamma$ and $\theta_- = \delta - \gamma$ for the CP-conjugate state. The original suggestion to extract γ was to use interference between the Cabibbo-favoured mode $D^0 \to K^+\pi^-\pi^0$ and the doubly Cabibbo-suppressed mode $\bar{D}^0 \to K^+\pi^-\pi^0$, with the obvious limitations in statistics for the latter. Recently it has been suggested to use the Cabibbo-favoured mode $K_s\pi^+\pi^-$, which is common to both D^0 and $\bar{D}^0$. A pilot study performed by Belle [6] provides a value $\gamma = (68^{+14}_{-15} \pm 11 \pm 13)^\circ$ for a combined sample of $B^\pm \to D^\pm K$ and $B^\pm \to D^* K^\pm$. The method proposed by Belle has also been implemented by BaBar [7], giving $\gamma = (70 \pm 31^{+12+14}_{-10-11})^\circ$.

2.5 Some complications for γ extraction

A model for the D^0 amplitude is, of course, needed, and it turns out to be the dominant source of systematics. This is not surprising since a set of 15 two-body resonances has to be introduced to describe the $(K\pi)\pi$ and $K_s(\pi\pi)$ states. In addition two *ad hoc* resonances are required to reproduce the excess of events in the $\pi\pi$ spectrum, one at the low-mass threshold, the other at $1.1\,\mathrm{GeV}^2$. Masses and widths of the two states, named σ_1 and σ_2, have been fitted to

the data themselves and found to be $M_{\sigma_1} = 539 \pm 9\,\text{MeV}$, $\Gamma_{\sigma_1} = 453 \pm 13$ and $M_{\sigma_2} = 1048 \pm 7\,\text{MeV}$, $\Gamma_{\sigma_2} = 109 \pm 11$ respectively. This procedure of "effectively" fitting data invites a word of caution. Do we really understand our systematics? Are we confident of controlling strong-dynamics effects in the analysis?

3 A way to proceed: the charm experience

The experience and expertise gleaned from the charm sector can inspire the beauty community as to how to proceed and overcome the above-mentioned difficulties. As a matter of fact, the same parametrization problems of strong dynamics effects have been already encountered in the charm analysis. It is thus worth remarking that BaBar has recently implemented the *K-matrix* formalism for the $\pi^+\pi^-$ S-wave parametrization in the $K_s\pi^+\pi^-$ analysis of the $D^0\bar{D}^0$ decays, just following the work suggested by the FOCUS collaboration [8] for D^+ and D_s to three pions. The implementation of this new formalism for the description of the BaBar $\pi^+\pi^-$ spectrum has been successful: no *ad-hoc* resonances [9] had to be inserted and the preliminary systematic error on the angle γ has been quoted at about 3°. Although I consider this analysis to be only in its preliminary stages and many refinements will certainly be necessary, I do believe this is the right track to pursue to reliably gauge the level of confidence in the final results.

3.1 The FOCUS D_s^+ and $D^+ \to \pi^+\pi^-\pi^+$ case

Many charm amplitude analyses require detailed knowledge of the light-meson sector. In particular, the need to model intermediate scalar particles contributing to the charm meson in the decays has caused the FOCUS collaboration to question the validity of the Breit–Wigner approximation for the description of the relevant scalar resonances [10, 11].

A formalism for studying overlapping and many-channel resonances was proposed long ago and is based on the *K-matrix* [12, 13, 14] parametrization. The *K-matrix* approach allows us to include the positions of the poles in the complex plane directly in our analysis, incorporating the results from spectroscopy experiments [15, 16]. In addition, the *K-matrix* formalism provides a direct way of imposing the two-body unitarity constraint, which is not explicitly guaranteed in the simple isobar model. Minor unitarity violations are

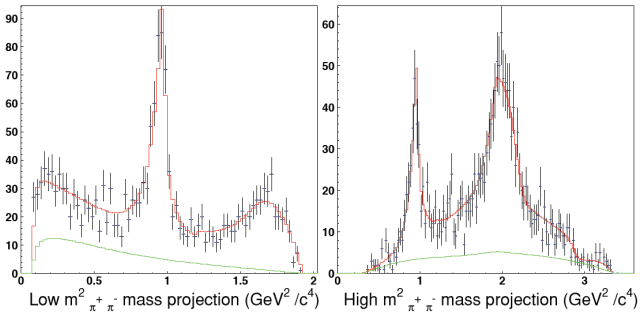

Figure 1: *FOCUS D_s^+ Dalitz-plot projections with fit results superimposed. The background shape under the signal is also shown.*

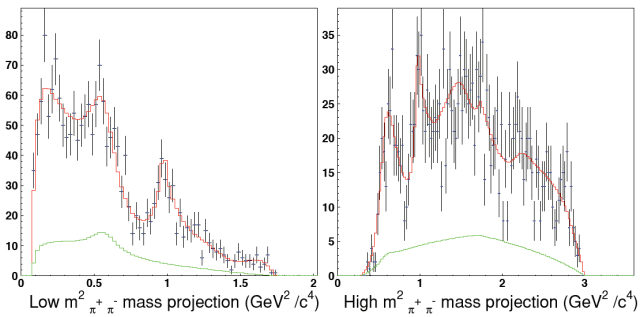

Figure 2: *FOCUS D^+ Dalitz-plot projections with fit results superimposed. The background shape under the signal is also shown.*

expected for narrow, isolated resonances but more severe ones exist for broad, overlapping states. The validity of the assumed quasi two-body nature of the process in the *K-matrix* approach can only be verified by a direct comparison of the model predictions with data. The FOCUS collaboration has implemented the *K-matrix* approach in the D_s and $D^+ \to \pi^+\pi^-\pi^+$ analyses. Details can be found in [8]: here I only present plots of the final results. In Fig. 1) and Fig. 2) the Dalitz-plot projections are shown for D_s and D^+ into three pions. In Fig. 3 the FOCUS adaptive binning schemes for D_s^+ (left) and D^+ (right) are plotted.

This analysis represents the first application of the *K-matrix* formalism to the charm sector. The confidence levels of the final fits are 3.0 % and 7.7 % for the D_s and D^+ respectively. The results are extremely encouraging since the same *K-matrix* description gives a coherent picture of both two-body scat-

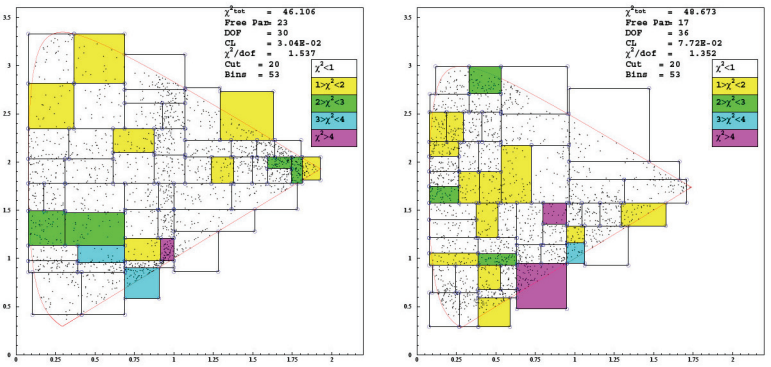

Figure 3: *D_s^+ (left) and D^+ (right) adaptive binning Dalitz-plots for the FOCUS K-matrix fit.*

tering measurements in light-quark experiments *as well as* charm-meson decay. This result was not obvious beforehand. Furthermore, the same model is able to reproduce features of the $D^+ \to \pi^+\pi^-\pi^+$ Dalitz plot that would otherwise require an *ad hoc* σ resonance. In addition, the non-resonant component of each decay seems to be described by known two-body S-wave dynamics without the need to include constant amplitude contributions. In addition, the better treatment of the S-wave contribution provided by the *K-matrix* model can reproduce the low-mass $\pi^+\pi^-$ structure of the D^+ Dalitz plot. This suggests that any σ-like object in the D decay should be consistent with the same σ-like object measured in $\pi^+\pi^-$ scattering. Of course, additional studies with higher statistics will be required to completely understand the σ puzzle. Nevertheless, the FOCUS experience can guide the $K_s\pi^+\pi^-$ analysis crucial for the measurement of the angle γ in beauty decays.

4 The effort in the beauty field continues, matures and grows

The application of the Dalitz-plot technique is intensifying. The statistical accuracy of the γ extraction can be improved by adding excited K states to the analysis. Belle has provided a preliminary result based on about 60 events [17] selected from a statistics of $253\,\mathrm{fb}^{-1}$. The angle γ is measured to be $\gamma = 112 \pm 35 \pm 9 \pm 11 \pm 8$; the last two systematics errors come from the

D model uncertainty and from the $K_s\pi$ non-resonant component underneath the K*. Analysis of $B \to DK^*$ has been performed by Babar too: data are published along with $B \to D^{(*)}K^{\pm}$ in [9]. A study of all the hadronic final states is important to cross check results and learn from one channel for the other. Both BaBar and Belle have started systematic analyses of the various K and π combinations. More precisely, Belle has analyzed $B^+ \to K^+\pi^+\pi^-$, $B^+ \to K^+K^-K^+$ and $B^0 \to K^0\pi^+\pi^-$ [18]. A few observations are interesting. CP asymmetry is predicted very small in $B^+ \to K^{*0}(892)\pi^+$, offering the opportunity to search for New Physics in $B^+ \to K^+\pi^+\pi^-$. Of course, a robust model for $K\pi$ states is required. The three-kaon final states demands a proper parametrization of all the KK resonances, such as $f_0(980)$ and $f_0(1300)$, which are typically coupled-channel functions. The $\pi\pi$ states present all the complications already discussed. BaBar, in turn, has analyzed $B^+ \to \pi^+\pi^+\pi^-$ [19], $B^+ \to K^+\pi^+\pi^-$ [20] and $B^0 \to K^+K^-K_s$ [21]. This last channel deserves some considerations. A promising way to search for New Physics is indeed $B^0 \to \phi K_s$. A reliable Standard Model prediction estimates $\sin 2\beta(J/\Psi K_s) = \sin 2\beta(\phi K_s)$. BaBar and Belle have provided $\sin 2\beta((\phi K_s) = 0.50 \pm 0.25^{+0.07}_{-0.04}$ and $\sin 2\beta((\phi K_s) = 0.44 \pm 0.27 \pm 0.05$ respectively, to be compared with the average $\sin 2\beta(J/\Psi K_s) = 0.685 \pm 0.032$. As soon as the statistical accuracy increases, it will be crucial to understand how the resonant (e.g, $f_0(980)$) and non-resonant components underneath the ϕ affect the phase, i.e. it will be imperative to measure all the contributions and the related interferences via a Dalitz-plot analysis.

5 CPV in charm

I have insisted on the relationship between charm and beauty and on how beauty physics can benefit from the expertise coming from a mature field, as is that of charm. We should not think, however, that charm is only enslaved to beauty. Charm possesses a dignity of its own. In the Standard Model the D system is not as sensitive to CP as B and K mesons. The small predicted effect could leave open a window onto New Physics. Furthermore, charm is unique since non-Standard Model effects might exhibit different patterns for up and down classes of quarks. Charm decays are the only up-type decays that afford a probe of such physics. It is important to measure CP in charm and it is important to exploit new methods of analysis. Various attempts have been

made in the last few years by different experiments and in different channels. Just to mention a few: a study by BaBar on $D^0 \to K^+K^-K_s$ [22], a study by CLEO on $D^0 \to \pi^+\pi^-\pi^0$ [23] and on $D^0 \to K_s\pi^+\pi^-$ [24].

The possibility to exploit the Dalitz-plot technique to investigate CP in the charm sector was first suggested by FOCUS on $D^+ \to K^+K^-\pi^+$ [25]. The decay presents all the characteristics to be a good candidate to search for CPV effects: two amplitudes (DCS and penguin) interfere, the statics is rather high (about 7000 events) and Final State Interactions (FSI) are copious, providing the strong phases. The simple, original idea was to analyse the two conjugate state D^+ and D^- separately. The results are based on a simple Breit–Wigner fit: amplitudes and phases for the two conjugate states are shown in Fig. 4 and Fig. 5 along with the full sample results. It was in just this analysis that we realized problems in the $f_0(980)$ and $a_0(980)$ KK coupled-channel lineshapes and $K\pi$ broad resonances, went back to the textbooks and learnt about the *K-matrix*.

Not surprisingly, no CPV has been reported so far in the charm sector: higher accuracy will be needed.

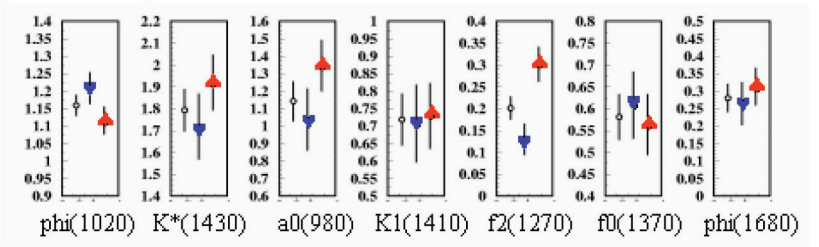

Figure 4: *D^+ (downward triangle) D^- (upward triangle) and full sample (circle) amplitudes from the $KK\pi$ FOCUS Dalitz-plot analysis.*

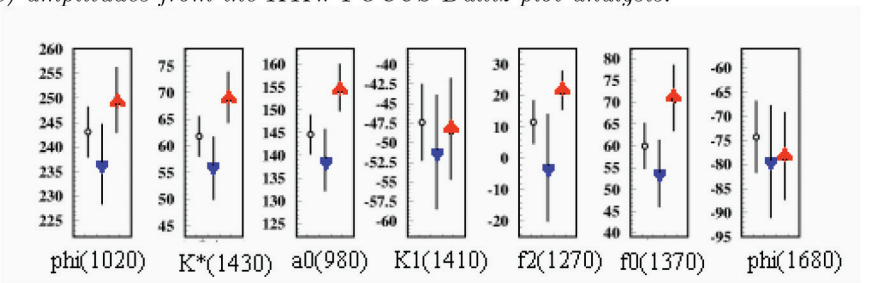

Figure 5: *D^+ (downward triangle) D^- (upward triangle) and full sample (circle) phases from the $KK\pi$ FOCUS Dalitz-plot analysis.*

6 The perspective of the hadronic physics

There is another perspective to take, precisely the "hadronic physics challenge." It is true that, if we want to interpret Heavy Flavour dynamics reliably, we need to keep the strong effects induced by light hadrons in the final states under control, but it is also true that very clean samples of Heavy Flavour offer an unprecedented opportunity to investigate light-meson physics. BaBar, Belle, BES and Cleo-c have (and/or) will have sufficient statistics to provide precise phase-shift behavior, measure resonance parameters to compare with the experiments at low and intermediate energy, to find consistency/inconsistency and enrich our knowledge of hadronic physics.

7 Conclusions

Dalitz-plot analysis represents a powerful, unique and promising tool for studying CP violation in the beauty sector. There is a new, vigorous effort to perform amplitude analysis: a more robust formalism has been implemented, many channels have been investigated. The beauty community can benefit from charm experience and expertise. Dalitz-plot analysis will definitely keep us company over the next few years. There will be a lot of work for both experimentalists and theorists alike: synergy will be invaluable. Some complications have already emerged, especially in the charm field, others, unexpected, will only become clearer when we delve deeper into the beauty sector. B_s will be a completely new chapter. The analysis is challenging but there are no shortcuts toward ambitious and high-precision studies and, ultimately, New Physics searches.

References

1. A. E. Snyder, H R. Quinn *et al.*, Phys. Rev. D **48**, 2139 (1993).
2. B. Aubert *et al.*, hep-ex/0408099 (ICHEP04 contribution)
3. C.C. Wang *et al.*, hep-ex/0408003; Phys. Rev. Lett. **94**, 121801 (2005).
4. B. Aubert *et al.*, hep-ex/0503049; Phys. Rev. Lett. **95**, 0401805 (2005).
5. A. Somov *et al.*, hep-ex/0601024.

6. P. Krokovny for the Belle Collaboration, hep-ex/0506033.
7. B. Aubert *et al.*, hep-ex/0504039; Phys. Rev. Lett. **95**, 121802 (2005).
8. J.M Link *et al.*, Phys. Lett. B **585**, 200 (2004).
9. B. Aubert *et al.*, hep-ex/0507101.
10. S. Spanier and N. A. Törnqvist, Scalar Mesons (rev.), Particle Data Group, Phys. Rev. D **66**, 010001-450 (2002).
11. M. R. Pennington, *Proc. of Oxford Conf. in honour of R. H. Dalitz*, Oxford, July, 1990, Ed. by I. J. R. Aitchison, *et al.*, (World Scientific) pp. 66–107; *Proc. of Workshop on Hadron Spectroscopy* (WHS 99), Rome, March 1999, Ed. by T. Bressani *et al.*, (INFN, Frascati).
12. E. P. Wigner, Phys. Rev. **70**, 15 (1946).
13. S. U. Chung *et al.*, Ann. Physik 4 (1995) 404.
14. I. J. R. Aitchison, Nucl. Phys. A **189**, 417 (1972).
15. K. L. Au, D. Morgan, and M. R. Pennington, Phys. Rev. D **35**, 1633 (1987).
16. V. V. Anisovich and A. V. Sarantsev, Eur. Phys. J. A **16**, 229 (2003).
17. K. Abe *et al.*, hep-ex/0504013
18. A. Garmash for the Belle collaboration, hep-ex/0510059
19. B. Aubert *et al.*, hep-ex/0507025; Phys. Rev. D **72**, 052002 (2005).
20. B. Aubert *et al.*, hep-ex/0507004; Phys. Rev. D **72**, 072003 (2005).
21. B. Aubert *et al.*, hep-ex/0507094.
22. B. Aubert *et al.*, hep-ex/050702; Phys. Rev. D **72**, 052008 (2005).
23. D. Cronin-Hennessy *et al.*, hep-ex/0503052; Phys. Rev. D **70**, 031102 (2005).
24. D.M Asner *et al.*, hep-ex/0311033; Phys. Rev. D **70**, 091101 (2004).
25. S.Malvezzi for the FOCUS collaboration, Nucl. Phys. B Proc. Suppl. **117**, 636-640 (2003).

Frascati Physics Series Vol. XLI (2006), pp. 217-230
DISCOVERIES IN FLAVOUR PHYSICS AT e^+e^- COLLIDERS
Frascati, February 28th - March 3rd, 2006

SEARCHES FOR D^0-$\overline{D}^0$ MIXING: FINDING THE (SMALL) CRACK IN THE STANDARD MODEL

A. J. Schwartz
University of Cincinnati, P.O. Box 120011, Cincinnati, Ohio 45221

Abstract

We review results from searches for mixing and CP violation in the D^0-$\overline{D}^0$ system. No evidence for mixing or CP violation is found, and limits are set for the mixing parameters x, y, x', y', and several CP-violating parameters.

1 Introduction

Despite numerous searches, mixing between D^0 and $\overline{D}^0$ flavor eigenstates has not yet been observed. Within the Standard Model (SM), the short-distance "box" diagram (which plays a large role in K^0-$\overline{K}^0$ and B^0-$\overline{B}^0$ mixing) is doubly-Cabibbo-suppressed (DCS) and GIM-suppressed; since the D^0 decay width is dominated by Cabibbo-favored (CF) amplitudes, D^0-$\overline{D}^0$ mixing is expected to be a rare phenomenon. Observing mixing at a rate significantly above the SM expectation could indicate new physics.

The formalism describing D^0-$\overline{D}{}^0$ mixing is given in several papers. [1, 2] The parameters used to characterize mixing are $x = \Delta m/\overline{\Gamma}$ and $y = \Delta\Gamma/(2\overline{\Gamma})$, where Δm and $\Delta\Gamma$ are the mass and decay width differences between the two mass eigenstates, and $\overline{\Gamma}$ is the mean decay width. Within the SM, x and y are difficult to calculate as there are long-distance contributions. For $m_q \gg \Lambda_{\rm QCD}$, these contributions can be estimated using the heavy-quark expansion; however, m_c may not be large enough for this calculation to be reliable. Current theoretical predictions [3] span a wide range: $|x| \sim |y| \sim (10^{-7}$ to $10^{-2})$, with the majority being $\lesssim 10^{-3}$.

For decay times $t \ll 1/\Delta m$, $1/\Delta\Gamma$, which is well-satisfied for charm decay, the time-dependent $D^0(t) \to f$ and $\overline{D}{}^0(t) \to \bar{f}$ decay rates are

$$R_{D^0} = |\mathcal{A}_f|^2 e^{-\overline{\Gamma}t}\left[1 + [\,y\,\mathrm{Re}(\lambda) - x\,\mathrm{Im}(\lambda)\,](\overline{\Gamma}t) + |\lambda|^2\frac{(x^2+y^2)}{4}(\overline{\Gamma}\,t)^2\right] \quad (1)$$

$$R_{\overline{D}{}^0} = |\bar{\mathcal{A}}_{\bar{f}}|^2 e^{-\overline{\Gamma}t}\left[1 + [\,y\,\mathrm{Re}(\bar{\lambda}) - x\,\mathrm{Im}(\bar{\lambda})\,](\overline{\Gamma}t) + |\bar{\lambda}|^2\frac{(x^2+y^2)}{4}(\overline{\Gamma}\,t)^2\right], \quad (2)$$

where $\lambda = (q/p)(\bar{\mathcal{A}}_f/\mathcal{A}_f)$, $\bar{\lambda} = (p/q)(\mathcal{A}_{\bar{f}}/\bar{\mathcal{A}}_{\bar{f}})$, q and p are complex coefficients relating flavor eigenstates to mass eigenstates, and $\mathcal{A}_f\,(\bar{\mathcal{A}}_f)$ and $\mathcal{A}_{\bar{f}}\,(\bar{\mathcal{A}}_{\bar{f}})$ are amplitudes for a pure D^0 $(\overline{D}{}^0)$ state to decay to f and $\bar{f}$, respectively.

In this paper we discuss five methods used to search for D^0-$\overline{D}{}^0$ mixing and CP violation (CPV). These methods use the following decay modes:[1] semileptonic $D^0 \to K^+\ell^-\nu$ decays, decays to CP-eigenstates K^+K^- and $\pi^+\pi^-$, DCS $D^0 \to K^+\pi^-$ decays, $D^0 \to K^0_S\,\pi^+\pi^-$ decays, and multi-body DCS $D^0 \to K^+n(\pi)$ decays. A newer method based on quantum correlations [4] in $e^+e^- \to \psi''(3770) \to D^0\overline{D}{}^0$ production is not discussed here. The flavor of a D^0 when produced is determined by requiring that it originate from a $D^{*+} \to D^0\pi_s^+$ decay; the charge of the low momentum ("slow") π_s^+ determines the charm flavor at $t = 0$. As the kinetic energy released in $D^{*+} \to D^0\pi_s^+$ decays is only 5.8 MeV (very near threshold), requiring that $Q \equiv M_{K\pi\pi_s} - M_{K\pi} - m_\pi$ be small greatly reduces backgrounds.

[1] Charge-conjugate modes are implicitly included throughout this paper unless noted otherwise.

2 $D^0(t) \to K^{(*)+}\ell^-\nu$ Semileptonic Decays

Because the $K^{(*)+}\ell^-\nu$ final state can only be reached from a $\overline{D}{}^0$ decay, observing $D^0(t) \to K^{(*)+}\ell^-\nu$ would provide clear evidence for mixing. In Eq. (1) only the third term is nonzero; integrating this term over all times and assuming $|q/p| = 1$ (i.e., neglecting CPV in mixing) gives

$$\frac{\int R(D^0 \to K^+\ell\nu)\,dt}{\int R(D^0 \to K^-\ell\nu)\,dt} \;\approx\; \frac{x^2+y^2}{2} \;\equiv\; r_D\,. \tag{3}$$

Several experiments [5, 6] have used this method to constrain r_D; the most stringent constraint is from the Belle experiment using 253 fb^{-1} of data. [6] Due to the neutrino, the final state is not fully reconstructed; however, at an e^+e^- collider there are enough kinematic constraints to infer the neutrino momentum. Specifically, momentum conservation prescribes $P_\nu = P_{CM} - P_{\pi_s K\ell} - P_{\rm rest}$, where P_{CM} is the four-momentum of the e^+e^- center-of-mass (CM) system, π_s, K, and ℓ are daughters from $D^* \to D^0\pi_s \to \pi_s K\ell\nu$, and $P_{\rm rest}$ is the four-momentum of the remaining particles in the event. In the Belle analysis the magnitude $|P_{\rm rest}|$ is rescaled to satisfy $(P_{CM} - P_{\rm rest})^2 = m^2_{D^*}$, and after this rescaling the direction of $\vec{\mathbf{p}}_{\rm rest}$ is adjusted to satisfy $P^2_\nu\,(= m^2_\nu) = 0$.

The $\Delta M \equiv M_{\pi_s K\ell\nu} - M_{K\ell\nu}$ distributions for "right-sign" (RS) $D^0 \to K^-\ell^+\nu$ and "wrong-sign" (WS) $D^0 \to K^+\ell^-\nu$ samples are shown in Fig. 1. Sensitivity to mixing is improved by utilizing information on the decay time, which is calculated by projecting the D^0 flight distance onto the (vertical) y axis: $t = (M_{D^0}/c) \times (y_{\rm vtx} - y_{\rm IP})/p_y$. This projection has superior decay time resolution, as the beam profile is only a few microns in y and thus the interaction point ($y_{\rm IP}$) is well-determined. Events satisfying $t > \tau_{D^0}$ are divided into six t intervals, and the event yields $N^{(t)}_{\rm RS}$ and $N^{(t)}_{\rm WS}$, acceptance ratio $\varepsilon^{(t)}_{\rm WS}/\varepsilon^{(t)}_{\rm RS}$, and resulting mixing parameter $r^{(t)}_D$ are calculated separately for each. $N^{(t)}_{\rm RS}$ and $N^{(t)}_{\rm WS}$ are obtained from fitting the ΔM distributions. Doing a χ^2 fit to the six $r^{(t)}_D$ values gives an overall result $r_D = [0.20 \pm 0.47\,({\rm stat}) \pm 0.14\,({\rm syst})] \times 10^{-3}$, or $r_D \leq 0.10\%$ at 90% C.L. No evidence for mixing is observed. The total number of signal candidates in all t intervals is 90601 ± 372 RS events and 10 ± 80 WS events.

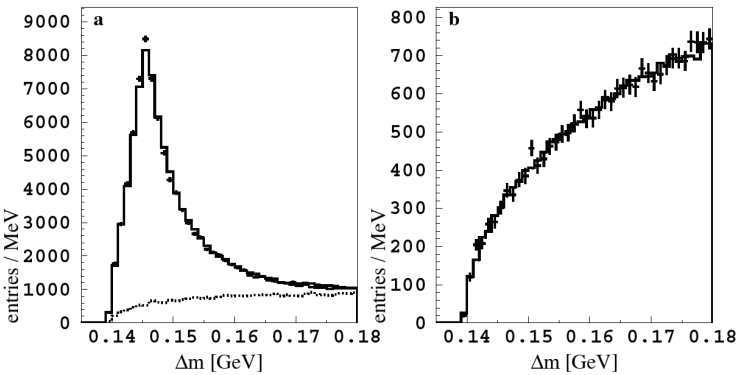

Figure 1: *ΔM distributions for RS $D^0 \to K^-\ell^+\nu$ candidate decays (left) and WS $D^0 \to K^+\ell^-\nu$ candidate decays (right), from Belle using 253 fb^{-1} of data.* [6] *The WS plot shows no visible signal above background.*

3 $D^0(t) \to K^+K^-$, $\pi^+\pi^-$ CP-Eigenstate Decays

When the final state is self-conjugate, e.g., K^+K^-, there is no strong phase difference between $\bar{\mathcal{A}}_f$ and $\mathcal{A}_f$. Assuming $|\bar{\mathcal{A}}_f| = |\mathcal{A}_f|$ (no direct CPV), $\lambda = -|q/p|\, e^{i\phi}$ and $\bar{\lambda} = -|p/q|\, e^{-i\phi}$, where ϕ is a weak phase difference and the leading minus sign is due to the phase convention $\boldsymbol{CP}|D^0\rangle = -|\overline{D}{}^0\rangle$. Inserting these terms into Eqs. (1) and (2) and dropping the very small last term gives

$$R(D^0 \to K^+K^-) = |\mathcal{A}_{K^+K^-}|^2\, e^{-\overline{\Gamma}t}\left[1 - \left|\frac{q}{p}\right|(y\cos\phi - x\sin\phi)\overline{\Gamma}t\right]$$

$$\approx |\mathcal{A}_{K^+K^-}|^2\, e^{-\overline{\Gamma}t}\, e^{-|q/p|(y\cos\phi - x\sin\phi)\overline{\Gamma}t} \quad (4)$$

$$R(\overline{D}{}^0 \to K^+K^-) \approx |\mathcal{A}_{K^+K^-}|^2\, e^{-\overline{\Gamma}t}\, e^{-|p/q|(y\cos\phi + x\sin\phi)\overline{\Gamma}t}\,. \quad (5)$$

Eqs. (4) and (5) imply that the measured D^0 and $\overline{D}{}^0$ inverse lifetimes are $\overline{\Gamma}[1+|q/p|(y\cos\phi - x\sin\phi)]$ and $\overline{\Gamma}[1+|p/q|(y\cos\phi + x\sin\phi)]$, respectively. We define $y_{CP} \equiv \tau_{K^-\pi^+}/\tau_{K^+K^-} - 1$, which equals $|q/p|(y\cos\phi - x\sin\phi)$ for D^0 decays and $|p/q|(y\cos\phi + x\sin\phi)$ for $\overline{D}{}^0$ decays. For $|q/p| = 1$, i.e., no CPV in mixing, $y_{CP} = y\cos\phi$ for equal numbers of D^0 and $\overline{D}{}^0$ decays together. If also $\phi = 0$ (no CPV), $y_{CP} = y$. The observable y_{CP} is measured by fitting the $D^0 \to K^+K^-$ and $D^0 \to K^-\pi^+$ decay time distributions.

To date, five experiments [7, 8, 9] have measured y_{CP}; the most precise

value is from BaBar using 91 fb^{-1} of data. [8] To increase statistics, BaBar used both K^+K^- and $\pi^+\pi^-$ decays. In addition, the $D^0 \to K^+K^-$ analysis used both a large inclusive D^0 sample and a smaller, higher purity sample in which the D^0 was required to originate from $D^{*+} \to D^0\pi^+$. The respective decay time distributions are shown in Fig. 2. Doing an unbinned maximum likelihood fit to each sample, combining results for K^+K^- and $\pi^+\pi^-$, and taking the ratio of lifetimes gives $y_{CP} = [0.8 \pm 0.4\,(\text{stat})\,^{+0.5}_{-0.4}\,(\text{syst})]\%$. This value is consistent with, but smaller than, the relatively large value measured by FOCUS: [9] $y_{CP} = [3.4 \pm 1.4\,(\text{stat}) \pm 0.7\,(\text{syst})]\%$.

BaBar also measures $\Delta Y \equiv (\tau^+ - \tau^-)/(\tau^+ + \tau^-) \times \tau_{K^-\pi^+}/\langle\tau\rangle$, where τ^+ (τ^-) is the lifetime for $D^0 \to K^+K^-$ ($\overline{D}{}^0 \to K^+K^-$) and $\langle\tau\rangle = (\tau^+ + \tau^-)/2$. For $|q/p| = 1$, $\Delta Y = x \sin\phi$. The result is $\Delta Y = [-0.8 \pm 0.6\,(\text{stat}) \pm 0.2\,(\text{syst})]\%$, which indicates that either x is small or ϕ is small.

4 $D^0(t) \to K^+\pi^-$ Doubly-Cabibbo-Suppressed Decays

For $D^0 \to K^+\pi^-$, $\mathcal{A}_f$ is DCS, $\bar{\mathcal{A}}_f$ is CF, and thus $|\mathcal{A}_f| \ll |\bar{\mathcal{A}}_f|$. In addition, there may be a strong phase difference (δ) between the amplitudes. Defining $R_D \equiv |\mathcal{A}_f/\bar{\mathcal{A}}_f|^2$ and $\overline{R}_D \equiv |\bar{\mathcal{A}}_{\bar{f}}/\mathcal{A}_{\bar{f}}|^2$, $\lambda = |q/p|\, R_D^{-1/2}\, e^{i(\phi+\delta)}$ and $\bar{\lambda} = |p/q|\, \overline{R}_D^{-1/2}\, e^{i(-\phi+\delta)}$. Inserting these terms into Eqs. (1) and (2) gives

$$R(D^0 \to K^+\pi^-) \propto e^{-\overline{\Gamma}t}\left[R_D + \left|\frac{q}{p}\right|\sqrt{R_D}\,[y'\cos\phi - x'\sin\phi]\,(\overline{\Gamma}t) + \left|\frac{q}{p}\right|^2 \frac{(x'^2+y'^2)}{4}(\overline{\Gamma}t)^2\right] \quad (6)$$

$$R(\overline{D}{}^0 \to K^-\pi^+) \propto e^{-\overline{\Gamma}t}\left[\overline{R}_D + \left|\frac{p}{q}\right|\sqrt{\overline{R}_D}\,[y'\cos\phi + x'\sin\phi]\,(\overline{\Gamma}t) + \left|\frac{p}{q}\right|^2 \frac{(x'^2+y'^2)}{4}(\overline{\Gamma}t)^2\right], \quad (7)$$

where $x' \equiv x\cos\delta + y\sin\delta$ and $y' \equiv -x\sin\delta + y\cos\delta$. These "rotated" mixing parameters absorb the unknown strong phase difference δ. CPV enters Eqs. (6) and (7) in three ways: $|q/p| \neq 1$ (CPV in mixing), $R_D \neq \overline{R}_D$ (CPV in the DCS amplitude), and $\phi \neq 0$ (CPV via interference between the DCS and mixed amplitudes). Assuming no CPV gives the simpler expression

$$R \propto e^{-\overline{\Gamma}t}\left[R_D + \sqrt{R_D}\,y'(\overline{\Gamma}t) + \frac{(x'^2+y'^2)}{4}(\overline{\Gamma}t)^2\right]. \quad (8)$$

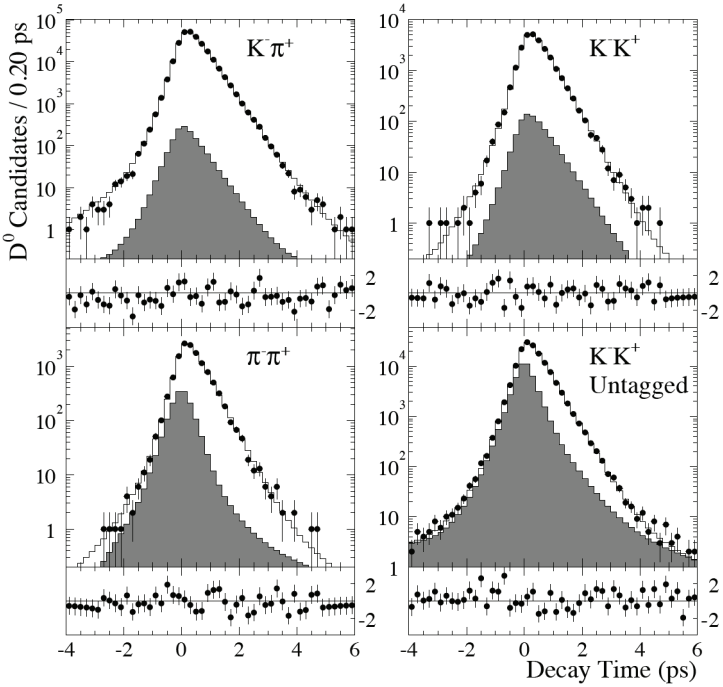

Figure 2: *Decay time distributions for CF $D^0 \to K^-\pi^+$ (upper left), $D^0 \to K^+K^-$ (upper right), $D^0 \to \pi^+\pi^-$ (lower left), and $D^0 \to K^+K^-$ selected without using a D^{*+} tag (lower right), from BaBar using 91 fb^{-1} of data.* [8] *The shaded histograms show the signal component obtained from the fit; residuals from the fit are plotted below each distribution.*

To date, six experiments [10, 11, 12] have done a time-dependent analysis of $D^0 \to K^+\pi^-$ decays; the most stringent constraints on x'^2 and y' are from Belle using 400 fb^{-1} of data. [12] The reconstructed $M_{K\pi}$ and Q distributions after all selection criteria are shown in Fig. 3; fitting these distributions yields 1073993 $\pm$ 1108 RS signal events and 4024 $\pm$ 88 WS signal events. Those events satisfying $|M_{K\pi} - M_{D^0}| < 22$ MeV/c^2 and $|Q - 5.8\ \text{MeV}| < 1.5$ MeV (4σ intervals) have their decay times fitted for x'^2, y', and R_D. The results are listed in Table 1; projections of the fit are shown in Fig. 4(left).

A 95% C.L. region in the x'^2-y' plane is obtained using a frequentist technique based on "toy" Monte Carlo (MC) simulation. For points $\vec{\alpha} = (x'^2, y')$,

Table 1: *Limits on mixing parameters obtained from fitting the decay time distribution of WS $D^0 \to K^+\pi^-$ decays, from Belle using 400 fb^{-1} of data.* [12]

Fit Case	**Parameter**	**Fit Result ($\times 10^{-3}$)**	**95% C.L. interval ($\times 10^{-3}$)**
No CPV	x'^2	$0.18\,^{+0.21}_{-0.23}$	< 0.72
	y'	$0.6\,^{+4.0}_{-3.9}$	$(-9.9, 6.8)$
	R_D	3.64 ± 0.17	$(3.3, 4.0)$
	R_M	–	$(0.63 \times 10^{-5},\ 0.40)$
CPV allowed	x'^2	–	< 0.72
	y'	–	$(-28, 21)$
	R_M	–	< 0.40
	A_D	23 ± 47	$(-76, 107)$
	A_M	670 ± 1200	$(-995, 1000)$
No mixing/CPV	R_D	$3.77 \pm 0.08\,(\text{stat}) \pm 0.05\,(\text{syst})$	

one generates ensembles of MC experiments and fits them using the same procedure as that used for the data. For each experiment, the difference in likelihood $\Delta L \equiv \ln L_{\max} - \ln L(\vec{\alpha})$ is calculated, where $L_{\max}$ is evaluated for $x'^2 \geq 0$. The locus of points $\vec{\alpha}$ for which 95% of the ensemble has ΔL less than that of the data is taken as the 95% C.L. contour. This contour is shown in Fig. 4(right); projections of the contour are listed in the right-most column of Table 1.

CPV is accounted for by fitting the $D^0 \to K\pi$ and $\overline{D}{}^0 \to K\pi$ samples separately; this yields six values: $x'^{2\,\pm}$, $y'^{\pm}$, and $R_D^{\pm}$. Defining $R_M^{\pm} \equiv (x'^{2\,\pm} + y'^{2\,\pm})/2$ and $A_M \equiv (R_M^+ - R_M^-)/(R_M^+ + R_M^-)$, one finds

$$x'^{\pm} = \left(\frac{1 \pm A_M}{1 \mp A_M}\right)^{1/4} (x' \cos\phi \ \pm \ y' \sin\phi) \tag{9}$$

$$y'^{\pm} = \left(\frac{1 \pm A_M}{1 \mp A_M}\right)^{1/4} (y' \cos\phi \ \mp \ x' \sin\phi)\,, \tag{10}$$

where there is an implicit sign ambiguity in $x'^{\pm}$ due to Eqs. (6) and (7) being quadratic in x'. To allow for CPV, one obtains separate $1-\sqrt{0.05} = 77.6\%$ C.L. contours for $(x'^{+\,2},\ y'^{+})$ and $(x'^{-\,2},\ y'^{-})$; points on the $(x'^{+\,2},\ y'^{+})$ contour are

then combined with points on the (x'^{-2}, y'^{-}) contour and the combination used to solve Eqs. (9) and (10) for x'^2 and y'. Because the relative sign of x'^{+} and x'^{-} is unknown, there are two solutions (one for each sign); Belle plots both in the (x'^2, y') plane and takes the outermost envelope of points as the 95% C.L. contour allowing for CPV. This contour has a complicated shape [see Fig. 4(right)] due to the two solutions. Projections of the contour are listed in the right-most column of Table 1. In the case of no CPV, the no-mixing point $x'^2 = y' = 0$ lies just outside the 95% C.L. contour; this point corresponds to 3.9% C.L. with systematic uncertainty included.

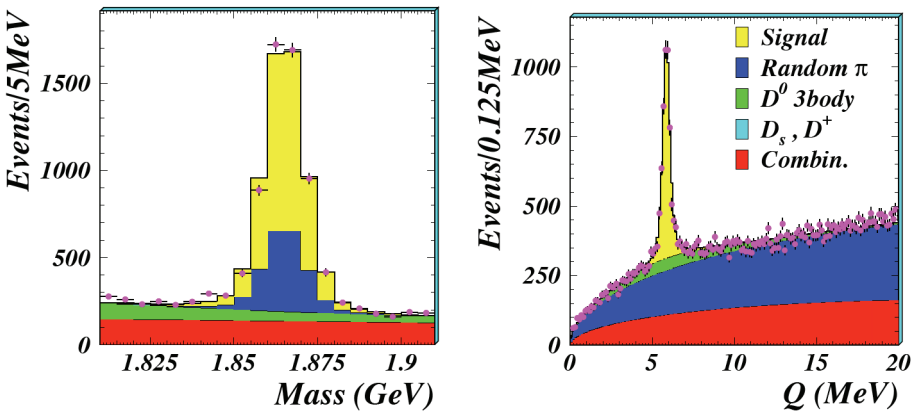

Figure 3: *WS* $D^0 \to K^+\pi^-$ *decays:* $M_{K\pi}$ *spectrum for events satisfying* $Q \in (5.3, 6.5)$ *MeV (left), and* Q *spectrum for events satisfying* $M_{K\pi} \in (1.845, 1.885)$ *GeV/*c^2*, from Belle using 400* fb^{-1} *of data.* [12)]

5 $D^0(t) \to K^0_S\,\pi^+\pi^-$ Dalitz Plot Analysis

In this method one considers a self-conjugate final state that is *not* a CP eigenstate, e.g., a three-body decay that can have either $L = 0$ (CP-even) or $L = 1$ (CP-odd). If CPV is negligible, CP-eigenstates (denoted D_-, D_+) are mass eigenstates (denoted D_1, D_2), and the amplitude for $D^0(t) \to K^0_S\,\pi^+\pi^-$ is:

$$\begin{aligned} \mathcal{A}_{K^0\pi\pi} &= \frac{1}{2p}\Big(\langle K^0_S\,\pi^+\pi^-|H|D_-(t)\rangle \;+\; \langle K^0_S\,\pi^+\pi^-|H|D_+(t)\rangle\Big) \\ &\equiv \mathcal{A}_-\,e^{-(\Gamma_1/2+im_1)\,t} \;+\; \mathcal{A}_+\,e^{-(\Gamma_2/2+im_2)\,t} \end{aligned} \tag{11}$$

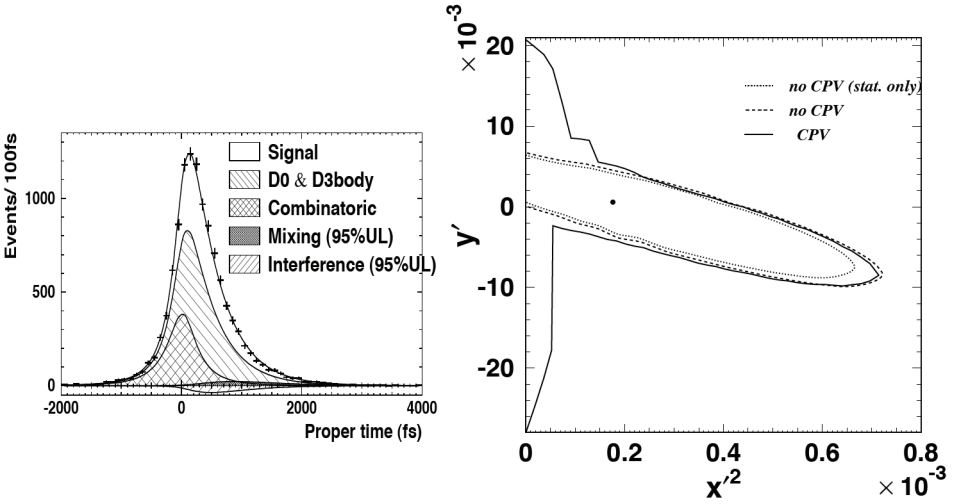

Figure 4: *Left: WS* $D^0 \to K^+\pi^-$ *decay-time distribution and fit projections. Right: 95% C.L. region for* x'^2, y'. *From Belle using 400* fb^{-1} *of data.* [12].

$$\Rightarrow R_{K^0\pi\pi} = |\mathcal{A}_-|^2\, e^{-\overline{\Gamma}(1-y)t} + |\mathcal{A}_+|^2\, e^{-\overline{\Gamma}(1+y)t} + 2e^{-\overline{\Gamma}t}\left[\,\mathrm{Re}(\mathcal{A}_+\,\mathcal{A}_-^*)\cos(\Delta m\, t) + \mathrm{Im}(\mathcal{A}_+\,\mathcal{A}_-^*)\sin(\Delta m\, t)\,\right], \quad (12)$$

where $\mathcal{A}_{+,-}$ is the amplitude for $D_{+,-} \to K^0_S\,\pi^+\pi^-$ multiplied by $1/(2p)$. Note that $x = (m_2 - m_1)/\overline{\Gamma}$ and $y = (\Gamma_2 - \Gamma_1)/(2\overline{\Gamma})$. For a three-body final state, one can distinguish the $\mathcal{A}_+$ and $\mathcal{A}_-$ components via a Dalitz plot analysis; i.e., a $K^0_S\, f_0(980)$ intermediate state is CP-even and contributes to $\mathcal{A}_+$, $K^0_S\,\rho^0$ is CP-odd and contributes to $\mathcal{A}_-$, $K^*(890)^+\,\pi^-$ is a flavor-eigenstate and contributes to both $\mathcal{A}_+$ and $\mathcal{A}_-$, etc. Thus one models $\mathcal{A}_{+,-}$ by separate sums of amplitudes $\sum_j a_j\, e^{i\delta_j} A_j$, where A_j is the Breit-Wigner amplitude [13] for resonance j and is a function of the Dalitz plot position $M^2_{K^0\pi^+}$, $M^2_{K^0\pi^-}$. Using the probability density function of Eq. (12), one does an unbinned maximum likelihood fit to $M^2_{K^0\pi^+}$, $M^2_{K^0\pi^-}$, and the decay time t to determine a_j, δ_j, x, and y. There is systematic uncertainty arising from the decay model, i.e., one must decide which intermediate states to include in the fit. Unlike Eq. (6), Eq. (12) depends linearly on x ($x \ll 1$) and is therefore sensitive to its sign.

This analysis was developed by CLEO, and their result [14] based on 9.0 fb^{-1} has not yet been superseded. To minimize backgrounds, the D^0 can-

didate is required to originate from $D^{*+} \to D^0\pi^+$. The final Dalitz plot sample (Fig. 5) contains 5299 events with only $(2.1 \pm 1.5)\%$ background. [15)]

The decay model used consists of $D^0 \to K^*(890)^- \pi^+$, $K^*(1430)^-_{0,2}\,\pi^+$, $K^*(1680)^-\,\pi^+$, $K^0_S\,\rho$, $K^0_S\,\omega$, $K^0_S\,f_0(980)$, $K^0_S\,f_2(1270)$, $K^0_S\,f_0(1370)$, WS $D^0 \to K^*(890)^+\,\pi^-$, and a nonresonant component. The fit results are listed in Table 2; the 95% C.L. intervals correspond to the values at which $-2\ln\mathcal{L}$ rises by 3.84 units, where $\mathcal{L}$ is the likelihood function. CPV is included in the fit by introducing parameters $\varepsilon \equiv (p-q)/(p+q)$ (in analogy with K^0 decays) and ϕ, the weak phase difference between $\bar{\mathcal{A}}_{K^0\pi\pi}$ and $\mathcal{A}_{K^0\pi\pi}$. The results listed are consistent with no mixing or CPV.

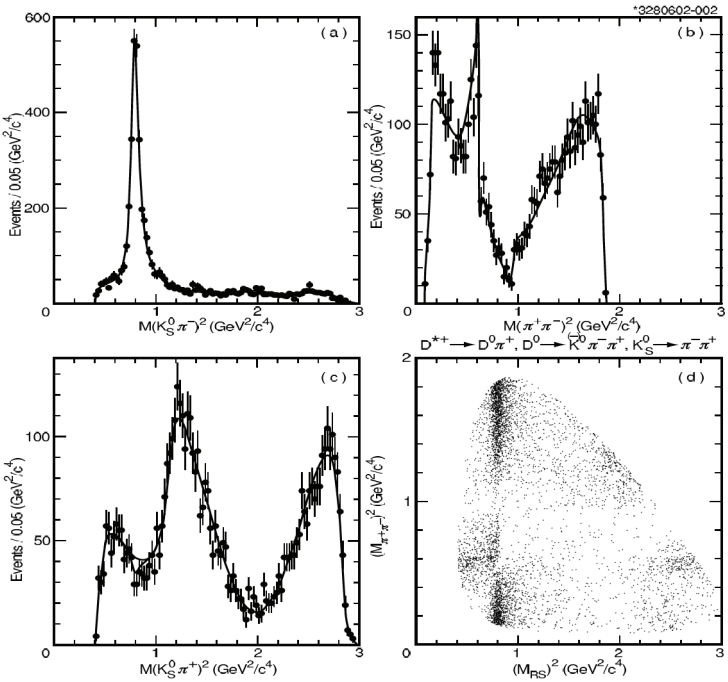

Figure 5: *Dalitz plot (lower right) and projections (lower left, upper plots) for* $D^0 \to K^0_S\,\pi^+\pi^-$ *decays, from CLEO using 9.0* fb^{-1} *of data.* [15)]

Table 2: *Limits on mixing and CPV parameters from a t-dependent fit to the* $D^0 \to K^0_S \pi^+\pi^-$ *Dalitz plot, from CLEO using 9.0 fb*$^{-1}$. [14] *The errors are statistical, experimental systematic, and modelling systematic, respectively.*

Fit	Param.	Fit Result (%)	95% C.L. Inter. (%)
No CPV	x	$1.8\,^{+3.4}_{-3.2} \pm 0.4 \pm 0.4$	$(-4.7, 8.6)$
	y	$-1.4\,^{+2.5}_{-2.4} \pm 0.8 \pm 0.4$	$(-6.3, 3.7)$
CPV Allowed	x	$2.3\,^{+3.5}_{-3.4} \pm 0.4 \pm 0.4$	$(-4.5, 9.3)$
	y	$-1.5\,^{+2.5}_{-2.4} \pm 0.8 \pm 0.4$	$(-6.4, 3.6)$
	ϵ	$1.1 \pm 0.7 \pm 0.4 \pm 0.2$	$(-0.4, 2.4)$
	ϕ	$(5.7 \pm 2.8 \pm 0.4 \pm 1.2)^\circ$	$(-0.3^\circ, 11.7^\circ)$

6 $D^0(t) \to K^+\pi^-\pi^0$ and $K^+\pi^-\pi^+\pi^-$ Multibody Decays

Mixing has also been searched for in WS multibody final states [10, 16, 17] $K^+\pi^-\pi^0$ and $K^+\pi^-\pi^+\pi^-$; the most recent measurement is from Belle using 281 fb^{-1} of data. [17] The final signal yields are 1978 ± 104 $D^0 \to K^+\pi^-\pi^0$ decays and 1721 ± 75 $D^0 \to K^+\pi^-\pi^+\pi^-$ decays. For this analysis no decay time information is used, i.e., Belle measures the time-integrated ratio of WS to RS decays:

$$R_{\rm WS} \;=\; \frac{\int R[D^0 \to K^+\pi^-(n\pi)]\,dt}{\int R[D^0 \to K^-\pi^+(n\pi)]\,dt} \;\approx\; R_D + \sqrt{R_D}\,y' + \frac{x'^2 + y'^2}{2}\,, \quad (13)$$

where R_D is the ratio of the DCS rate to the CF rate as previously defined for $D^0 \to K^+\pi^-$ decays. The results are $R_{\rm WS} = [0.229 \pm 0.015\,({\rm stat})\,^{+0.013}_{-0.009}\,({\rm syst})]\%$ for $K^+\pi^-\pi^0$ and $[0.320 \pm 0.018\,({\rm stat})\,^{+0.018}_{-0.013}\,({\rm syst})]\%$ for $K^+\pi^-\pi^+\pi^-$. Inserting these values into Eq. (13) allows one to determine R_D as a function of x' or y'. Assuming $x' = 0$ and $|x'| = 0.027$ gives the curves shown in Fig. 6; the latter $|x'|$ value corresponds to Belle's 95% C.L. upper limit from $D^0 \to K^+\pi^-$ decays (see Table 1). However, the value of x' from $D^0 \to K^+\pi^-$ may differ from that from $D^0 \to K^+\pi^- n(\pi)$ due to the strong phase differences (δ) being different.

7 Summary

The 95% C.L. allowed ranges for x' and y' are plotted in Fig. 7; for simplicity we assume negligible CPV. The most stringent constraints are $|x'| < 2.7\%$

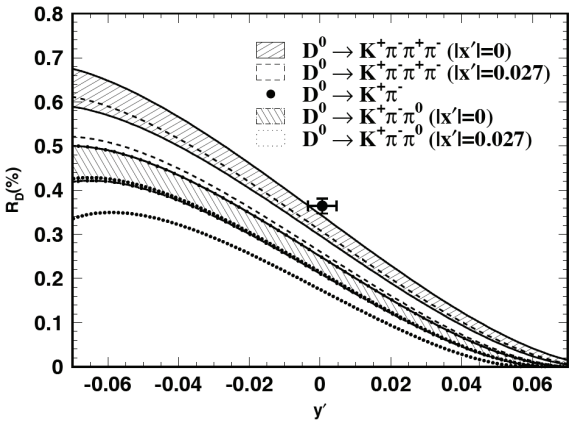

Figure 6: *WS* $D^0 \to K^+\pi^- n(\pi)$ *decays: 95% C.L. range for* R_D *as a function of* y' *for* $|x'| = 0$ *and* $|x'| = 0.027$, *from Belle using 281* fb^{-1} *of data.* [17] *The point with* 1σ *error bars is Belle's result from* $D^0 \to K^+\pi^-$ *decays (see Table 1).*

and $y' \in (-1.0\%, 0.7\%)$. These ranges are projections of the two-dimensional 95% C.L. region for x'^2, y' from Belle [Fig. 4(right)].

The results for y_{CP} are plotted in Fig. 8. Here the central values and 1σ errors are shown; combining the results assuming the errors uncorrelated gives $y_{CP} = (1.09 \pm 0.46)\%$. This value differs from zero by 2.4σ and indicates a nonzero decay width difference $\Delta\Gamma$. Assuming negligible CPV, one can combine this value with Belle's central value for y', $(0.06\,^{+0.40}_{-0.39})\%$. The result is $y'/y = \cos\delta - (x/y)\sin\delta = 0.05\,^{+0.39}_{-0.37}$, where the error is obtained from an MC calculation as the fractional errors on y and y' are large. This small central value (albeit with a large error) implies $\tan\delta \approx y/x$; i.e., if $x \ll y$, then δ is near 90°. Such a strong phase difference would be much larger than expected.

References

1. Z.-Z. Xing, Phys. Rev. D **55**, 196 (1997).

2. S. Bianco, F. L. Fabbri, D. Benson, and I. Bigi, Riv. Nuovo Cim. **26N7-8**, 1 (2003).

3. A. A. Petrov, Charm physics: theoretical review, in: Proc. of the Second In-

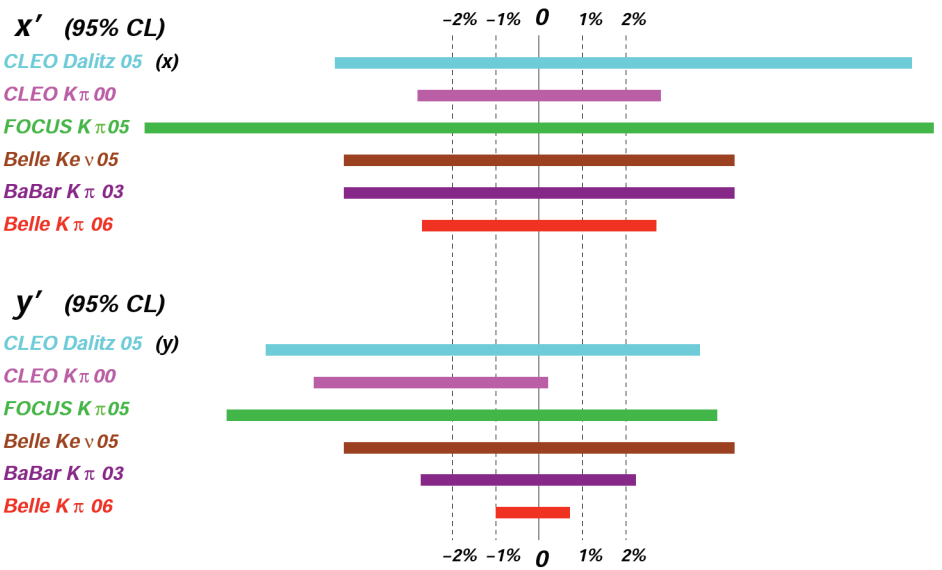

Figure 7: *95% C.L. allowed ranges for x' (top) and y' (bottom) from various experiments assuming no CPV. The CLEO Dalitz results are for x and y.*

ternational Conference on CP Violation and Flavor Physics (ed. P. Perret, Ecole Polytechnique, Paris, June 2003), eConf **C030603**, hep-ph/0311371. See also: A. A. Petrov, hep-ph/0409130 (2004).

4. D. M. Asner and W. M. Sun, Phys. Rev. D **73**, 034024 (2006).

5. E. M. Aitala *et al.* (FNAL E791), Phys. Rev. Lett. **77**, 2384 (1996).

   B. Aubert *et al.* (BaBar), Phys. Rev. D **70**, 091102 (2004).

   C. Cawlfield *et al.* (CLEO), Phys. Rev. D **71**, 077101 (2005).

6. U. Bitenc *et al.* (Belle), Phys. Rev. D **72**, 071101(R) (2005).

7. E. M. Aitala *et al.* (FNAL E791), Phys. Rev. Lett. **83**, 32 (1999).

   S. E. Csorna *et al.* (CLEO), Phys. Rev. D **65**, 092001 (2002).

   K. Abe *et al.* (Belle), BELLE-CONF-347, hep-ex/0308034 (2003); Phys. Rev. Lett. **88**, 162001 (2002).

8. B. Aubert *et al.* (BaBar), Phys. Rev. Lett. **91**, 121801 (2003).

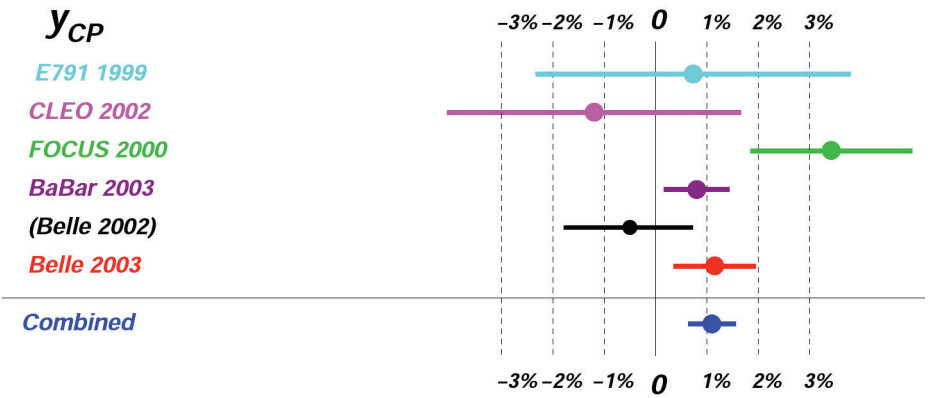

Figure 8: *y_{CP} central values and 1σ errors measured by various experiments, and the combined result assuming the individual errors uncorrelated. The Belle 2002 data sample (23 fb^{-1}) has some overlap with the Belle 2003 data sample (158 fb^{-1}), and thus this result is not included in the average.*

9. J. M. Link *et al.* (FOCUS), Phys. Lett. B **485**, 62 (2000).

10. E. M. Aitala *et al.* (FNAL E791), Phys. Rev. D **57**, 13 (1998).

11. R. Barate *et al.* (ALEPH), Phys. Lett. B **436**, 211 (1998).
    R. Godang *et al.* (CLEO), Phys. Rev. Lett. **84**, 5038 (2000).
    J. M. Link *et al.* (FOCUS), Phys. Lett. B **618**, 23 (2005); Phys. Rev. Lett. **86**, 2955 (2001).
    B. Aubert *et al.* (BaBar), Phys. Rev. Lett. **91**, 171801 (2003).

12. L. Zhang *et al.* (Belle), Phys. Rev. Lett. **96**, 151801 (2006); J. Li *et al.* (Belle), Phys. Rev. Lett. **94**, 071801 (2005).

13. S. Kopp *et al.* (CLEO), Phys. Rev. D **63**, 092001 (2001).

14. D. M. Asner *et al.* (CLEO), Phys. Rev. D **72**, 012001 (2005).

15. H. Muramatsu *et al.* (CLEO), Phys. Rev. Lett. **89**, 251802 (2002).

16. G. Brandenburg *et al.* (CLEO), Phys. Rev. Lett. **87**, 071802 (2001).
    S. A. Dytman *et al.* (CLEO), Phys. Rev. D **64**, 111101 (2001).

17. X. C. Tian *et al.* (Belle), Phys. Rev. Lett. **95**, 231801 (2005).

Frascati Physics Series Vol. XLI (2006), pp. 231-238
DISCOVERIES IN FLAVOUR PHYSICS AT e^+e^- COLLIDERS
Frascati, February 28th - March 3rd, 2006

RARE CHARM AND BOTTOM DECAYS AT TEVATRON

Frank Lehner*
Physik Institut der Universität Zürich

Abstract

The Tevatron accelerator at Fermilab delivers $p\bar{p}$ collisions at $\sqrt{s} = 1.96$ TeV with a peak luminosity of 1.7×10^{32} cm^{-2}s^{-1}. The two main detectors, CDF and DØ, are taking continuously collision data and have recorded more than 1 fb^{-1} of collision data up to now. In the following we will present results on rare charm and bottom decays that were obtained with the CDF and DØ detectors.

1 Introduction

Flavor-changing neutral current (FCNC) decays are absent in the Standard Model (SM) at tree level but proceed at low rate through higher order box and penguin diagrams. The experimental study of FCNC decays is a good opportunity to look for effects of new physics since (new) virtual particles can

be probed in loops that allow to discern new physics at high scales. In the SM the FCNC transition rate is governed by the GIM mechanism which dictates a suppressing quark mass difference dependence in the loops for all quark FCNC decays. Due to the large mass of the top quark the GIM suppression for down-type quark decay is relaxed giving rise to observable FCNC rates for B and K mesons and thus tight experimental constraints on new physics. In case of the corresponding FCNC charm decays however, the GIM suppression mechanism is much more effective such that charm FCNC decays proceed at very low rate and are still experimentally widely unexplored.

2 The Tevatron and the Experiments CDF and DØ

The so-called Run II of the Tevatron collider at Fermi National Accelerator Laboratory started to deliver $p\bar{p}$ collisions at $\sqrt{s} = 1.96$ TeV in April 2002. Since then the two operational experiments CDF and DØ have recorded with high data taking efficiency about 1.4 fb^{-1} of collision data with a recent peak luminosity of 1.7×10^{32} cm$^{-2}s^{-1}$ corresponding to a more than 10-fold increase in statistics compared to the previous Run I (1992-1995). Hadron colliders such as the Tevatron are copious sources of heavy quark ($c\bar{c}$, $b\bar{b}$) production. For instance, the $b\bar{b}$ cross section at Tevatron is about 100 μb, leading to $b\bar{b}$ production rates of a few kHz, while charm quarks are even produced at a 10$\times$ higher rate. Only approximately every 1000^{th} event in $p\bar{p}$ collisions contains a b ($\bar{b}$) quark, making event triggering and online selection for B physics a very delicate and complex task. In contrast to B physics studies at e^+e^- annihilation machines running at the $\Upsilon(4S)$ state, experimental investigations at the Tevatron have the distinct advantage of accessing all b-flavored mesons and baryons such as the $B_{s,c}$ mesons and Λ_b baryons. The high b-production rate on the one hand, and the availability to study several b-flavored species on the other hand, make the Tevatron collider an important laboratory for B physics, that is complementary to the present e^+e^- machines.

The two collider detectors CDF and DØ at the Tevatron were significantly upgraded [1)] in order to improve their physics capabilities while being able to cope with the high luminosity of Run II. The detector components that are crucial for a successful flavor physics program are silicon vertex detectors with good position resolution to resolve secondary vertices of heavy quark decays,

a tracking system within a magnetic field to provide efficient tracking and good momentum resolution, and a muon system with good coverage in pseudo-rapidity η. To select heavy quark events DØ is triggering mainly on single and di-muons coming from semi-leptonic heavy quark decays and from $B \to J/\psi X$ decays. Those muon triggers are found to be robust against higher luminosity and are used as unbiased triggers for mass and lifetime measurements as well as for rare decay searches. CDF employs in addition a two track trigger which reconstructs a secondary vertex from two charged hadrons with large impact parameter allowing to collect samples of two-body charmless B decays and charm meson decays.

3 Result on rare charm decays

3.1 $D^0 \to \mu^+\mu^-$

The leptonic decay $D^0 \to \mu^+\mu^-$ is a rare process that is mediated at short distance through a $c \to u\,\mu^+\mu^-$ FCNC quark transition. The branching ratio in the SM is estimated [2] to be $\mathcal{B}(D^0 \to \mu^+\mu^-) \approx 3 \times 10^{-13}$ and is almost completely dominated by long-distance two-photon processes. Although the SM prediction is many orders of magnitude beyond the reach of present experiments a considerable enhancement of this decay mode might exist in R_p violating SUSY models. Currently, the best experimental bound [3] at a 90% C.L. on this decay is given by Babar with $\mathcal{B}(D^0 \to \mu^+\mu^-) < 1.3 \times 10^{-6}$. As a very early Run II result CDF has carried out a search [4] for this decay using only 65 pb^{-1} of data. The data were collected with a two-track trigger and the topological similar decay $D^0 \to \pi\pi$ was used for normalization. Since the reconstructed mass of the normalization mode completely overlaps with the search window of the signal process a good understanding of misidentified $\pi \to \mu$ rates is crucial. This fake probability was estimated from a sample of D^* tagged $D \to \pi K$ events to be $(1.3 \pm 0.1)\%$. After optimizing cuts on discriminating variables while keeping the signal box hidden zero events were finally found with 1.8 ± 0.7 expected background events estimated from extrapolated sideband data. The obtained CDF limit is then $\mathcal{B}(D^0 \to \mu^+\mu^-) < 2.5 \times 10^{-6}$ at a 90% C.L. Note that this analysis used only 65 pb^{-1} of data and an updated limit on $\mathcal{B}(D^0 \to \mu^+\mu^-)$ with much higher statistics is expected to be released

soon. This updated analysis will also pursue the investigation of other rare D^0 decay modes such as $D^0 \to e^+e^-$ as well as the lepton-flavor violating decay $D^0 \to e^{\pm}\mu^{\mp}$.

3.2 $D^+ \to \pi^+\mu^+\mu^-$

The decay $D^+ \to \pi^+\mu^+\mu^-$ is another $c \to u\,\mu^+\mu^-$ FCNC transition that has a short-distance branching ratio in the SM of $\sim 10^{-8}$. The dominant long-distance contribution is a Cabbibo-suppressed resonant decay with the $\phi \to \mu^+\mu^-$ meson as intermediate state. There are several scenarios of new phenomena such as R_p violating SUSY or little Higgs models where deviations from the SM could be seen [5]. The decay $D_s^{\pm} \to \phi(\to \mu^+\mu^-)\pi^{\pm}$ has no short-distance contribution and decays only through the ϕ resonance. One of the first goals in an experimental charm FCNC program of DØ is thus the observation of this resonant decay as an essential step towards the study of $c \to u\,\mu^+\mu^-$ processes. Establishing the resonant signal allows then to search for $D^{\pm}$ decays in the non-resonant region. The most recent DØ search [6] is based on 1 fb^{-1} of data. Candidate $D^+_{(s)}$ mesons are formed by combining two muons with a track having $p_t > 0.18$ GeV/c that is associated with the same track jet and vertex as the muon pair. Backgrounds are further reduced using discriminating variables that are based on isolation and decay length information of the $D^+_{(s)}$ candidates. In a loose selection the $D^+_{(s)} \to \phi\pi^+ \to \pi\mu^+\mu^-$ signal events are extracted from a likelihood fit establishing as a first benchmark a clear signal of 133 ± 25 D_s^+ candidates at a significance above background of 7.5σ. After further optimization using signal MC and sideband data a 3σ evidence for $D^+ \to \phi\pi^+$ intermediate states is seen. The branching ratio can then be determined to be $\mathcal{B}(D^+ \to \phi\pi^+ \to \pi^+\mu^+\mu^-) = (1.75 \pm 0.7 \pm 0.5) \times 10^{-6}$ consistent with the product of $D^+ \to \phi\pi^+$ and $\phi \to \mu^+\mu^-$ branching ratios. A search in the non-resonant region excluding the area of the di-muon invariant mass around the ϕ enables DØ to place an upper limit at 90% C.L. on the short-distance FCNC process of $\mathcal{B}(D^+ \to \pi^+\mu^+\mu^-) < 4.7 \times 10^{-6}$, being the most stringent limit up to date.

4 Results on rare bottom decays

4.1 $B^0_{d,s} \to \mu^+\mu^-$

The purely leptonic decays $B^0_{d,s} \to \mu^+\mu^-$ are FCNC processes which are highly (helicity-) suppressed in the SM with decay rates [7] of $\mathcal{B}(B^0_s \to \mu^+\mu^-) = (3.42 \pm 0.54) \times 10^{-9}$ and $\mathcal{B}(B^0_d \to \mu^+\mu^-) = (1.00 \pm 0.14) \times 10^{-10}$ respectively. In particular new physics contributions at high $\tan\beta$ can enhance these branching ratios significantly. Due to the great sensitivity of this decay to new physics the search for $B^0_{d,s} \to \mu^+\mu^-$ belongs now to the core physics channels at Tevatron. CDF and DØ are using very similar methodologies to search for $B^0_s \to \mu^+\mu^-$ decays: Oppositely charged muon pairs are selected in a mass window around the B^0_s mass. The analyses are performed with multivariate optimization methods and a hidden signal box to avoid any bias in the results using sideband data for background determination. The widths of the signal box and of the sidebands are determined by the expected mass resolution for the signal channel and are drastically different between the CDF and DØ detectors. The mass resolution of CDF is estimated to be 24 MeV/c^2 while DØ evaluates its resolution to be 90 MeV/c^2. The superior mass resolution allows CDF an unique separation of B^0_s from B^0_d decays and to perform an independent search on $B^0_d \to \mu^+\mu^-$ decays as well. In the absence of a signal the limit on the branching ratio is then computed using the measured decay $B^+ \to J/\psi K^+$ with $J/\psi \to \mu^+\mu^-$ as normalization mode, such that systematic errors in triggering and selection tend to cancel. Normalizing the signal to $B^+ \to J/\psi K^+$ rather than to the $B^0_s \to J/\psi\phi$ decays has the advantage that the former mode has a higher statistics and the branching ratio and life time are well known from measurements at e^+e^- experiments. In addition, understanding the efficiency to detect $B^0_s \to J/\psi\phi$ events is complicated by the presence of CP even and odd decay components with significant different lifetimes. Using 300 pb^{-1} of data DØ sets [8] an upper limit at a 90% C.L. of $\mathcal{B}(B^0_s \to \mu^+\mu^-) < 3.0 \times 10^{-7}$. An update of the DØ search analysis exploiting the full available data set of more than 1 fb^{-1} is expected to be presented by the summer conferences. Presently, the world-best limits on $B^0_{s,d} \to \mu^+\mu^-$ decays are given by a recently released CDF analysis [9] based on 780 pb^{-1} of data. They obtain limits at a 90% C.L. of

$$\mathcal{B}(B_s^0 \to \mu^+\mu^-) < 8.0 \times 10^{-8}$$
$$\mathcal{B}(B_d^0 \to \mu^+\mu^-) < 2.3 \times 10^{-8}$$

which already reduce the available parameter space of certain SUSY models at high $\tan\beta$. The projected Tevatron reach for the DØ and CDF combined searches for $B_s^0 \to \mu^+\mu^-$ decays has been evaluated as function of the luminosity collected per experiment assuming that analysis techniques are unchanged and that the trigger and reconstruction efficiencies are unaffected with increasing luminosity. If, then, each experiment collects 8 fb^{-1} the Tevatron combination will allow for 90% C.L. exclusion limits down to branching ratios of 2×10^{-8}. Both experiments are pursuing further improvements to the analysis sensitivity, which would push the Tevatron combined sensitivity to still lower branching ratios. If no signal is observed, the resulting stringent limit would eliminate a very large part of the parameter space in many supersymmetric models at high $\tan\beta$.

4.2 $B_s^0 \to \phi\,\mu^+\mu^-$

The decay $B_s^0 \to \phi\,\mu^+\mu^-$ is an exclusive FCNC decay related to the transition of $b \to s\,\mu^+\mu^-$ at quark level. Within the SM the decay rate is predicted [10] to be of the order of 1.6×10^{-6} excluding long-distance effects from charmonium resonances with about 30% uncertainties due to poorly known form factors. DØ has conducted a blind analysis search [11] for $B_s^0 \to \phi\mu^+\mu^-$ decays using about 400 pb^{-1} of Run II data collected with di-muon triggers. To separate experimentally the FCNC-mediated process one has to restrict the invariant mass of the final state lepton pair to be outside the charmonium resonances. Those events are then normalized to reconstructed resonant $B_s^0 \to J/\psi(\mu^+\mu^-)\,\phi$ events. Cuts based on decay length information and on isolation of the B_s^0 candidate were optimized on signal MC and on expected background in the signal box as determined from the sidebands. After unblinding the analysis zero events were found with an expected number of background events of 1.6±0.4 corresponding to a Poisson probability of $p = 0.22$ in case of no signal hypothesis. The obtained limit relative to the resonant decay is then

$$\mathcal{B}(B_s^0 \to \phi\,\mu^+\mu^-)/\mathcal{B}(B_s^0 \to J/\psi\,\phi) < 3.5 \times 10^{-3}$$

at a 90% C.L. Using only the central value of the world average branching fraction of $\mathcal{B}(B_s^0 \to J/\psi\,\phi) = 9.3 \pm 3.3 \cdot 10^{-4}$, a limit at a 90% C.L. of $\mathcal{B}(B_s^0 \to \phi\,\mu^+\mu^-) = 3.2 \times 10^{-6}$ is derived. This is presently the most stringent limit of $B_s^0 \to \phi\,\mu^+\mu^-$ and only a factor 2 above the SM value.

5 Summary

The Tevatron collider is a copious source for heavy flavor. Its two experiments CDF and DØ allow to investigate rare FCNC decays of charm and bottom quarks which are good places to search for new physics. Upper limits on several rare charm decays are provided that are either competitive or better than other existing experiments. Moreover, the rare decay $B_s^0 \to \mu^+\mu^-$ is a prime candidate decay in searches for new physics. The most stringent limit recently obtained by CDF is already an important constraint for new physics at high $\tan\beta$ in several SUSY scenarios. Finally, Tevatron will approximately double the statistics every year such that rare FCNC decays are further experimentally scrutinized.

References

1. V. Abazov et al. [D0 Collab.], physics/0507191, submitted to Nucl. Instrum. Methods Phys. Res. A; D. Acosta et al. [CDF Collab.], Phys. Rev. D71, 032001 (2005).
2. G. Burdman and I. Shipsley, Ann. Rev. Nucl. Part. Sci. 53 (2003) 431.
3. B. Aubert et al. [Babar Collab], Phys. Rev. **D70**, 091101R (2004).
4. D. Acosta et al. [CDF Collab.], Phys. Rev. **D68**, 091101 (2003).
5. G. Burdman et al., Phys. Rev. **D66**, 014009 (2004); S. Fajfer these proceedings.
6. V. Abazov et al. [D0 Collab.], D0 Note 5038-CONF (2005).
7. G. Buchalla and A.J. Buras, Nucl. Phys. **B400**, 225 (1993); A.J. Buras, Phys. Lett. B **566**, 115 (2003).

8. V. Abazov et al. [D0 Collab.], Phys. Rev. Lett. **94**, 071802 (2005), updated in D0 Note 4733-CONF (2005).

9. A. Abulencia et al. [CDF Collab.], Phys. Rev. Lett. **95**, 221805 (2005), updated in CDF public note 8176 (2006).

10. C. Q. Geng and C. C. Liu, J. Phys. G **29**, 1103 (2003).

11. V. Abazov et al. [D0 Collab.], hep-ex/0604015, submitted to PRL.

Frascati Physics Series Vol. XLI (2006), pp. 239
DISCOVERIES IN FLAVOUR PHYSICS AT e^+e^- COLLIDERS
Frascati, February 28th - March 3rd, 2006

FLAVOUR PHYSICS FROM LATTICE QCD

Damir Becirevic
Lab. Physique Theorique, Université de Paris Sud, France

Written contribution not received

Frascati Physics Series Vol. XLI (2006), pp. 241
DISCOVERIES IN FLAVOUR PHYSICS AT e^+e^- COLLIDERS
Frascati, February 28th - March 3rd, 2006

SEARCH FOR NON-$\overline{D}$ DECAYS OF $\psi(3770)$ AND MEASUREMENT OF THE PARTIAL WIDTHS

Gang Rong
IHEP, Institute of High Energy Physics, Academia Sinica, People's Republic o

Written contribution not received

Frascati Physics Series Vol. XLI (2006), pp. 243
DISCOVERIES IN FLAVOUR PHYSICS AT e^+e^- COLLIDERS
Frascati, February 28th - March 3rd, 2006

CONSTRAINTS ON CHARM MIXING, STRONG PHASES AND DOUBLY-CABIBBO-SUPPRESSED DECAYS FROM CLEO-c

David M. Asner
Carleton University, 1125 Colonel By Drive
Ottawa, Ontario, Canada, K1S 5B6

Written contribution not received

Frascati Physics Series Vol. XLI (2006), pp. 245-252
DISCOVERIES IN FLAVOUR PHYSICS AT e^+e^- COLLIDERS
Frascati, February 28th - March 3rd, 2006

SEARCHES FOR EFFECTS OF LITTLEST HIGGS MODEL IN $D^+ \to \pi^+ l^+ l^-$ AND $D^0 \to \rho^0 l^+ l^-$ DECAYS

S. Fajfer and Saša Prelovšek
Department of Physics, University of Ljubljana, Jadranska 19, 1000 Ljubljana and J. Stefan Institute, Jamova 39, P. O. Box 300, 1001 Ljubljana, Slovenia

Abstract

The Littlest Higgs model allows $c \to u l^+ l^-$ decay at tree level. We investigate possible effects of this model in the $D^+ \to \pi^+ l^+ l^-$ and $D^0 \to \rho^0 l^+ l^-$ decays. After determining the effects of new physics in the relevant Wilson coefficents and reevaluating the standard model long-distance contributions, we calculate the differential branching ratio for both decay modes and determine the forward- backward asymmetry for the $D^0 \to \rho^0 l^+ l^-$ decay. The effects of the Littlest Higgs model are not significant.

1 Introduction

The Littlest Higgs (LH) model (see e.g. refs. [1)5)]) is one of many extension of the Standard Model. It offers a simple and appealing solution to the gauge hierarchy problem. The quadratic divergences in the Higgs mass due to the SM

gauge bosons are cancelled by the contributions of the new heavy gauge bosons with spin 1. The divergence due to top quark is cancelled by the contribution of the new heavy quark with the charge 2/3 and spin 1/2. It was pointed out by author of ref. [4] that the existence of this new quark which is a $SU(2)_L$ singlet has an interesting consequence: It extends the 3×3 CKM matrix in SM to a 4×3 matrix and it also allows Z-mediated FCNC at tree-level in the up sector but not in the down sector [4]. In ref. [4] the author has studied effects of this new FCNC coupling in $D\to\mu^+\mu^-$, $D^0\leftrightarrow\bar{D}^0$ oscillations and $t\to cZ$ decay.

Motivated by this study we investigate possible effects of the tree-level $c\to uZ$ coupling from the Littlest Higgs model in charm meson decays. In ref. [6] we focus on the decays $D^+\to\pi^+l^+l^-$ and $D^0\to\rho^0 l^+l^-$, which are the most suitable for the experimental studies among all $D\to Xl^+l^-$ decay modes as explained in ref. [6]

In the SM there is no neutral-current interactions which change flavor at the tree level due to the GIM mechanism. However, in the Littlest Higgs model the neutral current interactions change the flavor already at the tree level. The electromagnetic current is the same as in the SM, while $J^\mu_{W^3}$ is given by [4]

$$J^\mu_{W^3}=\frac{1}{2}\bar{U}^m_L\gamma^\mu\Omega U^m_L-\frac{1}{2}\bar{D}^m_L\gamma^\mu D^m_L \tag{1}$$

with $L=\frac{1}{2}(1-\gamma_5)$ and mass eigenstates $U^m_L=(u_L,c_L,t_L,T_L)^T$, $D^m_L=(d_L,s_L,b_L)^T$. The neutral current for the down-like quarks is the same as in the SM, while the up sector has additional currents since $\Omega\neq I$ due to the new heavy quark [4] . In ref. [4] Ω_{uc} was releted to the scale f by $|\Omega_{uc}|\simeq 10^{-5}\left(\frac{1\text{ TeV}}{f}\right)^2$, which implies upper bound on Ω_{uc} since the scale f can not be arbitrarily small.

At present, the scale f is already severely constrained by the precision electro-weak observables. The lowest bound on f ranges between 1 TeV to 4 TeV or even higher, depending on the specific model [5], and we will vary the scale between 0.5 TeV– 4 TeV [6]. The LH model contains the tree-level coupling $\bar{u}_L\gamma_\mu c_L Z^\mu$ and modifies coefficients C_9 and C_{10}

$$V^*_{cb}V_{ub}\;\delta C^{LH}_9=\frac{8\pi}{\alpha}\Omega_{uc}g^l_V,\quad V^*_{cb}V_{ub}\;\delta C^{LH}_{10}=-\frac{8\pi}{\alpha}\Omega_{uc}g^l_A \tag{2}$$

with $g^l_V=-1/2+2\sin^2\theta_W$ and $g_A=-1/2$. This model can moderately

enhance the rate for the inclusive decay $c \to u l^+ l^-$, as illustrated for various scales f in Fig. 1 in ref. [6].The enhancement over the SM rate is practically negligible for the scales f of few TeV or more while it is appreciable for $f \simeq 0.5$ TeV and we explore whether this could lead to any modifications of hadron observables in the $D^+ \to \pi^+ l^+ l^-$ and $D^0 \to \rho^0 e^+ e^-$ decays.

2 Effects on $D^+ \to \pi^+ l^+ l^-$ and $D^0 \to \rho^0 e^+ e^-$ decays

The FCNC effects of LH model in the $c \to u l^+ l^-$ transition can be probed in $D^+ \to \pi^+ l^+ l^-$ ($l = e, \mu$) decay. As we presented in ref. [6] resonant decay channels $D^+ \to \pi^+ V_0 \to \pi^+ l^+ l^-$ with intermediate vector resonances $V_0 = \rho^0, \omega, \phi$ constitute an important long-distance contribution to the hadronic decay, which may shadow interesting short-distance contribution induced by $c \to u l^+ l^-$ transition. Our determination of short and long distance contributions to $D^+ \to \pi^+ l^+ l^-$ takes advantage of the available experimental data. The amplitudes which arise from contributions given in eq. (14) and eq. (19) in ref. [6] give decay distributions in Figure 1, while the corresponding total rates are given in Table 1. The rates in Standard and Littlest Higgs models are dominated by the resonant long distance contribution over the entire kinematical region of m_{ll}^2. Although the LH model with scale as low as $f = 0.5$ TeV would enhance the short distance contribution, it would not affect appreciably the dilepton mass distribution for $D^+ \to \pi^+ l^+ l^-$.

The long-distance contribution in $D^0 \to \rho^0 V_0 \to \rho^0 l^+ l^-$ ($V_0 = \rho^0, \omega, \phi$) is induced by $V_{cd}^* V_{ud} Q_1^d + V_{cs}^* V_{us} Q_1^s$ as explained in detail in refs. [7, 8].We are unable to determine its amplitude using the measured rates for $D^0 \to \rho^0 V_0$ since only the rate of $D^0 \to \rho^0 \phi$ is known experimentally. We are forced to use a model and we apply the approach of [7] (an improved version of [8]), which was developed to describe all $D \to V l^+ l^-$ and $D \to V \gamma$ decays. As explained in ref. [6], the long-distance contribution completely dominates the dilepton mass distributions in SM and LH models (see Fig. 2). It also dominates the total rate given in Table 1. The short distance contributions are completely negligible in SM [7, 8] as well as in LH model even for the scale as low as $f = 0.5$ TeV. Our study shows that the LH model has negligible effect on the rate of $D^0 \to \rho^0 l^+ l^-$, but it might have sizable effect on forward-backward asymmetry as defined in eq. (20) of ref. [6]. The non-zero asymmetry in $D \to \rho l^+ l^-$ decay arises only when $C_{10} \neq 0$ (assuming $m_l \to 0$), so the asymmetry is practically

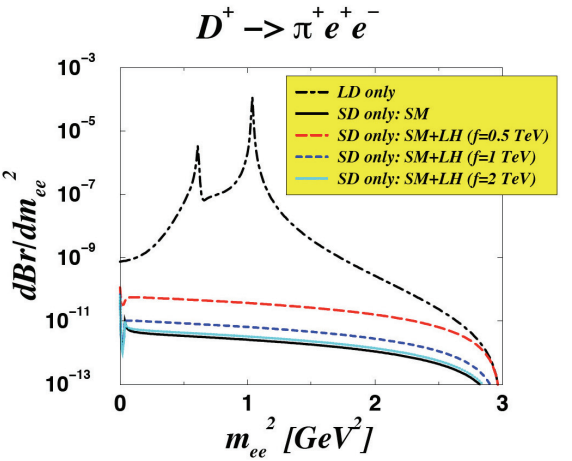

Figure 1: *The dilepton mass distribution* dBr/dm_{ee}^2 *for the decay* $D^+ \to \pi^+e^+e^-$ *as a function of the dilepton mass square* $m_{ee}^2 = (p_+ + p_-)^2$.

zero in SM where $C_{10} \simeq 0$. The enhancement of the C_{10} in the LH model (2) is due to the tree-level $\bar{u}_L\gamma_\mu c_L Z^\mu$ coupling and leads to nonzero asymmetry $A_{FB}(m_{ll}^2)$ shown in Fig. 3.

3 Conclusions

We have investigated the impact of the tree-level flavor changing neutral transition $c \to uZ$ on the rare D meson decay observables. First we determined the effects of the LH model on the effective Wilson coefficients C_9^{eff} and C_{10}^{eff}. Both coefficients have the same magnitude in the LH model, contrary to the result of SM where $C_{10}^{eff} \simeq 0$. The LH model can appreciably modify the inclusive $c \to ul^+l^-$ decay only for the scales close to $f = 1$ TeV or less.

Among exclusive rare $D \to Xl^+l^-$ decays, the $D^+ \to \pi^+l^+l^-$ and $D^0 \to \rho^0l^+l^-$ decays are the best candidates for the experimental searches and have most stringent upper bounds at present. However, these decays are found to be completely dominated by the long distance contributions in SM as well as in LH models. Even the LH model with scale as low as $f = 0.5$ TeV can not sizably modify the total rates and the dilepton mass distributions for $D^+ \to \pi^+l^+l^-$ and $D^0 \to \rho^0l^+l^-$. The forward-backward asymmetry for $D^0 \to \rho^0l^+l^-$ vanishes in SM, while it is of the order of 10^{-3} in LH model with

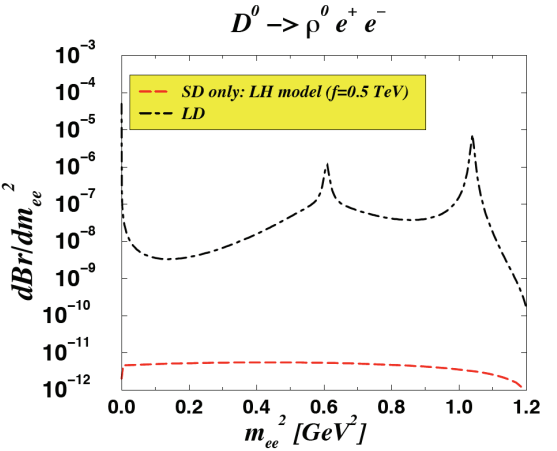

Figure 2: *The figure shows the dilepton mass distribution for* $D^0 \to \rho^0 e^+ e^-$.

the scale f around 1 TeV. Such asymmetry is still too small to be observed in the present or planned experiments given that the rate itself is already small.

We conclude that the LH model has insignificant effects on the charm meson observables in spite of its tree-level flavour changing couplings among up-like quarks. The eventual observation of the dilepton mass distribution and forward-backward asymmetry that disagree with the standard model prediction would indicate the presence of some other scenario of physics beyond standard model.

Table 1: *Branching ratios for the hadronic decays, which are most suitable to probe* $c \to u l^+ l^-$ *transition experimentally.*

Br	SD cont. only		total rate $\simeq$ LD contr.	experiment
	SM	SM + LH ($f = 0.5$ TeV)		
$D^+ \to \pi^+ e^+ e^-$	6×10^{-12}	8×10^{-11}	1.9×10^{-6}	$< 7.4 \times 10^{-6}$
$D^+ \to \pi^+ \mu^+ \mu^-$	6×10^{-12}	8×10^{-11}	1.9×10^{-6}	$< 8.8 \times 10^{-6}$
$D^0 \to \rho^0 e^+ e^-$	negligible	5×10^{-12}	1.6×10^{-7}	$< 1.0 \times 10^{-4}$
$D^0 \to \rho^0 \mu^+ \mu^-$	negligible	5×10^{-12}	1.5×10^{-7}	$< 2.2 \times 10^{-5}$

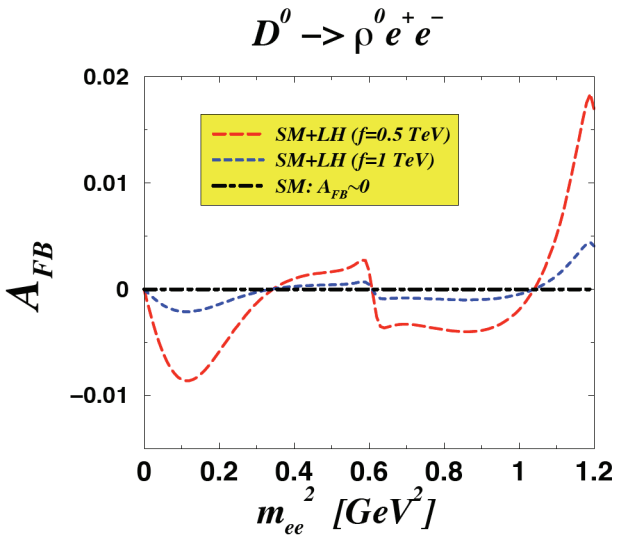

Figure 3: *The figure shows the forward-backward asymmetry for* $D^0 \to \rho^0 e^+ e^-$.

References

1. N. Arkani-Hamed, A.G. Cohen, E. Katz and A. E. Nelson, JHEP **0207**, 034 (2002).

2. T. Han, H.E. Logan, B. McElrath and L.T. Wang, Phys. Rev. D **67**, 095004 (2003).

3. M. Schmaltz, Nucl. Phys. Proc. Suppl. **117**, 40 (2003).

4. Lae Yong Lee, JHEP **0412**, 065 (2004).

5. C. Csaki *et al.*, Phys. Rev. D **67** (2003) 115002, M. Perelstein, `hep-ph/0512128`.

6. S. Fajfer and Sasa Prelovsek, Phys. Rev. **D** 73 (2006) 054026.

7. S. Prelovsek, Ph.D. Thesis, `hep-ph/0010106`.

8. S. Fajfer, S. Prelovsek, P. Singer, Phys. Rev. D

τ-LEPTON PHYSICS

Frascati Physics Series Vol. XLI (2006), pp. 253-262
DISCOVERIES IN FLAVOUR PHYSICS AT e^+e^- COLLIDERS
Frascati, February 28th - March 3rd, 2006

LEPTON FLAVOR VIOLATION IN TAU LEPTON DECAY AND THE RELATED TOPICS

Junji Hisano
ICRR, University of Tokyo
5-1-5 Kashiwa-no-Ha Kashiwa City, 277-8582, Japan

Abstract

Tau lepton flavor violation in supersymmetric models and the related topics are reviewed. Lepton flavor conservation is not exact in nature, and then charged lepton flavor violating processes are good probes to study models beyond the standard model. Especially, those for tau lepton are a unique window to discriminate models.

1 Introduction

Neutrino oscillation was discovered in 98' [1], and now the neutrino oscillation experiments is going to next phase of precision measurement. Following is the latest result of global fit to three neutrinos [2],

$$\begin{aligned} \delta m^2_{23} &= 2.4(1^{+0.21}_{-0.15}) \times 10^{-3}\text{eV}, & \sin^2\theta_{\mu 3} &= 0.44(1^{+0.41}_{-0.22}), \\ \delta m^2_{12} &= 7.92(1 \pm 0.09) \times 10^{-5}\text{eV}, & \sin^2\theta_{e2} &= 0.314(1^{+0.18}_{-0.15}), \\ \sin^2\theta_{e3} &= 0.9^{+2.3}_{-0.9} \times 10^{2}. \end{aligned} \tag{1}$$

Now we have no doubt that lepton flavor conservation is not exact in nature. The seesaw mechanism, in which superheavy right-handed neutrinos are introduced, is the simplest model to explain tiny neutrino masses. The lepton

flavor violation (LFV) in charged lepton sector is negligibly small in the model. However, we have many reasons that we have to extend the standard model (SM), such as a viewpoint of naturalness, and we have no apparent reason that the lepton flavor conservation is exact in those models.

Various models beyond the SM are proposed, and many models predict lepton flavor violation in the charged lepton sector. The supersymmetric (SUSY) extension of the SM (SUSY SM) is the leading candidate of the model beyond SM. In this model, the SUSY breaking terms for sleptons may be lepton flavor violating, and induce rare LFV charged lepton processes. The extra-dimension models, whose compact scale is close to the weak scale, may predict the rare processes when the SM fermions stay in the extra-dimensional space, since the bulk fermion mass terms can be introduced in addition to the Yukawa coupling to the SM Higgs boson. Tiny neutrino masses might come from some weak-scale physics. The search for the LFV in the charged lepton sector is important to explore these models.

The current experimental bounds on the rare LFV charged lepton processes are following,

$$\begin{aligned} Br(\tau \to \mu(e)\gamma) &< 6.8(0.11) \times 10^{-8}, \\ Br(\tau \to \mu(e)\eta) &< 1.5(2.3) \times 10^{-7}, \\ Br(\tau \to 3l) &\lesssim 10^{-7}, \\ Br(\mu \to e\gamma) &< 1.2 \times 10^{-11}, \\ Br(\mu \to 3e) &< 1.0 \times 10^{-12}, \\ R(\mu - e : Ti) &< 4.3 \times 10^{-12}. \end{aligned} \tag{2}$$

In the past five years, the bounds on the rare tau lepton decay modes were improved by the Belle and Babbar experiments. Further improvement may be possible in super B factories. While the bounds in the rare muon decays were not improved in the past five years, the MEG experiment will start to search for $\mu \to e\gamma$ this year, and it may cover the branching ratio down to $10^{-13} - 10^{-14}$. Furthermore, the $\mu - e$ conversion experiment, the PRISM experiment, is proposed, and it may push the bound on the rate down to 10^{-18}.

In this review, we discuss the charged lepton flavor violation in the SUSY SM and the extensions. The SUSY SM is the most promising model beyond the SM, and it is also a good prototype of the models beyond the SM. Various studies of the LFV in the models were done. In next section LFV in the SUSY SM is reviewed, and the flavor violation in the tau lepton decay is summarized.

We discuss the branching ratios in SUSY GUTs and the SUSY seesaw model in the following section and compare the LFV rare tau lepton and muon decays.

2 LFV in SUSY SM

In the SUSY SM, the superpartners are introduced for every SM particles. The mass term for squarks and sleptons, which are superpartners of quarks and leptons, are schematically given as

$$(m^2_{\tilde{f}})_{ij} \quad = \quad (m^\dagger_f m_f)_{ij} + (\overline{m}^2_{\tilde{f}})_{ij} \tag{3}$$

where m_f is the fermion mass and $\overline{m}^2_{\tilde{f}}$ is the SUSY breaking contribution. New flavor violation appears when the SUSY breaking terms are introduced.

Flavor physics plays an important role in construction and establishment of the SUSY SM as it has been in the history of the SM. The stringent constraints on the SUSY breaking terms are derived from the $K^0 - \bar{K}^0$ mixing and $\mu \to e\gamma$. There are several scenarios to solve this SUSY flavor problem:

- *Universality.* The SUSY breaking terms have a universal flavor structure at a very high energy scale.
- *Alignment.* Squarks and Sleptons can be diagonalized in the same basis as quarks and leptons due to some flavor symmetries or some mechanism.
- *Decoupling.* Squarks and sleptons in the first and second generations are so heavy ((10-100)TeV) that the flavor violation in the first and second generations is suppressed.

In the universality scenario, the flavor violation is suppressed. However, this does not necessarily imply that the LFV effects should not exist. If some physics has LFV interactions below the SUSY breaking mediation scale, the LFV slepton mass terms are induced radiatively by the renormalization-group effect [3]. In this case the LFV mass terms are not suppressed by powers of the energy scale for the LFV interactions. The seesaw mechanism and the GUTs are nowadays ones of attractive models from the phenomenological and theoretical points of view. In these models, LFV Yukawa interactions are introduced. Thus, if the SUSY breaking mediation scale is higher than the GUT [4] or the right-handed neutrino mass scale [5], sizable LFV processes might be predicted. In the next subsection we discuss the LFV tau lepton decay in these models.

In the decoupling scenario, squarks and sleptons in the third generation may have large flavor violation. If the alignment between lepton and slepton masses is not complete in the second scenario, the LFV is predicted. Thus, search for the LFV tau lepton decay is also an important probe in these scenarios.

Now we discuss LFV tau lepton processes in the SUSY models. In a broad parameter space, $\tau \to \mu(e)\gamma$ is the largest tau LFV processes, unless it is suppressed by the accidental cancellation or much heavier SUSY particle masses. The other LFV tau lepton decay modes are dominantly induced by the photon-penguin contributions, and they are correlated with $\tau \to \mu(e)\gamma$ as 6)

$$Br(\tau \to \mu(e)ee)/Br(\tau \to \mu(e)\gamma) \simeq 1/94, \quad (4)$$

$$Br(\tau \to \mu(e)\mu\mu)/Br(\tau \to \mu\gamma) \simeq 1/440, \quad (5)$$

$$Br(\tau \to \mu(e)\rho)/Br(\tau \to \mu(e)\gamma) \simeq 1/400. \quad (6)$$

When sleptons are much heavier than the weak scale, $Br(\tau \to \mu(e)\gamma)$ is suppressed. In this case, $\tau \to \mu(e)\mu\mu$ and $\tau \to \mu(e)\eta$ induced by Higgs boson exchange become relatively important [7]. The LFV Yukawa coupling for the Higgs bosons is generated by the radiative correction, and it is not suppressed by powers of the slepton masses. While these processes are suppressed by a small Yukawa coupling constant for muon or strange quark, they may become sizable branching ratios when $\tan\beta$ is large since the branching ratios are proportional to $\tan^6\beta$ [7]. It is argued in Refs. [7] that $Br(\tau \to \mu\mu\mu)$ and $Br(\tau \to \mu\eta)$ can reach to $10^{-(6-7)}$ in the SUSY seesaw mechanism when $\tan\beta = 60$ and the heavier Higgs mass is about 100GeV. Notice that $\tau \to \mu\gamma$ also has a comparable branching ratio to them since the Higgs loop diagram is enhanced by the tau lepton Yukawa coupling constant [8].

3 LFV in SUSY seesaw model and SUSY GUTs

The processes $\tau \to \mu\gamma$ might be very important because the large mixings between $\nu_\mu - \nu_\tau$ is observed in the atmospheric neutrino oscillation experiments. The most economical model to generate tiny neutrino masses is the seesaw mechanism. Neutrino Yukawa coupling Y_ν is introduced in the seesaw mechanism and it is lepton flavor violating. In the supersymmetric extension, the off-diagonal components in the left-handed slepton mass matrix are radiatively

induced, and they are approximately given as

$$(\delta m^2_{\tilde{L}})_{ij} \simeq -\frac{1}{8\pi^2}(3m_0^2 + A_0^2)\sum_k (Y_\nu^\dagger)_{ki}(Y_\nu)_{kj}\log\frac{M_G}{M_{N_k}}, \quad (7)$$

where M_{N_i} and M_G are the i-th right-handed neutrino masses and the Planck scale, respectively. Now we assume the gravity mediation scenario, and the parameters m_0 and A_0 are the universal scalar mass and the universal trilinear scalar coupling. The predicted small neutrino mass matrix is

$$(m_\nu)_{ij} = \sum_k \frac{(Y_\nu)_{ki}(Y_\nu)_{kj}\langle H_2\rangle^2}{M_{N_k}}. \quad (8)$$

Eq. (7) has the different structure from Eq. (8). Thus, we can get independent information about the seesaw mechanism from the charged LFV searches and the neutrino oscillation experiments [9].

In Fig. 1 we show $Br(\tau \to \mu\gamma)$ and $Br(\tau \to e\gamma)$ in the SUSY seesaw mechanism, assuming the gravity mediation scenario for the SUSY breaking. We fix the neutrino Yukawa coupling using the neutrino oscillation data under some assumptions for the neutrino Yukawa coupling Y_ν, which suppress $Br(\mu \to e\gamma)$. The experimental bounds on $Br(\tau \to \mu\gamma)$ and $Br(\tau \to e\gamma)$ have already excluded some parameter space. While a natural expectation for the largest LFV tau lepton decay mode is $\tau \to \mu\gamma$ from the atmospheric neutrino result, some model parameters in the seesaw model predict larger $Br(\tau \to e\gamma)$ [9]. This is because that Eq. (7) and Eq. (8) have different dependence on Y_ν and M_N as mentioned above.

In Fig. 2 the correlation between $Br(\tau \to \mu\gamma)$ and $Br(\mu \to e\gamma)$ in the SUSY seesaw mechanism. Here, we assume that the right-handed neutrino mixing angles are negligible so that $(Y_\nu)_{ij} \propto m_{\nu i} M_{Ni} U^\dagger_{ij}$. Here, U is the MNS matrix, and $m_{\nu i}(i = 1 - 3)$ is for light-neutrino masses. This is a bottom-up approach, in which Y_ν can be constructed from the low energy observables in addition to three right-handed neutrino masses. In this assumption, $(\delta m^2_{\tilde{L}})_{23} \propto U_{\mu 3} U^\star_{\tau 3} m_{\nu 3} M_{N3}$ and $(\delta m^2_{\tilde{L}})_{12} \propto U_{e2} U^\star_{\mu 2} m_{\nu 2} M_{N2} + U_{e3} U^\star_{\mu 3} m_{\nu 3} M_{N3}$, $Br(\mu \to e\gamma)$ is sensitive to U_{e3}. Then

$$\frac{Br(\mu \to e\gamma)}{Br(\tau \to \mu\gamma)} \gtrsim 10^{-3} \times \left|\frac{U_{e3}}{0.01}\right|^2. \quad (9)$$

This ratio depends on the models, however, the lowerbound in Eq. (9) is valid in many class of the models.

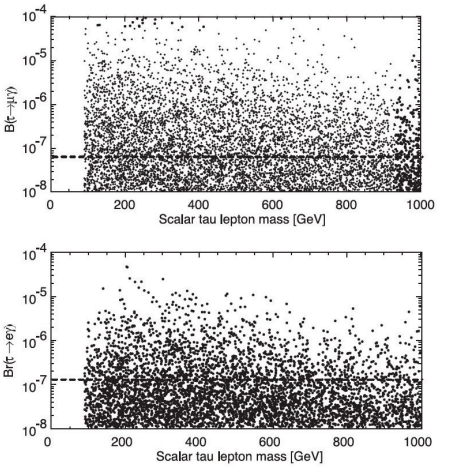

Figure 1: $Br(\tau \to \mu\gamma)$ and $Br(\tau \to e\gamma)$ in the SUSY seesaw mechanism, assuming the gravity mediation scenario for the SUSY breaking. Dashed lines show the current experimental bounds. We fix the neutrino Yukawa coupling using the neutrino oscillation data under assumptions of the neutrino Yukawa coupling.

It is straight-forward to extend the seesaw mechanism to the SU(5) SUSY GUT. However, even if the neutrino Yukawa contribution is negligible, the LFV processes are predicted. The right-handed charged leptons are embedded in the **10**-dimensional multiplets with the left-handed quarks and the right-handed up-type quarks in the SU(5) SUSY GUT. The LFV SUSY breaking terms for the right-handed sleptons are generated by the top quark Yukawa coupling Y_t above the GUT scale. The off-diagonal components in the right-handed slepton mass matrix are given as

$$(\delta m^2_{\tilde{E}})_{ij} \simeq -\frac{3}{8\pi^2}(3m_0^2 + A_0^2)V_{i3}V^\star_{j3}|Y_t|^2 \log\frac{M_G}{M_{GUT}}, \qquad (10)$$

where V_{ij} is the Cabibbo-Kobayashi-Maskawa (CKM) matrix in the SUSY SU(5) GUT and M_{GUT} is the GUT scale.

In Fig. 3 we show $Br(\mu \to e\gamma)$ and $Br(\tau \to \mu\gamma)$ in the SU(5) SUSY GUT without the neutrino Yukawa coupling. While the processes are enhanced by the top-quark Yukawa coupling, they are suppressed by the CKM matrix

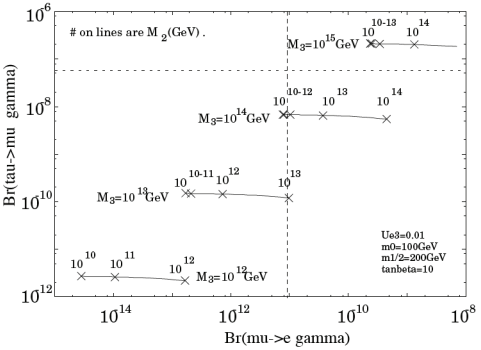

Figure 2: Correlation between $Br(\tau \to \mu\gamma)$ and $Br(\mu \to e\gamma)$ in the SUSY seesaw mechanism. Here, we take a bottom-up approach to construct the neutrino Yukawa coupling from low energy observables.

element and the $U(1)_Y$ gauge coupling constant. Furthermore, when the right-handed sleptons have the LFV mass terms, accidental cancellation among the diagrams tends to suppress the branching ratio. The ratio of $Br(\mu \to e\gamma)$ and $Br(\tau \to \mu\gamma)$ is roughly $O(\lambda^6) \sim 10^{-4}$.

Here, notice that the CKM matrix elements at the GUT scale may not be the same as ones extrapolated from the low energy data. This is because the quark and lepton mass ratios are not well explained in this model and we need to care of it. If V_{32} is larger, the LFV processes for tau lepton are enhanced.

In the SUSY GUTs, the SUSY breaking terms for sleptons are correlated with those of squarks. Thus, if we observe either LFV tau lepton processes or deviation from the SM predictions in the B decays, the other is a good test for the models. In Fig. (4) the correlations between $Br(\tau \to \mu\gamma)$ and CP asymmetries in $B \to \phi K_S$ and $B_s \to J/\psi\phi$ in the SUSY SU(5) GUT with right-handed neutrinos [10]. The neutrino Yukawa coupling induces the flavor-violating mass terms for the left-handed sleptons and also for the right-handed down-type squarks [11].

4 Summary

I reviewed tau lepton flavor violation in the SUSY models and the related topics. Lepton flavor conservation is not exact in nature, and then charged lepton flavor violating processes are good probe to study models beyond the

SM. Especially, those for tau lepton are a unique window. We hope that further experimental studies will continue.

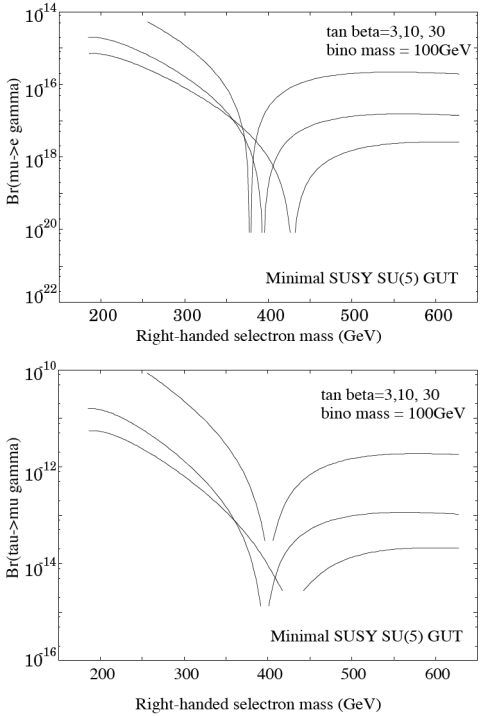

Figure 3: $Br(\tau \to \mu\gamma)$ and $Br(\mu \to e\gamma)$ in the SUSY GUT assuming the gravity mediation scenario for the SUSY breaking. Here, we ignore the neutrino Yukawa coupling constants.

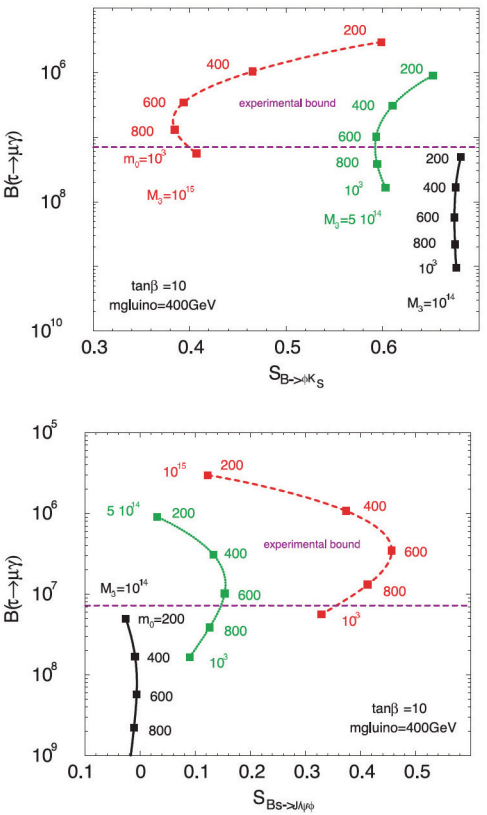

Figure 4: Correlations between $Br(\tau \to \mu\gamma)$ and CP asymmetries in $B \to \phi K_S$ and $B_s \to J/\psi\phi$ in the SUSY SU(5) GUT with right-handed neutrinos.

References

1. Y. Fukuda *et al.* [Super-Kamiokande Collaboration], Phys. Rev. Lett. **81** 1562, (1998).

2. G. L. Fogli, E. Lisi, A. Marrone and A. Palazzo, hep-ph/0506083.

3. L. J. Hall, V. A. Kostelecky and S. Raby, Nucl. Phys. B **267** 415, (1986).

4. R. Barbieri and L. J. Hall, Phys. Lett. B **338** 212, (1994); R. Barbieri, L. J. Hall and A. Strumia, Nucl. Phys. B **445** 219, (1995); J. Hisano, T. Moroi, K. Tobe and M. Yamaguchi, Phys. Lett. B **391**341, (1997) [Erratum-ibid. B **397**357, (1997)].

5. F. Borzumati and A. Masiero, Phys. Rev. Lett. **57** 961, (1986); J. Hisano, T. Moroi, K. Tobe, M. Yamaguchi and T. Yanagida, Phys. Lett. B **357** 579, (1995); J. Hisano, T. Moroi, K. Tobe and M. Yamaguchi, Phys. Rev. D **53** 2442, (1996); J. Hisano and D. Nomura, Phys. Rev. D **59** 116005, (1999).

6. A. Brignole and A. Rossi, Nucl. Phys. B **701**, 3 (2004).

7. K. S. Babu and C. Kolda, Phys. Rev. Lett. **89** 241802, (2002) ; M. Sher, Phys. Rev. D **66** 057301, (2002).

8. P. Paradisi, JHEP **0602**, 050 (2006).

9. J. A. Casas and A. Ibarra, Nucl. Phys. B **618** 171, (2001); S. Davidson and A. Ibarra, JHEP **0109**, 013 (2001); J. R. Ellis, J. Hisano, M. Raidal and Y. Shimizu, Phys. Rev. D **66** 115013, (2002).

10. J. Hisano and Y. Shimizu, Phys. Lett. B **565**, 183 (2003).

11. T. Moroi, Phys. Lett. B **493** 366, (2000).

Frascati Physics Series Vol. XLI (2006), pp. 263
DISCOVERIES IN FLAVOUR PHYSICS AT e^+e^- COLLIDERS
Frascati, February 28th - March 3rd, 2006

FUTURE PERSPECTIVES AND EXPERIMENTAL REQUIREMENTS IN τ-PHYSICS

Michael Roney
University of Victoria, CA

Written contribution not received

Frascati Physics Series Vol. XLI (2006), pp. 265-274
DISCOVERIES IN FLAVOUR PHYSICS AT e^+e^- COLLIDERS
Frascati, February 28th - March 3rd, 2006

τ PHYSICS AT B-FACTORIES

Olga Igonkina
Physics Department, University of Oregon, Eugene, Oregon 97403, USA

Abstract

Today the B-factories BaBar and Belle have accumulated largest samples of $\tau^+\tau^-$ events and are competing to be called τ-factories. Among the problems to be tested and measurements to be done by BaBar and Belle are check of CP and CPT invariance in tau decays, measurement of strange and non-strange spectral functions, extraction of mass of strange quark and $|V_{us}|$, searches for lepton flavor violation processes. In this paper, the latest results in tau physics by these two experiments and measurements to be done within next few years are reviewed.

1 Introduction

BaBar [1)] and Belle [2)] are the e^+e^- collider experiments running at $\sqrt{s}$ equal to $\Upsilon(4S)$ mass. In spite of their commonly used name *B-factories* they also

provide largest and cleanest samples today for study of tau physics. Indeed, the cross-section of $e^+e^- \to \tau^+\tau^-$ ($\sigma_{\tau^+\tau^-}$) at this energy is 0.89 nb, of the same order as $B\bar{B}$ cross section at $\Upsilon(4S)$ and just a bit smaller than $\sigma^{thr}_{\tau^+\tau^-} \simeq 1.2$ nb at $\tau^+\tau^-$ production threshold [3].

The $\tau^+\tau^-$ event produced at $\Upsilon(4S)$ has very characteristic topology. The decay products of two taus are well separated in space, such that if space is split on two hemispheres with respect to the axis of the event thrust, the decay products of two taus are mostly contained within opposite hemispheres. From other side, the boost is not as large as at LEP experiments, and the tracks are well separated. As both BaBar and Belle are multipurpose spectrometers, the full particle identification of the event can be performed. Usually tau decays have one (1-prong) or three (3-prong) charged particles in the final state, therefore the multiplicity of the $\tau^+\tau^-$ events is relatively small. The typical backgrounds are radiative Bhabha and di-muon events which can be suppressed by vetoing leptons or high momentum tracks, and hadronic $q\bar{q}$ events which are more isotropic and have in average more neutral particles.

Currently, BaBar has recorded about $6 \cdot 10^8$ tau decays, and Belle has recorded about 10^9 tau decays with large part of the statistics used in the analyzes presented below. In section 2, we review high precision measurements of tau mass and lifetime, which allow test of CPT invariance, and discuss perspectives of measuring CP-violation in tau decays. Section 3 is concentrated on the description of the measurements of the hadronic tau decays. In the section 4 the searches of lepton flavor violation in tau decays are described and the conclusions are drawn in section 5. The future perspectives and limitations of different measurements are discussed throughout the paper.

2 Standard Model tests

The basic tasks of the τ-factories are to measure mass m_τ and time of life τ_τ of tau lepton. Belle has recently presented a preliminary measurement of $m_\tau = (1776.71 \pm 0.25_{stat} \pm 0.62_{sys})$ MeV [5] using pseudo-mass technique pioneered by ARGUS [6]. The sample of 253 fb^{-1} was used. Although the measurement is dominated by systematic uncertainties, it is largely due to the size of the control samples, and therefore is likely to be improved with increased statistics. The sample is also used to probe the difference between m_{τ^+} and m_{τ^-} which is found to be negligible, $|m_{\tau^+} - m_{\tau^-}|/m_\tau < 5.0 \cdot 10^{-4}$ at 90% confidence level

(CL). This number is statistically limited as most systematic uncertainties are canceled in the ratio.

At the same time BaBar has concentrated on the tau lifetime measurement. The flight distance transverse to the beam λ_T is measured and corrected by polar angle of 3-prong system (Θ_{3pr}) to calculate the total decay length $\lambda = \lambda_T / \sin\Theta_{3pr}$. The dependence on azimuthal angle ϕ ($\lambda(\phi)$) is fitted to minimize the systematic uncertainties due to alignment of the vertex detector. The preliminary result is $\tau_\tau = 289.40 \pm 0.91_{stat} \pm 0.90_{sys}$ fs [7]. It is in agreement with PDG value $\tau_\tau = 290.6 \pm 1.1$ fs [14] and is the most precise measurement up to date. 80 fb^{-1} were used in the analysis. As in case of m_τ measurement, the systematic uncertainty are partially limited by statistics of control samples and is likely to be improved with luminosity, although not more than by factor of two. The preliminary study of τ_{τ^+} and τ_{τ^-} showed no difference $\tau_{\tau^-} - \tau_{\tau^+}/\tau_{\tau^-} + \tau_{\tau^+} = (0.12 \pm 0.32_{stat})\%$, where the systematic uncertainty is to be estimated but likely to be small.

Using the above numbers averaged with PDG values and leptonic branching fractions [14] of tau one can compare lepton charged current coupling constants:

$$\frac{g_e}{g_\mu} = \sqrt{\frac{B(\tau \to e\nu\nu)}{B(\tau \to \mu\nu\nu)} \frac{(1 + C_{\tau\mu})}{(1 + C_{\tau e})}} = 0.9997 \pm 0.0024 \qquad (1)$$

$$\frac{g_\mu}{g_\tau} = \sqrt{\frac{(1 + C_{\tau e})}{(1 + C_{\mu e})} \frac{\tau_\tau}{\tau_\mu} (\frac{m_\tau}{m_\mu})^5 \frac{1}{B(\tau \to e\nu\nu)}} = 0.9980 \pm 0.0022, \qquad (2)$$

where $C_{\tau e} = -0.004$, $C_{\tau\mu} = -0.0313$ and $C_{\mu e} = -0.0044$ are radiative corrections. No significant deviation from SM is observed.

The subject which is still in *to do* list of both experiments is a search of CP-violation in tau decays. While no such CP-violation is expected in SM, other contribution, like e.g. charged Higgs exchange can result in non-negligible effect in angular and visible mass distributions of tau decay products due to interference of vector and scalar parts. CLEO has searched for such effect in the decays $\tau \to K^0_S \pi\nu$ [8] and $\tau \to \pi\pi^0\nu$ [9] with 13.3 fb^{-1}. While no signal was found, the CLEO collaboration has put limits on imaginary part of charged Higgs coupling of $-0.172 < Im(\Lambda) < 0.067$ from $\tau^- \to K^0_S \pi^- \nu$ data assuming $K^*(1430)$ scalar contribution and $-0.046 < Im(\Lambda) < 0.022$ from $\tau \to \pi\pi^0\nu$ for maximal scalar contribution. The limits are at 90% CL. The largest source of the uncertainty here is the size of the sample recorded. Given

that B-factories have almost two orders of magnitude more data, it should be possible to improve CLEO result significantly. It is clear, however, that the understanding of the systematic uncertainty will require a careful work, in particular, study of possible charge asymmetry in the detector.

Of course, there are more SM tests to be performed, such as measurement of tau electric and anomalous magnetic dipole moments, Michael parameters, measurement of ν_τ helicity. However, it is unlikely, that either BaBar or Belle will be able to improve previous measurements soon.

3 Study of hadronic tau decays

Due to simplicity of the SM tau decays involving W^- exchange, it is possible to study the hadronization process in details. All hadronic tau decays are of interest, starting from the most common 1-prong $\tau \to \pi\pi^0\nu$ up to not yet observed 7-prong tau decay. The analysis of spectral function of $\pi\pi^0$ is to be used for comparing the measurement of anomalous magnetic moment of muon with SM prediction. The analysis of tau strange decays provides an information on mass of strange quark and $|V_{us}|$ element of CKM matrix. The 5-prong tau decays are studied with large statistics and not observed 7-prong decays are used to probe non-SM contributions.

3.1 Non-strange spectral function

The calculation of hadronic part of the anomalous magnetic moment of muon $a_\mu^{had,LO}$ includes integral of the cross-section $e^+e^- \to$ hadrons multiplied with QED kernel $K(s)$. The structure of $K(s)$ is such, that 75% of $a_\mu^{had,LO}$ is covered by two pion final state dominated by $\rho(770)$ resonance. Assuming isospin invariance, $\sigma(e^+e^- \to \pi^+\pi^-)$ can be estimated from the branching fraction $B(\tau^- \to \pi^-\pi^0\nu)$ [10]. Currently, the results based on tau data together with results of Muon g-2 experiment [4] give $a_\mu^{exp} - a_\mu^{SM} = (9.4 \pm 10.5) \cdot 10^{-10}$, while calculation based solely on e^+e^- data is $a_\mu^{exp} - a_\mu^{SM} = (25.2 \pm 9.2) \cdot 10^{-10}$ [10]. Belle has recently presented new preliminary study of $\tau \to \pi\pi^0\nu$ decay [11]. The measured $\pi^-\pi^0$ invariant mass spectrum is corrected for the detector deficiency and distortions using the unfolding technique and then fitted with Gounaris-Sakurai function as shown on Fig. 1a. The distribution also exposes ρ'' resonance, evident in this decay for the first time. The obtained $\pi\pi$

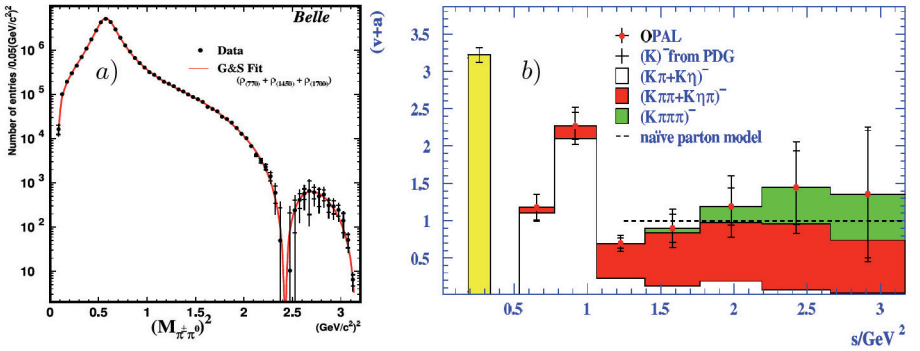

Figure 1: *a) Fully corrected* $m^2_{\pi\pi^0}$ *distribution for* $\tau \to \pi\pi^0\nu$. *The solid curve is the result of a fit to the Gounaris-Sakurai model with* $\rho(770)$, $\rho'(1450)$ *and* $\rho''(1770)$ *resonances. b) The spectral function from strange tau decays. The dots show the inclusive spectrum as measured in OPAL* [13]. *The histograms show exclusive spectra as described on the plot.*

contribution to a_μ is $a_\mu^{\pi\pi} = (462.4 \pm 0.6_{stat} \pm 3.2_{sys} \pm 2.3_{isospin}) \cdot 10^{-10}$, which yields $a_\mu^{exp} - a_\mu^{SM} = (11.0 \pm 10.5) \cdot 10^{-10}$, in good agreement with ALEPH and CLEO data. Although, only 72 fb^{-1} were used in this analysis, the systematic uncertainties, such as on the track and π^0 reconstruction efficiency, dominate and it is unlikely to be improved with larger statistics.

3.2 Strange spectral function

Analysis of strange tau decays allows to extract mass of strange quark m_s and $|V_{us}|$ element of CKM matrix via moments of the strange spectral function (SSF):

$$R_\tau^{kl} = \int_0^{M_\tau^2} ds(1 - \frac{s}{m_\tau^2})^k (\frac{s}{m_\tau^2})^l \frac{B(\tau \to X^{(S=-1)}\nu)}{B(\tau \to e\nu\nu)} \frac{dN_{X^{(S=-1)}}}{N_{X^{(S=-1)}} ds}. \qquad (3)$$

R_τ^{kl} are calculable within operator product expansion framework with phenomenological hadronic parametrization [12].

The $R_\tau^{(0,0)}$ moment is most sensitive to the $|V_{us}|$, while its dependence on m_s is small and can be neglected [12]. This allows to extract $|V_{us}| = 0.2208 \pm 0.0033_{exp} \pm 0.0009_{th}$ from results of OPAL [13] assuming $m_s(2\text{GeV}) = 95$ MeV. The value is already very competitive with the estimate from $K \to \pi e\nu$ decays

$|V_{us}| = 0.2200 \pm 0.0026$ [14] and unlike in $K \to \pi e \nu$ case the theoretical uncertainty is significantly smaller than experimental. Higher order moments are more sensitive to the m_s and one extracts $m_s(2\text{GeV}) = (81 \pm 22)$ MeV from the same data. The authors of [12] anticipate simultaneous extraction of m_s and $|V_{us}|$ from the data in future.

The OPAL result is largely statistics limited with total of 162 thousands of identified tau events. While there is only a preliminary result from BaBar on $B(\tau \to K\pi^0\nu) = (4.38 \pm 0.04_{stat} \pm 0.22_{sys}) \cdot 10^{-3}$ available, one can expect a significant improvement of knowledge of SSF from B-factories. The statistical uncertainties is very small, and systematic uncertainties are largely correlated for different $\tau \to X^{(S=-1)}\nu$ exclusive channels, and the measurement is expected to be few times more precises than current PDG value of $B(\tau \to X^{(S=-1)}\nu) = (29.1 \pm 0.8) \cdot 10^{-3}$ [14].

3.3 5- and 7-prong tau decays

With such big sample at hand, one can look into underlying structure of rare tau decays. BaBar has recently published a study of 5-prong decays $\tau^- \to 3h^-2h^+\nu$ [15]. The branching fraction is $(8.56 \pm 0.05 \pm 0.42) \cdot 10^{-4}$ in agreement with previous measurements [14]. However, the invariant mass of five hadrons is different from the phase-space distribution assumed before (see Fig. 2). The contribution of ρ meson is evident in the mass of two pion, and f_1 resonance is observed in the four pion mass distribution, $B(\tau^- \to f_1 h^- \nu_\tau) = (3.9 \pm 0.7 \pm 0.5) \cdot 10^{-4}$ [15]. BaBar has also searched for 7-prong tau decays. If observed, they would signal of non-SM contribution, as SM predicts $B(\tau^- \to 4\pi^- 3\pi^+ \nu) < 10^{-9}$. No signal is found in either exclusive or inclusive 7-prong tau decays and the obtained upper limits are

$$\begin{array}{lcl} B(\tau^- \to 4\pi^- 3\pi^+ (\pi^0)\nu_\tau) & < & 3.0 \cdot 10^{-7} \\ B(\tau^- \to 4\pi^- 3\pi^+ \nu_\tau) & < & 4.3 \cdot 10^{-7} \\ B(\tau^- \to 4\pi^- 3\pi^+ \pi^0 \nu_\tau) & < & 2.5 \cdot 10^{-7} \end{array} \qquad (4)$$

at 90% CL [16]. 232 fb^{-1} is used in both analyzes.

4 Searches for Lepton Flavor Violation

One of the most interesting question in tau physics now is there a sizable lepton flavor violation (LFV) or not. Given the observation of neutrino oscillation by

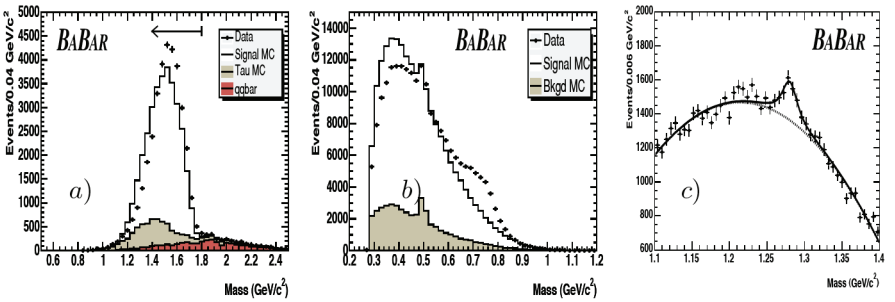

Figure 2: *Invariant mass of a) five charged particles b) h^+h^- pairs c) $2h^+2h^-$ combinations. All tracks are taken as pions. The points are the data and the histograms are the Monte Carlo simulation. The unshaded and shaded histograms are the signal and background events, respectively. The Monte Carlo sample is normalized to the luminosity of the data sample. The solid line on plot c is a fit to the data.*

experiment [17], one expects charged LFV even in Standard Model extended with massive neutrinos. However, the expected branching fractions are negligible and far beyond reach of the current experiments. From other side, many other extensions of SM, e.g. supersymmetry, predict LFV on the level of $10^{-10} - 10^{-7}$ [18], which can be probed with currently accumulated statistics. Analysis of different channels is important. While $\tau \to \mu\gamma$ is expected to be the largest tau LFV decay in most models, $\tau \to 3\ell$ can expose supersymmetric Higgs contribution [19], and $\tau^- \to \ell^+ h^- h^-$ violates not only lepton flavor, but also lepton number. If LFV process would be observed in an experiment, the combined analysis of different channels will allow to understand underlying mechanism and to differentiate between the models.

Both BaBar and Belle are very active in searches of lepton flavor violation. Unfortunately, no signal is found in any channel and upper limits are set on the level of 10^{-7} (see table 1). Both experiments plan to increase their samples by factor of 2 by 2008.

The obtained limits can already be used to restrict parameter space of the models. The Fig 3a [21] shows the exclusion plot for mSUGRA with right handed neutrinos as function of gaugino ($m_{1/2}$) and scalar (m_0) masses at grand unification scale $m_{GUT} = 5 \cdot 10^{15}$ GeV for $\tan\beta = 50$. The latest measurements

Table 1: *90% CL upper limits on LFV tau decays obtained by B-factories* [20]. *Numbers given in* 10^{-7} *units.*

	BaBar		Belle	
$\tau^- \to \mu^-\gamma$	0.7	232 fb^{-1}	3.1	86 fb^{-1}
$\tau^- \to e^-\gamma$	1.1	232 fb^{-1}	3.9	87 fb^{-1}
$\tau^- \to e^-e^+e^-$	2.0	91 fb^{-1}	3.5	87 fb^{-1}
$\tau^- \to \mu^-\mu^+\mu^-$	1.9	91 fb^{-1}	2.0	87 fb^{-1}
$\tau^- \to \ell^-\ell^\pm\ell'^\mp$	(1-3)	91 fb^{-1}	(2-4)	87 fb^{-1}
$\tau^- \to \ell^-h^+h^-$	(1-3)	221 fb^{-1}		
$\tau^- \to \ell^+h^-h^-$	(0.7-5)	221 fb^{-1}		
$\tau^- \to \ell^-\pi^0, \eta, \eta'$			2-10	154 fb^{-1}
$\tau^- \to \Lambda\pi^-$			0.7	154 fb^{-1}
$\tau^- \to \bar{\Lambda}\pi^-$			1.4	154 fb^{-1}

of neutrino mixing matrix and masses [22] are used for Yukawa couplings. The mass of right handed neutrinos is set to $M_{\nu_R} = 5 \cdot 10^{14}$ and normal hierarchy is assumed for left handed neutrinos. Everything but a green area is excluded by theory or cold dark matter density measurement, while the area below blue curves (towards center of coordinates) is excluded by tau LFV searches. The blue curves from center of coordinates onwards correspond to the $6.8 \cdot 10^{-8}$, $1 \cdot 10^{-8}$ and $1 \cdot 10^{-9}$. One can expect that by 2008 the combined sensitivity of BaBar and Belle will reach $1 \cdot 10^{-8}$ level, while running super-B factory will be necessary to reach $1 \cdot 10^{-9}$ level.

Figure 3b [21] shows the upper limits set on off-diagonal elements of slepton mixing matrix M^2_{L23}/M^2_{L22} (*model independent approach*) as function of m_0 for $\tan\beta = 50$ and $m_{1/2} = 100 + 0.8 \cdot m_0$. The uppermost curve corresponds to $6.8 \cdot 10^{-8}$, followed by curves of $5 \cdot 10^{-8}$, $2 \cdot 10^{-8}$ and $1 \cdot 10^{-8}$.

5 Conclusions

Current B-factories have a large and interesting program to study tau physics. The accumulated statistics reaches 10^9 tau decays which allows very precise measurements and searches of very rare or forbidden tau decays. Among the most important measurements are mass and tau lifetime (systematics limited) and tests of CPT/CP violation (statistics limited). The study of the spectral

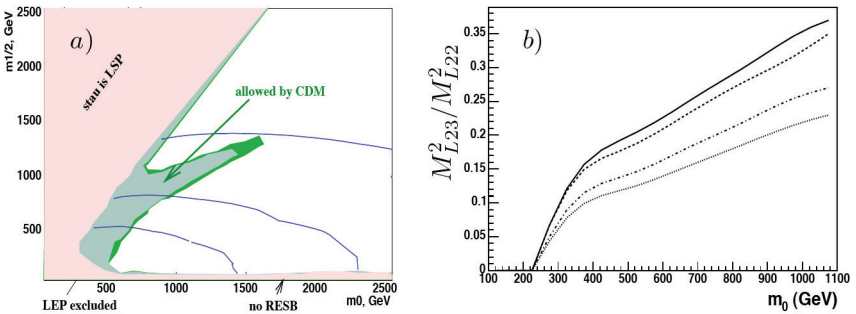

Figure 3: *a) Exclusion plot of mSUGRA with right handed neutrinos as function of gaugino ($m_{1/2}$) and scalar (m_0) masses for* $\tan\beta = 50$. *The green area is allowed by cold dark matter searches and blue curves show area excluded by* $\tau \to \mu\gamma$ *as described in the text. b) Model independent upper limits of off-diagonal element of slepton mixing matrix* M^2_{L23}/M^2_{L22} *as function of* m_0 *from* $B(\tau \to \mu\gamma)$ *as described in the text.*

function of $\tau \to \pi\pi^0\nu$ decay would help to clarify the comparison of measurement of anomalous magnetic moment of muon with its SM prediction, while strange spectral functions are to be used for m_s and $|V_{us}|$ estimates.

Among very interesting studies are searches of lepton flavor violation tau decays. While BaBar and Belle can be lucky to discover LFV and this way to probe the physics beyond Standard Model, one would need statistics of super-B factory to be able to measure mixing of sleptons accurately.

References

1. B. Aubert *et al.* [BABAR Coll.], Nucl. Instrum. Meth. A **479**, 1 (2002)
2. A. Abashian *et al.* [BELLE Coll.], Nucl. Instrum. Meth. A **479**, 117 (2002).
3. J. Z. Bai *et al.* [BES Coll.], Phys. Rev. D **53**, 20 (1996).
4. G. W. Bennett *et al.* [Muon g-2 Coll.], Phys. Rev. Lett. **89**, 101804 (2002)
5. K. Abe *et al.* [BELLE Coll.], arXiv:hep-ex/0511038.
6. H. Albrecht *et al.* [ARGUS Coll.], Phys. Lett. B **292**, 221 (1992).

7. A. Lusiani *et al.* [BABAR Coll.], Nucl. Phys. Proc. Suppl. **144**, 105 (2005).

8. G. Bonvicini *et al.* [CLEO Coll.], Phys. Rev. Lett. **88**, 111803 (2002)

9. P. Avery *et al.* [CLEO Coll.], Phys. Rev. D **64**, 092005 (2001)

10. M. Davier *et al.*, Eur. Phys. J. C **27**, 497 (2003)

11. K. Abe *et al.* [BELLE Coll.], arXiv:hep-ex/0512071

12. E. Gamiz *et al.*, Nucl. Phys. Proc. Suppl. **144**, 59 (2005)

13. G. Abbiendi *et al.* [OPAL Coll.], Eur. Phys. J. C **35**, 437 (2004)

14. S. Eidelman *et al.*, Phys. Lett. B **592**, 1 (2004)

15. B. Aubert *et al.* [BABAR Coll.s], Phys. Rev. D **72**, 072001 (2005)

16. B. Aubert *et al.* [BABAR Coll.], Phys. Rev. D **72**, 012003 (2005)

17. K. Eguchi *et al.* [KamLAND Coll.], Phys. Rev. Lett. **90**, 021802 (2003); Q. R. Ahmad *et al.* [SNO Coll.], Phys. Rev. Lett. **89**, 011301 (2002); Y. Fukuda *et al.* [Super-Kamiokande Coll.], Phys. Rev. Lett. **81**, 1562 (1998)

18. E. Ma, Nucl. Phys. Proc. Suppl. **123**, 125 (2003)

19. K. S. Babu and C. Kolda, Phys. Rev. Lett. **89**, 241802 (2002)

20. B. Aubert *et al.* [BABAR Coll.], Phys. Rev. Lett. **95**, 041802 (2005); Phys. Rev. Lett. **96**, 041801 (2006) Phys. Rev. Lett. **92**, 121801 (2004); Phys. Rev. Lett. **95**, 191801 (2005)

    K. Abe *et al.* [BELLE Coll.], Phys. Rev. Lett. **92**, 171802 (2004); K. Hayasaka *et al.*, Phys. Lett. B **613**, 20 (2005); Y. Yusa *et al.* [BELLE Coll.], Phys. Lett. B **589**, 103 (2004); arXiv:hep-ex/0603036. Y. Enari *et al.* [BELLE Coll.], Phys. Lett. B **622**, 218 (2005) Y. Miyazaki *et al.* [BELLE Coll.], Phys. Lett. B **632**, 51 (2006);

21. O. Igonkina,The 13th International Conference on Supersymmetry and Unification of Fundamental Interactions, (Durham, UK), Jul 18-23, 2005

22. M. C. Gonzalez-Garcia, arXiv:hep-ph/0410030

Frascati Physics Series Vol. XLI (2006), pp. 275-284
DISCOVERIES IN FLAVOUR PHYSICS AT e^+e^- COLLIDERS
Frascati, February 28th - March 3rd, 2006

EDM AND CPV IN THE τ-SYSTEM

G. A. González-Sprinberg
Facultad de Ciencias, Universidad de la República,
Iguá 4225, 11400 Montevideo, Uruguay
J.Bernabéu and J.Vidal
Departament de Física Teòrica Universitat de València,
E-46100 Burjassot, València, Spain
and
IFIC, Centre Mixt Universitat de València-CSIC, València, Spain

Abstract

The new proposals for high statistics at B/Flavor factories allow a detailed investigation of CP-odd observables related to the τ-pair production. In particular, stringent bounds on the tau electric dipole moment can be obtained. We review some already published results in spin-spin correlations at low energy and we show that new CP-odd asymmetry observables, associated to the normal polarization term, can be measured at these low energy accelerators, both at resonant and non resonant energies. The cases for unpolarized and longitudinal polarized electron beams are analyzed in detail.[1]

1 Introduction

The time reversal odd electric dipole moment (EDM) of the τ is the source of CP violation in the τ-pair production vertex. In the framework of local

[1]Invited talk, speaker G.A.G-S., email: gabrielg@fisica.edu.uy

quantum field theories the CPT theorem states that CP violation is equivalent to T violation. While the electric dipole moments (EDM) of the electron and muon have been extensively investigated both in experiment and theory, the case of the tau is somewhat different, both from the theoretical and experimental point of view. The Standard Model prediction for the τ-EDM is a 4-loops effect and can be estimated to be of the order of $10^{-33} - 10^{-34}\, e\, cm$. Besides, the tau lepton has a relatively high mass: this means that tau lepton physics is expected to be more sensitive to contributions coming from high energy scales and new physics. Furthermore, the tau decays into hadrons, so different techniques to those for the (stable) electron or muon case are needed in order to measure the dipole moments. There are very precise bounds on the EDM magnitude of nucleons and leptons, and the most precise one is the electron EDM, $d_\gamma^e = (0.07 \pm 0.07) \times 10^{-26}\ e\ cm$, while the looser one is the τ EDM [1], $-0.22\, e\, cm < Re(d_\gamma^\tau) \times 10^{16} < 0.45\, e\, cm$. The dipole moments flip chirality and therefore they may provide some insight into the mass mechanism of the underlying theory. CP-odd observables related to the EDM would not receive an appreciable contribution from the standard model and any experimental signal should be identified with beyond the standard model physics. Following the ideas of [2] and [3], the tau weak-EDM has been studied [4, 5] at high energies in CP-odd observables sensitive to spin linear terms and spin-spin correlations respectively. In [6] the sensitivity to the WEDM is also studied in the tau-charm-factories, for polarized electrons, using spin-spin correlation observables. While most of the statistics for the tau pair production was dominated by high energy physics, mainly at LEP, nowadays the situation has changed. High luminosity B factories and their upgrades at resonant energies (Υ thresholds) have the largest τ pair samples. Besides, the possibility of a polarized beam opens the possibility of studying new observables. In this note we review the tau EDM at low energies (section 2) the low energy spin correlations observables (section 3) studied in [7] and we introduce new observables (section 4) that may be measured in the future at polarized beam facilities. We conclude with some remarks on the CPV physics in the tau system at Super B or Super Flavor factories.

2 τ EDM at Low Energies

The standard model describes with high accuracy most of the physics found in present experiments. Deviations from the standard model, at low energies, can be parameterized by an effective Lagrangian built with the standard model symmetry and particle spectrum, having as zero order term just the standard model Lagrangian, and containing higher dimension gauge invariant operators suppressed by the scale of new physics [8]. The leading non-standard CP-odd effects come from dimension six operators, that at low energy can be written as the effective chirality-flip operators corresponding to the WEDM and EDM (more details in [7]):

$$\mathcal{L}_{eff}^{\gamma,Z} = -id_{\gamma}^{\tau}\,\overline{\tau}\sigma_{\mu\nu}\gamma^{5}\tau F^{\mu\nu} - id_{Z}^{\tau}\,\overline{\tau}\sigma_{\mu\nu}\gamma^{5}\tau Z^{\mu\nu} \quad (1)$$

where $F_{\mu\nu} = \partial_{\mu}A_{\nu} - \partial_{\nu}A_{\mu}$ and $Z_{\mu\nu} = \partial_{\mu}Z_{\nu} - \partial_{\nu}Z_{\mu}$ are the abelian field strength tensors of the photon and Z gauge boson, respectively.

The $e^{+}e^{-} \longrightarrow \tau^{+}\tau^{-}$ cross section has contributions coming from the standard model and the effective Lagrangian Eq.(1). At low energies the tree level contributions come from γ or Υ exchange (at the Υ peak) in the s-channel. The interference with the Z-exchange ($\gamma - Z$, $\Upsilon - Z$ at the Υ peak) and the $Z-Z$ diagrams are suppressed by powers of $\left(q^{2}/M_{Z}^{2}\right)$. The tree level contributing diagrams are shown in Fig.1 where diagrams (a) and (b) are standard model contributions, and (c)and (d) come from beyond the standard model terms in the Lagrangian.

3 Unpolarized beams observables

Following the notation of reference [7], we now discuss CP-odd low energy observables related to the EDM. For unpolarized beams and at low energies the EDM gives contributions to leading order in the Normal-Transverse and Normal-Longitudinal correlation terms of the $e^{+}e^{-} \longrightarrow \tau^{+}(s_{+})\tau^{-}(s_{-})$ differential cross section. Polarization along the directions x, y, z correspond to what is called transverse (T), normal (N) and longitudinal (L) polarizations, respectively.

We consider the τ-pair production in $e^{+}e^{-}$ collisions through direct γ exchange (diagrams (a) and (c) in Fig. 1.). As will be discuss later, the results of this section still hold for resonant Υ production. For the tau production

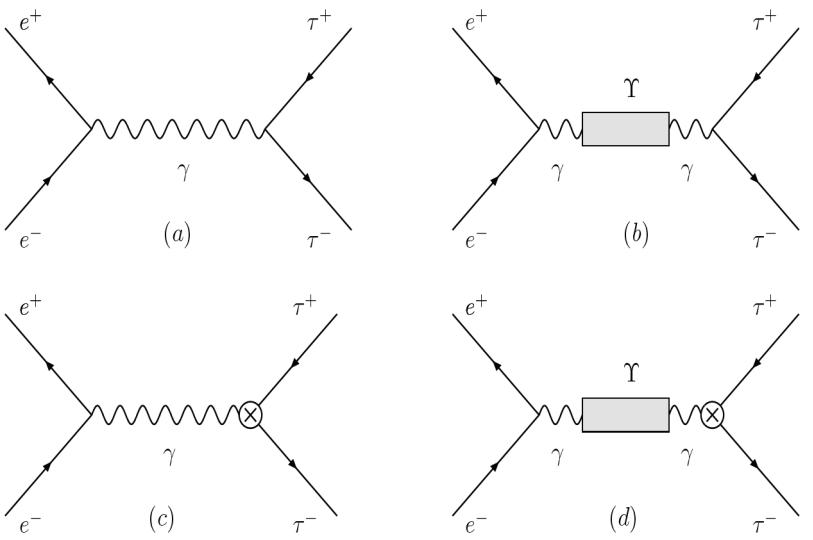

Figure 1: *Diagrams: (a) direct γ-exchange, (b) Υ-production, (c) EDM in γ-exchange, (d) EDM in Υ-production.*

plane and direction of flight fully reconstructed, as it is the case if both τ's decay semileptonically, all the production angles can be determined [9].

The normal -to the scattering plane- polarization (P_N) of each tau is the only component which is T-odd. For a CP-violating interaction, such as an EDM, the $(s_+ - s_-)_N$ CP-odd term gets a non-vanishing value without the need of absorptive parts. As P_N is even under parity (P) symmetry, a linear observable in the EDM can not receive contribution from only γ or Υ exchange. Therefore, there is no contribution to the single normal polarization (P_N) of the tau at this level. As a consequence, for unpolarized beams, only the spin-spin correlation observables of both taus may have sensitivity to the EDM. The T-odd, P-odd Normal-Transverse $(\overrightarrow{s}_+ \times \overrightarrow{s}_-)_{NT}$ and Normal-Longitudinal $(\overrightarrow{s}_+ \times \overrightarrow{s}_-)_{NL}$ spin correlation terms (antisymmetric $y - x$ and $y - z$ terms respectively) will be proportional to the EDM term interfering with photon

exchange. The spin-spin correlation terms in the differential cross section for τ pair production are:

$$\begin{aligned}\frac{d\sigma^{SS}}{d\Omega_{\tau^-}} &= \frac{\alpha^2}{16s}\beta\left(s_+^x s_-^x C_{xx} + s_+^y s_-^y C_{yy} + s_+^z s_-^z C_{zz} + \right.\\ &(s_+^x s_-^y + s_+^y s_-^x)C_{xy}^+ + (s_+^x s_-^z + s_+^z s_-^x)C_{xz}^+ + (s_+^y s_-^z + s_+^z s_-^y)C_{yz}^+ + \\ &\left.(\overrightarrow{s}_+ \times \overrightarrow{s}_-)_x C_{yz}^- + (\overrightarrow{s}_+ \times \overrightarrow{s}_-)_y C_{xz}^- + (\overrightarrow{s}_+ \times \overrightarrow{s}_-)_z C_{xy}^-\right) \qquad (2)\end{aligned}$$

where

$$\begin{aligned} C_{xx} &= (2-\beta^2)\sin^2\theta_{\tau^-} & C_{yy} &= -\beta^2\,\sin^2\theta_{\tau^-} \\ C_{zz} &= (\beta^2 + (2-\beta^2)\cos^2\theta_{\tau^-}) & C_{xy}^- &= 2\beta\left(\sin^2\theta_{\tau^-}\right)\frac{2m_\tau}{e}\,d_\tau^\gamma \qquad (3)\\ C_{yz}^- &= -\gamma\beta\left(\sin(2\theta_{\tau^-})\right)\frac{2m_\tau}{e}\,d_\tau^\gamma & C_{xz}^+ &= \tfrac{1}{\gamma}\sin(2\theta_{\tau^-}) \end{aligned}$$

and $C_{xy}^+ = C_{yz}^+ = C_{xz}^- = 0$. C_{xy}^+ and C_{yz}^+ are zero in our hypothesis. They are CP-even and P-odd but for photon exchange there is no source of P violation to produce these terms. C_{xz}^- is zero because it is CP-odd and P-even, while the EDM in interference with photon exchange would be CP-odd but P-odd instead, and cannot contribute. The complete cross section for the process $e^+e^- \to \gamma \to \tau^+\tau^- \to h^+\bar{\nu}_\tau h^-\nu_\tau$ can be written as a function of the kinematical variables of the hadrons into which each tau decays [10] as:

$$\begin{aligned} d\sigma\left(e^+e^- \to \gamma \to \tau^+\tau^- \to h^+\bar{\nu}_\tau h^-\nu_\tau\right) &= 4\,d\sigma\left(e^+e^- \to \tau^+(\overrightarrow{n}_+^*)\,\tau^-(\overrightarrow{n}_-^*)\right) \\ \times Br(\tau^+ \to h^+\bar{\nu}_\tau)Br(\tau^- \to h^-\nu_\tau)&\frac{d\Omega_{h^+}}{4\pi}\,\frac{d\Omega_{h^-}}{4\pi} \qquad (4)\end{aligned}$$

with

$$\overrightarrow{n}_\pm^* = \mp\alpha_\pm\frac{\overrightarrow{q}_\pm^*}{|\overrightarrow{q}_\pm^*|} = \mp\alpha_\pm(\sin\theta_\pm^*\,\cos\phi_\pm, \sin\theta_\pm^*\,\sin\phi_\pm, \cos\theta_\pm^*) \qquad (5)$$

$\alpha_\pm$ are the polarization parameters of the τ decay and $\overrightarrow{q}_\pm^*$ are the momenta of the hadrons with moduli fixed to $P_\pm = \dfrac{m_\tau^2 - m_{h^\pm}^2}{2m_\tau}$. The $*$ means that all affected quantities are given in the respective τ-at-rest reference frame.

We now show how to get an observable proportional to the EDM term from the NT correlation. Taking into account that the angular dependence of each correlation term is unique, it is this particular dependence that allows to select one of the correlation terms in the cross section. Indeed, it is by

a combination of an integration on the hadronic angles plus, eventually, an integration on the θ_{τ^-} angle, that one can select a polarization or correlation term, and there, the contribution of the EDM.

For the NT term, for example, this works as follows. The integration over the τ^- variables $d\Omega_{\tau^-}$ erases all the information on the EDM in the Normal-Longitudinal (C_{zy}^-) correlation, together with the C_{xz}^+ term of the cross section. Integrating in all angles except the hadron azimuthal angles we get:

$$\begin{aligned}\frac{d^2\sigma^{SS}}{d\phi_- d\phi_+} &= -\frac{\pi\alpha^2\beta}{96s}\,(\alpha_-\,\alpha_+)\;Br(\tau^+\to h^+\bar{\nu}_\tau)Br(\tau^-\to h^-\nu_\tau)\times \\ &\Big[(2-\beta^2)\cos(\phi_-)\;\cos(\phi_+)-\beta^2\,\sin(\phi_-)\;\sin(\phi_+)+ \\ &2\beta\,\sin(\phi_-^*-\phi_+^*)\,\frac{2m_\tau}{e}\,d_\tau^\gamma\Big] \qquad (6)\end{aligned}$$

Now, to get an observable related to the EDM in the NT correlation we define the azimuthal asymmetry:

$$A_{NT}=\frac{\sigma_{NT}^+-\sigma_{NT}^-}{\sigma_{NT}^++\sigma_{NT}^-} \qquad (7)$$

where

$$\sigma_{NT}^\pm=\int_{w\gtrless 0}\frac{d^2\sigma}{d\phi_-\,d\phi_+}\,d\phi_-\,d\phi_+\;,\quad \text{with}\qquad w=\sin(\phi_--\phi_+) \qquad (8)$$

Finally, the Normal-Transverse correlation azimuthal asymmetry is:

$$A_{NT}=-\alpha_-\alpha_+\,\frac{\pi\beta}{4(3-\beta^2)}\,\frac{2m_\tau}{e}\,d_\tau^\gamma \qquad (9)$$

All other terms in the cross section are eliminated when we integrate in the way we have shown above. Thus, the only source for this azimuthal asymmetry is exactly the term C_{xy}^- we are interested in. We have a genuine CP-odd Normal-Transverse correlation observable which is directly proportional to the EDM.

For the normal-longitudinal correlation term we can also define a different observable, and for the details we refer to [7], where this is discussed in detail. Besides, some observables related to the imaginary part of the EDM have also been studied in this approach. Although of not much theoretical interest, because a non zero imaginary part for the EDM comes from very low mass new particles, not found up to now in other experiments, these observables open the possibility to study CPT violation observables in the tau system.

4 Polarized beams observables

EDM leading order effects can also be studied in the angular distribution of the $e^+e^- \longrightarrow \tau^+(s_+)\tau^-(s_-)$ differential cross section for a longitudinal polarized electron beam. The complete results and more details will be published elsewhere [12].

As we have already discuss, the normal polarization (P_N) of each tau is the only component which is T-odd. While P_N is even under parity (P) symmetry, the observable sensitive to the EDM should need, in addition to d_γ^τ, a P-odd contribution coming from a longitudinal polarized electrons term.

The EDM contributes to leading order to the single normal polarization terms in the $e^+e^- \longrightarrow \tau^+(s_+)\tau^-(s_-)$ differential cross section. The main results for τ-pair production in e^+e^- collisions through direct γ-exchange (diagrams (a) and (c) in Fig. 1.) still hold for resonant Υ production. In the differential cross section the term $\dfrac{d\sigma^S}{d\Omega_{\tau^-}}$ is the one that is linear in the tau spin variables and has sensitivity to the EDM (in the normal polarization). We now show how to get an observable proportional to the EDM term from the Normal polarization of a single tau. The linear tau spin terms depend on several angles and it is by an integration on the production θ_{τ^-} angle, followed by a dedicated integration on the hadronic angles, that one can select a polarization term and there, the contribution of the EDM.

For the single *tau* normal polarization, subtracting for opposite helicities of the incoming e^- and performing a convenient integration over the hadron variables, we get sensitivity to the EDM (d_τ^γ) by defining the following normal polarization azimuthal asymmetry:

$$A_N^{\mp} = \frac{\sigma_L^{\mp} - \sigma_R^{\mp}}{\sigma} \simeq \gamma\beta \frac{2m_\tau}{e}\, d_\tau^\gamma \tag{10}$$

where

$$\sigma_L^{\mp} = \int_0^{2\pi} d\phi_\pm \left[\int_0^{\pi} d\phi_\mp \left. \frac{d^2\sigma^S}{d\phi_- d\phi_+} \right|_{Pol(e^-)} \right] \tag{11}$$

$$\sigma_R^{\mp} = \int_0^{2\pi} d\phi_\pm \left[\int_\pi^{2\pi} d\phi_\mp \left. \frac{d^2\sigma^S}{d\phi_- d\phi_+} \right|_{Pol(e^-)} \right] \tag{12}$$

Notice that all other terms in the cross section are eliminated when we integrate in the convenient way.

5 Observables at the Υ resonances

As discussed in [7, 12], all these ideas can be applied for polarized or unpolarized electron beams in e^+e^- collisions at the Υ peak, where the τ pair production is mediated by the resonance. We assume that the resonant diagrams (b) and (d) of Fig. 1. dominate the process on the Υ peaks.

The amplitudes A_b and A_d for the tau pair production diagrams (see Fig. 1.) at the Υ-peak can be related to those of the direct production (A_a and A_c) as:

$$A_{\binom{b}{d}} = A_{\binom{a}{c}} \cdot H(s)\,, \quad \text{with} \quad H(s) \equiv \frac{4\pi\alpha Q_b^2}{s}\,|F_\Upsilon(s)|^2\,P_\Upsilon(s)\,, \qquad (13)$$

so that the tau pair production at the Υ peak introduces the same tau polarization matrix terms as the direct production with γ exchange (diagrams (a) and (c)). The only difference is the overall factor $|H(s)|^2$ introduced in the cross section which is responsible for the enhancement at the resonant energies, with $H(M_\Upsilon^2) = -i\,\frac{3}{\alpha}Br\,(\Upsilon \to e^+e^-)$.

Then, at the Υ-peak, the interference of diagrams (a) and (d) plus the interference of diagrams (b) and (c) is exactly zero and the same for the interference of diagrams (a) and (b). Finally, the only contributions with EDM in polarization terms come with the interference of diagrams (b) and (d), while diagram (b) squared gives the leading contribution to the cross section.

Finally, we obtain no changes in the asymmetries, and the expression of all the observables remain the same.

6 Bounds on the EDM

We can now estimate the bounds on the EDM that can be achieved using these observables. For numerical results we assume a set of data of 5×10^{10} tau pairs produced at high statistics factories. We also consider the $\pi^\pm\ \bar{\nu_\tau}$ or $\rho^\pm\ \bar{\nu_\tau}$ (*i.e.* $h_1,\ h_2 = \pi,\ \rho$) decay channels for the traced $\tau^\pm$, while we sum up over $\pi^\mp\ \nu_\tau$ and $\rho^\mp\ \nu_\tau$ hadronic decay channels for the non traced $\tau^\mp$.

The bounds for the observables of section 2 are [7]:

NT asymmetry and $\pi^\pm$ *tau* decay channel: $|d_\tau^\gamma| < \{\ 7 \times 10^{-19}\ e\,cm \quad (14)$

NL asymmetry and $\pi^\pm$ *tau* decay channel: $|d_\tau^\gamma| < \{\ 1.7 \times 10^{-16}\ e\,cm \quad (15)$

For the imaginary part of the EDM the bounds of [7] are also of the order $10^{-19}\ e\,cm$.

The preliminary bounds one gets from the polarized observables for the EDM are:

$$|d_\tau^\gamma| \leq 8\ 10^{-20}\ e\,cm \quad \text{for the } \pi \text{ channel} \tag{16}$$

$$|d_\tau^\gamma| \leq 1\ 10^{-19}\ e\,cm \quad \text{for the } \rho \text{ channel} \tag{17}$$

A combined analysis of all possible channel will lower these bounds by an important figure. The high statistics of a high luminosity facility would improve the present PDG bounds by two orders of magnitude.

7 Conclusions

To summarize, we would like to point out that:

- low energy observables, as defined in this paper, are different and complementary to the high energy ones studied in the past,
- polarized electrons beams allow to put bounds on the EDM looking at single tau polarization observables,
- these bounds are closer to the prediction of many extended models [11],
- high resolution in the determination of the production vertex by means of micro-vertex detectors allows a detailed treatment of the data, avoiding statistical methods that are usually used in order to resolve the two-fold ambiguity in the determination of the tau reference.

8 Acknowledgements

The speaker (G.G-S.) would like to thank the organizers for a very interesting Workshop and for the opportunity they have given to me to participate. This work has been supported by MEC and FEDER, under the grants FPA2005-00711 and FPA2005-01678, and by Gen-ralitat Valenciana under the grant GV05/264.

References

1. S. Eidelman *et al.*, *Phys. Lett.* *B***592**, 1 (2004); K. Inami *et al.* [BELLE Collaboration], *Phys. Lett.* *B***551**, 16 (2003).

2. J. Bernabéu, G.A. González-Sprinberg and J. Vidal, *Phys. Lett. B***326**, 168 (1994).

3. W. Bernreuther, U. Low, J. P. Ma and O. Nachtmann, Z. Phys. C **43**, 117 (1989).

4. M. Acciarri *et al.* [L3 Collaboration], *Phys. Lett. B***434**, 169 (1998).

5. D. Buskulic *et al.* [ALEPH Collaboration], Phys. Lett. B **346**, 371 (1995); K. Ackerstaff *et al.* [OPAL Collaboration], Z. Phys. C **74**, 403 (1997); H.Albrecht *et al.* [ARGUS Collaboration], *Phys. Lett. B***485**, 37 (2000).

6. B. Ananthanarayan and S.D. Rindani, *Phys. Rev. D***51**, 5996 (1995).

7. J. Bernabéu, G.A. González-Sprinberg and J. Vidal, *Nucl. Phys. B***701**, 87 (2004).

8. W. Buchmuller and D. Wyler, *Nucl. Phys. B***268**, 621 (1986); C.N. Leung, S.T. Love and S. Rao, Z. Phys. C **31**, 433 1986; M. Bilenky and A. Santamaria, *Nucl. Phys. B***420**, 47 (1994).

9. J. H. Kuhn, Phys. Lett. B **313**, 458 (1993).

10. Y.S. Tsai, *Phys. Rev. D***4**, 2821 (1971).

11. T.Huang, W. Lu, Z. Tao, Phys. Rev. D **55**, 1643 (1997); W. Bernreuther, A. Brandenburg, P . Overmann, Phys. Lett. B **412**, 413 (1997), Eur. Phys. J. C **11**, 293 (1999).

12. Work in preparation.

Frascati Physics Series Vol. XLI (2006), pp. 285
DISCOVERIES IN FLAVOUR PHYSICS AT e^+e^- COLLIDERS
Frascati, February 28th - March 3rd, 2006

LEPTON FLAVOUR VIOLATION IN RARE MUON DECAYS

Donato Nicoló
Laboratori Nazionali di Frascati, Via E. Fermi 40, 00044 Frascati, Italy

Written contribution not received

BOTTOM-QUARK PHYSICS II

A. Masiero	The B–tau FCNC Connection in SUSY Unified Theories
M.E. Biagini	Challenges of High–Luminosity B-Factories
W. Wisniewski	Requirements For a Detector at the Super B-Factory
T. Nakada	Physics of B_s Mesons, Status and Perspectives
H. Yamamoto	Future Perspectives for B Physics at a Super B-Factory
T. Hurth	Rare B Decays as a Window on Physics Beyond the Standard Model
K.-F. Chen	Review of Time-Dependent *CP* Violation in $b \to s$ Transitions
A. Stocchi	Developments of CKM Fits
H. Kim	New Physics at BaBa
T.J. Orimoto	New Measurements of the angle γ from the BaBar Experiment

Frascati Physics Series Vol. XLI (2006), pp. 289-299
DISCOVERIES IN FLAVOUR PHYSICS AT e^+e^- COLLIDERS
Frascati, February 28th - March 3rd, 2006

THE B – τ FCNC CONNECTION IN SUSY UNIFIED THEORIES

A. Masiero
Univ. of Padova and INFN, Padova
P. Paradisi
Department of Physics, Technion-Israel Institute of Technology, Technion City, 32000 Haifa, Israel

Abstract

In the context of SUSY grand unification a link is established between the hadronic and leptonic soft breaking sectors. Such relation is here exploited in particular for FCNC processes in B physics. It is shown how bounds on leptonic FCNC involving the third generation translate into constraints on FC B decays. In the second part of the contribution we show that tests of lepton universality in K and B decays can represent an interesting handle to obtain relevant information on the amount of FCNC in the second and third fermion generation.

1 Grand Unification of Quark and Lepton FCNCs

Supersymmetry (SUSY) breaking (SB) remains one of the biggest issues in physics beyond the Standard Model (SM). In spite of various proposals, we still miss a realistic and theoretically satisfactory model of SB.

Flavor violating processes have been instrumental in guiding us towards consistent SB models. Indeed, even in the absence of a well-defined SB mechanism and, hence, without a precise knowledge of the SUSY lagrangian at the

electroweak scale, it is still possible to make use of the FCNC bounds to infer relevant constraints on the part of the SUSY soft breaking sector related to the sfermion mass matrices.

The model-independent method which is adopted is the so-called Mass-Insertion approximation (MIA). In this approach, the experimental limits lead to upper bounds on the parameters (or combinations of) $\delta^f_{ij} \equiv \Delta^f_{ij}/m^2_{\tilde{f}}$; where Δ^f_{ij} is the flavour-violating off-diagonal entry appearing in the $f = (u, d, l)$ sfermion mass matrices and $m^2_{\tilde{f}}$ is the average sfermion mass. The mass-insertions include the LL/LR/RL/RR types, according to the chirality of the corresponding SM fermions.

Detailed bounds on the individual δs have been derived by considering limits from various FCNC processes [1]. As long as one remains within the simple picture of the Minimal Supersymmetric Standard Model (MSSM), where quarks and leptons are unrelated, the hadronic and leptonic FCNC processes yield separate bounds on the corresponding δ^q's and δ^l's, respectively.

The situation changes when one embeds the MSSM within a Grand Unified Theory (GUT). In a SUSY GUT, quarks and leptons sit in same multiplets and are transformed into each other through GU symmetry transformations. If the supergravity lagrangian, and, in particular, its Kähler function are present at a scale larger than the GUT breaking scale, they have to fully respect the underlying gauge symmetry which is the GU symmetry itself. The subsequent SUSY breaking will give rise to the usual soft breaking terms in the lagrangian. In particular, if the mediation mechanism responsible for the transmission of the SUSY breaking to the visible sector is gravitational, the sfermion mass matrices, whose structure is dictated by the Kähler potential, will have to respect the underlying GU symmetry. Hence we expect quark-lepton correlations among entries of the sfermion mass matrices [2]. In other words, the quark-lepton unification seeps also into the SUSY breaking soft sector.

Imposition of a GU symmetry on the $\mathcal{L}_{\rm soft}$ entails relevant implications at the weak scale. This is because the flavour violating (FV) mass-insertions do not get strongly renormalized through RG scaling from the GUT scale to the weak scale in the absence of new sources of flavor violation. On the other hand, if such new sources are present, for instance due to the presence of new neutrino Yukawa couplings in SUSY GUTs with a seesaw mechanism for

neutrino masses, then one can compute the RG-induced effects in terms of these new parameters. Hence, the correlations between hadronic and leptonic flavor violating MIs survive at the weak scale to a good approximation. As for the flavor conserving (FC) mass insertions (i.e., the diagonal entries of the sfermion mass matrices), they get strongly renormalized but in a way which is RG computable.

The connection between quark and lepton δ parameters can have significant implications on flavor phenomenology [2, 3]. Indeed, using these relations, a quark δ parameter can be probed in a leptonic process or vice versa. In this way, it is possible that constraints in one sector are converted to the other sector where previously only weaker or perhaps even no bounds existed. A thorough analysis along these lines has been performed by our group and is going to appear very soon [4]. This extends and quantitatively accomplishes the research project outlined in our previous work [2]. Here we present a limited selection of such results, in particular concerning B physics.

To be specific, we concentrate on the SUSY $SU(5)$ framework and derive all the relations between squark and sleptonic mass insertions. We then study the impact of the limit from $\tau \to \mu\,\gamma$ on the $b \to s$ transition observables, such as $A_{CP}(B \to \phi K_s)$.

The soft terms are assumed to be generated at some scale above M_{GUT}. Note that even assuming complete universality of the soft breaking terms at M_{Planck}, as in mSUGRA, the RG effects to M_{GUT} will induce flavor off-diagonal entries at the GUT scale [5, 6]. Hence we assume generic flavor violating entries to be present in the sfermion matrices at the GUT scale. Let us consider the scalar soft breaking sector of the MSSM:

$$
\begin{aligned}
-\mathcal{L}_{\rm soft} = {} & m^2_{Q_{ii}} \tilde{Q}^\dagger_i \tilde{Q}_i + m^2_{u^c_{ii}} \tilde{u^c}^\star_i \tilde{u^c}_i + m^2_{e^c_{ii}} \tilde{e^c}^\star_i \tilde{e^c}_i + m^2_{d^c_{ii}} \tilde{d^c}^\star_i \tilde{d^c}_i + m^2_{L_{ii}} \tilde{L}^\dagger_i \tilde{L}_i \\
& + m^2_{H_1} H^\dagger_1 H_1 + m^2_{H_2} H^\dagger_2 H_2 \\
& + A^u_{ij}\ \tilde{Q}_i \tilde{u^c}_j H_2 + A^d_{ij}\ \tilde{Q}_i \tilde{d^c}_j H_1 + A^e_{ij}\ \tilde{L}_i \tilde{e^c}_j H_1 + \\
& + \quad (\Delta^l_{ij})_{\rm LL} \tilde{L}^\dagger_i \tilde{L}_j + (\Delta^q_{ij})_{\rm LL} \tilde{Q}^\dagger_i \tilde{Q}_j \\
& + (\Delta^e_{ij})_{\rm RR} \tilde{e^c}^\star_i \tilde{e^c}_j + (\Delta^u_{ij})_{\rm RR} \tilde{u^c}^\star_i \tilde{u^c}_j + (\Delta^d_{ij})_{\rm RR} \tilde{d^c}^\star_i \tilde{d^c}_j \\
& + (\Delta^e_{ij})_{\rm LR} \tilde{e_L}^\star_i \tilde{e^c}_j + (\Delta^u_{ij})_{\rm LR} \tilde{u_L}^\star_i \tilde{u^c}_j (\Delta^d_{ij})_{\rm LR} \tilde{d_L}^\star_i \tilde{d^c}_j + \ldots
\end{aligned}
\tag{1}
$$

Table 1: Links between various transitions between up-type, down-type quarks and charged leptons for SU(5). The suffix '0' implies GUT scale parameters.

	Weak-scale	GUT scale
(1)	$(\delta^u_{ij})_{\rm RR} \approx (m^2_{e^c}/m^2_{u^c})\ (\delta^l_{ij})_{\rm RR}$	$m^2_{u^c{}_0} = m^2_{e^c{}_0}$
(2)	$(\delta^q_{ij})_{\rm LL} \approx (m^2_{e^c}/m^2_{Q})\ (\delta^l_{ij})_{\rm RR}$	$m^2_{Q_0} = m^2_{e^c{}_0}$
(3)	$(\delta^d_{ij})_{\rm RR} \approx (m^2_{L}/m^2_{d^c})\ (\delta^l_{ij})_{\rm LL}$	$m^2_{d^c{}_0} = m^2_{L_0}$
(4)	$(\delta^d_{ij})_{\rm LR} \approx (m^2_{L}/m^2_{Q})(m_b/m_\tau)(\delta^l_{ij})^\star_{\rm RL}$	$A^e_{ij_0} = A^d_{ji_0}$

where we have used the standard notation for the MSSM fields and have explicitly written down the various Δ parameters.

Consider that $SU(5)$ be the relevant symmetry at the scale where the above soft terms firstly show up. Then, taking into account that matter is organized into the SU(5) representations $\mathbf{10} = (q, u^c, e^c)$ and $\overline{\mathbf{5}} = (l, d^c)$, one obtains the following relations

$$m^2_Q = m^2_{\tilde{e^c}} = m^2_{\tilde{u^c}} = m^2_{\mathbf{10}} \tag{2}$$

$$m^2_{\tilde{d^c}} = m^2_L = m^2_{\overline{\mathbf{5}}} \tag{3}$$

$$A^e_{ij} = A^d_{ji}\,. \tag{4}$$

Eqs. (2, 3, 4) are matrices in flavor space. These equations lead to relations between the slepton and squark flavor violating off-diagonal entries Δ_{ij}. These are:

$$(\Delta^u_{ij})_{\rm LL} = (\Delta^u_{ij})_{\rm RR} = (\Delta^d_{ij})_{\rm LL} = (\Delta^l_{ij})_{\rm RR} \tag{5}$$

$$(\Delta^d_{ij})_{\rm RR} = (\Delta^l_{ij})_{\rm LL} \tag{6}$$

$$(\Delta^d_{ij})_{\rm LR} = (\Delta^l_{ji})_{\rm LR} = (\Delta^l_{ij})^\star_{\rm RL}. \tag{7}$$

These GUT correlations among hadronic and leptonic scalar soft terms are summarized in table 1. Assuming that no new sources of flavor structure are present from the $SU(5)$ scale down to the electroweak scale, apart from the usual SM CKM one, one infers the relations in the first column of table 1 at low scale. Two comments are in order when looking at table 1. First, the boundary conditions on the sfermion masses at the GUT scale (last column

in table 1) imply that the squark masses are *always* going to be larger at the weak scale compared to the slepton masses. As a second remark, notice that some of the relations between hadronic and leptonic δ MIs in table 1 exhibit opposite "chiralities", i.e. LL insertions are related to RR ones and vice-versa. This stems from the arrangement of the different fermion chiralities in $SU(5)$ five- and ten-plets (as it clearly appears from the final column in table 1). This restriction can easily be overcome if we move from $SU(5)$ to left-right symmetric unified models like SO(10) or the Pati-Salam (PS) case.

In Fig.1, we plot the probability density in the $\mathrm{Re}(\delta^d_{23})_{RR}$–$\mathrm{Im}(\delta^d_{23})_{RR}$ plane for different upper bounds on $BR(\tau \to \mu\,\gamma)$. NLO branching ratios and CP asymmetries for $B \to X_s\gamma$, $B \to \phi K_s$, $BR(B \to X_s\ell^+\ell^-)$ and ΔM_s were considered. As shown in Fig.1, the bound on $(\delta^d_{23})_{RR}$ induced by $BR(\tau \to \mu\,\gamma)$ is already at present much stronger than the bounds from hadronic processes, reducing considerably the room left for SUSY effects in B decays.

Note that making use of the relation (3) with $|(\delta^l_{23})_{LL}| < 1$, implies $|(\delta^d_{23})_{RR}| \lesssim 0.5$ as the ratio $(m^2_L/m^2_{d^c})$ varies roughly between $(0.2 - 0.5)$ at the weak scale, for the chosen high scale boundary conditions. The effect on $(\delta^d_{23})_{RR}$ of the upper bound on $BR(\tau \to \mu\,\gamma)$ is dramatic already with the present experimental value.

2 Lepton Universality in $K \to \ell\nu$

High precision electroweak tests represent a powerful tool to probe the SM and, hence, to constrain or obtain indirect hints of new physics beyond it. Kaon and pion physics are obvious grounds where to perform such tests, for instance in the well studied π_{l2} ($\pi \to l\nu_l$) and K_{l2} ($K \to l\nu_l$) decays, where $l = e$ or μ. Unfortunately, the relevance of these single decay channels in probing the SM is severely hindered by our theoretical uncertainties on non perturbative quantities like f_π and f_K, which still remain at the percent level. On the other hand, in the ratios $R_\pi = \Gamma(\pi \to e\nu)/\Gamma(\pi \to \mu\nu)$ and $R_K = \Gamma(K \to e\nu)/\Gamma(K \to \mu\nu)$ of the electronic and muonic modes, the hadronic uncertainties cancel to a very large extent. As a result, the SM predictions of R_π and R_K are known with excellent accuracy [7] and this makes it possible to fully exploit the great experimental resolutions on R_π [8] and R_K [8, 9] to constrain new physics effects. Given our limited predictive power on f_π and f_K, deviations from the

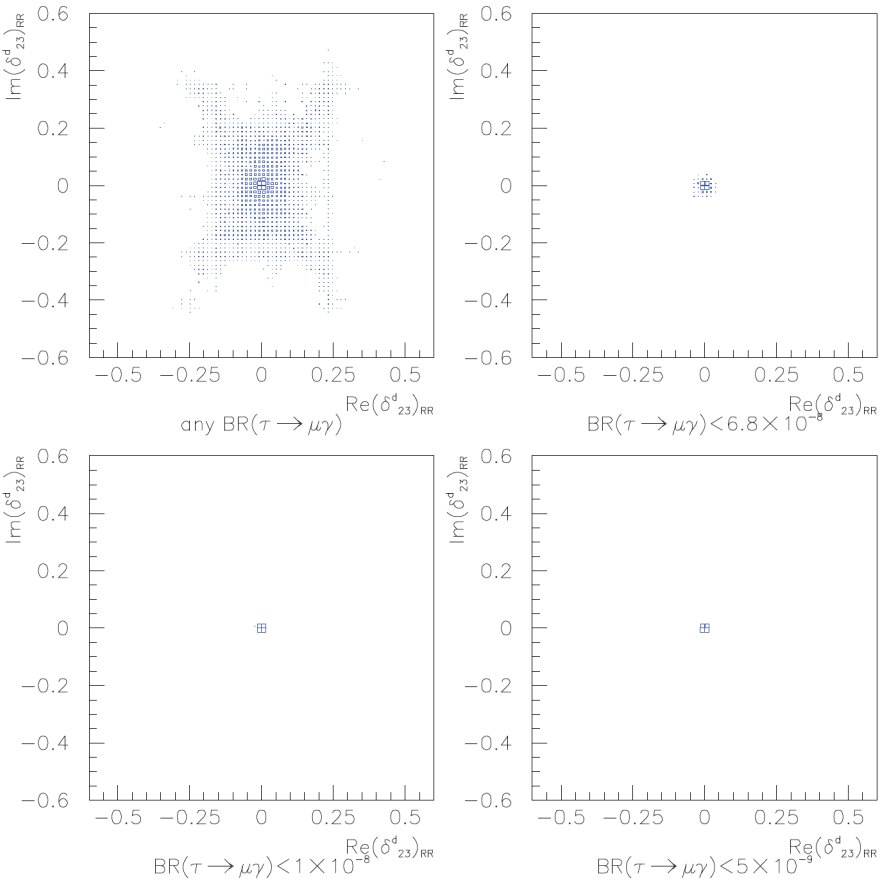

Figure 1: Allowed regions in the $\mathrm{Re}(\delta^d_{23})_{RR}$–$\mathrm{Im}(\delta^d_{23})_{RR}$ plane for different values of $Br(\tau \to \mu\gamma)$. Constraints from $B \to X_s\gamma$, $BR(B \to X_s\ell^+\ell^-)$, $B \to \phi K_s$ and ΔM_s have been used.

$\mu - e$ universality represent the best hope we have at the moment to detect new physics effects in π_{l2} and K_{l2}. The most recent NA48/2 result on R_K:

$$R_K^{exp.} = (2.416 \pm 0.043_{stat.} \pm 0.024_{syst.}) \cdot 10^{-5} \quad \text{NA48/2}$$

which will further improve with current analysis, significantly improves on the previous PDG value, $R_K^{exp.} = (2.44 \pm 0.11) \cdot 10^{-5}$. This is to be compared with the SM prediction which reads:

$$R_K^{SM} = (2.472 \pm 0.001) \cdot 10^{-5}.$$

Denoting by $\Delta r_{NP}^{e-\mu}$ the deviation from $\mu - e$ universality in R_K due to new physics, i.e.:

$$R_K = \frac{\Gamma_{SM}^{K \to e\nu_e}}{\Gamma_{SM}^{K \to \mu\nu_\mu}} \left(1 + \Delta r_{NP}^{e-\mu}\right), \tag{8}$$

the NA48/2 result requires (at the 2σ level):

$$-0.063 \leq \Delta r_{NP}^{e-\mu} \leq 0.017 \quad \text{NA48/2}. \tag{9}$$

In the following, we consider low-energy supersymmetric extensions of the SM (with R parity) as the source of new physics to be tested by R_K [10]. The question we intend to address is whether SUSY can cause deviations from $\mu - e$ universality in K_{l2} at a level which can be probed with the present attained experimental sensitivity, namely at the percent level. We will show that i) it is indeed possible for regions of the minimal supersymmetric standard model (MSSM) to obtain $\Delta r_{NP}^{e-\mu}$ of $\mathcal{O}(10^{-2})$ and ii) such large contributions to K_{l2} do not arise from SUSY lepton flavor conserving (LFC) effects, but, rather, from lepton flavor violating (LFV) ones. Finally, being the NA48/2 R_K central value below the SM prediction, one may wonder whether SUSY contributions could have the correct sign to account for such an effect. We will show that there exist regions of the SUSY parameter space where the total R_K arising from all such SM and SUSY terms is indeed lower than R_K^{SM}.

The SM contributions to π_{l2} and K_{l2} are helicity suppressed; hence, these processes are very sensitive to non-SM effects. In particular, charged Higgs bosons ($H^\pm$) appearing in any model with two Higgs doublets (including the SUSY case) can contribute at tree level to the above processes inducing the

following effects [11]:

$$\frac{\Gamma(M\to l\nu)}{\Gamma_{SM}(M\to l\nu)} = r_H = \left[1-\left(\frac{m_d}{m_d+m_u}\right)^2 \tan^2\beta \frac{m_M^2}{m_H^2}\right]^2 \qquad (10)$$

where m_u is the mass of the up quark while $m_{s,d}$ stands for the down-type quark mass of the M meson ($M = K, \pi$). ¿From Eq. (10) it is evident that such tree level contributions do not introduce any lepton flavour dependent correction. The first SUSY contributions violating the $\mu - e$ universality in $M \to l\nu$ decays arise at the one-loop level with various diagrams involving exchanges of (charged and neutral) Higgs scalars, charginos, neutralinos and sleptons. For our purpose, it is relevant to divide all such contributions into two classes: i) LFC contributions where the charged meson M decays without FCNC in the leptonic sector, i.e. $M \to l\nu_l$; ii) LFV contributions $M \to l_i\nu_k$, with $i \neq k$ (in particular, the interesting case will be for $i = e, \mu$, and $k = \tau$). A typical contribution of the first class is of order

$$\Delta r_{SUSY}^{e-\mu} \sim \frac{\alpha_2}{4\pi}\left(\frac{m_\mu^2 - m_e^2}{m_H^2}\right)\tan^2\beta\,, \qquad (11)$$

where H denotes a heavy Higgs circulating in the loop. Then, even if we assume particularly favorable circumstances like $\tan\beta = 50$, we end up with $\Delta r_{SUSY}^{e-\mu} \leq 10^{-6}$ much below the percent level of experimental sensitivity. One could naively think that contributions of the second class (LFV contributions) are further suppressed with respect to the LFC ones. On the contrary, we show that charged Higgs mediated SUSY LFV contributions, in particular in the kaon decays into an electron and a tau neutrino, can be strongly enhanced. The quantity which now accounts for the deviation from the $\mu - e$ universality is $R_{\pi,K}^{LFV} = \sum_i \Gamma(\pi(K) \to e\nu_i)/\sum_i \Gamma(\pi(K) \to \mu\nu_i)$ (with $i = e, \mu, \tau$) with the sum extended over all (anti)neutrino flavors (experimentally one determines only the charged lepton flavor in the decay products). The dominant SUSY contributions to $R_{\pi,K}^{LFV}$ arise from the charged Higgs exchange. The effective LFV Yukawa couplings we consider are:

$$l^\mp H^\pm \nu_\tau \to \frac{g_2}{\sqrt{2}}\frac{m_\tau}{M_W}\Delta_R^{3l}\tan^2\beta \qquad l = e, \mu. \qquad (12)$$

The Δ_R^{3l} terms are induced at one loop level by non holomorphic corrections through the exchange of gauginos and sleptons, provided LFV mixing among

the sleptons [12] (for phenomenological applications, see [12, 13, 14, 15]). Since the Yukawa operator is of dimension four, the quantities Δ_R^{3l} depend only on ratios of SUSY masses, hence avoiding SUSY decoupling. Δ_R^{3l} is proportional to the off-diagonal flavor changing entries of the slepton mass matrix $\delta_{RR}^{3j} = (\tilde{m}_\ell^2)_{3_R j_R}/\langle\tilde{m}_\ell^2\rangle$. Following the thorough analysis in [13], it turns out that $\Delta_R^{3l} \leq 10^{-3}$. Making use of the LFV Yukawa coupling in Eq. (12), it turns out that the dominant contribution to $\Delta r_{NP}^{e-\mu}$ reads [10]:

$$R_K^{LFV} \simeq R_K^{SM}\left[1 + \left(\frac{m_K^4}{M_H^4}\right)\left(\frac{m_\tau^2}{m_e^2}\right)|\Delta_R^{31}|^2\,\tan^6\beta\right]. \tag{13}$$

Taking $\Delta_R^{31} \simeq 5\cdot 10^{-4}$ accordingly to what said above, $\tan\beta = 40$ and $M_H = 500GeV$ we end up with $R_K^{LFV} \simeq R_K^{SM}(1+0.013)$. Turning to pion physics, one could wonder whether the analogous quantity $\Delta r_{\pi\,SUSY}^{e-\mu}$ is able to constrain SUSY LFV. However, the correlation $\Delta r_{\pi\,SUSY}^{e-\mu} \leq (m_\pi^4/m_k^4)\Delta r_{K\,SUSY}^{e-\mu} < 10^{-4}$ clearly shows that the constraints on $\Delta r_{K\,susy}^{e-\mu}$ force $\Delta r_{\pi\,susy}^{e-\mu}$ to be much below its actual experimental upper bound. LFV effects to $\Delta r_{K\,SUSY}^{e-\mu}$ at the per cent level are allowed by the experimental bounds on LFV tau decays ($Br(\tau \to l_j X) \leq 10^{-7}$, with $X = \gamma, \eta, \mu\mu$). In fact, $\Delta r_{K\,SUSY}^{e-\mu}$ at the percent level corresponds to $Br(\tau \to eX) \leq 10^{-10}$ [15, 16]. The above SUSY dominant contribution to $\Delta r_{NP}^{e-\mu}$ increases the value of R_K with respect to the SM expectation. On the other hand, the recent NA48/2 result exhibits a central value lower than R_K^{SM}. One may wonder whether SUSY could account for such a lower R_K. Obviously, the only way it can is through terms which, contributing to the LFC $K \to l\nu_l$ channels, can interfere (destructively) with the SM contribution. One can envisage the possibility of making use of the large LFV contributions to give rise to LFC ones through double LFV mass insertions in the scalar lepton propagators.

The corrections to the LFC $H^\pm l\nu_l$ vertices induced by LFV effects are:

$$l^\mp H^\pm \nu_l \to \frac{g_2}{\sqrt{2}}\frac{m_l}{M_W}\tan\beta\left(1 + \frac{m_\tau}{m_l}\Delta_{RL}^{ll}\tan\beta\right) \quad l = e, \mu \tag{14}$$

where the second term is generated by a double LFV source that, as a final effect, preserves the flavour. Indeed Δ_{RL}^{ll} is proportional to $\delta_{RR}^{l3}\delta_{LL}^{3l}$. In the large slepton mixing case, Δ_{RL}^{ll} terms are of the same order of Δ_R^{3l}. These new

effects modify the previous R_K^{LFV} expression in the following way [10]:

$$R_K^{LFV} \simeq R_K^{SM} \left[\left| 1 - \frac{m_K^2}{M_H^2} \frac{m_\tau}{m_e} \Delta_{RL}^{11} \tan^3\beta \right|^2 + \left(\frac{m_K^4}{M_H^4} \right) \left(\frac{m_\tau^2}{m_e^2} \right) |\Delta_R^{31}|^2 \tan^6\beta \right]. \quad (15)$$

Setting the parameters as in the example of the above section and if $\Delta_{RL}^{11} = 10^{-4}$ we get $R_K^{LFV} \simeq R_K^{SM}(1 - 0.032)$.

The results of the above section can be easily applied also to the case of charged B mesons, namely to the $B \to \ell\nu$ (with $\ell = e, \mu, \tau$) processes.

Finally, we remark that a key ingredient of all the effects discussed in the present section are large $\tan\beta$ values so, it is legitimate to ask how natural is this framework. The regime of large $\tan\beta$ [$\tan\beta = (m_t/m_b)$] has an intrinsic theoretical interest since it allows the unification of top and bottom Yukawa couplings, as predicted in well-motivated grand-unified models. Moreover, as recently discussed in [17], this scenario is particularly appealing also from a phenomenological point of view. In fact, in this framework, one could naturally accommodate the present central values of both $BR(B \to \tau\nu)$ and $(g-2)_\mu$, explain why the lightest Higgs boson has not been observed yet, and why no signal of new physics has been observed in $BR(B \to X_s\gamma)$ and ΔM_{B_s} without requiring any fine tuning. So, one of the virtues of the large $\tan\beta$ regime of the MSSM is its naturalness in flavor physics and in precise electroweak tests.

References

1. F. Gabbiani, E. Gabrielli, A. Masiero and L. Silvestrini, Nucl. Phys. B **477**, 321 (1996) [arXiv:hep-ph/9604387].

2. M. Ciuchini, A. Masiero, L. Silvestrini, S. K. Vempati and O. Vives, Phys. Rev. Lett. **92**, 071801 (2004) [arXiv:hep-ph/0307191].

3. T. Moroi, Phys. Lett. B **493**, 366 (2000) [arXiv:hep-ph/0007328]; D. Chang, A. Masiero and H. Murayama, Phys. Rev. D **67**, 075013 (2003) [arXiv:hep-ph/0205111].

4. M. Ciuchini, A. Masiero, L. Silvestrini, P. Paradisi, S. K. Vempati and O. Vives, work in progress

5. F. Borzumati and A. Masiero, Phys. Rev. Lett. **57**, 961 (1986).

6. R. Barbieri, L. J. Hall and A. Strumia, Nucl. Phys. B **445** (1995) 219 [arXiv:hep-ph/9501334].

7. W.J. Marciano and A. Sirlin, Phys.Rev.Lett. 71 3629 (1993); M.Finkemeier, Phys.Lett. B 387 391 (1996).

8. S.Eidelman et al. (Particle Data Group), Phys. Lett. B 592, 1 (2004).

9. L.Fiorini, for the NA48/2 Collaboration at ICHEP 2005.

10. A. Masiero, P. Paradisi and R. Petronzio, Phys. Rev. D **74** (2006) 011701 [arXiv:hep-ph/0511289].

11. W.S.Hou, Phys. Rev. D 48, 2342 (1992).

12. K.S. Babu and C. Kolda, Phys.Rev.Lett.**89**, 241802 (2002).

13. A. Brignole and A. Rossi, Phys. Lett. B 566, 217 (2003); A. Brignole and A. Rossi, Nucl. Phys. **B 701**, 3 (2004).

14. M. Sher, Phys. Rev. D 66, 057301 (2002); R. Kitano, M. Koike, S. Komine and Y. Okada, Phys. Lett. B 575, 300 (2003); A. Dedes, J. R. Ellis and M. Raidal, Phys. Lett. **B 549**, 159 (2002); E. Arganda, A. M. Curiel, M. J. Herrero and D. Temes, Phys. Rev. D 71, 035011 (2005).

15. P. Paradisi, JHEP **0602**, 050 (2006); P. Paradisi, [arXiv:hep-ph/0601100].

16. P. Paradisi, JHEP **0510** (2005) 006.

17. G. Isidori and P. Paradisi, Phys. Lett. B **639** (2006) 499 [arXiv:hep-ph/0605012].

Frascati Physics Series Vol. XLI (2006), pp. 301-318
DISCOVERIES IN FLAVOUR PHYSICS AT e^+e^- COLLIDERS
Frascati, February 28th - March 3rd, 2006

CHALLENGES OF HIGH LUMINOSITY B-FACTORIES

Maria Enrica Biagini
Laboratori Nazionali di Frascati, INFN

Abstract

Operation of the two B-Factories (PEP-II and KEKB) has been very successful, both having exceeded their design peak and integrated luminosity and provided a huge amount of good data to the experiments. Proposal for upgrades, in order to achieve about two order of magnitude larger luminosity, are in progress in Japan, Us and Europe. High intensity, short bunch length, very low IP β-functions are the key points of these designs, these schemes being very challenging for the hardware components (RF, vacuum). In this talk the present status of the existing B-Factories will be shortly reviewed. The main luminosity related issues will be addressed, and a short review of the present Super B-Factories designs, together with new ideas, will be presented.

1 Present B-Factories performances

Presently operating B-Factories (PEP-II and KEKB) have exceeded their design goals, both in peak and integrated luminosity. PEP-II [1], running since mid-1999, has reached $1.\times10^{34}\mathrm{cm}^{-2}\ \mathrm{s}^{-1}$ (see Fig.1a) against a design luminosity of $3.\times10^{33}\mathrm{cm}^{-2}\mathrm{s}^{-1}$, delivering to the BaBar experiment an integrated luminosity of about 360 fb^{-1} (March 2006, Fig.1b). KEKB [2] also started

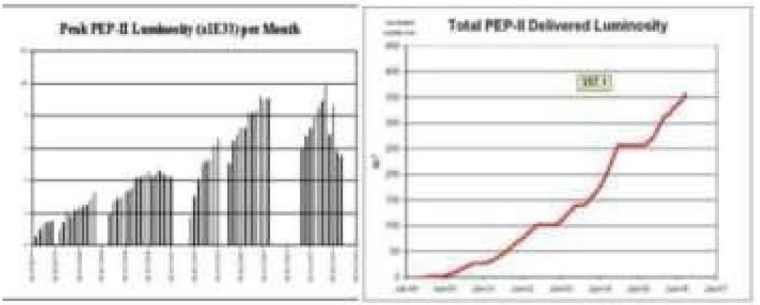

Figure 1: *a) PEP-II Peak Luminosity, b) PEP-II Integrated Luminosity*

operation in 1999 and reached a peak luminosity of $1.6\times10^{34}\text{cm}^{-2}\ \text{s}^{-1}$, having a design value of $1.\times10^{34}\text{cm}^{-2}\ \text{s}^{-1}$ (see Fig.2a) and delivering 560 fb^{-1} (March 2006, Fig.2b) to Belle.

Very good performances and high operation reliability represent a big success for all the Factories included those at lower energy like the DAΦNE Φ-Factory in Frascati [3]. An upgrade of an order of magnitude or more in luminosity is desirable for investigation on particle physics beyond the Standard Model and both B-Factories have studied upgrades.

Tables I and II show the relevant machine parameters for PEP-II and KEKB: it is worthwhile to notice that both have exceeded their peak luminosity goals (of a factor of 3 PEP-II and of 60% KEKB) and consequently the integrated one (a factor 5 in integrated luminosity per day for PEP-II, twice for KEKB) and the design beam-beam tune shifts. These top performances are not due to any magical receipt but rather to the hard work spent in addressing every single problem, leading to a profound knowledge of the accelerator in all its aspects.

In the following a short, not exhaustive list of some of these studies is presented.

- Machine optics has been refined to reproduce real life behaviors, allowing for example β-beat correction. This has also allowed to decrease β_y^*, with

Table 1: PEP-II Parameters

Parameter	Design	Best in collision	Future 2007 goal
I^+ (mA)	2140	2995	4500
I^- (mA)	750	1745	2200
N. bunches	1658	1732	1715
$\beta_y^\star$ (mm)	15-20	11	8.5
ξ_y	0.03	0.045 - 0.07	0.055-0.08
$\mathcal{L} \times 10^{33}$ (cm^{-2}s^{-1})	3.0	10	23
$\int \mathcal{L}$/day (pb^{-1})	130	710	1800

Table 2: KEKB Parameters

Date	**May 2005**		**March 2004**		**Design**		
	LER	**HER**	**LER**	**HER**	**LER**	**HER**	
Current	1.75	1.24	1.58	1.19	2.6	1.1	A
Bunches	1389		1289		5000		
Bunch current	1.26	0.89	1.23	0.92	0.52	0.22	mA
Spacing	1.8-2.4		1.8-2.4		0.6		m
Emittance ϵ_x	18	24	18	24	18	18	nm
$\beta_x^\star$	59	56	59	56	33	33	cm
$\beta_y^\star$	0.65	0.62	0.52	0.65	1.0	1.0	cm
Hor. size @ IP	103	116	103	118	77	77	μm
Ver. size @ IP	2.0	2.0	2.1	2.1	1.9	1.9	μm
Beam-beam ξ_x	0.104	0.077	0.107	0.075	0.039	0.039	
Beam-beam ξ_y	0.089	0.059	0.070	0.057	0.052	0.052	
Luminosity	16.27		13.92		10		/nb/s
$\int$ Lum/day	1178		944		$\sim$ 600		/pb
$\int$ Lum/7 day	7.36		6.01		-		/fb
$\int$ Lum/30 day	29.02		24.00		-		/fb

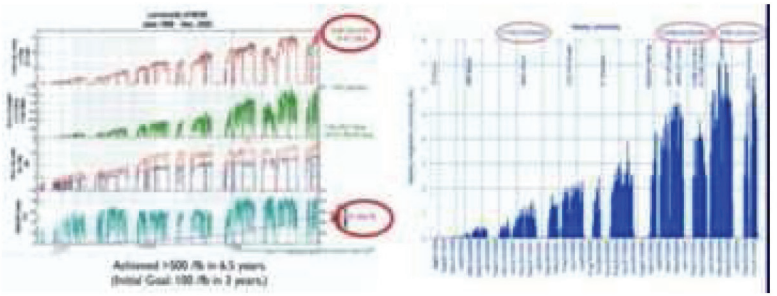

Figure 2: *a) KEKB Peak Luminosity, b) KEKB Integrated Luminosity*

an immediate impact on luminosity.

- Working point in the tunes plane has been changed, going closer to the half integer, with continuous tuning during collisions to optimize at the same time luminosity, lifetimes and backgrounds in the detector.
- Horizontal-vertical coupling correction was performed to get the smallest possible vertical size.
- Use of the continuous injection ("trickle") allowed gaining in integrated luminosity while keeping acceptable backgrounds.
- Orbit feedbacks are used to maintain beams in collision (PEP-II has a dithering feedback using the fast luminosity monitor) and control beam orbits.
- Beam dynamics feedbacks, longitudinal and transverse, control instabilities and were upgraded to cope with shorter bunch spacing and higher currents.
- RF cavities are controlled and upgraded, through feedbacks, comb loops, ARES and Super Conducting cavities.

- Capillary beam measurements, including use of the detector to infer beam sizes at the Interaction Point (IP) were performed.
- Any issue that can influence machine performances was addressed: for example in KEKB the ring circumference is controlled via RF frequency adjustments and the Beam Position Monitors cables outside, responsible for a 20% night-day change in luminosity, have been shielded.
- Background control, with synchrotron radiation masks, collimators and tunes, has decreased the rate of detector induced beam aborts.

Of course the main contribution to the luminosity growth comes from the increasing beam currents. A particular care has been devoted to the design of the vacuum pipe, in particular the bellows which contribute a lot to the chamber impedance and can be responsible for increasing wakefield effects and instability raise.

A limit to the maximum positron current in collision has come from the electron-cloud instability, a phenomenon common to both Factories, with the formation of a cloud of secondary emitted electrons extracted by the vacuum pipe, which interacts with the positron bunches, thus increasing their sizes. This instability has been intensively studied theoretically, with simulations and measurements. Fig.3 shows calculations of the Secondary Emission Yield and measurements of beam sizes for KEKB. Both machines have installed low field solenoidal coils wrapped around the pipe which have been quite effective up to the present currents. However an "e-cloud remediation" international task force is at present evaluating other solutions, for example curved electrodes are being studied at PEP-II, and the best material to be used for the beam pipe is object of experiments.

2 Lessons learned from high luminosity operation

¿From B-Factories operation it is clear that asymmetric beam energies work well. The transparency condition, with beam current ratio inverse to energy ratio, seems to be a weak condition, since both accelerators operate with a much larger electron current in the HER. However, at least for KEKB this is probably a condition necessary to compensate the LER blow-up due to the e-cloud instability. High currents can be stored: both B-Factories have a smaller

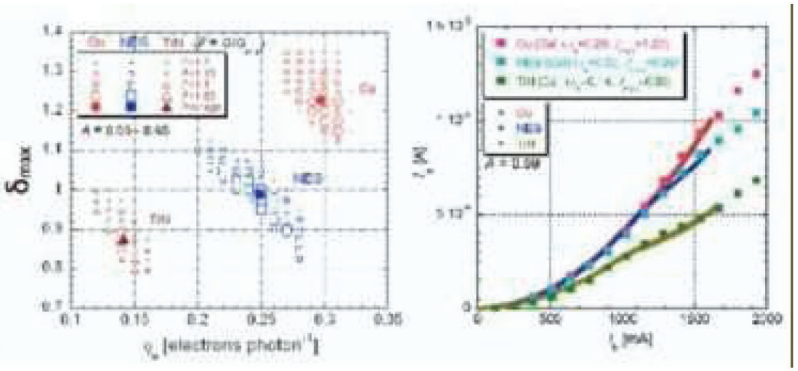

Figure 3: *KEKB Secondary Yield Electrons simulations (a), measurements (b)*

number of bunches with a much higher current per bunch than the design and higher beam-beam tune shifts.

The crossing angle in KEKB, ±11 mrad, has proved not to be a fundamental limit for the luminosity; however a further improvement will come from the installation of a crab cavity in order to restore head-on collision.

Detector backgrounds are still an issue; however they can be handled playing with tunes and collimators.

Bunch-by-bunch feedbacks work very well even with a short (4 nsec) bunch spacing.

Continuous injection works also very well for both machines and it is surely a mode of operation to consider in future designs of extremely high luminosity accelerators.

The beam-beam tune shifts (0.08 to 0.1) are the largest ever reached in electron-positron colliders, proving that operation in such a regime is possible. This means that these values can be reasonably assumed for the design of new machines of the same kind.

Last but not least it should be remarked that these successes are also due to the possibility to have runs dedicated to machine development, which proved to be absolutely necessary in order to understand beam behavior and to apply corrections to the lattice or new operation schemes.

3 Super B-Factories challenges

What are the challenges for a Super B-Factory design is straightforward when looking at the simplified luminosity formula below:

$$L \approx \frac{\gamma_\pm}{2er_e} \frac{I_\pm \xi_{\pm y}}{\beta_y^*} \tag{1}$$

The key parameters are beam currents, beam-beam tune shifts and the β_y^*. In Table III the main parameters of proposed upgrades are listed. They of course all include high currents, increased collision frequency, short bunch length and crossing angle schemes. Lets examine pros and cons of them.

3.1 High current issues

As it is clear from the previous section, high current operation poses severe constraints on RF power, beam pipe cooling, powerful and reliable injector, vacuum pipe design - with antechamber to cope with High Order Modes (HOM) power and improved bellows. The threshold current for the e-cloud instability, if no other cure is found, can be probably overcome with charge exchange in the LER and HER rings. Thermal heating of the beam pipe, responsible for many hardware failures, needs efficient cooling. The background rates increase with the current, so do instabilities like the resistive wall. Beam loading in RF cavities increases: KEKB considered the use of a 1.5 GHz cavity, but the design of such an unusually high frequency cavity was judged difficult and costly in terms of money and manpower. At high currents the Coherent Synchrotron Radiation (CSR) emitted in bending magnets, already observed in KEKB LER, can also become an issue. Due to the high circulating currents both PEP-II and KEKB suffered serious hardware damages, for example in bellows, longitudinal feedback feedthroughs, BPMs, masks, and many vacuum leaks.

3.2 Interaction Region issues

A smaller β_y^* means smaller physical aperture available, smaller dynamical aperture due to the increased chromaticity, shorter lifetime, more backgrounds,

Table 3: SuperB-Factories Parameters

	PEP-II		Super PEP		KEKB		Super KEKB	
	LER	HER	LER	HER	LER	HER	LER	HER
E, GeV	3.1	9.0	3.5	8.0	3.5	8.0	3.5	8.0
Particle	e^+	e^-	e^-	e^+	e^+	e^-	e^-	e^+
C, m	2200		2200		3016		3016	
I, A	2.45	1.55	15.5	6.8	1.73	1.26	9.4	4.1
Bunches	1588		6900		1388		5000	
I/bunch, mA	1.54	0.98	2.25	0.99	1.25	0.91	1.88	0.82
Spacing, m	1.26		0.31		1.77 or 2.36		0.59	
θ_{cros}, mrad	0		30		22		30	
ϵ, nm ϵ_x	27	51	28	28	19	24	24	24
$\beta_x^\star$, cm	50	32	15	15	59	56	20	20
$\beta_y^\star$, cm	1.05	1.05	0.15	0.15	0.65	0.62	0.30	0.30
$\sigma_x^\star$, μm	170 (Σ)		65	65	103	116	69	69
$\sigma_y^\star$, μm	7.2 (Σ)		0.6	0.6	2.1	2.1	0.73	0.73
σ_l, mm	11	11	1.75	1.75	~ 7	~ 7	3.0	3.0
V_{RF}, MV	3.8	16.5	43	33	8	15	15	20
F_{RF}, MHz	476		962		509		509	
ξ_x	0.053	0.055	0.105	0.105	0.110	0.073	0.152	0.152
$\xi_{x,\text{dyn. eff.}}$							0.041	0.041
ξ_y	0.064	0.046	0.107	0.107	0.092	0.056	0.215	0.215
$\xi_{x,\text{dyn. eff.}}$							0.187	0.187
L, $\text{cm}^{-2}\text{s}^{-1}$	10^{34}		70 10^{34}		1.6 10^{34}		40 10^{34}	

and the need to re-design the IR, possibly with a local chromaticity correction scheme. The bunch length σ_l does not appear explicitly in the luminosity equation, however the β_y^* cannot be smaller than σ_l: due to the parabolic behavior of the β-function at the IP particles colliding outside the IP experience a much larger β_y value and a much stronger tune shift, with a net loss in luminosity ("hourglass effect"). Possible solutions have been suggested, as the "traveling focus" method with a RF quadrupole at the IP to move the bunch waist along the z direction, or the "crabbed waist" solution [4)] that with the help of a couple of sextupoles moves the waist along x and z. Such schemes have not been applied yet to any operating machine, but the crabbed waist method seems to be very powerful and could be tested in the near future in DAΦNE.

Additional luminosity reduction comes from the crossing angle, introducing synchro-betatron resonances and additional increase in the horizontal size, since the projected beam size along the IR will be larger. On the other hand this scheme is needed since in head-on collision with a short bunch spacing the bunches collide not only at the IP but also before and after, in high β locations, experiencing beam-beam tune shifts comparable to the IP one ("parasitic crossing" collisions). In PEP-II, where beams collide head-on, a small permanent magnet dipole is used to separate the beams after collision, but the synchrotron radiation emitted introduces further backgrounds. A possible scheme with ± 3 mrad, the maximum achievable with the present layout, has been studied. However the benefits of less harmful parasitic crossings probably would not compensate the loss in luminosity and the design has been abandoned. At KEKB the installation of a crab cavity to restore head-on collision at the IP will take place in next summer shutdown. Beam-beam simulations with weak-strong and strong-strong codes, showed in Fig.4a, confirmed that this scheme can increase the maximum achievable beam-beam tune shift by a factor 2 at least. In Fig.4b is a sketch of how the crab-crossing works and in Fig.5 is a picture of the cavity.

3.3 Bunch length issues

Making short bunches is an issue, since the RF voltage is a weak parameter (σ_l is proportional to the square root of Vrf) and very high voltages are difficult and

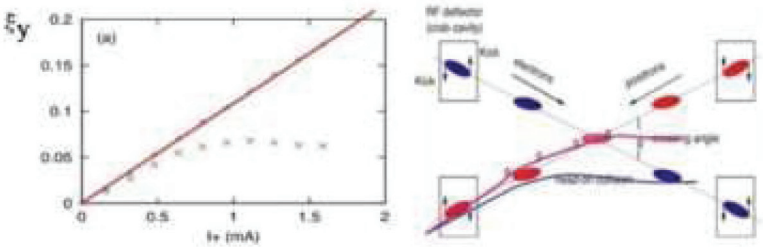

Figure 4: *a) Beam-beam simulations with and without crab crossing, b) Crab crossing principle*

expensive. Other scheme have been proposed, such as the negative momentum compaction lattice experimented in DAΦNE [5] or the "Strong RF Focusing" [6] method proposed for the DAΦNE upgrade (DANAE [3]), to modulate the bunch length along the ring so to have a minimum σ_l at the IP and a maximum at the cavity location. However short bunch lengths are an issue "per se" since HOM heating increases with the peak current and CSR instability can arise. Moreover shorter bunch length means shorter lifetime and more backgrounds due to the Touschek effect in the LER ring.

4 Super PEP-II

In the past 2 years a possible upgrade of PEP-II has been studied, in order to reach a peak luminosity of $7.\times10^{35}\mathrm{cm}^{-2}\mathrm{s}^{-1}$ [7]. Key points of the upgrade are:

- replace present RF with SC 952 MHz frequency;
- use 8 x 3.5 GeV energies with up to 15.5 A x 6.8 A beam currents;
- new LER and HER vacuum chambers with antechambers for higher power;

Figure 5: *KEKB Crab Cavity*

- replace LER magnets to soften radiation and resistive wall losses; rework HER magnets as well;
- new bunch-by-bunch feedback for 6900 bunches (every bucket) at 1 nsec spacing;
- push β_y^* to 1.7 mm: need new IR (SC quadrupoles) with 15 mrad crossing angle and crab cavities with bunch lengths of 1.8 mm.

A new cavity design has been studied [8)] as well as bellows with HOM absorber and an improved vacuum system. Fig.6 shows the new bellow design.

The change in RF frequency is dictated by the necessity of reducing the wall power, as it is shown in Fig.7. For about 100 MW of total power, Linac and campus included, 476 MHz provides a luminosity of about 2 to $4.\times10^{35}\mathrm{cm}^{-2}\mathrm{s}^{-1}$ and 952 MHz provides about 0.7 to $1.\times10^{36}\mathrm{cm}^{-2}\mathrm{s}^{-1}$.

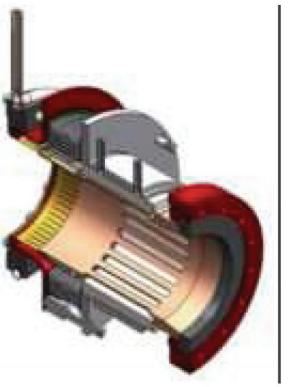

Figure 6: *PEP-II New bellows design with HOM absorber*

5 Super KEKB

The KEKB upgrade has been described in a Letter of Intent presented in 2004 [9]. The design follows basically the same philosophy. The high beam currents require upgrade of:

- RF system for:
  - RF power
  - Frequency detuning due to beam loading
  - Handling of high HOM power
- Vacuum System for:
  - Handling of high SR power
  - Tolerance against high HOM power
  - Electron cloud instability
- Linac for:
  - Energy switch between electrons and positrons

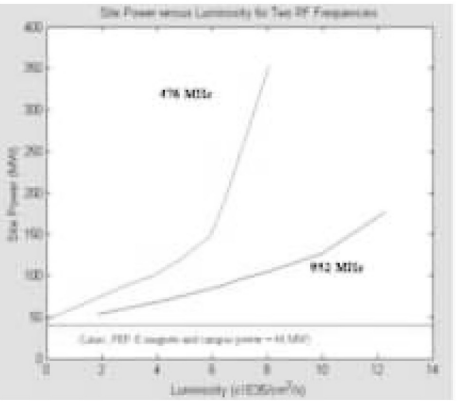

Figure 7: *Super-PEP-II: Site Power including Linac and Campus for Two RF Frequencies*

- Bunch-by-bunch feedback for:
  - Faster damping (transverse)
  - Longitudinal feedback (no need at present KEKB)

The high beam-beam parameters require a combination of choice of betatron tunes and head-on collision:

- Horizontal tune very close to half integer
- Crab crossing

The smaller β_y^* will require:

- New IR design
- Shorter bunch length

The IR has to be modified in order to increase the crossing angle to ± 30 mrad and the physical aperture, as well as to handle HOM power and synchrotron radiation from the first IR quadrupole that will be brand new and closer to the IP. A small damping ring for the positrons is also foreseen. Fig.8

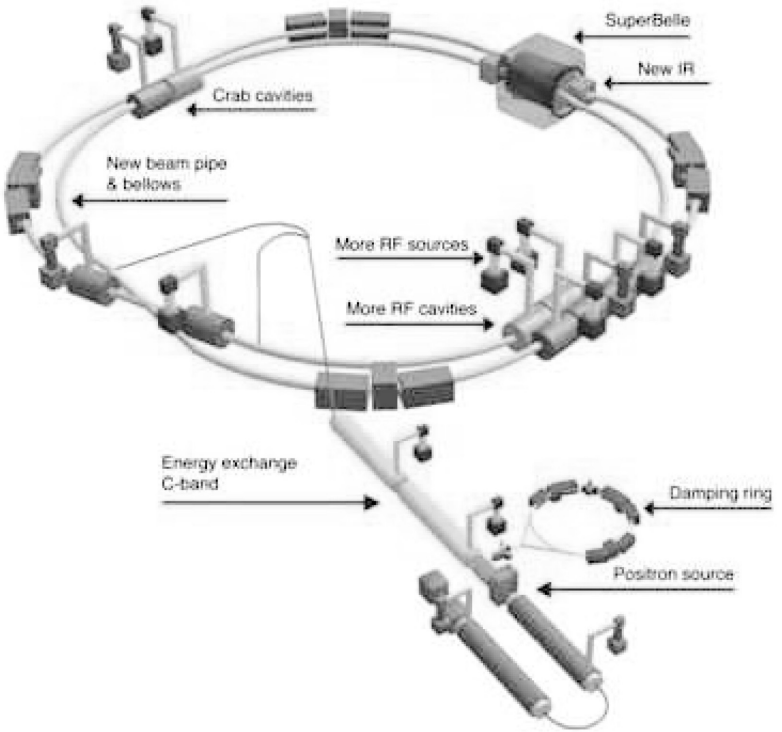

Figure 8: *Super-KEKB Layout*

shows a sketch of the upgraded layout. Cost estimates for this project is around 415 M$ total, without detector upgrade. A decision is expected by the end of this year, so to be able to commission the rings in early 2011.

6 A new Scheme: the SuperB

From both present designs for very high luminosity B-Factories, in the $10^{36}\mathrm{cm}^{-2}\mathrm{s}^{-1}$ range, higher currents ("brute force") seem the only way to increase the luminosity. However both upgrades hit fundamental limits in beam-beam parameters and bunch length, being HOM and CSR a big issue. Moreover many technical and cost issues are expected with a new RF system. It seems that a completely different scheme is highly desirable. The concept of combin-

ing linear and circular collider ideas to make a linear-circular B-Factory was discussed in the late 1980s, although only circular B-Factories were built in the 1990s. Recent advances in B-Factory performance and solid linear collider design progress has reopened this design avenue. The basic idea [10] came from the ATF2-Final-Focus experiment at KEK: it seems possible to achieve spot sizes at the focal point of about 2 μ m*20 nm at very low energy (1 GeV), out from the damping ring. Rescaling at about 10 GeV in center of mass we should get sizes of about 1μ m*10nm. It seemed worthwhile to explore the potential of a collider based on a scheme similar to the Linear Collider one. This idea was first presented at the Hawaii Workshop on Super-B-Factory on March 2005 [10]. The idea was further studied and discussed in a First Super-B Workshop at LNF, Frascati [11] in November 2005. A schematic drawing of the Super-B-Factory as initially considered is shown in Fig.9 [12]. A positron bunch from a 2 GeV damping ring (DR) is extracted and accelerated to 7 GeV in a superconducting (SC) linac. Simultaneously, an electron bunch is generated in a gun and accelerated in a separate SC linac to 4 GeV. The two bunches are prepared to collide in a transport line where the bunch lengths are shortened by a bunch compressor. These bunches are then focused to a small spot at the collisions point and made to collide. The spent beams are returned with transport lines to their respective linacs where they return their energies to the SC accelerator. The 2 GeV positrons are returned to the damping ring to restore the low emittances. The spent electron beam is discarded. The process is repeated with the next bunch. It is expected that each bunch will collide about 120 times each second and that there will be about 10000 bunches. Thus, the collision rate is about 1.2 MHz. A small electron linac and a positron source are used to replenish lost positrons in the colliding process and natural beam lifetime.

Such a scheme was necessary in order to save power for cooling the beams that are heavily disrupted after the collision, the vertical emittance growth in a single collision being a factor of about 300. Running the rings at low energy seemed the only way to bring the power requirements for the facility to the 100 MW level. However this design presents several complexities and challenging requirements for several subsystems. In particular the low energy required for the DR, in combination with the high current, low emittance, small energy spread and short bunch length, is more challenging than the already advanced

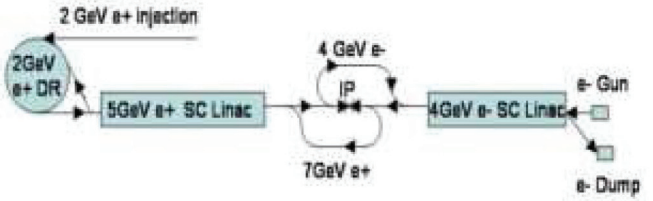

Figure 9: *Linear SuperB scheme*

schemes studied for the International Linear Collider (ILC). Moreover, several technical solutions proposed have never been tested and significant R&D and detailed studies, in order to ensure success, was required.

A second Workshop at LNF, Frascati, has been held on March 2006 [13], when new solution came out from the optimization work of the beam-beam parameters [4]. This new scheme [14] makes use of the ILC Damping Rings, rescaled to 4 and 7 GeV, and of the ILC Final Focus with a crossing angle of ± 25 mrad. The IP parameters have been re-optimized in order to minimize the disruption due to the beam-beam forces. The proposed values are nearly the ones proposed for ILC, except for the number of bunches that is about 4 times larger, and do produce a much smaller luminosity for a single pass, but the emittance blowup for a single crossing is of the order of a few parts in 10^3 and thus only modest damping is needed between collisions. With the new scheme it is then possible to increase the collision frequency, and to collide continuously in the rings with ILC-like parameters. The required Final Focus is also exactly the one designed for ILC with rescaled energies. In Fig. 10 is shown a schematic layout.

With this scheme it will be possible to operate at the τ energy also, with a luminosity of the order of $1.\times 10^{35}\mathrm{cm}^{-2}\mathrm{s}^{-1}$, while it has still to be studied the possibility to run down to the Φ. The wall power in the new design is below 35 MW, considering a 60% transfer efficiency, to be further optimized. The possibility to reuse the PEP-II RF system, power supplies, magnets, vacuum pumps, etc., reducing the overall costs, will also be considered. The injector system will be standard, probably a C-band 7 GeV linac as in the KEKB upgrade.

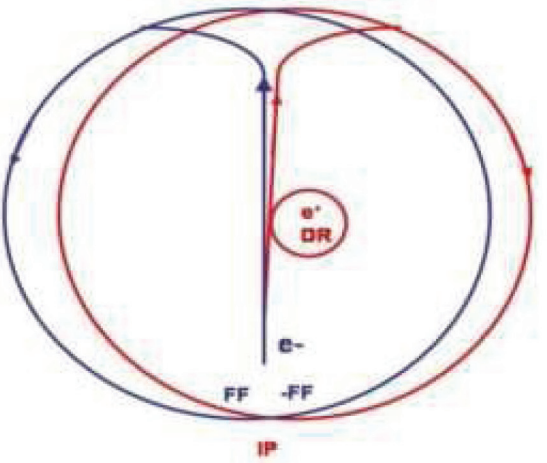

Figure 10: *SuperB ILCDR-like layout*

7 Conclusions

Operation of present B-Factories has been very successful, but going to higher luminosities is much more challenging: the brute force approach seems hard to pursue and new ideas need to be tested. Solutions to problems can come from the collaboration between international laboratories, as it is done for the ILC. The study of a novel accelerator is in progress, and R&D can be done in full synergy with the ILC. For future accelerators, requiring a big commitment of people and money, an international collaboration seems to be the only solution. A global SuperB project is the way to pursue.

References

1. J. Seeman *et al*, Performance of the PEP-II B-Factory collider at SLAC, in: Proc. of 2005 Particle Accelerator Conference, Knoxville, Tennessee,US, p.2369 (May 2005)

2. Y. Funakoshi *et al*, Recent progress at KEKB, in: Proc. of 2005 Particle Accelerator Conference, Knoxville, Tennessee,US, p.1045 (May 2005)

3. C. Biscari, Status and perspectives of Φ-Factories, this Workshop

4. P. Raimondi, Introduction to Super-B Accelerators, in: Second LNF SuperB Workshop, Frascati, Italy, March 16-17, 2006, http : //www.lnf.infn.it/conference/superb06/

5. M. Zobov *et al*, DAΦNE Operation and Plans for DAFNE2, in: Proc. of 2005 Particle Accelerator Conference, Knoxville, Tennessee,US, p.112 (May 2005)

6. C. Biscari *et al*, Proposal of an experiment on bunch length modulation in DAΦNE, in: Proc. of 2005 Particle Accelerator Conference, Knoxville, Tennessee,US, p.336 (May 2005)

7. J. Seeman, PEP SuperB Parameters and design, in: Super-B-Factory Workshop in Hawaii, April 20-22, 2005, http : //www.phys.hawaii.edu/superb/

8. A. Novokhatski, RF cavity designs, in: Super-B-Factory Workshop in Hawaii, April 20-22, 2005, http : //www.phys.hawaii.edu/superb/

9. SuperKEKB Letter of Intent, KEK Report 04-4, arXiv hep-ex/0406071m, 2004

10. P. Raimondi, Exotic approach to a Super-B-Factory, in: Super-B-Factory Workshop in Hawaii, April 20-22, 2005, http : //www.phys.hawaii.edu/superb/

11. First LNF Workshop on SuperB, Frascati, Italy, November 11-13, 2005, http : //www.lnf.infn.it/conference/superbf05/

12. J. Albert *et al*, SuperB: a linear high-luminosity B-Factory, INFN-AE 05-08, hep-ex/0512235, 2005

13. Second LNF SuperB Workshop, Frascati, Italy, March 16-17, 2006, http : //www.lnf.infn.it/conference/superb06/

14. M. Giorgi on behalf of the SuperB group, SuperB: High Luminosity Flavour Factory, INFN Roadmap report, March 2006

Frascati Physics Series Vol. XLI (2006), pp. 319
DISCOVERIES IN FLAVOUR PHYSICS AT e^+e^- COLLIDERS
Frascati, February 28th - March 3rd, 2006

REQUIREMENTS FOR A DETECTOR AT THE SUPER B-FACTORY

William Wisniewski
SLAC, Stanford

Written contribution not received

Frascati Physics Series Vol. XLI (2006), pp. 321
DISCOVERIES IN FLAVOUR PHYSICS AT e^+e^- COLLIDERS
Frascati, February 28th - March 3rd, 2006

PHYSICS OF B_s MESONS, STATUS AND PERSPECTIVES

Tatsuya Nakada
CERN and EPFL

Written contribution not received

Frascati Physics Series Vol. XLI (2006), pp. 323
DISCOVERIES IN FLAVOUR PHYSICS AT e^+e^- COLLIDERS
Frascati, February 28th - March 3rd, 2006

FUTURE PERSPECTIVES FOR B PHYSICS AT A SUPER B-FACTORY

Hitoshi Yamamoto
Tohoku University

Written contribution not received

Frascati Physics Series Vol. XLI (2006), pp. 325-336
DISCOVERIES IN FLAVOUR PHYSICS AT e^+e^- COLLIDERS
Frascati, February 28th - March 3rd, 2006

RARE B DECAYS AS A WINDOW ON PHYSICS BEYOND THE STANDARD MODEL

Tobias Hurth
CERN, Dept. of Physics, Theory Unit, CH-1211 Geneva 23, Switzerland
SLAC, Stanford University, Stanford, CA 94309, USA

Abstract

We discuss the opportunities offered by rare decays in our search for new physics beyond the SM. We discuss three strategies to disentangle hadronic physics from possible new physics effects, including the new tools QCD factorization and soft collinear effective theory. We illustrate them by the rare decay modes $b \to s\gamma$, $b \to s\ell^+\ell^-$ and $B \to \pi\pi$ in an exemplory mode.

1 Introduction

Rare B and also kaon decays representing loop-induced processes are highly sensitive probes for new degrees of freedom beyond the SM. Through virtual (loop) contributions of new particles to such observables, one can investigate high-energy scales even before such energies are accessible at collider experiments.

Such flavour information is complementary to the collider data of the Large Hadron Collider (LHC); for example the present flavour data from the B

factories in the $b \to s$ sector is not very restrictive (yet). Within a supersymmetric new physics scenario, present bounds on squark mixing still allow for large contributions to flavour-violating squark decays at tree level, which can be measured at the LHC. In these cases, additional information from future flavour experiments will be necessary to interpret those LHC data properly [1].

Quark-flavour physics is governed by the interplay of strong and weak interactions. One of the main difficulties in examining the observables in flavour physics is the influence of the long-distance strong interaction. The resulting hadronic uncertainties restrict the opportunities in flavour physics significantly. If new physics does not show up in B physics through large deviations, as recent experimental data indicate, the focus on theoretically clean variables within the indirect search for new physics is mandatory.

Nevertheless there are new tools, such as QCD factorization and the soft-collinear effective theory (SCET), to tackle the strong interaction within B decays. The large data sets from the B experiments should be used to sharpen these new tools and improve our present understanding of the strong interaction.

1.1 Hadronic uncertainties

Thus, the crucial problem in the new physics search within flavour physics is the optimal separation of new physics effects and hadronic uncertainties. This can be successfully solved only for a selected number of *golden* observables in flavour physics, where hadronic physics can be disentangled to a large extent and clean tests of the SM are possible. In principle there are three strategies:

• One can focus on inclusive decays modes (for a review see [2]). These modes are dominated by the partonic contributions because bound-state effects of the final states are eliminated by averaging over a specific sum of hadronic states. Moreover, also long-distance effects of the initial state are accounted for, through the heavy mass expansion in which the inclusive decay rate of a heavy B meson is calculated, using an expansion in inverse powers of the b-quark mass. In fact, one can use quark-hadron duality to derive a heavy mass expansion of the decay rates in powers of $\Lambda_{\rm QCD}/m_b$ (HME). For example, it turns out that the decay width of the $\bar{B} \to X_s\gamma$ is well approximated by the partonic decay rate, which can be calculated in renormalization-group-improved perturbation

theory:

$$\Gamma(\bar{B} \to X_s\gamma) = \Gamma(b \to X_s^{parton}\gamma) + \Delta^{nonpert.}$$

Non-perturbative corrections occur at the order Λ_{QCD}^2/m_b^2 only. The absence of first-order power corrections is a consequence of the fact that there is no independent gauge-invariant operator of dimension 4 in the operator product expansion because of the equations of motion. The latter fact implies a rather small numerical impact of the non-perturbative corrections to the decay rate of inclusive modes. Nevertheless, there are additional nonperturbative corrections within inclusive modes due to necessary cuts in the experimental spectra like the photon energy spectrum in $\bar{B} \to X_s\gamma$ (see [3]).

• In exclusive processes, however, one cannot rely on quark-hadron duality and has to face the difficult task of estimating matrix elements between meson states. Therefore, exclusive modes are not well-suited to the new physics search in general. Nevertheless, one can focus on ratios of exclusive decay modes such as asymmetries, where large parts of the hadronic uncertainties partially cancel out. In particular, there are CP asymmetries that are governed by one weak phase only. In that specific case the hadronic matrix elements cancel out completely.

• There are also specific decays like $K \to \pi\nu\bar{\nu}$ modes where the hadronic uncertainties can be eliminated by experimental data. In these kaon decays the hadronic matrix element can be related to the well-known rare semileptonic K_{l3} decays.

Regarding the hadronic matrix elements of exclusive modes, the method of QCD-improved factorization has been systemized for non-leptonic decays in the heavy-quark limit. This method allows for a perturbative calculation of QCD corrections to naive factorization and is the basis for the up-to-date predictions for exclusive rare B decays in general [4]. However, within this approach, a general, quantitative method to estimate the important $1/m_b$ corrections to the heavy-quark limit is missing.

A more general quantum field theoretical framework was proposed – known under the name of SCET – which allows for a deeper understanding of the QCD factorization approach [5, 6]. In contrast to the well-known heavy-quark effective theory (HQET), the recently proposed SCET does not

correspond to a local operator expansion. While HQET is only applicable to B decays, when the energy transfer to light hadrons is small, for example to $B \to D$ transitions at small recoil to the D meson, it is not applicable, when some of the outgoing, light particles have momenta of order m_b; then one faces a multi scale problem:
a) Λ = few $\times \Lambda_{\rm QCD}$, the *soft* scale set by the typical energies and momenta of the light degrees of freedom in the hadronic bound states; b) m_b the *hard* scale set by the heavy-b-quark mass (we note, that in the B-meson rest frame, for $q^2 \simeq 0$ also the energy of the final-state hadron is given by $E \simeq m_b/2$); c) the hard-collinear scale $\mu_{\rm hc} = \sqrt{m_b \Lambda}$ appears through interactions between soft and energetic modes in the initial and final states. The dynamics of hard and hard-collinear modes can be described perturbatively in the heavy-quark limit $m_b \to \infty$.

The separation of the two perturbative scales from the non-perturbative hadronic dynamics is formalized, within the framework of SCET, with the small expansion parameter $\lambda = \sqrt{\Lambda/m_b}$. Thus, SCET describes B decays to light hadrons with energies much larger than their masses, assuming that their constituents have momenta collinear to the hadron momentum. On a technical level, the implementation of power counting in λ, at the level of momenta, field and operators, corresponds directly to the well-known method of regions for Feynman diagrams [7].

2 Exploration of higher scales via rare decays

Rare B and kaon processes often represent flavour changing neutral currents (FCNCs) and occur in the SM only at the loop level. This fact leads to the high sensitivity to potential new degrees of freedom beyond the SM. Such potential new contributions are not suppressed with respect to the SM contributions. This indirect search for new physics signatures within flavour physics takes place today in complete darkness, given that we have no direct evidence of new particles beyond the SM. However, the day the existence of new degrees of freedom is established by the LHC, the searches for anomalous phenomena in the flavour sector will become mandatory. The problem then will no longer be to discover new physics, but to measure its (flavour) properties. In this context, the measurement of theoretically clean rare decays, *even when found*

to be SM-like, will lead to important and valuable information of the structure of the new physics models and will lead to complementary information to the LHC collider data.

Because new physics effects beyond the SM seem to be rather small it is important to go beyond the pure study of branching ratios and also look at complex kinematic distributions, in particular at CP, forward-backward, isospin and polarization asymmetries. Only the measurements of a large over-constraining set of these observables allow us to detect specific pattern and to distinguish between various new-physics scenarios.

Finally, rare decays are also important tools to analyse the famous flavour problem, namely how FCNCs are suppressed beyond the SM. This problem has to be solved by any viable new physics model. One solution of the flavour problem is given by minimal flavour violation (MFV). In [14], a consistent definition of this scenario was presented, which essentially requires that all flavour and CP-violating interactions be linked to the known structure of Yukawa couplings. The constraint within an effective field approach is introduced with the help of a symmetry concept and can be shown to be renormalization-group-invariant [14].

Perhaps this MFV-based effective field theory approach is too pessimistic from the current point of view. One of the key predictions of the MFV is the direct link between the $b \to s$, $b \to d$, and $s \to d$ transitions. This prediction within the $\Delta F = 1$ sector is definitely not well-tested at the moment and there is still room for new flavour structures to be discovered. Nevertheless, in contrast to the scale of the electroweak symmetry breaking, there is no similarly strong argument that new flavour structures have to appear at the electroweak scale.

In the following we discuss some inclusive and exclusive decays in an exemplory mode.

2.1 $b \to s/d\gamma$ and $b \to s\ell^+\ell^-$ modes

The inclusive $b \to s\gamma$ mode is still the most prominent rare decay, because it has already measured by several independent experiments and the present experimental accuracy has reached the 10% level The HFAG world average of

these measurements with a photon energy cut $E_\gamma > 1.6$ GeV is [8]:

$$\mathrm{BR}[\bar{B} \to X_s\gamma] = \left(3.55 \pm 0.24 \,{}^{+\,0.09}_{-\,0.10} \pm 0.03\right) \times 10^{-4}\,, \tag{1}$$

where the errors are combined statistical and systematic, the systematic ones due to shape functio, and due to the $d\gamma$ contamination. In the near future, more precise data on this mode are expected from the B factories. Thus, it is mandatory to reduce the present theoretical uncertainty accordingly. A systematic improvement certainly consists in performing a complete NNLL calculation which will reduce the well-known large uncertainty due to the definition of the charm mass [9] by a factor 2 as was recently shown [10]. In a recent theoretical update of the NLL prediction of this branching ratio, the uncertainty related to the definition of m_c was taken into account by varying m_c/m_b in the conservative range $0.18 \leq m_c/m_b \leq 0.31$ which covers both, the pole mass (with its numerical error) value and the running mass $\bar{m}_c(\mu_c)$ value with $\mu_c \in [m_c, m_b]$ [11]: $\mathrm{BR}[\bar{B} \to X_s\gamma] = (3.70 \pm 0.35|_{m_c/m_b} \pm 0.02|_{\mathrm{CKM}} \pm 0.25|_{\mathrm{param.}} \pm 0.15|_{\mathrm{scale}}) \times 10^{-4}$. The stringent bounds obtained from the $B \to X_s\gamma$ mode on various non-standard scenarios (see e.g. [12, 13, 14, 15, 16, 17]) are a clear example of the importance of clean FCNC observables in discriminating new-physics models.

Besides the $b \to s\gamma$ mode, also the $b \to s\ell^+\ell^-$ transitions are already accessible at the B factories [18, 19, 20], inclusively and exclusively. Quite recently also the $b \to d\gamma$ transition was measured for the first time [21] (for a recent review see [22]). The inclusive decay $b \to s\ell^+\ell^-$ is particularly attractive because of kinematic observables such as the invariant dilepton mass spectrum and the forward–backward (FB) asymmetry. This inclusive decay is also dominated by perturbative contributions if the $c\bar{c}$ resonances that show up as large peaks in the dilepton invariant mass spectrum are removed by appropriate kinematic cuts. In the 'perturbative windows', namely in the low-s (dilepton mass) region ($0.05 < s = q^2/m_b^2 < 0.25$ and also in the high-s region with $0.65 < s$, a theoretical precision comparable with the one reached in the decay $b \to s\gamma$ is in principle possible. The recently calculated NNLL contributions [23, 24, 25, 26, 27, 28] have significantly improved the sensitivity of the inclusive $\bar{B} \to X_s\ell^+\ell^-$ decay in testing extensions of the SM in the sector of flavour dynamics, in particular the value of the dilepton invariant mass (q_0^2), for which the differential forward–backward asymmetry vanishes, is one of the

precise predictions in flavour physics:

$$q^2_{0,\,\mathrm{NNLL}} = (3.90 \pm 0.25)\ \mathrm{GeV}^2.$$

Let us briefly comment on the impact of the exclusive $B \to K^{(*)}\ell^+\ell^-$ modes. Hadronic uncertainties on these exclusive rates are dominated by the errors on form factors and are much larger than in the corresponding inclusive decays. In fact, following the analysis presented in Ref. [29], we see that inclusive modes already put much stronger constraints on the various Wilson coefficients. Concerning the measurement of a zero in the spectrum of the forward-backward asymmetry, things are different. According to Refs. [30] the value of the dilepton invariant mass (q_0^2), for which the differential forward–backward asymmetry vanishes, can be predicted in quite a clean way. In the QCD factorization approach at leading order in $\Lambda_{\mathrm{QCD}}/m_b$, the value of q_0^2 is free from hadronic uncertainties at order α_s^0 (a dependence on the soft form factor $\xi_\perp$ and the light cone wave functions of the B and K^* mesons appear at NLL). Within the SM, the authors of Ref. [30] find: $q_0^2 = (4.2 \pm 0.6)\,\mathrm{GeV}^2$. As in the inclusive case, such a measurement will have a huge phenomenological impact.

2.2 Charmless rare B decays

Charmless rare B decays are an ideal testing ground for the QCD factorization approach. Let us discuss the $B \to \pi\pi$ in an examplory mode.

The QCD factorization theorems on non-leptonic decay modes in general, first proposed in [4], identify short-distance effects (T_{I} and T_{II}) that can be systematically calculated in perturbation theory: $\langle PP|H_{\mathrm{eff}}|B\rangle = F^{B\to P}\cdot T_{\mathrm{I}}\otimes\phi_P + T_{\mathrm{II}}\otimes\phi_B\otimes\phi_P\otimes\phi_P + \text{terms suppressed by } 1/m_b$, where the symbol $\otimes$ represents convolution with respect to the light-cone momentum fractions of light quarks inside the mesons. Non-perturbative effects are parametrized in terms of a few universal functions such as form factors ($F^{B\to P}$) and light-cone distribution amplitudes (ϕ_B, ϕ_P), on which our information is rather restricted. Moreover, phenomenological applications are limited by the insufficient information on (power-suppressed) non-factorizable terms. Thus, the limiting factor of the QCD factorization theorems is twofold, namely the insufficient information on their non-perturbative input and on the power-suppressed (non-factorizable)

terms. This problem should be tackled by the large data sets made available by current and future B physics experiments and by the development of suitable new non-perturbative methods on the theory side.

If one does not want to rely on particular assumptions about the hadronic dynamics, the traditional model-independent approach to charmless non-leptonic B-decays is to decompose the various decay amplitudes according to isospin. The present experimental data on $B \to \pi\pi$ decays is consistent with this isospin decomposition. In [31] it was proposed to use the model-independent predictions from QCD factorization for the factorizable part of the decay amplitudes. The standard isospin analysis is then applied to the non-factorizable contributions only, which thus covers the model-dependent estimate of chirally enhanced power corrections, large deviations from the standard hadronic input parameters, etc. Comparing with the experimental data on branching ratios and CP asymmetries, this method allows to quantify the amount of non-factorizable effects in particular isospin amplitudes without additional theoretical bias.

From the present data on $B \to \pi\pi$ decays, one finds that small non-factorizable contributions are disfavoured. Clearly, the dynamical origin of these non-factorizable corrections remains a theoretical challenge. At present, different phenomenological assumptions can accommodate the data. For instance, the latest update [33] of the BBNS approach [32] advocates scenarios where certain hadronic input parameters are put to the edges of the allowed regions and the estimate about the size of a particular class of $1/m_b$ corrections is included in the theoretical uncertainties. Other authors assume the dynamical enhancement of certain flavour topologies to explain the experimental data, for instance the charming penguin approach of [34]. Also a new analysis using SCET methods was recently presented [35], where SCET relations in leading order are combined with $SU(3)$ flavour relations. This leads to a further reduction of hadronic parameters due to the vanishing of some strong phases in the $m_b \to \infty$ limit.

Often only dominant $1/m_b$ corrections are identified corresponding to simple $1/m_b$ SCET operators. However, the $1/m_b$ corrections also include more power-suppressed decay current operators and more insertions of subleading Lagrangian terms which lead to terms sensitive to higher Fock-state-contributions which are not necessarily suppressed.

It should be stressed that any dynamical assumption which further constrains the isospin analysis may lead to a strong bias when used in CKM fits. Therefore, one should rather use the experimental data itself to distinguish between different alternatives, and to measure the power-suppressed non-factorizable matrix elements in QCD factorization/SCET.

In the long run, the large variety of experimental data on exclusive modes from the B factories and from the LHC experiments will allow us to learn about the size of $1/m_b$ corrections and also of $SU(3)$ breaking effects and to reach sufficient accuracy within charmless B decays for the determination of the CKM parameters and perhaps also for the detection of new physics.

3 Outlook

It is expected that the experiments at the LHC will lead to discoveries of new degrees of freedom at the TeV energy scale. The precise nature of this new physics is unknown, but it is strongly expected that it will answer some of the fundamental questions related to the origin of electroweak symmetry breaking. Independently of the nature of the new physics, a flavour physics program parallel to the LHC's will be crucial to disentangle the precise features of the newly uncovered phenomena and to discriminate between different new physics scenarios.

In particular, the measurement of loop-induced rare B- and K-meson decays as highly sensitive probes for new degrees of freedom beyond the SM will lead to important information complementary to collider data; here it is crucial to go beyond the analysis of branching ratios and to measure more complex kinematical distributions. Moreover, if new physics effects do not show up through large deviations, as recent experimental data indicate, the focus on theoretically clean observables is mandatory.

There are important fundamental questions that will be addressed exclusively by future flavour experiments, for example how FCNCs are suppressed beyond the SM (flavour problem), if there exist new sources of flavour and CP violation beyond those in the SM, if there is CP violation in the QCD gauge sector, how neutrino masses are generated, and what the relation between the flavour structure in the lepton and quark sectors is. All these questions include exciting options to learn something about physics at a scale much higher

than our current experiments. Thus, a diversified and thorough experimental programme in flavour physics will continue to be an essential element for the understanding of nature.

References

1. T. Hurth and W. Porod, Eur. Phys. J. C **33** (2004) S764 [arXiv:hep-ph/0311075].
2. T. Hurth, Rev. Mod. Phys. **75** (2003) 1159 [arXiv:hep-ph/0212304].
3. M. Neubert, Eur. Phys. J. C **40** (2005) 165 [arXiv:hep-ph/0408179].
4. M. Beneke et al., Phys. Rev. Lett. **83** (1999) 1914 [arXiv:hep-ph/9905312].
5. C. W. Bauer et al., Phys. Rev. D **63** (2001) 114020 [arXiv:hep-ph/0011336].
6. M. Beneke et al., Nucl. Phys. B **643** (2002) 431 [arXiv:hep-ph/0206152].
7. M. Beneke and V. A. Smirnov, Nucl. Phys. B **522** (1998) 321 [hep-ph/9711391].
8. Heavy Flavor Averaging Group (HFAG), http://www.slac.stanford.edu/xorg/hfag/rare
9. P. Gambino and M. Misiak, Nucl. Phys. B **611**, 338 (2001) [arXiv:hep-ph/0104034].
10. H. M. Asatrian, C. Greub, A. Hovhannisyan, T. Hurth and V. Poghosyan, Phys. Lett. B **619** (2005) 322 [arXiv:hep-ph/0505068].
11. T. Hurth, E. Lunghi and W. Porod, Nucl. Phys. B **704** (2005) 56 [arXiv:hep-ph/0312260].
12. G. Degrassi, P. Gambino and G. F. Giudice, JHEP **0012**, 009 (2000) [arXiv:hep-ph/0009337].
13. M. Carena, D. Garcia, U. Nierste and C. E. M. Wagner, Phys. Lett. B **499**, 141 (2001) [arXiv:hep-ph/0010003].
14. G. D'Ambrosio, G. F. Giudice, G. Isidori and A. Strumia, Nucl. Phys. B **645**, 155 (2002) [arXiv:hep-ph/0207036].
15. F. Borzumati, C. Greub, T. Hurth and D. Wyler, Phys. Rev. D **62**, 075005 (2000) [arXiv:hep-ph/9911245].

16. T. Besmer, C. Greub and T. Hurth, Nucl. Phys. B **609**, 359 (2001) [arXiv:hep-ph/0105292].

17. M. Ciuchini, E. Franco, A. Masiero and L. Silvestrini, Phys. Rev. D **67**, 075016 (2003) [Erratum-ibid. D **68**, 079901 (2003)] [arXiv:hep-ph/0212397].

18. M. Iwasaki [Belle Collaboration], arXiv:hep-ex/0503044.

19. B. Aubert *et al.* [BABAR Collaboration], Phys. Rev. Lett. **93** (2004) 081802 [arXiv:hep-ex/0404006].

20. K. Abe *et al.* [The Belle Collaboration], arXiv:hep-ex/0508009.

21. K. Abe *et al.*, arXiv:hep-ex/0506079.

22. T. Hurth and E. Lunghi, eConf **C0304052** (2003) WG206 [arXiv:hep-ph/0307142].

23. H. H. Asatryan, H. M. Asatrian, C. Greub and M. Walker, Phys. Rev. D **65** (2002) 074004 [arXiv:hep-ph/0109140].

24. A. Ghinculov, T. Hurth, G. Isidori and Y. P. Yao, Nucl. Phys. B **648** (2003) 254 [arXiv:hep-ph/0208088].

25. A. Ghinculov, T. Hurth, G. Isidori and Y. P. Yao, Nucl. Phys. B **685** (2004) 351 [arXiv:hep-ph/0312128].

26. H. M. Asatrian, K. Bieri, C. Greub and A. Hovhannisyan, Phys. Rev. D **66** (2002) 094013 [arXiv:hep-ph/0209006].

27. C. Bobeth, M. Misiak and J. Urban, Nucl. Phys. B **574** (2000) 291 [arXiv:hep-ph/9910220].

28. C. Bobeth, P. Gambino, M. Gorbahn and U. Haisch, JHEP **0404**, 071 (2004) [arXiv:hep-ph/0312090].

29. A. Ali, E. Lunghi, C. Greub and G. Hiller, Phys. Rev. D **66** (2002) 034002. [arXiv:hep-ph/0112300].

30. M. Beneke, T. Feldmann and D. Seidel, Nucl. Phys. B **612** (2001) 25 [arXiv:hep-ph/0106067].

31. T. Feldmann and T. Hurth, JHEP **0411** (2004) 037 [arXiv:hep-ph/0408188].

32. M. Beneke et al., Nucl. Phys. B **606** (2001) 245 [arXiv:hep-ph/0104110].

33. M. Beneke and M. Neubert, Nucl. Phys. B **675** (2003) 333 [arXiv:hep-ph/0308039].

34. M. Ciuchini et al., Phys. Lett. B **515** (2001) 33 [arXiv:hep-ph/0104126].

35. C. W. Bauer, I. Z. Rothstein and I. W. Stewart, arXiv:hep-ph/0510241.

Frascati Physics Series Vol. XLI (2006), pp. 337-343
DISCOVERIES IN FLAVOUR PHYSICS AT e^+e^- COLLIDERS
Frascati, February 28th - March 3rd, 2006

REVIEW OF TIME-DEPENDENT CP VIOLATION IN $b \to s$ TRANSITIONS

Kai-Feng Chen
Department of Physics, National Taiwan University, Taipei, Taiwan

Abstract

We review on the experimental results of time-dependent CP-violation measurements in the decays that are sensitive to the $b \to s$ transitions. These studies provide a promising way to probe the additional CP-violating phases beyond the framework of Standard Model. The best measurements given by the decay $B^0 \to \phi K^0$ and $B^0 \to \eta' K^0$ provide only 1.1 and 2.0 standard deviations from the Standard Model predictions. An improved sensitivity is expected with the high integrated luminosity provided by a Super B-factory.

1 Introduction

CP violation was first observed in the neutral Kaon system in 1964, and many theories attempt to solve the origin of CP violation. The theory proposed by M. Kobayashi and T. Maskawa points out that an irreducible complex phase in

quark mixing matrix, the Cabibbo-Kobayashi-Maskawa (CKM) matrix, enables CP violation to take place [1]. The relations between the elements of CKM matrix can be described as unitarity triangles, while precise measurements of the unitarity triangles are good tests for the KM model. The KM mechanism could lead to a large CP violating asymmetry in the B-meson system. The CP asymmetries can be extracted from the partial time-dependent decay rate difference between B^0 and $\overline{B}^0$, while one of the B-mesons decays to a common CP eigenstate. The decay daughters of accompanying B-meson provide the b-flavor information. The time-dependent decay rate is given by

$$\mathcal{P}(\Delta t) = \frac{e^{-|\Delta t|/\tau_{B^0}}}{4\tau_{B^0}}\{1 + q \cdot [\mathcal{S}\sin(\Delta m_d \Delta t) + \mathcal{A}\cos(\Delta m_d \Delta t)]\} \ , \qquad (1)$$

where $\mathcal{S}$ and $\mathcal{A}(= -\mathcal{C})$ are CP violating parameters, τ_{B^0} is the B^0 lifetime, and Δm_d is the mass difference between the two B^0 mass eigenstates. A precise determination of the proper time difference (Δt) is required to measure the time-dependent CP violation.

The most important decay mode where this scenario works is the decay $B^0 \to J/\psi K^0$. It provides a direct measurement to the CKM angle $\phi_1(\beta)$ in the unitarity triangle [2]. This value has been precisely measured by both B-factories and agrees with the prediction of the Standard Model. The latest world average of $\sin 2\phi_1(\beta)$ is 0.687 ± 0.032 using all $B^0 \to c\bar{c}K^0$ decays. The CP violation in the B-meson system is already well established within the framework of the Standard Model, but the possibility existing other New Physics beyond the KM Model is still open and may play an important role in the CP violation phenomena. CP violation in flavor-changing $b \to s$ transitions are sensitive to physics at a very high energy scale [3], indicating that a large deviation from the prediction based on Standard Model is allowed. Measurements on the decay channels that are sensitive to the $b \to s$ penguin amplitude may be able to establish the existence of New Physics. Thus, the decay modes $B^0 \to \phi K^0$ (including both K^0_S and K^0_L), $\eta' K^0$, $K^+K^-K^0$, $f_0 K^0_S$, $\pi^0 K_S$, $K^0_S K^0_S K^0_S$, ωK^0_S, and $\pi^0\pi^0 K^0_S$ are examined with the a large data sample. The best candidate is $B^0 \to \phi K^0_S$, while the theoretical error is expected to be very small and the background level is low. The $B^0 \to \eta' K^0_S$ mode has a relative large branching fraction and is a very good candidate to search for New Physics as well. The $B^0 \to \pi^0 K_S$, $K^0_S K^0_S K^0_S$, and $\pi^0\pi^0 K^0_S$ decays require a special K_S vertex finding technique, an advance study on the vertex detector

is necessary. The measurement on $B^0 \to \pi^0 K^0_S$ mode may provide some additional information that is related to the direct CP violation in $B^0 \to K^-\pi^+$ decays. The $B^0 \to K^+K^-K^0$ decay is measured to have a large branching fraction, but the undefined CP state introduces an extra dilution factor for the measurement.

2 Experimental Results

Experimental results from two B-factories, Belle and BABAR, are summarized by the Heavy Flavor Averaging Group (HFAG). The results from the summer 2005 averages [4] (after the summer 2005 conferences) are included here. Figure 1 shows the effective $\sin 2\phi_1$ measurements with $b \to s$ related decay channels from Belle and BABAR, together with their averages. These averages are calculated by assuming a single weak phase, corresponding to a single $\mathcal{S}_f$) for each final state f. The naïve expectation on $\mathcal{S}_f$ is $-\eta_f \times \sin 2\phi_1$ as indicated by $b \to c\bar{c}s$ average on the figure, where η_f is the CP eigenvalue for the final state f. However, the decay $B^0 \to K^+K^-K^0$ involves both CP-even and CP-odd contributions. The fraction of two CP states are estimated from an isospin analysis [5] by Belle and a moment analysis [6] by BABAR. None of the measured $\mathcal{S}_f$ is significant enough to claim a signal of New Physics phase. Even the golden modes, $B^0 \to \phi K^0$ and $B^0 \to \eta' K^0$ decays, only provide a significance of 1.1σ and 2.0σ away from the Standard Model expectations, respectively. However, an overall shift to the left (negative $\delta\mathcal{S}_f = \mathcal{S}_f - \mathcal{S}_{c\bar{c}s}$) is observed, although most of the measured $\delta\mathcal{S}_f$ are relatively small.

3 Standard Model Uncertainties

Even in the Standard Model, the expectation value of $\mathcal{S}_f$ is not exactly equal to $\sin 2\phi_1$. For example, the contributions from CKM-suppressed $b \to u$ penguin amplitudes are usually neglected, and they could provide some additional weak phases. Several theoretically based approaches, such as using SU(3) relations [7], QCD factorization [8], PQCD [9], SCET [10], and final state interaction [11], provide some non-zero deviations.

SU(3) relations can be used to estimate the contributions from the amplitudes related to $V_{ub}V_{us}$. These amplitudes lead to a deviation on the prediction of $\mathcal{S}_f$ for $B^0 \to \phi K^0$, $K^+K^-K^0$, $\eta' K^0$, $\pi^0 K^0_S$, and $K^0_S K^0_S K^0_S$ decays

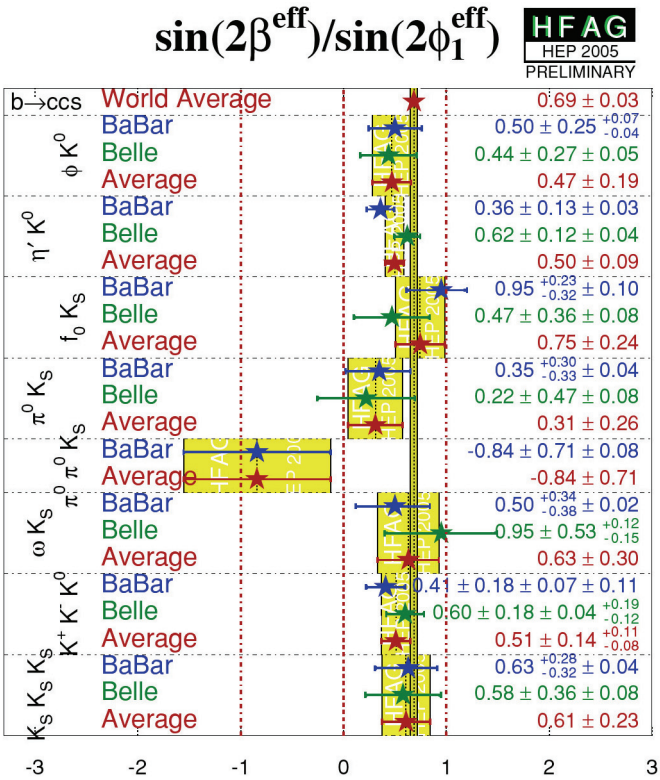

Figure 1: *Comparison of results for* $-\eta_f \times \mathcal{S}_f$ *from* $b \to c\bar{c}s$ *and* $b \to sq\bar{q}$ *penguin decays.*

from $\sin 2\phi_1$. We insert HFAG 2005 averages on several charmless branching fractions into the equations given by the paper, and illustrate the two dimensional boundaries on $\delta\mathcal{S}$ and $\mathcal{A}_f$ in the Figure 2. Deviations of order 0.1 for $B^0 \to \pi^0 K^0_S$, of order 0.2 for $K^+K^-K^0$ and $\eta' K^0$, and of order 0.4 for $K^0_S K^0_S K^0_S$ are predicted. A dynamical assumption is added to the SU(3) analysis due to the unavailable experimental result to get an upper bound for the deviation for $B^0 \to \phi K^0$. It yields an upper bound of order 0.25.

The other model-dependent estimations assume the factorization property in the decays. The estimations provided by several theory groups are summarized in the Figure 3. If measurements yield $|-\eta_f \mathcal{S}_f - \sin 2\phi_1|$ that are much larger than these upper bounds, it would provide a convincing hint for

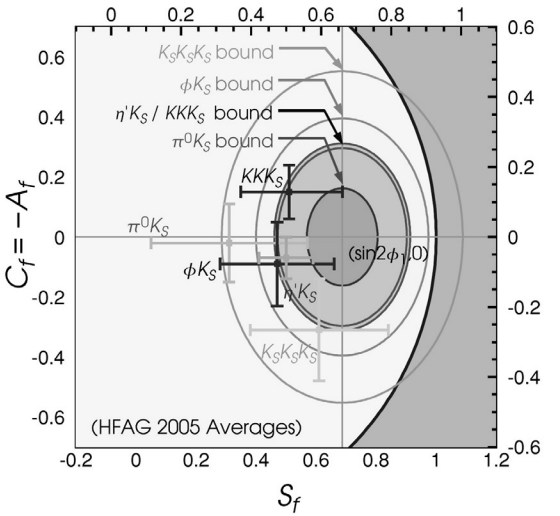

Figure 2: *A Summary of 2D upper bounds based on SU(3) relations. These bounds follow the equation* $\mathcal{A}_f^2 + \left(\frac{\eta_f \mathcal{S}_f + \sin 2\phi_1}{\cos 2\phi_1}\right)^2 = 4 \sin \phi_3 \, |\xi_f|^2$ *and form ellipses in* $\mathcal{S}_f$–$\mathcal{A}_f$ *space. The values of* $\phi_3 \approx 63^\circ$ *and* $\sin 2\phi_1 = 0.687$ *are assumed. All the experimental results are based on the HFAG summer 2005 release.*

New Physics. However, none of the current measured $\mathcal{S}_f$ values exceed these limits if the experimental errors are considered.

4 Conclusion

In the year 2003, a hint for large deviation for effective $\sin 2\phi_1$ value was shown in the $B^0 \to \phi K_S^0$ measurement [12]. A natural question is asked: whether this observation is really a result of New Physics phase in the penguin loops, or is just a result of statistical fluctuation. The direct solution is to extend the analysis to all the $b \to s$ penguin sensitive decays. After a 2-year investigation, the time-dependent CP asymmetries have been measured for various decay channels as summarized above. There is an overall shift observed in the effective $\sin 2\phi_1$ of these $b \to s$ decays; the experimental data yields negative $\delta \mathcal{S}_f$, but most of the theoretical predictions are positive. The disagreement is not significant, but there is still room for having a New Physics effect to take place. A super B-factory will be one of the routes to discover physics beyond the

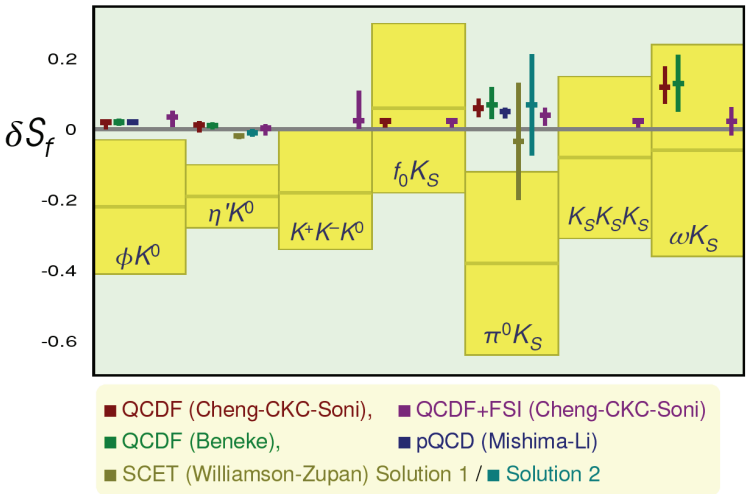

Figure 3: *A summary of experimental measurements (shaded band) and theoretical expectations (squre dots) for the time-dependent CP-violating parameters for $b \to s$ sensitive modes. Results are presented by $\delta\mathcal{S}_f = -\eta_f \mathcal{S}_f - \sin 2\phi_1$.*

Standard Model. A data set corresponding to 5 ab^{-1} integrated luminosity per year is expected for the super KEKB. An error of 0.08 on $\delta\mathcal{S}_{\phi K^0}$ is expected without any ambiguity, while the best precision will be provided by $\delta\mathcal{S}_{\eta' K^0}$ with an error of 0.04. The existence of New Physics can be proved clearly if a significantly large $\delta\mathcal{S}_f$ is measured.

References

1. M. Kobayashi and T. Maskawa, CP Violation in the Renormalizable Theory of Weak Interaction, Prog. Theor. Phys. **49** (1973) 652657.

2. I. I. Y. Bigi and A. I. Sanda, Notes on the Observability of CP Violations in B Decays, Nucl. Phys. **B193** (1981) 85.

3. K. Sasaki and T. Uematsu, Mass Eects in the Polarized Virtual Photon Structure, Nucl. Phys. Proc. Suppl. **135** (2004) 178182.

4. Heavy Flavor Averaging Group (HFAG), E. Barberio *et al.*, Averages of b-hadron Properties at the End of 2005, hep-ex/0603003 (2006).

5. Belle Collaboration, A. Garmash *et al.*, Study of B Meson Decays to Three-body Charmless Hadronic Final States, Phys. Rev. D **69** (2004) 012001.

6. BaBar Collaboration, B. Aubert *et al.*, Measurement of CP Asymmetries in $B^0 \to \phi K^0$ and $B^0 \to K^+K^-K^0_S$ Decays, Phys. Rev. D **71** (2005) 091102.

7. Y. Grossman, Z. Ligeti, Y. Nir, and H. Quinn, SU(3) Relations and the CP Asymmetries in B decays to $\eta' K_S$, ϕK_S and $K^+K^-K_S$, Phys. Rev. D **68** (2003) 015004; M. Gronau, Y. Grossman, and J. L. Rosner, Interpreting the Time-dependent CP Asymmetry in $B^0 \to \pi^0 K_S$, Phys. Lett. **B579** (2004) 331339; G. Engelhard, Y. Nir, and G. Raz, SU(3) Relations and the CP Asymmetry in $B \to K_S K_S K_S$, Phys. Rev. D **72** (2005) 075013.

8. M. Beneke and M. Neubert, QCD Factorization for $B \to PP$ and $B \to PV$ Decays, Nucl. Phys. **B675** (2003) 333415; M. Beneke, Corrections to $sin(2\beta)$ from CP Asymmetries in $B^0 \to (\pi^0, \rho^0, \eta, \eta', \omega, \phi)K_S$ Decays, Phys. Lett. **B620** (2005) 143-150.

9. H. n. Li, S. Mishima and A. I. Sanda, Resolution to the $B \to \pi K$ Puzzle, Phys. Rev. D **72** (2005) 114005.

10. A. R. Williamson and J. Zupan, Two Body B Decays with Isosinglet Final States in SCET, hep-ph/0601214.

11. H. Y. Cheng, C. K. Chua and A. Soni, Effects of Final-state Interactions on Mixing-induced CP Violation in Penguin-dominated B Decays, Phys. Rev. D **72**, (2005) 014006; CP-violating Asymmetries in B^0 decays to $K^+K^-K^0_{S(L)}$ and $K^0_S K^0_S K^0_S$, Phys. Rev. D **72** (2005) 094003.

12. Belle Collaboration, K. Abe *et al.*, Measurement of Time-dependent CP-violating Asymmetries in $B^0 \to \phi K^0_S$, $K^+K^-K^0_S$, and $\eta' K^0_S$ Decays, Phys. Rev. Lett. **91** (2003) 261602.

Frascati Physics Series Vol. XLI (2006), pp. 345-353
DISCOVERIES IN FLAVOUR PHYSICS AT e^+e^- COLLIDERS
Frascati, February 28th - March 3rd, 2006

DEVELOPMENTS OF CKM FITS

UTfit Collaboration:
M. Bona
Dip. di Fisica,Università di Torino and INFN Sezione di Torino
M. Ciuchini
Dip. di Fisica, Università di Roma Tre and INFN Sezione di Roma III
E. Franco
Dip. di Fisica, Università di Roma "La Sapienza" and INFN, Sezione di Ro
V. Lubicz,
Dip. di Fisica, Università di Roma Tre and INFN, Sezione di Roma III
G. Martinelli,
Dip. di Fisica, Università di Roma Tre and INFN, Sezione di Roma III
F. Parodi
Dip. di Fisica, Università di Genova and INFN, Sezione di Genova
M. Pierini
Department of Physics, University of Wisconsin,Madison, WI 53706, USA
P. Roudeau
Laboratoire de l'Accélérateur Linéaire,IN2P3-CNRS et Université de Paris-S
C. Schiavi
Dip. di Fisica, Università di Genova and INFN, Sezione di Genova
L. Silvestrini
Dip. di Fisica, Università di Roma "La Sapienza" and INFN, Sezione di Ro
A. Stocchi
Laboratoire de l'Accélérateur Linéaire,IN2P3-CNRS et Université de Paris-S
V. Vagnoni
INFN, Sez. di Bologna.

Abstract

We review the status of the Unitarity Triangle in the Standard Model and beyond.

1 Introduction

Within the Standard Model (SM), all flavour and CP violating quark weak interactions are governed by the CKM matrix, which can be parameterized in terms of three angles and one phase, or, more conveniently, in terms of the parameters λ, A, $\bar{\rho}$ and $\bar{\eta}$. This implies very strong correlations among flavour and CP violating observables within the SM. The Unitarity Triangle (UT) is a very useful tool to analyze these correlations. With the recent data on B decays, the UT fit has become strongly overconstrained, thus it is now possible to test the CKM mechanism within the SM and to derive constraints on New Physics (NP). In this talk, we will quickly review these two aspects. More details on the procedure and on the results can be found in ref. [1, 2]. (results by other groups can be found in ref. [3]).

2 The SM UT analysis

The values and errors of the relevant quantities used in the standard analysis of the CKM parameters are summarized in Table 1. Additional inputs corresponding to the measurements of the angles γ and α can be found in ref. [4], while ref. [1] describes the procedure followed to extract these constraints from experimental data.

The main novelty in the last two years in the UT analysis is the measurement of the angles of the UT at the B factories. While $\sin 2\beta$ is by now part of the "classic" fit, it is only recently that the measurements of the CP asymmetry in $B \to J/\psi K^*$ (of $B \to D^0 h^0$ decays) have provided a determination of $\cos 2\beta$ (β). These determinations and the corresponding constraints on the $\bar{\rho}$ – $\bar{\eta}$ plane are shown in Fig. 1. It is evident how these additional measurements can suppress one of the two bands determined by $\sin 2\beta$.

The angle γ can be determined studying the interference of $b \to u$ and $b \to c$ transitions in $B \to D^{(*)}K^{(*)}$ decays, using the GLW, ADS or Dalitz methods. The resulting p.d.f. for γ is reported in Fig. 2.

Studying $B^0 \to D^{(*)}\pi(\rho)$ decays, it is possible to extract $\sin(2\beta+\gamma)$ from the time-dependent CP asymmetries. However, present data are insufficient to allow this determination, so that additional input is needed. This can come from SU(3)-related $B \to D_s$ channels, if one neglects annihilation contributions. The total theoretical error in this procedure can be estimated around 100%.

Table 1: Values of the relevant quantities used in the UT fit.

Parameter	Value	Gaussian	Uniform
λ	0.2258	0.0014	-
$\|V_{cb}\|$(excl.)	$41.4 \cdot 10^{-3}$	$2.1 \cdot 10^{-3}$	-
$\|V_{cb}\|$(incl.)	$41.6 \cdot 10^{-3}$	$0.7 \cdot 10^{-3}$	$0.6 \cdot 10^{-3}$
$\|V_{ub}\|$(excl.)	$38.0 \cdot 10^{-4}$	$2.7 \cdot 10^{-4}$	$4.7 \cdot 10^{-4}$
$\|V_{ub}\|$(incl.)	$43.9 \cdot 10^{-4}$	$2.0 \cdot 10^{-4}$	$2.7 \cdot 10^{-4}$
Δm_d	0.502 ps^{-1}	0.006 ps^{-1}	-
Δm_s	> 14.5 ps^{-1} @ 95% C.L.		
$f_{B_s}\sqrt{\hat{B}_{B_s}}$	276 MeV	38 MeV	-
ξ	1.24	0.04	0.06
$\hat{B}_K$	0.79	0.04	0.09
ε_K	$2.28 \cdot 10^{-3}$	$1.3 \cdot 10^{-5}$	-
f_K	159 MeV	fixed	
$\sin 2\beta$	0.687	0.032	-
$\overline{m}_t$	165.0 GeV	3.9 GeV	-
$\overline{m}_b$	4.21 GeV	0.08 GeV	-
$\overline{m}_c$	1.3 GeV	0.1 GeV	-
$\alpha_s(M_Z)$	0.119	0.003	-

Including this error, we obtain the constraint on $\sin(2\beta+\gamma)$ shown in Fig. 3, together with the impact on the $\bar{\rho}-\bar{\eta}$ plane.

The angle α can be extracted from the time-dependent CP asymmetry in $B \to \pi\pi$, $\rho\pi$, $\rho\rho$ decays, with the uncertainty related to penguin pollution. Given the presently unclear experimental situation and the large penguin pollution, we do not consider here $B \to \pi\pi$ decays. The determination of α from the other modes using the BaBar data and the corresponding constraint on the $\bar{\rho}-\bar{\eta}$ plane are reported in Fig. 4.

Using the angle measurements described above, it is possible to obtain a determination of the UT with an accuracy comparable to the determination obtained using all the other measurements (see Fig. 5). The UT fit is therefore now strongly overconstrained, and it tests in a highly nontrivial way the CKM picture of flavour and CP violation.

Combining all available information, we obtain the "state of the art" determination in Fig. 5, and the results for UT parameters reported in Table 2. Comparing the results of the fit with the input values, there is a small ($< 2\sigma$)

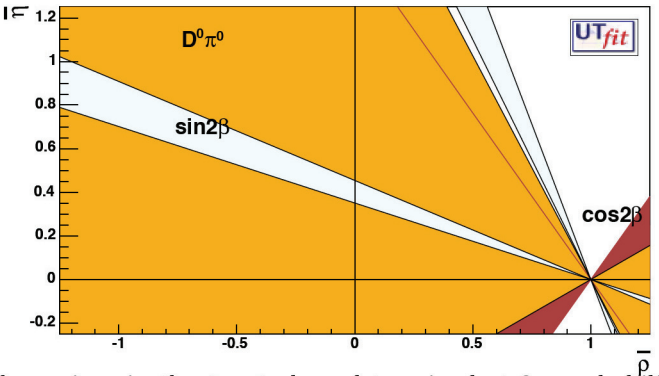

Figure 1: The regions in the $\bar{\rho} - \bar{\eta}$ plane determined at 2σ probability by the measurements of $\cos 2\beta$ and β. For reference, the region selected by $\sin 2\beta$ is also reported.

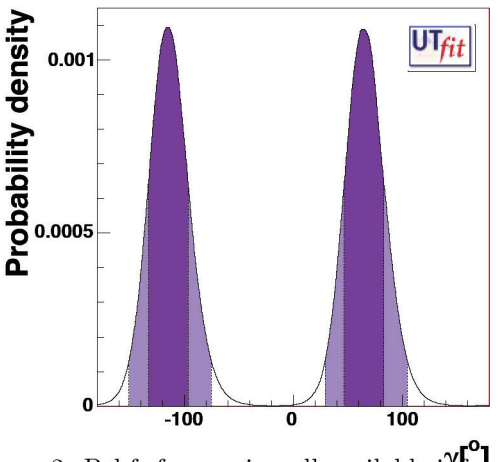

Figure 2: P.d.f. for γ using all available information.

discrepancy in the values of $\sin 2\beta$ and $|V_{ub}|$ from inclusive decays.

3 Constraints on NP from the UT

We remarked in the previous section that the UT fit is now strongly over-constrained. It is therefore possible to add NP contributions to all quantities entering the UT analysis and to perform a combined fit of NP contributions

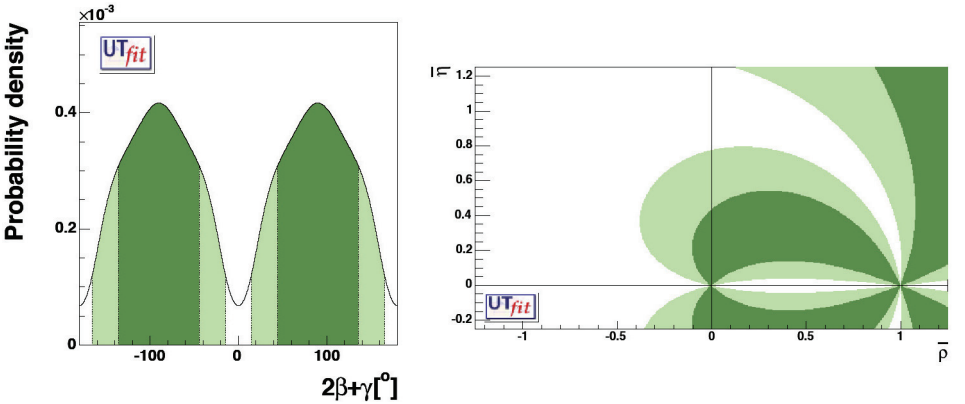

Figure 3: P.d.f. for $2\beta + \gamma$ and its impact on the $\bar{\rho} - \bar{\eta}$ plane.

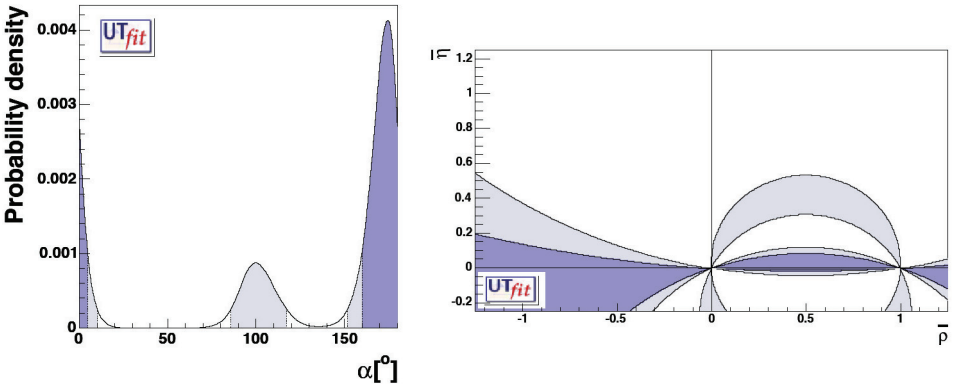

Figure 4: P.d.f. for α and its impact on the $\bar{\rho} - \bar{\eta}$ plane.

and SM parameters. In general, NP models introduce a large number of new parameters: flavour changing couplings, short distance coefficients and matrix elements of new local operators. The specific list and the actual values of these parameters can only be determined within a given model. Nevertheless, each

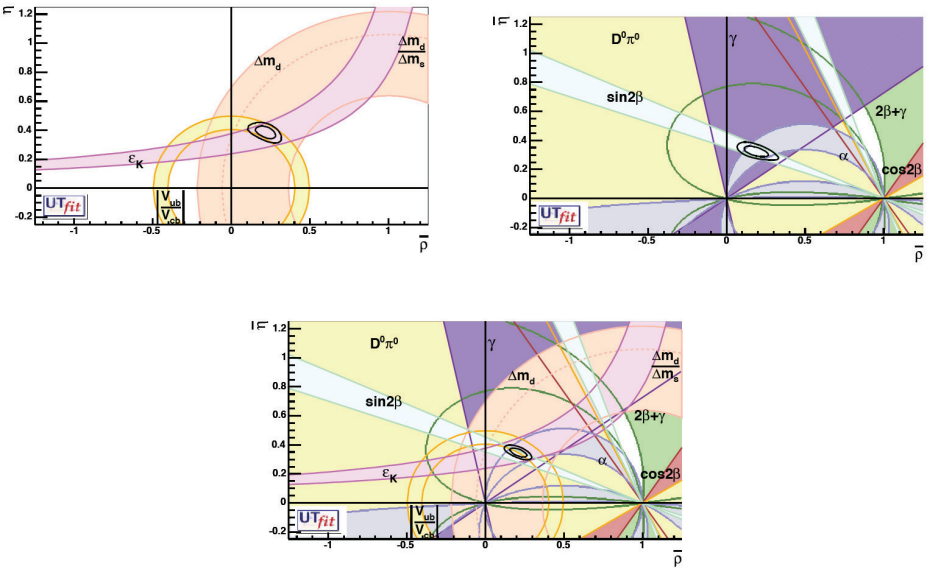

Figure 5: Determinations of the UT without using angle measurements (top), using only angles (middle) and using all information (bottom).

Table 2: Values and probability ranges for the UT parameters obtained from the UT fit using all constraints.

	68%	95%
$\bar{\rho}$	0.208 ± 0.036	$[0.135, 0.277]$
$\bar{\eta}$	0.347 ± 0.021	$[0.306, 0.388]$
$\alpha[^\circ]$	97.1 ± 5.6	$[86.0, 107.7]$
$\beta[^\circ]$	23.8 ± 1.4	$[21.3, 26.2]$
$\gamma[^\circ]$	58.9 ± 5.4	$[48.7, 69.9]$
$\sin 2\beta$	0.736 ± 0.023	$[0.690, 0.781]$
$\lvert V_{ub}\rvert\ [10^{-4}]$	38.5 ± 1.4	$[35.7, 41.4]$

of the meson-antimeson mixing processeses is described by a single amplitude and can be parameterized, without loss of generality, in terms of two parameters, which quantify the difference between the full amplitude snd the SM one.

Thus, for instance, in the case of $B_q^0 - \bar{B}_q^0$ mixing we define

$$C_{B_q} e^{2i\phi_{B_q}} = \frac{\langle B_q^0 | H_{\rm eff}^{\rm full} | \bar{B}_q^0 \rangle}{\langle B_q^0 | H_{\rm eff}^{\rm SM} | \bar{B}_q^0 \rangle}, \ (q = d, s) \tag{1}$$

where $H_{\rm eff}^{\rm SM}$ includes only the SM box diagrams, while $H_{\rm eff}^{\rm full}$ includes also the NP contributions. As far as the $K^0 - \bar{K}^0$ mixing is concerned, we find it convenient to introduce a single parameter C_{ϵ_K} which relates the imaginary part of the amplitude to the SM one. Therefore, all NP effects in $\Delta F = 2$ transitions are parameterized in terms of three real quantities, C_{B_d}, ϕ_{B_d} and C_{ϵ_K}. NP in the B_s sector is not considered, due to the lack of experimental information, since both Δm_s and $A_{\rm CP}(B_s \to J/\psi\phi)$ are not yet measured.

NP effects in $\Delta B = 1$ transitions can also affect some of the measurements entering the UT analysis, in particular the measurements of α and of the semileptonic asymmetry $A_{\rm SL}$ [2]. However, under the hypothesis that NP contributions are mainly $\Delta I = 1/2$, their effect can be taken into account in the fit of the $B \to \pi\pi, \rho\pi, \rho\rho$ decay amplitudes. Concerning $A_{\rm SL}$, penguins only enter at the Next-to-Leading order and therefore NP in $\Delta B = 1$ transitions produces subdominant effects with respect to the leading $\Delta B = 2$ contribution.

The results obtained in a global fit for C_{B_d}, C_{ϵ_K}, C_{B_d} vs. ϕ_{B_d}, and γ vs. ϕ_{B_d} are shown in Fig. 6, together with the corresponding regions in the $\bar{\rho}$–$\bar{\eta}$ plane [2]. The constraints on C_{B_d} and ϕ_{B_d} can be translated into bounds on the amplitude and phase of the NP contribution, writing

$$C_{B_d} e^{2i\phi_{B_d}} = \frac{A_{\rm SM} e^{2i\beta} + A_{\rm NP} e^{2i(\beta+\phi_{\rm NP})}}{A_{\rm SM} e^{2i\beta}}, \tag{2}$$

The result is reported in Fig. 7. We see that the NP contribution can be substantial if its phase is close to the SM phase, while for arbitrary phases its magnitude has to be much smaller than the SM one. Notice that, with the latest data, the SM ($\phi_{B_d} = 0$) is disfavoured at 68% probability due to the disagreement in the SM fit discussed in the previous section. This requires $A_{\rm NP} \neq 0$ and $\phi_{\rm NP} \neq 0$. For the same reason, $\phi_{\rm NP} > 90°$ at 68% probability and the plot is not symmetric around $\phi_{\rm NP} = 90°$. Assuming that the small but non-vanishing value for ϕ_{B_d} we obtained is just due to a statistical fluctuation, the result of our analysis points either towards models with no new source of flavour and CP violation beyond the ones present in the SM (Minimal Flavour Violation, MFV [5]), or towards models in which new sources of flavour and

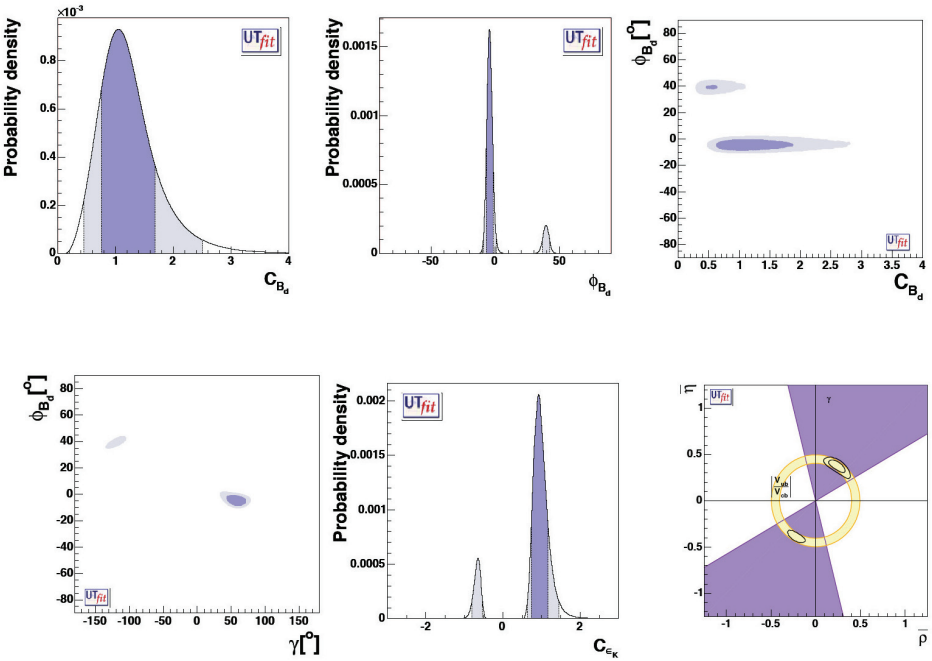

Figure 6: From top to bottom and from left to right, p.d.f.'s for C_{B_d}, ϕ_{B_d}, ϕ_{B_d} $vs.$ C_{B_d}, ϕ_{B_d} $vs.$ γ, C_{ϵ_K} and the selected region on the $\bar{\rho}-\bar{\eta}$ plane obtained from the NP analysis. In the last plot, selected regions corresponding to 68% and 95% probability are shown, together with 95% probability regions for γ (from DK final states) and $|V_{ub}/V_{cb}|$. Dark (light) areas correspond to the 68% (95%) probability region.

CP violation are only present in $b \to s$ transitions. The UT determination and rare decays in MFV models have been recently discussed in refs. [2, 6].

4 Acknowledgments

We would like to warmly thanks the organisers of the DIF06 Workshop for the invitation and for having set a very interesting workshop in a nice atmosphere.

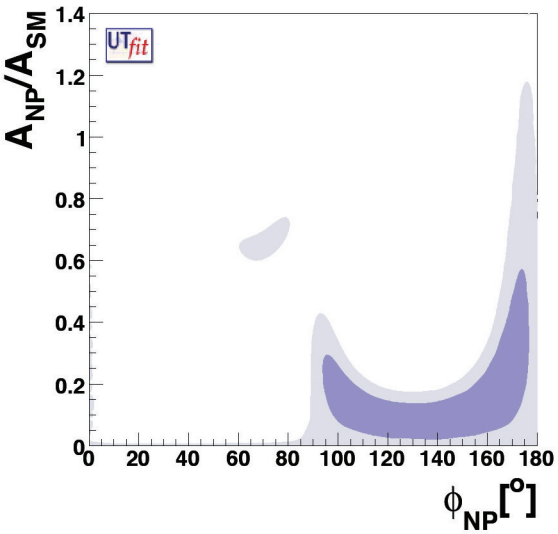

Figure 7: P.d.f. in the $(A_{\rm NP}/A_{\rm SM})$ vs. $\phi_{\rm NP}$ plane for NP in the $|\Delta B| = 2$ sector (see Eq. (2)).

References

1. M. Bona *et al.* [UTfit Collaboration], JHEP **0507** (2005) 028 [arXiv:hep-ph/0501199]; `www.utfit.org`.
2. M. Bona *et al.* [UTfit Collaboration], JHEP **0603** (2006) 080 [arXiv:hep-ph/0509219]; `www.utfit.org`.
3. J. Charles *et al.* [CKMfitter Group], Eur. Phys. J. C **41** (2005) 1; Z. Ligeti, arXiv:hep-ph/0408267; F. J. Botella *et al.*, Nucl. Phys. B **725** (2005) 155; K. Agashe *et al.*, arXiv:hep-ph/0509117.
4. The Heavy Flavour Averaging Group, summer 2005 averages. `http://www.slac.stanford.edu/xorg/hfag/`
5. E. Gabrielli and G. F. Giudice, Nucl. Phys. B **433** (1995) 3 [Erratum-ibid. B **507** (1997) 549]; G. D'Ambrosio *et al.*, Nucl. Phys. B **645** (2002) 155; A. J. Buras *et al.*, Phys. Lett. B **500** (2001) 161.
6. C. Bobeth *et al.*, Nucl. Phys. B **726** (2005) 252.

Frascati Physics Series Vol. XLI (2006), pp. 355-360
DISCOVERIES IN FLAVOUR PHYSICS AT e^+e^- COLLIDERS
Frascati, February 28th - March 3rd, 2006

NEW PHYSICS AT BABAR

Kim Hojeong
Department of Physics, McGill University, Montreal, QC, Canada

Abstract

Recent results from *BABAR* on leptonic or radiative rare B decays are presented. The first upper limit on $B^0 \to \tau^+\tau^-$ and updated upper limits on $B^+ \to \tau^+\nu$ and $B \to (\rho/\omega)\gamma$ are reported. Updated branching fraction measurements for $B \to X_s\gamma$ and $B \to K^{(*)}l^+l^-$ and *CP* asymmetries from those channels are presented.

1 Introduction

Rare decays of the B meson provide important tests of the Standard Model (SM). Purely leptonic decays of the B are predicted to exist, but have never been observed; radiative B decays are also a sensitive probe of the B meson structure. These decays are also sensitive to models of physics beyond the SM, and their study can place limits on such models. All the upper limits presented here are at 90% confidence level.

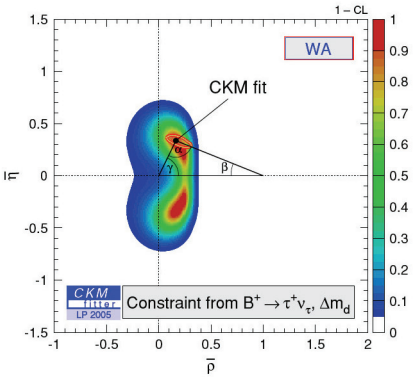

Figure 1: The constraint on $(\bar{\rho}, \bar{\eta})$ [3] from $\mathcal{B}\,(B^+ \to \tau^+\nu)$ combined with $\Delta m(B_d)$.

2 $B^+ \to \tau^+\nu$

Among $B^+ \to l^+\nu$ modes, $B^+ \to \tau^+\nu$ has the largest expected branching fraction, due to decreased helicity suppression. *BABAR* has a result [1] with 232 million $B\bar{B}$ pairs. One semileptonic B decay in each event is reconstructed, to reduce background. The neutrino four-momentum can be determined assuming the B momentum is small in the $\Upsilon(4S)$ rest frame. With one B meson accounted for, candidates are selected for the following decays of τ^+: $e^+\nu\bar{\nu}$, $\mu^+\nu\bar{\nu}$, $\pi^+(\pi^0)\nu$ and $\pi^+\pi^-\pi^+\nu$. The upper limit is set at 2.8×10^{-4}. The combined result with the statistically independent *BABAR* analysis using hadronic tag($< 4.2 \times 10^{-4}$) is $\mathcal{B}(B^+ \to \tau^+\nu) < 2.6 \times 10^{-4}$. This branching fraction, along with the mass difference $\Delta m(B_d)$ [2], constrains the unitarity triangle as shown in Fig. 1.

3 $B^0 \to \tau^+\tau^-$

As in the case of $B^+ \to \tau^+\nu$, among $B \to l^+l^-$ modes, $B^0 \to \tau^+\tau^-$ has the largest expected branching fraction. However, since the event has 2 to 4 neutrinos, the reconstruction is more difficult than in the e or μ channels. *BABAR* sets the first preliminary upper limit, with a sample of 232 million

$B\bar{B}$ events [4]. Any signal candidate must be accompanied by one hadronically decaying B. Using the tracks and neutrals not associated with this tagging B, a signal is reconstructed for the following decays of τ^+: $(\pi^+/\rho^+)\nu$ and $l^+\nu\bar{\nu}$. The upper limit is set: $\mathcal{B}(B^0 \to \tau^+\tau^-) < 3.2 \times 10^{-3}$. This measurement also sets an upper limit on the leptoquark couplings $\lambda_R^{33}\lambda_R^{13}$ at $1.1 \times 10^{-2}[m_{S_{1/2}}/100\,\mathrm{GeV}]^2$, where $m_{S_{1/2}}$ is the mass of leptoquark $S_{1/2}$ [5].

4 $B \to X_s\gamma$

There are two independent *BABAR* measurements of $B \to X_s\gamma$. One method is fully inclusive [6] which is insensitive to fragmentation effects but has a large background. The other is the sum of exclusive modes [7] which has a significant error on the fraction of unmeasured final states but has less background. The branching fractions are shown in Fig. 2 (a).

4.1 Fully Inclusive

Events with a high energy lepton and a high energy photon are selected from a sample of 90 million $B\bar{B}$ events. The lepton is from a semileptonically decaying B meson, and the photon is from the signal. Requiring a semileptonic B meson in the event reduces backgrounds from non $b\bar{b}$ events by a factor of about 1300. The preliminary partial branching fraction is $\mathcal{B}(B \to X_s\gamma) = (3.67 \pm 0.29_{stat} \pm 0.34_{syst} \pm 0.29_{theo}) \times 10^{-4}$, in the range of 1.9 to 2.7 GeV of the B-rest frame photon energy . The CP asymmetry[1] has been measured with X_{s+d}: $A_{CP}(B \to X_{s+d}\gamma) = 0.11 \pm 0.115_{stat} \pm 0.017_{syst}$. The SM prediction is of the order of 10^{-9} [8] but some models of new physics can enhance it up to the level of 10^{-2} [9].

4.2 Sum of Exclusive Modes

A total of 38 exclusive modes are reconstructed from a sample of 89 million $B\bar{B}$ events. One high energy photon is combined with a $K^\pm$ or a K_S, and several $\pi^\pm$ or π^0. This covers about 60% of all final states, or 80% assuming K_S and K_L have the same distribution. An unbinned maximum likelihood fit is made to extract the signal. The *BABAR* measurement with photon energy

[1] $A_{CP}(X) = \frac{\Gamma(X)-\Gamma(\bar{X})}{\Gamma(X)+\Gamma(\bar{X})}$

$E_\gamma > 1.9\,\mathrm{GeV}$ is $\mathcal{B}(B \to X_s\gamma) = (3.27 \pm 0.18^{+0.55+0.04}_{-0.40-0.09}) \times 10^{-4}$, where errors are statistical, systematic and theoretical, respectively. The *CP* asymmetry has been measured with X_s [10]: $A_{CP}(B \to X_s\gamma) = 0.025 \pm 0.050_{stat} \pm 0.015_{syst}$.

5 $B \to (\rho/\omega)\gamma$

The exclusive decay modes $B^+ \to \rho^+\gamma$, $B^0 \to \rho^0\gamma$ and $B^0 \to \omega\gamma$ stem from the quark level transition $b \to d\gamma$. These rates are related by the spectator quark model, and one can define an average branching fraction, $\mathcal{B}(B \to (\rho/\omega)\gamma) = \frac{1}{2}\{\mathcal{B}(B^+ \to \rho^+\gamma) + \frac{\tau_{B^+}}{\tau_{B^0}}[\mathcal{B}(B^0 \to \rho^0\gamma) + \mathcal{B}(B^0 \to \omega\gamma)]\}$, where $\tau_{B^+(B^0)}$ is the lifetime of the $B^+(B^0)$ meson. *BABAR* sets an upper limit for each mode with a sample of 211 million $B\bar{B}$ events [11]: $\mathcal{B}(B^+ \to \rho^+\gamma) < 1.8 \times 10^{-6}$, $\mathcal{B}(B^0 \to \rho^0\gamma) < 0.4 \times 10^{-6}$ and $\mathcal{B}(B^0 \to \omega\gamma) < 1.0 \times 10^{-6}$, and on the average branching fraction: $\mathcal{B}(B \to (\rho/\omega)\gamma) < 1.2 \times 10^{-6}$. These are summarized in Fig. 2 (b). The ratio $\Gamma(B \to (\rho/\omega)\gamma)/\Gamma(B \to K^*\gamma)$ is related to $|V_{td}/V_{ts}|$ [12], where V_{td} and V_{ts} are CKM matrix elements [13]. The *BABAR* measurements of $\mathcal{B}(B \to (\rho/\omega)\gamma)$ and $\mathcal{B}(B \to K^*\gamma)$ [14] allow for the measurement of $|V_{td}/V_{ts}| < 0.19$, neglecting theoretical uncertainties.

6 $B \to K^{(*)}l^+l^-$

A total of 8 modes are measured: $K^\pm$, K_S, $K^\pm\pi^\mp$ or $K_S\pi^\pm$ combined with e^+e^- or $\mu^+\mu^-$. An unbinned maximum likelihood fit is made to extract the signal. The preliminary *BABAR* results [15] with a sample of 229 million $B\bar{B}$ events are: $\mathcal{B}(B \to Kl^+l^-) = (0.34 \pm 0.07 \pm 0.03) \times 10^{-6}$ and $\mathcal{B}(B \to K^*l^+l^-) = (0.78^{+0.19}_{-0.17} \pm 0.12) \times 10^{-6}$. The errors are statistical and systematic, respectively. The results are summarized in Fig. 2 (c). The *CP* asymmetry has been measured using $K^\pm$ for B flavor tagging: $A_{CP}(B \to Kl^+l^-) = 0.08 \pm 0.22_{stat} \pm 0.11_{syst}$ and $A_{CP}(B \to K^*l^+l^-) = -0.03 \pm 0.23_{stat} \pm 0.11_{syst}$. The SM prediction is less than 1% [16] while some new physics can enhance it up to order of 1 [17]. The ratios $R_{K^{(*)}} = K^{(*)}\mu\mu/K^{(*)}e^+e^-$ are also measured: $R_K = 1.06 \pm 0.48_{stat} \pm 0.05_{syst}$ and $R^*_K = 0.93 \pm 0.46_{stat} \pm 0.06_{syst}$. The SM prediction is $R_K = 1$ and $R^*_K = 0.75$ while some new physics can enhance it up to 10% [18]. $R^*_K < 1$ is due to a photon pole at $m^2_{l^+l^-} = 0$.

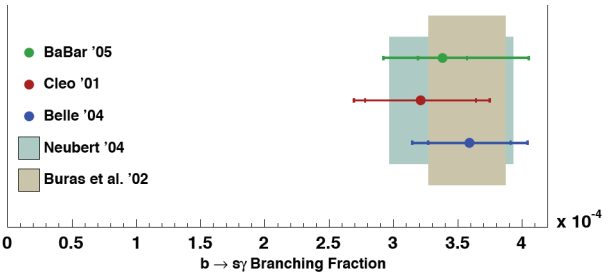

(a)

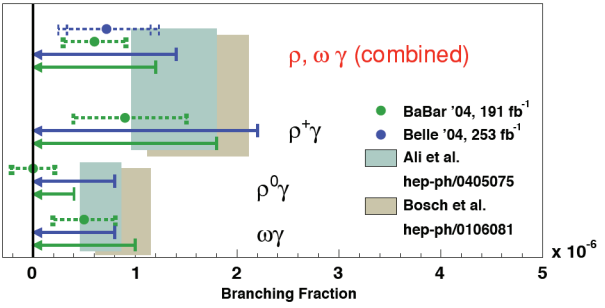

(b)

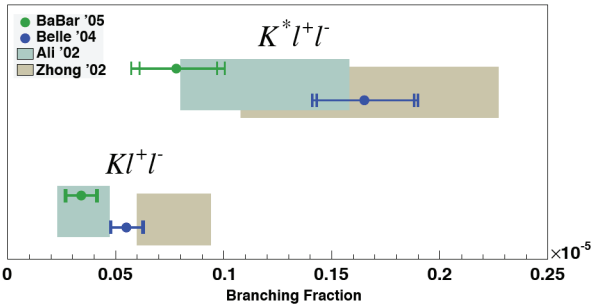

(c)

Figure 2: Measurements and models for (a) $\mathcal{B}\,(B \to X_s\gamma)$ (b) $\mathcal{B}\,(B \to (\rho/\omega)\gamma)$ (c) $\mathcal{B}\,(B \to K^{(*)}l^+l^-)$

7 Summary

The rich data samples at *BABAR* allow extensive studies of rare decays. No deviation from the SM has been observed. *BABAR* luminosity is expected to be 1 ab^{-1} by the year 2008. It will permit more stringent tests on the SM through studies on leptonic or radiative rare B decays.

References

1. B. Aubert *et al.*, Phys. Rev. D **73**, 057101 (2006).
2. Heavy Flavor Averaging Group, hep-ex/0412073.
3. http://www.slac.stanford.edu/xorg/ckmfitter/ckm_results_summer2005.html.
4. B. Aubert *et al.*, hep-ex/0511015.
5. Y. Grossman *et al.*, Phys. Rev. D **55**, 2768 (1997).
6. B. Aubert *et al.*, hep-ex/0507001.
7. B. Aubert *et al.*, Phys. Rev. D **72**, 052004 (2005).
8. T. Hurth and T. Manuel, Phys. Lett. B **511**, 196 (2001).
9. T. Hurth *et al.*, Nucl. Phys. B **704**, 56 (2005).
10. B. Aubert *et al.*, Phys. Rev. Lett. **93**, 021804 (2004).
11. B. Aubert *et al.*, Phys. Rev. Lett. **94**, 011801 (2005).
12. A. Ali *et al.*, Phys. Lett. B **595**, 323 (2004).
13. N. Cabibbo, Phys. Rev. Lett. **10**, 531 (1963).
14. B. Aubert *et al.*, Phys. Rev. D **70**, 112006 (2004).
15. B. Aubert *et al.*, hep-ex/0507005.
16. F. Krüger *et al.*, Phys. Rev. D **61**, 114028 (2000), Erratum-ibid. D **63**, 019901 (2001).
17. F. Krüger and E. Lunghi, Phys. Rev. D **63**, 014013 (2001).
18. G. Hiller and F. Krüger, Phys. Rev. D **69**, 074020 (2004).

Frascati Physics Series Vol. XLI (2006), pp. 361-370
DISCOVERIES IN FLAVOUR PHYSICS AT e^+e^- COLLIDERS
Frascati, February 28th - March 3rd, 2006

NEW MEASUREMENTS OF THE ANGLE γ FROM THE *BABAR* EXPERIMENT

Toyoko Jennifer Orimoto
(on behalf of the *BABAR* Collaboration)
Lawrence Berkeley National Laboratory, 1 Cyclotron Road, Berkeley, CA 94720

Abstract

Measuring the angle γ is an important part of over-constraining the Unitarity Triangle to test Standard Model predictions. There are a number of methods to measure γ, and we present results on the progress made in measuring γ with B meson decays, using data collected with the *BABAR* detector at the PEP-II asymmetric energy e^+e^- collider at SLAC.

1 Introduction

The Cabibbo-Kobayashi-Maskawa (CKM) quark flavor-mixing matrix [1] provides an elegant explanation of the origin of *CP* violation within the Standard Model of particle interactions. *CP* violation manifests itself as a non-zero area of the Unitarity Triangle of the CKM matrix [2]. While it is sufficient to measure one of the angles to demonstrate the existence of *CP* violation, the

Unitarity Triangle must be over-constrained to demonstrate that the CKM mechanism is the correct explanation of this phenomenon. We report on the latest measurements of the angle γ from the *BABAR* Experiment.

2 γ from $B^- \to D^{(*)0}K^{(*)-}$ Decays

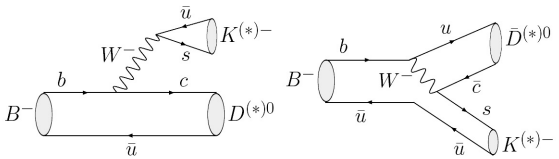

Figure 1: *Feynman diagrams for CKM and color-favored* $B^- \to D^{(*)0}K^{(*)-}$ *(left) and CKM and color-suppressed* $B^- \to \bar{D}^{(*)0}K^{(*)-}$ *(right).*

The decays $B^- \to \tilde{D}^{(*)0}K^{(*)-}$ can be used to probe γ since $b \to c\bar{u}s$ and $b \to u\bar{c}s$ transitions have a relative weak phase of γ. $\tilde{D}^0$ indicates either a D^0 or $\overline{D}^0$ meson, and "(*)" indicates either a D or D^* meson. These decays are particularly attractive for *CP* studies since they are tree-level processes, which lack the theoretical uncertainties that can arise from penguin processes. Figure 1 depicts the Feynman diagrams for the color-suppressed mode $B^- \to D^{(*)0}K^{(*)-}$ and the color-favored mode $B^- \to \bar{D}^{(*)0}K^{(*)-}$. The ratio of the suppressed amplitude to the favored amplitude is proportional to $r_B^{(*)} e^{i\delta_B^{(*)}} e^{i\gamma}$, where $r_B^{(*)} \equiv \frac{|A(B^- \to D^{(*)0}K^-)|}{|A(B^- \to \bar{D}^{(*)0}K^-|}$ is the ratio of the magnitudes of the suppressed and favored amplitudes, $\delta_B^{(*)}$ is the unknown relative strong phase, and γ is the relative weak phase between the decays, which can be written in terms of the CKM matrix elements as $\gamma \equiv \arg\left[-\frac{V_{ud}V_{ub}^*}{V_{cd}V_{cb}^*}\right]$. $r_B^{(*)}$ is estimated to be $\sim 0.1-0.3$ [3]. $r_B^{(*)}$ is a crucial parameter since it is a measure of the interference between these decays and thus indicates our sensitivity to measuring γ. In order to measure the phase γ, these decays must interfere, and this occurs when the same final state f is accessible by both the D^0 and $\bar{D}^0$.

A number of theoretically clean methods are available for measuring γ from $B^- \to \tilde{D}^{(*)0}K^{(*)-}$ decays. We report here measurements of γ from *BABAR* using the Gronau-London-Wyler (GLW) [4], the Atwood-Dunietz-Soni (ADS) [5], and the Giri-Grossman-Soffer-Zupan (GGSZ) Dalitz [6] methods. Although these methods similarly rely on the interference of B decays into $\tilde{D}^0K$, they differ in the use of the final state of the D meson.

2.1 γ from the Gronau-London-Wyler Method

The GLW method exploits the relationship between the *CP* and flavor states of the neutral D mesons to measure γ. The *CP* even states that are used are $\pi^+\pi^-$ and K^+K^-, while the *CP* odd states used are $K^0_S\pi^0$, $K^0_S\phi$, $K^0_S\omega$. The results are usually expressed in terms of the ratio of the charge-averaged partial rates $R_{CP\pm}$ and the partial-rate charge asymmetries $A_{CP\pm}$, which arise from the relationships between the *CP* and flavor states:

$$R_{CP\pm} = \frac{\Gamma(B^- \to D^0_{CP\pm}K^-) + \Gamma(B^+ \to D^0_{CP\pm}K^+)}{\left[\Gamma(B^- \to D^0K^-) + \Gamma(B^+ \to \overline{D}^0K^+)\right]/2} \tag{1}$$

$$A_{CP\pm} = \frac{\Gamma(B^- \to D^0_{CP\pm}K^-) - \Gamma(B^+ \to D^0_{CP\pm}K^+)}{\Gamma(B^- \to D^0_{CP\pm}K^-) + \Gamma(B^+ \to D^0_{CP\pm}K^+)}, \tag{2}$$

where $D^0_{CP\pm} = (D^0 \pm \overline{D}^0)/\sqrt{2}$ are *CP* eigenstates of the neutral D mesons, written in terms of the flavor states. In the absence of D^0–$\overline{D}^0$ mixing [7], $R_{CP\pm}$ and $A_{CP\pm}$ are related to r_B, δ_B, and γ through the following relationships:

$$R_{CP\pm} = 1 + r_B^2 \pm 2r_B \cos\delta_b \cos\gamma \tag{3}$$

$$A_{CP\pm} = \pm 2r_B \sin\delta_B \sin\gamma / R_{CP\pm} \tag{4}$$

This results in three unknowns, r_B, δ_B, and γ and three independent observables, since $A_{CP+}R_{CP+} = A_{CP-}R_{CP-}$. In addition, this method results in a four-fold ambiguity on γ.

The GLW method is theoretically clean since it exploits relationships that are exact, and the hadronic uncertainties associated with the decays are small. However, this method is experimentally challenging since the branching fractions for these B and D decays are relatively small.

The latest results from the GLW analyses of $B^\pm \to D^0_{CP}K^{(*)\pm}$ from *BABAR*, based on a sample of 232 million $B\overline{B}$ events, can be seen in Table 1 [8], [9]. The signal yields are 131 ± 17 *CP* even and 148 ± 17 *CP* odd events for $B^\pm \to D^0_{CP}K^\pm$ and 37.6 ± 7.4 *CP* even and 14.8 ± 5.9 *CP* odd states for $B^\pm \to D^0_{CP}K^{*\pm}$. The results for r_B^2 from these analysis are $-0.12 \pm 0.08(\text{stat}) \pm 0.03(\text{syst})$ for $B^\pm \to D^0_{CP}K^\pm$ and 0.30 ± 0.25 for $B^\pm \to D^0_{CP}K^{*\pm}$. Thus far the GLW analyses do not tightly constrain r_B and more statistics are needed.

Table 1: *Measured ratios $A_{CP\pm}$ and $R_{CP\pm}$ for CP-even and CP-odd D decay modes. The first error is statistical and the second is systematic.*

	$B^\pm \to D^0_{CP} K^\pm$	$B^\pm \to D^0_{CP} K^{*\pm}$
A_{CP+}	$0.35 \pm 0.13 \pm 0.04$	$-0.08 \pm 0.19 \pm 0.08$
A_{CP-}	$-0.06 \pm 0.13 \pm 0.04$	$-0.26 \pm 0.40 \pm 0.12$
R_{CP+}	$0.90 \pm 0.12 \pm 0.04$	$1.96 \pm 0.40 \pm 0.11$
R_{CP-}	$0.86 \pm 0.10 \pm 0.05$	$0.65 \pm 0.26 \pm 0.08$

2.2 γ from the Atwood-Dunietz-Soni Method

The ADS method is similar to the GLW method, except that it utilizes doubly Cabibbo-suppressed (DCS) decays rather than *CP* eigenstates. For the GLW method, *CP* asymmetries tend to be small because of the CKM and color suppression between the two interfering modes. In the ADS method, the *CP* violating effects can be enhanced when the final states are chosen to balance CKM and color suppression factors. For instance, the decays can be selected such that the color-favored B decay subsequently decays through a DCS D decay, and the color-suppressed B decay subsequently decays through a relatively CKM-favored D decay. However, the branching fractions for the DCS decays are small, and this method suffers from low yields. The D mode chosen for the analyses presented here is $D^0 \to K^+\pi^-$.

For the ADS method, the observables are:

$$R_{ADS} = \frac{\Gamma(B^- \to [K^+\pi^-]_D K^{(*)-}) + \Gamma(B^+ \to [K^-\pi^+]_D K^{(*)+})}{\Gamma(B^- \to [K^-\pi^+]_D K^{(*)-}) + \Gamma(B^+ \to [K^+\pi^-]_D K^{(*)+})} \quad (5)$$

$$A_{ADS} = \frac{\Gamma(B^- \to [K^+\pi^-]_D K^{(*)-}) - \Gamma(B^+ \to [K^-\pi^+]_D K^{(*)+})}{\Gamma(B^- \to [K^+\pi^-]_D K^{(*)-}) + \Gamma(B^+ \to [K^-\pi^+]_D K^{(*)+})} \quad (6)$$

As in the GLW method, neglecting D^0–$\overline{D}^0$ mixing [7], R_{ADS} and A_{ADS} can be related to γ, the strong phases for the B and D decays, δ_B and δ_D, and the ratios of the suppressed-to-favored modes for the B and D decays, r_B and r_D:

$$R_{ADS} = r_D^2 + r_B^2 + 2 r_D r_B \cos(\delta_B + \delta_D) \cos\gamma \quad (7)$$

$$A_{ADS} = 2 r_D r_B \sin(\delta_B + \delta_D) \sin\gamma / R. \quad (8)$$

The CKM suppression factor for the D decay, $r_D \equiv \frac{|A(D^0 \to K^+\pi^-)|}{|A(D^0 \to K^-\pi^+)|}$, is constrained to the experimental value of 0.060 ± 0.003 [10]. r_B and δ_B can be

Table 2: *Results for R_{ADS} and r_B for $B^{\mp} \to \tilde{D}^0 K^{\mp}$ and $B^{\mp} \to \tilde{D}^{*0} K^{\mp}$. The first error is statistical and the second is systematic. r_B for $B^{\mp} \to \tilde{D}^0 K^{*\mp}$ arises from combining the ADS and GLW results.*

	$B^{\mp} \to \tilde{D}^0 K^{\mp}$	$B^{\mp} \to \tilde{D}^{*0} K^{\mp}$ $\tilde{D}^{*0} \to \tilde{D}^0 \pi^0$	$B^{\mp} \to \tilde{D}^{*0} K^{\mp}$ $\tilde{D}^{*0} \to \tilde{D}^0 \gamma$	$B^{\mp} \to \tilde{D}^0 K^{*\mp}$
R_{ADS}	$0.013^{+0.011}_{-0.009}$	$-0.002^{+0.010}_{-0.006}$	$0.011^{+0.018}_{-0.013}$	$0.046 \pm 0.031 \pm 0.008$
R_{ADS} 90% C.L.	< 0.029	< 0.023	< 0.045	-
r_B	-	$0.004^{+0.014}_{-0.008}$		$0.28^{+0.06}_{-0.10}$
r_B 90% C.L.	< 0.23	-		-
r_B^{*2} 90% C.L.	-	$< (0.16)^2$		-

constrained to the values from the GLW analyses, leaving two unknowns, δ_D and γ, and two measurable observables in the ADS analysis.

The latest ADS results from *BABAR* are based on 232 million $B\overline{B}$ events [11], [12]. The analyses reconstruct 5^{+4}_{-3}, $-0.2^{+1.3}_{-0.7}$, $1.2^{+2.1}_{-1.4}$, and 4.2 ± 2.8 signal events for $\tilde{D}^0 K^-$, $\tilde{D}^{*0}(\tilde{D}^0\pi^0)K^-$, $\tilde{D}^{*0}(\tilde{D}^0\pi^0)K^-$, and $\tilde{D}^0 K^{*-}(K_S\pi^-)$ modes, respectively. No significant signal is observed in any of the channels studied. The results for R_{ADS} and r_B are shown in Table 2. For the $B \to \tilde{D}^0 K$ channel, a limit on r_B is placed by allowing any value for δ_D and γ and a 1σ variation of r_D. The r_B result for $B \to \tilde{D}^0 K^*$ comes from combining the results for the ADS and GLW methods. This combined result for $B \to \tilde{D}^0 K^*$ also excludes the interval $75^\circ \leq \gamma \leq 105^\circ$ at the 2σ level. As in the case of the GLW analyses, more statistics are needed to put strong constraints on r_B.

2.3 γ from the Giri-Grossman-Soffer-Zupan Dalitz Method

The GGSZ method utilizes D decays into three-body final states. Since the D can access the three-body final state through a number of resonances, a Dalitz analysis is done to fit the $D^0 - \overline{D}^0$ interference region in the Dalitz plot and extract the desired *CP* parameters. One of the main advantages of this method is that by using a Dalitz fit, we can use the entire resonant structure of the three-body decay, including not only DCS decays, but also CKM-allowed decays as well as decays into *CP* eigenstates, thereby increasing our sensitivity to γ. The analysis presented here uses the common final state $K_S\pi^+\pi^-$, employing $K^0 - \bar{K}^0$ mixing in order to attain the same final state needed for intereference.

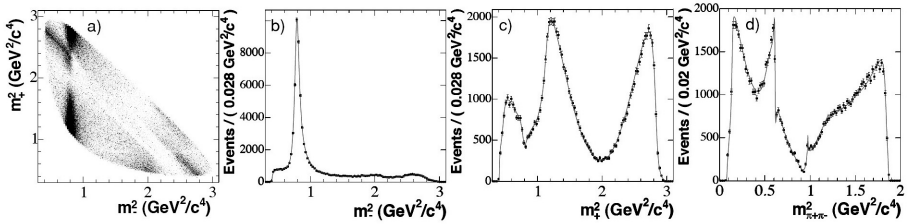

Figure 2: *(a) The $D^0 \to K_S\pi^-\pi^+$ Dalitz distribution from $D^{*+} \to D^0\pi^+$ events, and K-matrix model fit projections on (b) m_-^2, (c) m_+^2, and (d) $m_{\pi^+\pi^-}^2$. $\overline{D}^0 \to K_S\pi^+\pi^-$ from $D^{*-} \to \overline{D}^0\pi^-$ events are also included.*

The decay amplitude for $B^\mp \to \tilde{D}^{(*)0}K^\mp$ can be expressed as:

$$A_\mp^{(*)}(m_\mp^2, m_\pm^2) = A_D(m_\mp^2, m_\pm^2) + r_B^{(*)} e^{i(\delta_B^{(*)} \mp \gamma)} A_D(m_\pm^2, m_\mp^2) \qquad (9)$$

where m_-^2 and m_+^2 are the squared invariant masses $K_S\pi^-$ and $K_S\pi^+$, respectively, and A_D is the D decay amplitude.

The current data sample of $B \to \tilde{D}^{(*)0}K^{(*)}$ decays does not provide enough statisics to constrain A_D, which depends on the strong phase δ_D and ratio of amplitudes r_D, in addition to δ_B, r_B and γ. A high statistics sample of flavor tagged D^0 mesons from inclusive $D^{*0} \to D^0\pi^+$ decays is used to determine the D^0 decay amplitude. A fit model must be chosen when parametrizing the D^0 decay amplitude. The $B \to \tilde{D}^{(*)0}K$ analysis uses a Breit-Wigner model, which includes 13 relativistic Breit-Wigner resonances and one non-resonant term. This model has proved inadequate at describing $\pi\pi$ S-wave states, relying on the addition of $\sigma(500)$ and $\sigma'(1000)$ resonances, which are not well established, to improve the fit. A more accurate model based on the K-matrix formalism [14], [15] and better suited for describing broad-overlapping resonances is used for the $B \to \tilde{D}^0K^*$ analysis. Figure 2 shows the Dalitz distribution from the $D^{*+} \to D^0\pi^+$ sample and the projections from the fit.

Once the D^0 decay amplitude is determined, a simultaneous fit to the $|A_-^{(*)}(m_-^2, m_+^2)|^2$ and $|A_+^{(*)}(m_-^2, m_+^2)|^2$ distributions in the $B^\mp \to \tilde{D}^0K^\mp$ samples is used to extract $r_B^{(*)}$, $\delta_B^{(*)}$, and γ. Using a sample of 227 million $B\overline{B}$ events, 282 ± 20, 90 ± 11, 44 ± 8, and 42 ± 8 signal $\tilde{D}^0K^-$, $\tilde{D}^{*0}(\tilde{D}^0\pi^0)K^-$, $\tilde{D}^{*0}(\tilde{D}^0\gamma)K^-$, and $\tilde{D}^0K^{*-}(K_S\pi^-)$ events are reconstructed, respectively [13], [16]. Figure 3 shows the contour projections of the constraint regions for r_B and γ. For $B^- \to \tilde{D}^0K^{*-}$, a factor κ is introduced to take into account the contamination from $B^- \to \tilde{D}^0(K_S\pi^-)_{non-K^*}$ decays. There is two-fold ambiguity on γ

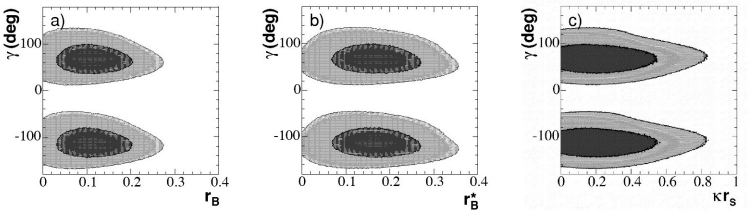

Figure 3: *Two-dimensional projections onto the (a) $r_B - \gamma$, (b) $r_B^{(*)} - \gamma$, and (c) $\kappa r_s - \gamma$ planes of the seven-dimensional one- (dark) and two- (light) standard deviation regions, for the combination of $B^- \to \tilde{D}^{*0} K^-$ and $B^- \to \tilde{D}^0 K^{*-}$.*

from this method. Combining the three modes results in $\gamma = (67 \pm 28(\text{stat}) \pm 13(\text{syst}) \pm 11(\text{model}))^\circ$, where the third error is due to the uncertainty in the Dalitz fit model.

3 $\sin(2\beta + \gamma)$ from $B^0 \to D\pi$, $B^0 \to D^*\pi$, and $B^0 \to D\rho$ Decays

The results presented thus far in this paper rely on time-independent methods for extracting γ. The study of time-dependent asymmetries in neutral B decays $B^0 \to D^{(*)}\pi$ and $B^0 \to D\rho$ can also be used to measure $\sin(2\beta + \gamma)$, and hence γ. Like the analyses described earlier, this method studies the interference between CKM-suppressed $b \to u$ and CKM-favored $b \to c$ transitions, which have a relative weak phase of γ. In the time-dependent study there is an additional weak phase of 2β from $B^0 - \overline{B}^0$ mixing. The dominant Feynman diagrams for the CKM-favored decay $B^0 \to D^-\pi^+$ and the doubly CKM-suppressed decay $B^0 \to D^+\pi^-$ can seen in Figure 4. The ratio between suppressed and favored decays is estimated to be ~ 0.02, and thus, the *CP* violating effects are expected to be small using this method.

The expression for time-dependent decay rate for the B^0 decaying to final state $\mu = D\pi, D^*\pi, D\rho$, neglecting the decay width difference, is:

$$f^{\pm,\mu}(\eta, \Delta t) = \frac{e^{-|\Delta t|/\tau}}{4\tau} \times [1 \mp (a^\mu \mp \eta b - \eta c^\mu) \sin(\Delta m_d \Delta t) \mp \eta \cos(\Delta m_d \Delta t)] \quad (10)$$

where τ is the B^0 lifetime, Δm_d is the $B^0 - \overline{B}^0$ mixing frequency, and Δt is the time difference between the $B^0 \to D^{(*)\pm}\pi^\mp$ or $B^0 \to D^\pm\rho^\pm$ decay (B_{rec}) and the decay of the other B from the $\Upsilon(4S)$ decay (B_{tag}). The upper (lower) sign refers to the flavor of the tagged B as B^0 ($\overline{B}^0$), while $\eta = +1(-1)$ for the

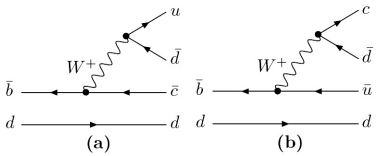

Figure 4: *Feynman diagrams for (a) the CKM-favored decay* $B^0 \to D^-\pi^+$ *and (b) the doubly CKM-suppressed decay* $B^0 \to D^+\pi^-$

final state with a $D^{(*)-}(D^{(*)+})$. a^μ, b and c^μ can be written in terms of the *CP* parameters r^μ, δ^μ, and $2\beta+\gamma$ as:

$$a^\mu = 2r^\mu \sin(2\beta+\gamma)\cos\delta^\mu \tag{11}$$

$$b = 2r' \sin(2\beta+\gamma)\cos\delta' \tag{12}$$

$$c^\mu = 2\cos(2\beta+\gamma)(r^\mu \sin\delta^\mu - r' \sin\delta'). \tag{13}$$

The parameters r' and δ' account for the non-negligible *CP* violating effects on the tagged side of the decay. Only c^μ from events tagged with leptons, which have do not suffer from such tag-side interference, and a^μ are used in determining $\sin(2\beta+\gamma)$.

Since our experimental sensitivity is limited by the small size of r^μ, it is not possible to extract $\sin(2\beta+\gamma)$, δ^μ and r^μ from the available dataset. External input for r^μ is therefore needed. A measurement of the branching fractions for the the favored and suppressed modes would give us the required input, but unfortunately, the direct measurement of the branching fractions for the doubly CKM-suppressed modes are not possible because of the overwhelming background from the favored mode. However, assuming SU(3) flavor symmetry, r^μ can be related to the branching ratios for $B^0 \to D_s^{(*)+}\pi^-$ or $B^0 \to D_s^+\rho^-$, the measurements for which are more experimentally feasible [17], [18].

Full and partial reconstruction methods are used for studying $B^0 \to D^{*-}\pi^+$ decays. In the full reconstruction method, the decay chain is fully reconstructed, which results in a high signal purity, but low efficiency. In the partial reconstruction method, only the daughter pion of the B^0 and the slow pion from $D^{*-} \to D^0\pi^-$ decays are reconstructed, which results in a high efficiency but also a high level of backgrounds.

The results from *BABAR* using 232 million $B\overline{B}$ events, from both the full and partial reconstruction methods, are shown in Table 3 [19], [20]. The

Table 3: *Results for CP parameters* a^μ *and* c^μ_{lepton} *for* $B^0 \to D^{(*)}\pi$ *and* $B^0 \to D\rho$ *from full and partial reconstruction methods.*

mode	a^μ	c^μ_{lepton}
$B^0 \to D\pi$ (full reco)	$-0.010 \pm 0.023 \pm 0.007$	$-0.033 \pm 0.042 \pm 0.012$
$B^0 \to D^*\pi$ (full reco)	$-0.040 \pm 0.023 \pm 0.010$	$0.049 \pm 0.042 \pm 0.015$
$B^0 \to D\rho$ (full reco)	$-0.024 \pm 0.031 \pm 0.009$	$-0.098 \pm 0.055 \pm 0.018$
$B^0 \to D^*\pi$ (partial reco)	$-0.034 \pm 0.014 \pm 0.009$	$-0.019 \pm 0.022 \pm 0.013$

signal yields from the full reconstruction method are 15038 ± 132, 14002 ± 123, 8736 ± 101 events for $D\pi$, $D^*\pi$, and $D\rho$, respectively. The signal yields from the partial reconstruction method for $D^*\pi$ are 18710 ± 270 events in the lepton-tag category and 70580 ± 660 events in the kaon-tag category. The resulting lower limits on $|\sin(2\beta+\gamma)|$ at the 68% (90%) C.L. are $|\sin(2\beta+\gamma)| > 0.64$ (0.40) for $D^{(*)}\pi$ and $D\rho$ from the full reconstruction method, and $|\sin(2\beta+\gamma)| > 0.62$ (0.35) for $D^*\pi$ from the partial reconstruction method.

4 Conclusions

Although direct measurement of γ was impossible at the B-factories a few years ago, much progress has been made and it is now an important and significant part of constraining the Unitarity Triangle. The errors on γ are still statistically limited, but as *BABAR* collects more data, with an expected 1 ab^{-1} by 2008, the error on γ is estimated to decrease to less than 10°. We are now entering a phase when the direct measurement of the angles of the Unitarity Triangle can determine (ρ, η) at a comparable precision as all data combined.

5 Acknowledgements

I would like to thank my *BABAR* and PEP-II colleagues whose expertise and dedication made these results possible. This work was supported in part by U.S. Department of Energy contract DE-AC02-76SF00515.

References

1. N. Cabibbo, Phys. Rev. Lett. **10**, 531 (1963); M. Kobayashi and T. Maskawa, Prog. Theor. Phys. **49**, 652 (1973).

2. C. Jarlskog, in *CP Violation*, C. Jarlskog ed., World Scientific, Singapore (1988).

3. M. Gronau, Phys. Lett. **B557**, 198 (2003).

4. M. Gronau, D. London, Phys. Lett. B **253**, 483 (1991); M. Gronau, D. Wyler, Phys. Lett. B **265**, 172 (1991).

5. D. Atwood, I. Dunietz, A. Soni, Phys. Rev. Lett. **78**, 3257 (1997); Phys. Rev. D **70**, 091503 (2004).

6. A. Giri, Y. Grossman, A. Soffer, and J. Zupan, Phys. Rev. D **68**, 054018 (2003).

7. Y. Grossman, A. Soffer, J. Zupan, Phys. Rev. **D72**, 031501 (2005).

8. *BABAR* Collaboration, B. Aubert *et al.*, Phys. Rev. **D73** 051105 (2006).

9. *BABAR* Collaboration, B. Aubert *et al.*, Phys. Rev. **D72** 071103 (2005).

10. *BABAR* Collaboration, B. Aubert *et al.*, Phys. Rev. Lett. **91**, 171801 (2003).

11. *BABAR* Collaboration, B. Aubert *et al.*, Phys. Rev. **D72**, 032004 (2005).

12. *BABAR* Collaboration, B. Aubert *et al.*, Phys. Rev. **D72**, 071104 (2005).

13. *BABAR* Collaboration, B. Aubert *et al.*, Phys. Rev. Lett. **95**, 121802 (2005).

14. E. P. Wigner, Phys. Rev. 70 (1946) 15; S. U. Chung *et al.*, Ann. Physik 4 (1995) 404.

15. I. J. R. Aitchison, Nucl. Phys. **A189**, 417 (1972).

16. hep-ex/0507101

17. I. Dunietz, Phys. Lett. **B427**, 179 (1998).

18. hep-ex/0604012

19. hep-ex/0602049

20. *BABAR* Collaboration, B. Aubert *et al.*, Phys. Rev. **D71**, 112003 (2005).

ROUND TABLE

Role of e^+e^- Meson Factories at the Luminosity Frontier in the LHC Era

L. Maiani (Chair), R. Petronzio, S. Bertolucci, M. Calvetti

H. Yamamoto	Why is Flavour Physics Interesting in the LHC Era?
M. Giorgi	Why Should we Need a Super B-Factory ?
D.M. Asner	On the Case for a Super τ Charm Factory
F. Ferroni	What are the Arguments against Future Electron-Positron Colliders for Flavour Physics

Frascati Physics Series Vol. XLI (2006), pp. 373
DISCOVERIES IN FLAVOUR PHYSICS AT e^+e^- COLLIDERS
Frascati, February 28th - March 3rd, 2006

WHY IS FLAVOUR PHYSICS INTERESTING IN THE LHC ERA ?

Hitoshi Yamamoto
Tohoku University

Written contribution not received

Frascati Physics Series Vol. XLI (2006), pp. 375
DISCOVERIES IN FLAVOUR PHYSICS AT e^+e^- COLLIDERS
Frascati, February 28th - March 3rd, 2006

WHY SHOULD WE NEED A SUPERB-FACTORY?

Marcello Giorgi
INFN and Univ. di Pisa

Written contribution not received

Frascati Physics Series Vol. XLI (2006), pp. 377-392
DISCOVERIES IN FLAVOUR PHYSICS AT e^+e^- COLLIDERS
Frascati, February 28th - March 3rd, 2006

ON THE CASE FOR A SUPER τ-CHARM FACTORY

David M. Asner
Carleton University, 1125 Colonel By Drive
Ottawa, Ontario, Canada, K1S 5B6

Abstract

Design studies for a Super Flavor Factory (SFF), an asymmetric energy e^+e^- collider utilizing International Linear Collider (ILC) techniques and technology, are in progress. The capability to run at $\sqrt{s} = 3.770$ GeV could be included in the initial design. This report discusses the physics that can be probed with luminosity of $10^{35}\,\mathrm{cm}^{-2}\mathrm{s}^{-1}$ near τ-charm threshold.

1 Introduction

Design studies for a Super Flavor Factory (SFF), an asymmetric energy e^+e^- collider utilizing International Linear Collider (ILC) techniques and technology, are in progress [1]. Energy flexibility is an important component of the design. Luminosities of $10^{36}\,\mathrm{cm}^{-2}\mathrm{s}^{-1}$ at the $\Upsilon(4S)$ and $10^{35}\,\mathrm{cm}^{-2}\mathrm{s}^{-1}$ at the $\psi(3770)$

are expected. This report summarizes the physics that can be probed at a τ-charm threshold. The physics case for a Super τ-charm Factory ($10^{35}\,\mathrm{cm}^{-2}\mathrm{s}^{-1}$) or equivalently the case for designing the SFF with the capability to run at energies near $D\overline{D}$ threshold must be evaluated relative to the physics reach with the enormous τ and charm samples available from $\sqrt{s} = 10.58$ GeV running as well as anticipated data samples from CLEO-c [2)] and BESIII [3)]. The physics to be probed generally falls into two categories: (1) Probes of QCD to enhance or validate the theoretical control over QCD. This program will likely be completed with CLEO-c and BESIII (except for charm baryon studies). (2) Searches for physics beyond the Standard Model. This program will not be completed by CLEO-c and BESIII.

The two existing asymmetric B-factories, BABAR at PEP-II and Belle at KEKB, have operated since 1999. PEP-II is running with peak luminosity of $10.0 \times 10^{33}\,\mathrm{cm}^{-2}\mathrm{s}^{-1}$ and KEKB with peak luminosity of $15.8 \times 10^{33}\,\mathrm{cm}^{-2}\mathrm{s}^{-1}$ both at the $\Upsilon(4S)$. The total integrated luminosity recorded by BABAR, 330 fb^{-1}, and Belle, 500 fb^{-1}, includes nearly 10^9 $B\bar{B}$ pairs. Also included in this data sample are nearly 10^9 τ-pairs and 4×10^9 charm mesons.

CLEO-c at CESR has been accumulating data in the charm threshold region since 2003. CESR is running with a peak luminosity of $7 \times 10^{31}\,\mathrm{cm}^{-2}\mathrm{s}^{-1}$. Data samples of 30 million $\psi(2S)$, 750 pb^{-1} at $\psi(3770)$, and 750 pb^{-1} at $\sqrt{s} = 4170$ MeV are anticipated before shutdown in 2008. This corresponds to a sample of 2.7 million $D^0\overline{D}^0$ pairs and 2.1 million D^+D^- from $\psi(3770)$. The higher energy data sample includes a comparable number of D mesons plus 700,000 $D_s^{*+}D_s^- + D_s^+D_s^{*-}$. BESIII at BEPCII expects first e^+e^- collisions at the end of 2007 and design luminosity, $0.6 \times 10^{33}\,\mathrm{cm}^{-2}\mathrm{s}^{-1}$ at the J/ψ, by the end of 2008. Large charmonium samples, 10×10^9 J/ψ and 3×10^9 $\psi(2S)$, are anticipated, however the τ and charm meson samples will still be much smaller than those from existing B-factories.

The physics output of a Super Flavor Factory *may* be maximized by including energy flexibility in the design of both the accelerator and the detector. Assuming the facility is optimized for asymmetric collisions at $\Upsilon(4S)$, little performance degradation is expected for center-of-mass energies ranging from $\Upsilon(1S)$ to $\Upsilon(5S)$. Including in the initial design the flexibility to run at energies in the τ-charm threshold region requires further study. Some open questions

include: (1) Should low energy running be symmetric or asymmetric? (2) Is the low energy physics reach compromised by a detector optimized for high energy running? (3) Is there a physics need for the low energy data given the enormous τ and charm samples produces at $\sqrt{s} = 10.58$ GeV?

2 The Advantages of Threshold Production

The production rate of charm during threshold running at a Super Flavor Factory and $\Upsilon(4S)$ running is comparable. Although the luminosity for charm threshold running is expected to be an order of magnitude lower, the production cross section is 3 times higher than at $\sqrt{s} = 10.58$ GeV. Charm threshold data has distinct and powerful advantages over continuum and $b \to c$ charm production data accumulated above B production threshold.

Charm Events at Threshold are Extremely Clean: The charged and neutral multiplicites in $\psi(3770)$ events are only 5.0 and 2.4 - approximately 1/2 the multiplicity of continuum charm production at $\sqrt{s} = 10.58$ GeV.

Charm Events at Threshold are pure $D\overline{D}$: No additional fragmentation particles are produced. The same is true for $\sqrt{s} = 4170$ MeV production of $D\overline{D}^*$, $D_s^+ D_s^-$, and $D_s^+ D_s^{*-}$. This allows use of kinematic constraints, such as total candidate energy and beam constrained mass, and permits effective use of missing mass methods and neutrino reconstruction. The crisp definition of the initial state is a uniquely powerful advantage of threshold production that is absent in continuum charm production.

Double Tag Studies are Pristine: The pure production of $D\overline{D}$ states, together with low multiplicity and large branching ratios characteristic of many D decays permits effective use of double-tag studies in which one D meson is fully reconstructed and the rest of the event is examined without bias but with substantial kinematic knowledge. The techniques pioneered by Mark III and extended by CLEO-c [4] allow precise absolute branching fraction determination. Backgrounds under these conditions are heavily suppressed which minimizes both statistical errors and systematic uncertainties.

Signal/Background is Optimum at Threshold: The cross section for the signal $\psi(3770) \to D\overline{D}$ is about 1/2 the cross section for the underlying continuum $e^+e^- \to$ hadrons background. By contrast, for $c\bar{c}$ production at $\sqrt{s} = 10.58$ GeV the signal is only 1/4 of the total hadronic cross section.

Neutrino Reconstruction: The undetected energy and momentum is interpreted as the neutrino four-vector. For leptonic and semileptonic charm decays the signal is observed in missing mass squared distributions and for double-tagged events these measurements have low backgrounds. The missing mass resolution is about one pion mass. For semileptonic decays the q^2 resolution is excellent, about 3 times better than in continuum charm reconstruction at $\sqrt{s} = 10.58$ GeV. Neutrino reconstruction at threshold is clean.
Quantum Coherence: The production of D and $\overline{D}$ in a coherent $C = -1$ state from $\psi(3770)$ decay is of central importance for the subsequent evolution and decay of these particles. The same is true for $D\overline{D}(n)\pi^0(m)\gamma$ produced at $\sqrt{s} \sim 4$ GeV where $C = -1$ for even m and $C = +1$ for odd m. The coherence of the two initial state D mesons allows both simple and sophisticated methods to measure $D\overline{D}$ mixing parameters, strong phases, CP eigenstate branching fractions, and CP violation [5, 6, 7, 8, 9].

3 Physics Reach of Low Energy Running

The low energy data at a Super Flavor Factory can be used to improve our knowledge of QCD, the Standard Model (SM), and search for New Physics (NP) with the study of the τ lepton, charmonia, total hadronic cross section, charm mesons, and charm baryons.

3.1 τ Studies

Studies of the τ lepton include measurement of absolute branching fractions, precision determination of τ properties - mass, lifetime, and dipole moment - to probe CPT and CP violation, lepton universality, measurements of hadronic currents - to probe QCD, measure V_{us} and m_s, searches for CP violation in weak τ decays, and searches for rare or Standard Model forbidden decays such as lepton flavor violation [10]. The τ mass determination benefits from the constrained kinematics of threshold production but will likely be limited by knowledge of the beam energy to ± 0.1 MeV at BESIII. This precision can be compared with the statistical error expected in 100 ab^{-1} of ± 0.023 MeV. Improved constraints on the τ neutrino mass in the range of 1-5 MeV might be attainable at threshold. The τ lifetime cannot be measured in symmetric

collisions at threshold. The choice of energy for the rest of the τ program is driven by the need for large statistics. The τ-pair production cross section is 0.89 nb at Υ(4S) and 1.2 nb at threshold. Combined with the expected luminosities there is no compelling reason to run at τ threshold.

3.2 Charmonium Physics at the J/ψ Resonance

The design luminosity at a Super Flavor Factory at the J/ψ resonance could exceed the design luminosity at BESIII by an order of magnitude. The BESIII samples will be orders of magnitude larger than current BES samples. It is challenging to predict quantitatively the sensitivities that can be achieved with the 10^{12} J/ψ sample that might be accumulated at the Super Flavor Factory. Below are described some of the physics topics that can be elucidated.

$J/\psi \rightarrow$**VS Transitions:** The primary motivation for acquiring a large J/ψ sample is the study of glueballs. More generally, it is the study of scalar ($J^{PC} = 0^{++}$) and tensor ($J^{PC} = 2^{++}$) mesons produced in radiative J/ψ decay. The Particle Data Group lists three light isoscalar mesons, the $f_0(1370)$, $f_0(1500)$, and $f_0(1710)$ while the quark model predicts two in this mass region. There is a strong bias that one of the f_0 is *the* glueball or that the three observed f_0 mesons are mixtures of the glueball and the two $q\bar{q}$ states. The double radiative decay $J/\psi \rightarrow \gamma f_0$ followed by $f_0 \rightarrow \gamma\rho, \gamma\phi$ [11, 12] and the decay $J/\psi \rightarrow Vf_0$ [12, 13, 14, 15] may elucidate the glueball content of the f_0 mesons.

Exclusive J/ψ Branching Fractions: Models of charmonium make definite predictions for the $\psi(2S)$ branching fractions based on J/ψ decay rates. Exclusive branching fractions are not well measured. A systematic program of precision J/ψ branching ratio measurements is desirable to test and improve our understanding of charmonium. Hadronic decays to charmless final states account for 87% of J/ψ decay - only 40% of that is measured exclusively.

Leptonic J/ψ Decays: The J/ψ is commonly identified through its decay to leptons. The relative branching ratios of J/ψ to leptons are known to 1% and do not pose a precision barrier to other measurements. The only exception is in the determination of $\Gamma_{ee}(J/\psi)$ through ISR [16].

Threshold Enhancements: BES reported an enhancement in the $M(p\bar{p})$ spectrum in $J/\psi \rightarrow \gamma p\bar{p}$ decays which they attribute to a sub-threshold resonance, the mass (1859 MeV) and width ($\Gamma < 30$ MeV at 90% C.L.) of which

are not consistent with any known particle hence it is called the $X(1860)$ [17]. An enhancement observed by BES in the $\pi^+\pi^-\eta'$ spectrum in $J/\psi \to \gamma\pi^+\pi^-\eta'$ may confirm this observation [18]. However, the enhancement is not observed in $J/\psi \to \pi^0 p\bar{p}$ decays at BES or in $\Upsilon(1S) \to \gamma p\bar{p}$ decay at CLEO [19]. BES has observed additional threshold enhancements [20, 21]. BESIII will accumulate a significant J/ψ data sample which may clarify the situation.

3.3 Charmonium Physics at the $\psi(2S)$ Resonance

The design luminosity at a Super Flavor Factory at the $\psi(2S)$ resonance could exceed the design luminosity at BESIII by an order of magnitude. The BESIII samples will be orders of magnitude larger than current BES (58 million) and anticipated CLEO-c (30 million) samples. It is challenging to predict the physics issues to be addressed with 10^{12} $\psi(2S)$ sample accumulated at the SFF.

Radiative $\psi(2S)$ Transitions: The η_c, the charmonium ground state, is of particular interest since its bottomonium counterpart is unobserved experimentally. The η_c mass and width have been determined utilizing multiple production mechanisms but without good agreement. Additionally, the exclusive decay modes measured account for about 25% of the total with substantial uncertainties. Relating the η_c branching fractions to the corresponding measurements on the η_c' tests our models of charmonium. Although η_c production rate is greater from radiative J/ψ decay, data accumulated at the $\psi(2S)$ allows for both $\psi(2S) \to \gamma\eta_c$ and $\psi(2S) \to \gamma\eta_c'$ processes.

Exclusive $\psi(2S)$ Branching Fractions: Models of charmonium make definite predictions for the $\psi(2S)$ based on J/ψ decay rates. Exclusive branching fractions are not well measured. A systematic program of precision $\psi(2S)$ branching ratio measurements at CLEO-c and BESIII will test our understanding of charmonium.

Properties of $h_c(1^1P_1)$: In 2005, CLEO reported first observation of the h_c [22, 23]. The h_c is the last of the eight bound states of charmonium expected to lie beneath open charm threshold. Precision determination of the properties of the h_c, mass, width, branching fractions will improve our understanding of the QCD potential – in particular, measuring $M(h_c)$ relative to the center of gravity of the χ_{cj} states. Predictions using a number of theoretical models [24, 25] span a wide range of values and therefore precise measurements

of the hyperfine splitting can distinguish among models. A precision of better than 0.1 MeV on $M(h_c)$ and 0.2 MeV on $\Gamma(h_c)$ is expected from a sample of 300 million $\psi(2S)$ - 10% of the sample anticipated in one year at BESIII.

J/ψ Sample from $\psi(2S)$: A large J/ψ sample can be obtained through the cascade production from $\psi(2S)$ decays to $\pi^+\pi^- J/\psi$ with $\mathcal{B} = 33.5\%$. This reduces and perhaps eliminates the need for running at the J/ψ.

χ_{cj} Sample from $\psi(2S)$: The $\psi(2S)$ is a factory for producing χ_{cj} through $\psi(2S) \to \gamma\chi_{cj}$. The branching ratios are around 9% and photon detection efficiencies (after π^0 suppression) are about 50% so that one detectable each of χ_{c0}, χ_{c1} and χ_{c2} are produced for every 20 $\psi(2S)$. Hadronic decay of the χ_{cj} offer a number of interesting measurements (1) study of mesons with manifestly exotic quantum numbers through the Dalitz plot analysis of $\chi_{cj} \to \eta\pi\pi$ (2) study of the quark content of the three isoscalar mesons, $f_0(1370)$, $f_0(1500)$, and $f_0(1710)$. Since $f_2(1270)$ is nearly entirely $u\bar{u}, d\bar{d}$ and the $f_2'(1525)$ is nearly entirely $s\bar{s}$, these two narrow resonances can be used to tag the flavor of the f_0. Therefore comparing the relative rates of $\chi_{c2} \to f_2(1270)f_0$ and $\chi_{c2} \to f_2'(1525)f_0$ can shed light on the quark content of the f_0 in question. (3) Multibody charmonium decays access most of the kinematic range accessible to B decays. Improved modelling of $\pi\pi$, $K\pi$, KK S-wave in charmonium samples, such as $\chi_{c0} \to \pi^+\pi^- K^+ K^-$ [26], will enable precision measurements of CKM angles α, β, and γ. Specifically, understanding the $\pi\pi$ S-wave is important for the determination of α ($B^0 \to \pi^+\pi^-\pi^0$) and γ ($B^- \to DK^-, D \to K_S^0\pi^+\pi^-$), understanding the $K\pi$ S-wave is important for the determination of γ ($B^- \to DK^-, D \to K_S^0 K\pi$), and the understanding of the KK S-wave is important of the determination of β using $b \to s$ penguin processes ($B \to K_S^0 K^+ K^-$).

The $M2/E1$ Ratio for $\chi_{cj} \to \gamma J/\psi$: The transitions $\chi_{c1} \to \gamma J/\psi$ and $\chi_{c2} \to \gamma J/\psi$ can each proceed through either an $E1$ or $M2$ transition. Current measurements are at odds with theoretical expectations [27, 28]. The BESIII sample of $\psi(2S)$ will be sufficient to conclusively measure this multipole ratio.

3.3.1 Using $\psi(2S)$ Running as Calibration Data

Data taken at the $\psi(2S)$ has a utilitarian value. The processes $\psi(2S) \to \pi^+\pi^- J/\psi$, $\pi^0\pi^0 J/\psi$, and $\gamma\chi_{cj}$ are particularly useful. They provide hadron and photon spectra of known momenta that are useful for measuring recon-

struction efficiencies in data, Monte Carlo tuning, and detector calibration. Such data, taken at intervals interspersed between higher energy running, can be used for monitoring software and detector performance, leading to better control of systematic uncertainties for studies of τ and charm at threshold.

3.4 Charmonium Physics above $c\bar{c}$ Threshold

The total e^+e^- cross section and R measurement: The BES measurements of the total cross section of e^+e^- annihilation to hadrons or R scan from 85 energy points between 2 and 5 GeV have an average statistical error of 6.6% and a systematic uncertainty of 3.3% using about 70 nb^{-1} per point [30]. The CLEO measurement of R with an accuracy of 2% in the vicinity of the Υ(4S) [31] and recent progress in the calculation of radiative corrections together with the hermeticity of the BESIII detector allows one to expect a systematic uncertainty of about 1% below and 2-4% above open charm threshold.

A second approach to measuring R in the 2-5 GeV range uses initial state radiation (ISR) from 10.58 GeV [32]. This approach should be competitive with results from the R scan. Existing data samples from BABAR and Belle are expected to be limited by systematic uncertainties to a precision of a few percent. If further advances in the calculation of radiative corrections enable R measurements with sub-percent precision the ISR data from the Υ(4S) running of a SFF will have more than sufficient statistics for the R measurement.

$c\bar{c}$ Hybrids, $Y(4260)$ and Other Resonances: The region at center-of-mass energies above open charm production threshold is of great interest to theory due to its richness of $c\bar{c}$ states, the properties of which are not well-understood. Prominent structures in the hadronic cross section are the $\psi(3770)$, $\psi(4040)$, and $\psi(4160)$. A dedicated scan, 1 fb^{-1}/per energy point at 100 energy points, to search for hybrid $c\bar{c}$ mesons coupling directly to e^+e^- through a virtual photon or produced in decay products of charmonia represented by the structure in the hadronic cross section would require 100 days of SFF running.

Recently, observations of new charmonium-like states decaying to open-charm have been reported in this energy region. Additionally, an enhancement, the $Y(4260)$, in the invariant mass spectrum of $\pi^+\pi^- J/\psi$ has been observed by BABAR in ISR [33] and in $B \to K(\pi^+\pi^- J/\psi)$ [34]. This observation was confirmed by CLEO is both ISR $(\pi^+\pi^- J/\psi)$ [35] and in e^+e^- collision at

$\sqrt{s}$ = 4260 MeV ($\pi^+\pi^- J/\psi$, $\pi^0\pi^0 J/\psi$, $K^+K^- J/\psi$) [36]. These observation help distinguish among the many models predicting properties of the $Y(4260)$.

3.5 D^0, D^+, and D_s^+ Decays

Leptonic Charm Decays - $D^+ \to \ell^+\nu$, $D_s^+ \to \ell^+\nu$: For the muonic decays, CLEO-c and BESIII, will determine the decay constants f_D and f_{D_s}, to precision of 1%. The decay constants measure the nonperturbative wave function of the meson at zero inter-quark separation. In the Standard Model the relative widths for $\tau^+\nu$, $\mu^+\nu$ and $e^+\nu$ are $2.65 : 1 : 2.3\times10^{-5}$. Comparison of electronic, muonic and tauonic rates [37, 38, 39] tests for physics beyond the SM.

Exclusive Semileptonic Charm Decays - $D \to (K, K^*, K\pi)\ell\nu$, $D \to (\pi, \eta, \rho, \omega, \pi\pi)\ell\nu$, $D_s \to (\eta, \phi)\ell\nu$, $D_s \to (K, K^*, K\pi)\ell\nu$, and $\Lambda_c \to \Lambda\ell\nu$: Absolute branching ratios, for the D and D_s, will be measured to $\sim 1\%$ and the form factor slopes to $\sim 2\%$ by CLEO-c [40, 41, 42] and BESIII. Threshold production enables form factor measurements with improved resolution over the full range of q^2. Semileptonic decay rates *and* accurate knowledge of form factors are required for CKM elements $|V_{ub}|$, $|V_{cb}|$, $|V_{cd}|$, and $|V_{cs}|$.

Inclusive Semileptonic Charm Decays - $D \to \ell X$, $D_s \to \ell X$, and $\Lambda_c \to \ell X$: Inclusive branching ratios, for the D and D_s, will be measured to $\sim 1\%$ by CLEO-c [29] and BESIII. Inclusive spectra have three advantages compared to semileptonic branching fractions as a probe of theory: (1) Theoretical interpretation is cleaner as spectra are independent of the hadronic width. (2) Spectra contain both shape and rate information. (3) Non-perturbative effects are pronounced in the lepton endpoint region. Low backgrounds associated with tagged events at threshold enable inclusive semileptonic studies. The theoretical description of semileptonic decays in the charm sector, coupled with heavy quark symmetry, will improve the description of semileptonic B decays and the determination of V_{ub} and V_{cb}.

Hadronic Charm Decays: CLEO-c and BESIII will measure the branching fractions for the normalizing modes $D^0 \to K\pi$, $D^+ \to K^-\pi^+\pi^+$, and $D_s^+ \to K^+K^-\pi^+$ to a precision of less than 1% [4, 43]. Sensitivity to Cabibbo suppressed modes, $D \to (n)\pi(m)\pi^0$, at $10^{-5} - 10^{-6}$ level [44, 43] and independent measurements of $D \to K_S^0 X$ and $D \to K_L^0 X$ are possible at threshold due to low backgrounds and constrained kinematics with these data samples.

3.6 Impact on CKM physics

Determination of V_{ub}: Limited by form factor calculations to $\sim 13\%$. Improving form factor calculation methods in the charm decays $D \to \pi\ell\nu$ and $D \to \rho\ell\nu$ with data from CLEO-c will enable 5% precision in $|V_{ub}|$. Improved understanding of weak annihilation contributions to inclusive semileptonic charm decay will improve the extraction of V_{ub} from inclusive semileptonic B meson decay. Improvement will be possible with the BESIII data sample.
Determination of V_{td} and V_{ts}: Limited by ignorance of $f_B\sqrt{B_{B_d}}$ and $f_{B_s}\sqrt{B_{B_s}}$. Determining $|V_{td}|$ and $|V_{ts}|$ from B mixing measurements requires improved determination of f_B and f_{B_s}. Precision measurements of f_D, f_{D_s} and f_D/f_{D_s} at CLEO-c and BESIII will enable the necessary theoretical advances.
Determination of V_{cd} and V_{cs}: Currently known to $\sim$10% level by direct measurement. CLEO-c is measuring absolute branching ratios of leptonic and semileptonic decays from which $|V_{td}|$ and $|V_{ts}|$ can be determined with few percent accuracy. Again form factor and decay constant calculations must achieve comparable precision for the few percent precision on CKM parameters to be realized. These measurements will enable Unitarity tests of the CKM matrix. Data from BESIII will enable additional improvement.
Determination of V_{cb}: Presently limited by several factors including theoretical control of form factors and experimental determination of $\mathcal{B}(D \to K\pi)$. CLEO-c will drive form factor technology and will measure the normalizing hadronic charm branching ratios at the percent level. Precision of 3% in V_{cb} is expected. Improved precision using BESIII data will require theoretical advances to better estimate corrections to form factors. The inclusive determination of V_{cb} will benefit from better knowledge of the inclusive lepton spectra which refine modeling of the "cascade" decays $b \to c \to s\ell\nu$.
CKM Angle γ/ϕ_3: Measurement of the CKM angle γ/ϕ_3 is challenging. Several methods have been proposed using $B^{\mp} \to DK^{\mp}$ decays; (1) the Gronau-London-Wyler (GLW) [45] method where the D decays to CP eigenstates (2) the Atwood-Dunietz-Soni (ADS) [46] method where the D decays to flavor eigenstates and (3) the Dalitz-plot method [47] where the D decays to a three-body final state. Uncertainties due to charm contribute to each of these methods. A variety of charm measurements impact the determination of γ/ϕ_3 from the Υ(4S): (1) Improved constraints on charm mixing amplitudes - important

for GLW, (2) Measurement of the relative rate and relative strong phase δ between D^0 and $\overline{D}^0$ decay to $K^+\pi^-$ - important for ADS, and (3) studies of charm Dalitz plots tagged by hadronic flavor or CP eigenstates. Charm threshold data is necessary for the measurement of δ and the study of CP tagged Dalitz plots. Only 1 fb^{-1} of charm threshold data is required to measure $\cos\delta$ to ± 0.1 [6] which will be accomplished by CLEO-c and BESIII. The CKM angle γ/ϕ_3 will be measured to 1^o (statistical) with 100 ab^{-1} of SFF data. The sample of 30 fb^{-1} at charm threshold - expected from BESIII - is needed to limit Dalitz-plot systematic uncertainties to 1^o [48].

4 D Mixing, CP Violation, and Rare Charm Processes

$\mathbf{D^0 - \bar{D}^0}$ Mixing: Neutral flavor oscillation in the D meson system is highly suppressed within the SM. The time evolution of a particle produced as a D^0 or $\bar{D}^0$, in the limit of CP conservation, is governed by four parameters: $x = \Delta m/\Gamma$, $y = \Delta\Gamma/2\Gamma$ characterize the mixing matrix, δ the relative strong phase between Cabibbo favored (CF) and doubly-Cabibbo suppressed (DCS) amplitudes and R_D the DCS decay rate relative to the CF decay rate [49]. The mass and width differences x and y can be measured in a variety of ways. The most precise limits are obtained by exploiting the time-dependence of D decays [49]. A time-dependent analysis of $D^0 \to K^0_S\pi^+\pi^-$ Dalitz plot [50] allows simultaneous determination of x and y without phase or sign ambiguity but with $\sim 4\times$ less sensistivity relative to the time-dependent study of $D^0 \to K^+\pi^-$ [51]. Time-dependent analyses are not feasible at CLEO-c and BESIII; however, the quantum-coherent $D^0\bar{D}^0$ state provides time-integrated sensitivity to x, y at $\mathcal{O}(1\%)$ level and $\cos\delta \sim 0.05$ [2, 6]. Asymmetric collisions near $\sqrt{s} = 4$ GeV at a SFF could enable time-dependent measurements.

CP Violation [5, 8]: Standard Model CP violation is strongly suppressed in charm as the effective weak phase is rather small - $\mathcal{O}(\lambda^4)$, arising only in singly-Cabibbo-suppressed transitions where expected CP asymmetries reach $\mathcal{O}(0.1\%)$. Significantly larger values would indicate NP. Any asymmetry in CF or DCS decays requires new physics - except for $D^\pm \to K^0_S\pi^\pm$, where the CP impurity due to the K^0_S induces an asymmetry of 3.3×10^{-3}. At $\sqrt{s} = 10.58$ GeV, the decay channel $D^{*\pm} \to D\pi^\pm$ is used to provide a flavor tag for the D meson. Threshold production provides a CP tag. CP conservation

forbids certain final states from the decay of the $D^0\overline{D}^0$ pair from correlated production. For $C = -1$ states produced from $\psi(3770) \to D\overline{D}$, the final state f_+f_+, such as $(K^+K^-)(\pi^+\pi^-)$, is forbidden; For $C = +1$ states produced from $e^+e^-(4170\,\mathrm{MeV}) \to D\overline{D}\gamma$, the final state f_+f_-, such as $(K^+K^-)(K^0_S\pi^0)$, is forbidden. The expected sensitivity to direct CP violation with tagged decays at CLEO-c and BESIII is $\sim 1\%$; at a SFF it is $\sim 0.1\%$. There are also methods to probe CP violation with untagged charm decays [53].

Decays to final states with more than two pseudoscalars or one pseudoscalar and one vector meson contain more dynamical information than given by their widths. Distribution on Dalitz plots or T odd moments can exhibit CP asymmetries considerably larger than those for the width. The Dalitz plots for $\psi(3770) \to D^0\bar{D}^0 \to f_+K_S\pi^+\pi^-$ and $\psi(3770) \to D^0\bar{D}^0 \to f_-K_S\pi^+\pi^-$ will be distinct and the Dalitz plot for the untagged sample $\psi(3770) \to D^0\bar{D}^0 \to XK_S\pi^+\pi^-$ will be distinct from that observed with uncorrelated D's from continuum production at ~ 10 GeV [54]. The sensitivity at charm threshold to CP violation with Dalitz plot analyses has not yet been evaluated. The sensitivity to CP violation with flavor tagged $D^0 \to K^0_S\pi^+\pi^-$ at $\sqrt{s} = 10.58$ GeV in 9 fb^{-1} is in the range (3.5 to 28.4)$\times 10^{-3}$ depending on the decay channel [55].

Rare and Forbidden Charm Decays: The Standard Model predicts vanishingly small branching ratios for processes such as $D \to \pi/K^{(*)}\ell^+\ell^-$ which is GIM suppressed. Rare decays of charmed mesons and baryons provide "background-free" probes of new physics effects that enhance rare or allow forbidden processes such as lepton flavor violation ($D \to Ke^+\mu^-$) and lepton number violation ($D^+ \to K^-e^+e^+$). Current limits are $\mathcal{O}(10^{-4})$ to $\mathcal{O}(10^{-6})$ and are limited by statistics. Limits from BESIII will improve to $\mathcal{O}(10^{-7})$ to $\mathcal{O}(10^{-8})$ [43]. It is noteworthy that long distance dynamics can generate some of these final states even within the SM such as $D^+ \to \phi\pi^+$, $\phi \to e^+e^-, \mu^+\mu^-$. In these cases distinguishing NP from SM contributions will be a challenge.

4.1 Charm Baryons

The absolute scale for charm baryon decays decays is not well determined. To date, the measurements of the charm baryon absolute rate are model dependent. The decay mode used to normalize all other decay rates is $\Lambda_c^+ \to pK^-\pi^+$ but it is only known to be $(5.0 \pm 1.3)\%$ [56]. Prospects for improving this situa-

tion are poor without data taken near $\Lambda_c\bar{\Lambda}_c$ threshold where a modest amount data, 20 fb^{-1}, could measure $\mathcal{B}(\Lambda_c)$ to within 1% of itself. Semileptonic decays of charm baryons are also of interest to test our theoretical understanding of form factors. Measuring Λ_c is important for understanding of b fragmentation and the study of Λ_b which is usually studied in $\Lambda_b \to \Lambda_c X$, $\Lambda_c \to pK^-\pi^+$.

5 Summary

Current questions in τ, open charm and charmonium have been summarized. For τ physics there is no compelling reason to run near threshold. Charmonium data samples will increase by several orders of magnitude before a 2011 as BESIII carries out it physics program. It is difficult to forecast what questions will remain and new question arise in this area. Although ISR from $\sqrt{s} = 10.58$ GeV renders an R scan unneccessary, the capability to study charm hybrids and charmonium above open charm threshold with direct production is desireable. Using open charm produced near threshold to improve the precision of CKM parameters determined by BABAR, Belle, CLEO-c and BESIII will require theoretical advances. Searches for D-mixing, CP violation charm and rare charm decays are driven by statistics. The enormous B and charm samples available at a Super Flavor Factory at $\sqrt{s} = 10.58$ GeV partially mitigate the need for charm threshold data. However, there are many advantages to running at threshold such as lower backgrounds, lower multiplicity, increased kinematical constraints and quantum coherence. Thus, it is prudent to design the Super Flavor Factory machine and detector with the flexibility to operate effetively with center-of-mass energies ranging from J/ψ to $\Upsilon(5S)$. More work is required and is ongoing to determine whether the benefit of charm threshold running is worth the cost and effort.

References

1. J. Albert *et al.*, INFN Roadmap Report, arXiv:physics/0512235.
2. R. A. Briere *et al.*, Cornell University, CLNS 01/1742 (2001) (unpublished).
3. Internal Report, IHEP-BEPCII-SB-13 (unpublished).
4. Q. He *et al.* [CLEO Collab.], Phys. Rev. Lett. **95**, 121801 (2005).

5. I. I. Y. Bigi, UND-HEP-89-BIG01 *Given at Tau Charm Factory Workshop, Stanford, CA, May 23-27, 1989*

6. D. M. Asner and W. M. Sun, Phys. Rev. D **73**, 034024 (2006).

7. M. Gronau, Y. Grossman and J. L. Rosner, Phys. Lett. B **508**, 37 (2001).

8. I. I. Y. Bigi and A. I. Sanda, Camb. Monogr. Part. Phys. Nucl. Phys. Cosmol. **9**, 1 (2000).

9. S. Bianco *et al.*, Riv. Nuovo Cim. **26N7**, 1 (2003)

10. J. M. Roney, *at the International Workshop on Discoveries in Flavour Physics at e^+e^- Colliders (DIF 06), Frascati, Italy, 28 Feb - 3 Mar 2006.*

11. F. E. Close and A. Kirk, Eur. Phys. J. C **21**, 531 (2001).

12. F. E. Close and Q. Zhao, Phys. Rev. D **71**, 094022 (2005).

13. M. Ablikim *et al.* [BES Collab.], Phys. Lett. B **607**, 243 (2005).

14. M. Ablikim *et al.* [BES Collab.], Phys. Lett. B **603**, 138 (2004).

15. Q. Zhao, B. s. Zou and Z. b. Ma, Phys. Lett. B **631**, 22 (2005).

16. B. Aubert *et al.* [BABAR Collab.], Phys. Rev. D **69**, 011103 (2004).

17. J. Z. Bai *et al.* [BES Collab.], Phys. Rev. Lett. **91**, 022001 (2003).

18. M. Ablikim *et al.* [BES Collab.], Phys. Rev. Lett. **95**, 262001 (2005).

19. S. B. Athar *et al.* [CLEO Collab.], Phys. Rev. D **73**, 032001 (2006).

20. M. Ablikim *et al.* [BES Collab.], Phys. Rev. Lett. **96**, 162002 (2006).

21. [BES Collab.], arXiv:hep-ex/0604045.

22. J. L. Rosner *et al.* [CLEO Collab.], Phys. Rev. Lett. **95**, 102003 (2005).

23. P. Rubin *et al.* [CLEO Collab.], Phys. Rev. D **72**, 092004 (2005).

24. T. Appelquist *et al.* Ann. Rev. Nucl. Part. Sci. **28**, 387 (1978).

25. S. Godfrey and J. L. Rosner, Phys. Rev. D **66**, 014012 (2002).

26. M. Ablikim *et al.* [BES Collab.], Phys. Rev. D **72**, 092002 (2005).

27. T. A. Armstrong *et al.* [E760 Collab.], Phys. Rev. D **48**, 3037 (1993).

28. M. Ambrogiani *et al.* [E835 Collab.], Phys. Rev. D **65**, 052002 (2002).

29. N. E. Adam [CLEO Collab.], hep-ex/0604044 - submitted to PRL.

30. J. Z. Bai *et al.* [BES Collab.], Phys. Rev. Lett. **88**, 101802 (2002).

31. R. Ammar *et al.* [CLEO Collab.], Phys. Rev. D **57**, 1350 (1998).

32. F. Anulli [BABAR Collab.], arXiv:hep-ex/0406017.

33. B. Aubert *et al.* [BABAR Collab.], Phys. Rev. Lett. **95**, 142001 (2005).

34. B. Aubert *et al.* [BABAR Collab.], Phys. Rev. D **73**, 011101 (2006).

35. M. R. Shepherd *et al.* [CLEO Collab.], to be submitted to Phys. Rev. D.

36. T. E. Coan *et al.* [CLEO Collab.], Phys. Rev. Lett. **96**, 162003 (2006).

37. G. Bonvicini *et al.* [CLEO Collab.], Phys. Rev. D **70**, 112004 (2004).

38. M. Artuso *et al.* [CLEO Collab.], Phys. Rev. Lett. **95**, 251801 (2005).

39. P. Rubin [CLEO Collab.], hep-ex/0604043, submitted to Phys. Rev. D.

40. T. E. Coan *et al.* [CLEO Collab.], Phys. Rev. Lett. **95**, 181802 (2005).

41. G. S. Huang *et al.* [CLEO Collab.], Phys. Rev. Lett. **95**, 181801 (2005).

42. M. Artuso, arXiv:hep-ex/0510052.

43. H. Li, "Charm Physics with BES-III at BEPC-II," arXiv:hep-ex/0605004.

44. P. Rubin *et al.* [CLEO Collab.], Phys. Rev. Lett. **96**, 081802 (2006).

45. M. Gronau and D. Wyler, Phys. Lett. B **265**, 172 (1991);
M. Gronau and D. London., Phys. Lett. B **253**, 483 (1991).

46. D. Atwood, I. Dunietz and A. Soni, Phys. Rev. Lett. **78**, 3257 (1997);
D. Atwood, I. Dunietz and A. Soni, Phys. Rev. D **63**, 036005 (2001).

47. A. Giri *et al.*, Phys. Rev. D **68**, 054018 (2003).

48. A. Bondar and A. Poluektov, arXiv:hep-ph/0510246.

49. D. Asner, "$D^0 - \overline{D}^0$ Mixing", Phys.Lett.B592: 1, 2004.

50. D. M. Asner *et al.* [CLEO Collab.], Phys. Rev. D **72**, 012001 (2005).

51. R. Godang *et al.* [CLEO Collab.], Phys. Rev. Lett. **84**, 5038 (2000).

52. F. Buccella, M. Lusignoli and A. Pugliese, Phys. Lett. B **379**, 249 (1996).

53. A. A. Petrov, Phys. Rev. D **69**, 111901 (2004).

54. H. Muramatsu *et al.* [CLEO Collab.], Phys. Rev. Lett. **89**, 251802 (2002).

55. D. M. Asner *et al.* [CLEO Collab.], Phys. Rev. D **70**, 091101 (2004).

56. P. R. Burchat, "Λ_c^+ Branching Fractions," Phys.Lett.B592: 1, 2004.

Frascati Physics Series Vol. XLI (2006), pp. 393-396
DISCOVERIES IN FLAVOUR PHYSICS AT e^+e^- COLLIDERS
Frascati, February 28th - March 3rd, 2006

WHAT ARE THE ARGUMENTS AGAINST FUTURE ELECTRON-POSITRON COLLIDERS FOR FLAVOUR PHYSICS

Fernando Ferroni
Università di Roma La Sapienza & INFN Roma
P.za A. Moro 5, I-00185, Roma, Italy

Abstract

Here it is reported one of contribution to the panel discussion held at the end of the DIF06 conference on the subject of the need of new low energy electron-positron colliders.

1 Introduction

The struggle of all the high energy physicists consists in trying to find any little bit of evidence that the Standard Model (SM) is indeed incomplete. As one of them it is extremely difficult for me to play the role of whom is able to find the killer arguments against the construction of new facilities that sideways with the one at the energy frontier might successfully contribute to break the wall of the SM orthodoxy. So I interpret my contribution as a one that might help the community in optimizing the (scarce) resources deciding for a single

machine rather than few. The argument of the resources is indeed one of the crucial element that we shall take into account in laying out the frame of future initiative. To my personal judgement the first step toward the future of experimental particle physics is a timely, positive decision on the construction of an electron-positron linear collider in the version that is known as ILC. This is a grand project (and a costly one). It will be a great opportunity to see it running at a point in parallel with LHC and possibly complementing it for a global fit of all the new particles that might appear at the TeV scale. However even in the case that SUSY would not appear at the LHC , The International Linear Collider will be the best of all the conceivable machines for looking at the subtle effect induced at low energy by a higher scale. The construction of ILC will drain a lot of resources and one should be careful in optimizing what else could be built, beside that machine at the same time scale.

2 Existing Facilities

There are three sets of energies that are, with good reasons, covered by electron-positron colliders. They correspond to the threshold of the resonance formed by strange, charmed and bottom quarks. DAFNE in Frascati is to-date the best tool at the Φ energy, CESR at the Ψ family region and PEPII and KEKB are the B-factories in operation. Soon the Chinese collider will get back in operation for charm physics.

2.1 Low (Strange) Energy

The physics case for a factory operating at the Φ threshold and around is clear. In short:

- K_S decays like $K_S \to \gamma\gamma, K_S \to \pi^0 e^+ e^-, K_S \to \pi^0\pi^0\pi^0, K_S \to \pi^+\pi^-\pi^0$
- Studies of CPT violation and Quantum Decoherence
- Ratio $K^+ \to \mu^+\nu / K^+ \to e^+\nu$

The measurement of R at energies lower than 1 GeV comes for free by exploiting the initial state radiation, and this measurement is of extreme importance for the correction to the QED calculation of the muon (g-2) value. As we said, the best tool existing is DAFNE that has integrated in excess of 2fb^{-1}. A

modest upgrade of this facility might allow to make a factor 10 and complete the program sketched above.

2.2 Intermediate (Charm) Energy

As mentioned there is a running facility (CESR) and soon another one will get into the game (BEPC). The exploitation of these facilities brings a terrific improvement to the understanding of charm decays and it is the best tool for validating the lattice calculation. See as the One example, the measurement of f_D, f_{D_s}. It is however difficult to see a future need for a machine tunable at different energies around charm resonances with a luminosity beyond the one attainable by the existing ones. For what concern the absolute number of charmed mesons produced a B-factory already produces more of them that you can hope to make with a new dedicated facility. For what physics is concerned there is one single outstanding topic in charm physics. It is $D^0\overline{D}^0$ mixing. However its observation requires a lot of luminosity and therefore a B-factory might be favoured and its interpretation might prove to be impossible in terms of disentangling New Physics effect by trivial long range interaction ones. True, a charm factory running at the $\Psi(3770)$ might have a chance to clarify but the perspectives are bleak. Tau physics is no justification either. A B-factory is better. Here, therefore, we might content ourselves with the present experimental situation.

2.3 High (Beauty) Energy

The two B-factories in operation (PEPII and KEKB) are performing spectacularly well. Before the end of their operation, at the end of the decade, they will have collected more than one inverse attobarn each. However, while the B-physics will be known much better than before, the chances that these machines will provide their twin experiments, BaBar and Belle, with the luminosity sufficient for making the case of the observation of significant deviation from the Standard Model in any of the channel scrutinized is really slim. Here and there indeed there are hints of discrepancy but you clearly see that a mere factor 4-5 of statistics will not be enough to ever make a claim. The feeling is that even a factor 10 more luminosity would not be enough.

So, is it really that we have run out of steam? Indeed new low energy electron-positrons colliders are useless for the future of high energy physics?

3 The future facility

The ideal machine for the future should run at the B-physics energy scale, so to provide access both to B and charm physics. It shall have a luminosity at least two order of magnitude higher than the existing facilities so to allow:

- Very precise measurement of the Unitary Triangle angles
- Explore the $b \to s$ transitions in depth ($B \to Kl^+l^-, B \to \Phi K$)
- Cast light on the SUSY couplings and/or measure its low energy effects
- Improve significantly the $\tau \to \mu\gamma$ limit

At this conference one project for s Super B-Factory has been presented that deserves a lot of attention. It has indeed the potentiality of satisfying all of the above requests and promises even more. It is in fact based almost entirely on the $R\&D$ performed for the Linear Collider preparation and this a great bonus because it reduces the costs and make it a credible project. More than this, given the technology it looks like the machine is so flexible that it might be run at the charm energy with a loss of luminosity only linear with the energy, allowing, just in case, a run at those energies.

It looks impossible, in spite of the title of the talk, therefore not to say that a Super Flavour Factory of the type that has been presented in this conference is the way to go.

4 Acknowledgements

Many thanks to the organizers of the conference for having trusted me for such an unusual task.

CONCLUSIONS

Frascati Physics Series Vol. XLI (2006), pp. 399-407
DISCOVERIES IN FLAVOUR PHYSICS AT e^+e^- COLLIDERS
Frascati, February 28th - March 3rd, 2006

A SEND-OFF AFTER DIF06: WHAT DO WE NEED TO KNOW TO UNDERSTAND MORE?

Ikaros I. Bigi
Physics Dept., University of Notre Dame du Lac,
Notre Dame, IN 46556, U.S.A
email: ibigi@nd.edu

Abstract

After a brief look back at the roles played by hadronic machines and e^+e^- colliders I emphasize that continuing dedicated studies of heavy flavour transitions should be central to our efforts of decoding nature's 'Grand Design'. For studies 'instrumentalizing' the high sensitivity of **CP** violation will presumably be essential to identify salient features of the New Physics anticipated for the TeV scale and hopefully discovered directly at the LHC. An e^+e^- Super-Flavour Factory would provide the optimal platform for such a program.

This is *not* a summary – to my considerable relief I was asked not to give one. These are not *the* conclusions either. You can never give the conclusions when the 'boss', in this case M. Calvetti, is speaking right after you. [1] Instead I will offer merely my personal reflections.

[1] A Justice on the US Supreme Court once said: "We are not the Supreme Court, because we are infallible. We are infallible, since we are the Supreme

1 A Short Look Back

Let us look at two exhibits from the past.

Exhibit A:

The weak bosons were first found at the CERN SPPS – a hadronic collider. It was LEP I & II – an e^+e^- collider – that established the electroweak gauge sector of the Standard Model (SM) with a *quantitative* accuracy *well beyond* original expectations.

Exhibit B:

Indirect and direct **CP** violation were first uncovered at BNL, CERN and FNAL – all hadronic machines. The B factories at KEK and SLAC – e^+e^- machines – established the Yukawa sector of the SM: CKM dynamics are able to describe (at least almost) all **CP** violation as observed in particle decays to a *quantitative* accuracy *well beyond* original expectations. The CKM paradigm has thus become a *tested* theory; **CP** violation has been 'demystified' in the sense that if the dynamics are sufficiently rich to be able to support **CP** violation the latter can be large; this demystification will be completed once **CP** violation is found anywhere in the lepton sector.

Let us remember also what happened with strangeness changing transitions: (i) The $\tau - \theta$ puzzle lead to the realization that **P** symmetry does not hold in the weak interactions. (ii) The observation that the production rate exceeds the decay rate by several orders of magnitude (giving rise to the name 'strangeness') lead to the notion of associated production and in due course to the concept of quark families. (iii) The huge suppression of strangeness changing neutral currents – as inferred from the tiny size of ΔM_K and of $\mathrm{BR}(K_L \to \mu^+\mu^-)$ – encouraged some daring minds to speculate about charm quarks. (iv) The observation of $K_L \to \pi^+\pi^-$ revealed **CP** violation and suggested the existence of a third quark family.

All these features, which are now pillars of the SM, were New Physics *at that time*!

(i.e. final) Court." Working at a Catholic University I am not unfamiliar with this issue.

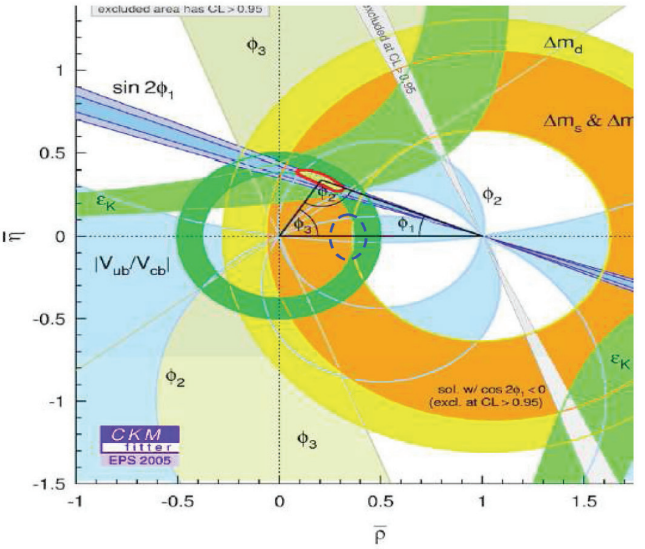

Figure 1: *Constraints on the CKM triangle as of the end of 2005.*

2 What to Do?

The SM is a very peculiar creation. On one hand more and more victories have been attached to its banner. The years around the turn of the millennium have witnessed novel successes in its description of heavy flavour dynamics: most spectacularly the 'Paradigm of truly large **CP** violation in B decays' has been verified. We can even see the next triumph of CKM theory emerging: Consider the constraints on the CKM triangle as of the end of 2005 shown in Fig.1. If you remove the constraints from **CP** violation, in particular from $|\epsilon_K|$ and sin$2\phi_1$ (as well as from $\phi_{2,3}$), thus retaining only those from $|V(ub)/V(cb)|$ and $\Delta M(B)$, then a completely flat triangle – i.e. one with zero area – while not favoured, is not ruled out, as indicated by the broken circle.

If – and that is admittedly a nontrivial 'if' – the evidence presented this spring by D0 [1] for an *upper* bound on the rate of B_s oscillations holds up – $\Delta M(B_s) \leq 21$ p^{-1} – one has a qualitatively new scenario as can be seen from Fig.2 [2]:

- **CP** *in*sensitive observables – namely $|V(ub)/V(cb)|$ and $\Delta M(B_{d,s})$ – imply a CKM triangle of *non*-zero area, i.e. the existence of **CP** violation.

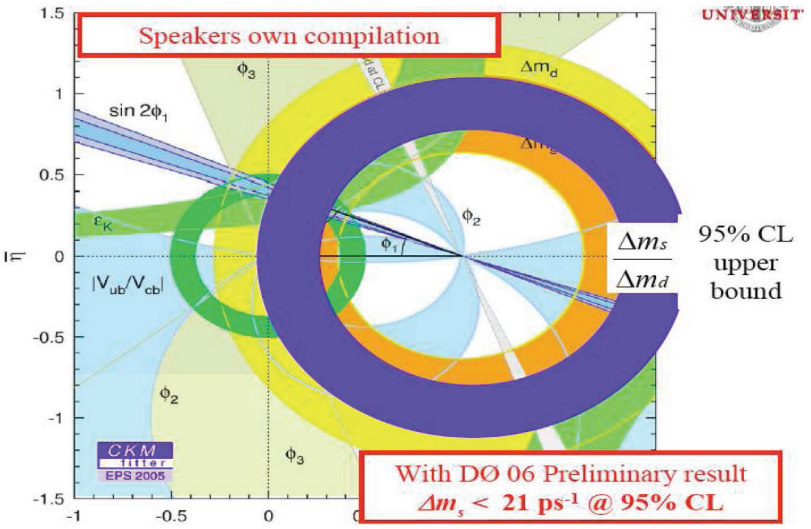

Figure 2: *Constraints on the CKM triangle as of the end of 2005.*

- This triangle is fully consistent with the observed **CP** violation as expressed through ϵ_K and $\sin 2\phi_1$.

Yet *none* of the successes of the SM – including those just sketched – invalidate the arguments for it being incomplete. This represents a virtual consensus in the community. New Physics is expected at the TeV scale.

A clear majority opinion holds that we need more answers from nature to figure out the variant(s) of New Physics realized in nature and to establish that we are 'on the right track'. After all 'experiment is the Supreme Court of Physics'.

Given the past history of searches for Physics beyond the SM this might remind you of Samuel Beckett's dictum:

Ever tried? Ever failed?
No matter.
Try again. Fail again. Fail better.

But we can cheer up – we know there is New Physics: With CKM dynamics being utterly irrelevant for baryogenesis, there has to be a 'New **CP** Paradigm'. Likewise the SM cannot account for neutrino oscillations, dark matter and dark

energy. In addition there are the SM's well known explanatory deficits. Thus we will not fail forever.

Yet history rarely if ever repeats itself in an identical manner. Recognizing that the SM has succeeded in putting a vast array of phenomena occurring at very diverse scales under its roof, we cannot *count* on *numerically* massive manifestations of New Physics in heavy flavour transitions – unlike what happened in the physics of strangeness before the era of the SM. It appears that nature has read the SM's book on flavour changing neutral currents – at least for *down*-type quarks.

Accordingly we need some luck to find this New Physics. Being lucky has of course to be part of the job description for a high energy physicist (in particular of the experimental variety). Accuracy in acquiring and interpreting data will do wonders for enhancing our luck.

3 The Future

I do not intend to beat around the bushes: in my view studies of heavy flavour dynamics

- are of fundamental importance,
- their lessons cannot be obtained any other way and
- they can*not* become obsolete.

I.e., no matter what studies of high $p_\perp$ physics at FNAL and the LHC will or will not show – and I am confident they will show a lot – detailed and comprehensive analysis of flavour physics will remain crucial in our efforts to reveal 'Nature's Grand Design'.

I see three possible scenarios of the next five to eight years:

Scenario A – the 'optimal' one:

New Physics has been observed at high $p_\perp$. It is then *mandatory* to study their impact on flavour dynamics, which is greatly facilitated by the mass scales of the New Physics being known. Even a negative result – i.e. no discernible impact on heavy flavour decays – would be a highly important result in this scenario, however frustrating it would be for our experimental colleagues.

Scenario B – the 'intriguing' one:

Deviations from the SM have been established in heavy flavour decays. Recently considerable excitement has been created by the '$b \to s\bar{s}s$ anomaly', i.e. by experimental evidence that modes driven by this effective 'Penguin-like' operator exhibit markedly lower **CP** asymmetries than predicted by the SM. While the spectacular discrepancies have faded away, some have remained [3], and I find those actually more believable than the original ones. Therefore we better keep a close watch on them,

Scenario C – the 'frustrating' one:
No further deviation from the SM has been established at high or low $p_\perp$.

While I am optimistic it will turn out to be Scenario A, I would like to emphasize that none of these scenarios weakens the importance of continuing heavy flavour studies for our quest of finding out about nature's basic forces.

Yet we do not live and work in isolation. Following what was said by Nakada at this meeting I would like to formulate a 'Generalized Nakada Concern': While more than ever before we have many promising avenues for exploring fundamental physics, while we have more technical tools and capabilities than ever, we live in a world with immense political, social and environmental problems; furthermore we have to deal with governments with less interest in basic research to a degree that goes well beyond a justified pre-occupation with these problems. How do we choose our priorities?

This is an excellent question, and I do not have a general answer to it. I can offer only one criterion, namely to aim for *comprehensive* research goals. In the case under discussion here I want to emphasize that a Super-B factory is also a Super-Tau as well as Super-Charm factory of truly unique capabilities. It allows precise studies of a *third* family *down*-type *quark*, a *third* family *down*-type *lepton* and a *second* family *up*-type *quark*. In this context the studies of **CP** violation, oscillations and rare decays are *instrumentalized* to probe TeV scale New Physics.

To achieve

- a luminosity of 10^{36} cm^{-2} s^{-1}
- with tiny beams and a hermetic detector allowing to study transitions with large amount of 'invisible' energy – like $B \to \tau^+\tau^-$, $\tau\nu$, $\tau\nu X$, $\tau \to l\nu\bar{\nu}$ etc. –
- maybe even with one beam being polarized,

- 'soon' and
- 'here', i.e. near Rome –

to me sounds better than paradise. There is the promise that such a Super-Flavour Factory can be run not only at the $\Upsilon(4S)$ and $\Upsilon(5S)$ resonances, but even at much lower energies close to charm and τ thresholds at an affordable cost in luminosity. While the primary goals in τ and charm physics – searching for and probing **CP** violation as well as rare decays – can profitably be pursued at the $\Upsilon(4S)$, future studies might show that lower energies are optimal for dealing with certain backgrounds. The statistically as well as systematically ambitious goals that need to be pursued in B physics have been listed repeatedly at this workshop. Let me remind you also of equally challenging goals in τ and charm studies [4], namely to go after **CP** asymmetries as small as $\mathcal{O}(10^{-3})$ or even smaller.

It has often been noted that when 'all is said and done' usually a lot more is said than done. We are seeing how the dream of a Super-Flavour Factory is turning into a vision. A whole lot needs to be done before it can be transformed into a project and finally elevated into reality.

I had mentioned in my opening remarks at this workshop [5] that the area around Rome has a long tradition of *linear* structures and shown you a historical example. In Biagini's talk [6] we have seen a brand new and very different 'Solution 2' for an ILC-inspired Super-Flavour Factory. The fascination of Rome is such that you can find an example for almost anything in its rich heritage. 'Solution 2' reminds me of the almost 2000 years old structure shown in Fig. 3 full of tunnels with round as well as straight beam lines. Another intriguing aspect of it is that such a design would be portable to other places – like KEK, which has its own heritage, see Fig.4.

4 A Final Thought

In my opening remarks [5] I had shown a picture as an allegory on the future of high energy physics. I am showing Fig.5 again for a related reason. You notice the sun between the two rocks. Just looking at the picture without taking recourse to additional information you might have about these structures (in particular if you are Italian) you cannot tell if the sun is rising or setting. To me one of the most impressive aspects of experimental high energy physics

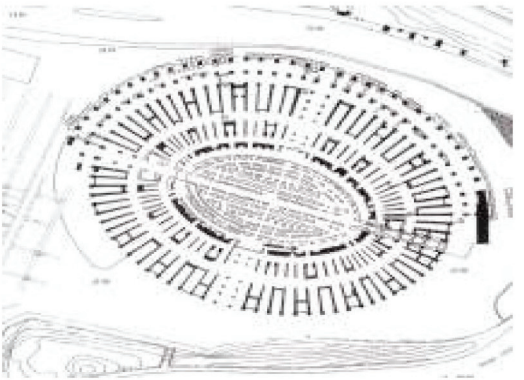

Figure 3: *A prominent machine in Rome.*

Figure 4: *The Baroque splendour of Nikko.*

is that when you give experimentalists resources and time it is most amazing what they can achieve. As an example just have a look at the 'Blue Book' that was written during the planning and constructing of LEP with a lot of quality time spent on it by theorists as well and compare it with what was actually done – which was so much more. This speaks most highly of the intellectual vigour of the field.

Likewise I firmly believe that if a Super-B factory is built, a proper time span is provided to utilize it and young people can fully participate in shaping its program, we will learn even more than what we envision now. In that sense I am confident the picture shows a rising rather than a setting sun.

Figure 5: *Another allegory on HEP's future landscape.*

Acknowledgments

It always is a most gratifying experience to come to the Rome area for discussing and marveling about nature's puzzles with colleagues. This was also true this time, and I am thankful for the organizers of this workshop for creating this opportunity. This work was supported by the NSF under grant PHY03-55098.

References

1. V.M. Abazov *et al.*, D0 Collab., hep-ex/0603029.
2. B. Casey, talk given at 'Moriond EW 2006', La Thuile, March 2006.
3. K.-F. Chen, these Proceedings.
4. I.I. Bigi, these Proceedings.
5. I.I. Bigi, these Proceedings; hep-ph/0603087.
6. M. Biagini, these Proceedings.

PARTICIPANTS

Alfonsi Matteo	INFN-LNF	matteo.alfonsi@lnf.infn.it
Antonelli Antonella	INFN-LNF	antonella.antonelli@lnf.infn.it
Antonelli Mario	INFN-LNF	mario.antonelli@lnf.infn.it
Asner David	Carleton Univ.	asner@physics.carleton.ca
Becirevic Damir	Lab. Physique Theorique	Damir.Becirevic@th.u-psud.fr
Bencivenni Giovanni	INFN-LNF	giovanni.bencivenni@lnf.infn.it
Benussi Luigi	INFN-LNF	luigi.benussi@lnf.infn.it
Bertani Monica	INFN-LNF	monica.bertani@lnf.infn.it
Bertolucci Sergio	INFN-LNF	sergio.bertolucci@lnf.infn.it
Biagini Maria Enrica	INFN-LNF	biagini@lnf.infn.it
Bianco Stefano	INFN-LNF	stefano.bianco@lnf.infn.it
Bigi Ikaros	University Notre Dame	ibigi@nd.edu
Bini Cesare	INFN-LNF	cesare.bini@lnf.infn.it
Biscari Caterina	INFN-LNF	caterina.biscari@lnf.infn.it
Bloise Caterina	INFN-LNF	caterina.bloise@lnf.infn.it
Boscolo Manuela	INFN-LNF	manuela.boscolo@lnf.infn.it
Bossi Fabio	INFN-LNF	fabio.bossi@lnf.infn.it
Bozek Andrzej	Inst.Nuclear Physics	andrzej.bozek@ifj.edu.pl
Cabibbo Nicola	INFN - Roma 1	nicola.cabibbo@roma1.infn.it
Cahn Robert	LBNL	rncahn@lbl.gov
Calvetti Mario	INFN-LNF	mario.calvetti@lnf.infn.it
Calvi Marta	Univ. of Milano Bicocca	marta.calvi@mib.infn.it
Campana Pierluigi	INFN-LNF	pierluigi.campana@lnf.infn.it
Capon Giorgio	INFN-LNF	giorgio.capon@lnf.infn.it
Ceradini Filippo	INFN-LNF	filippo.ceradini@lnf.infn.it
Chen Kai-Feng	National Taiwan Univ.	kfjack@hep1.phys.ntu.edu.tw
Ciambrone Paolo	INFN-LNF	paolo.ciambrone@lnf.infn.it
Crosetti Giovanni	UNICAL	crosetti@fis.unical.it
Crucianelli Fabio	INFN-LNF	fabio.crucianelli@lnf.infn.it

Petronzio Roberto	INFN	presidenza@presid.infn.it
Poli-Lener Marco	INFN-LNF	marco.polilener@lnf.infn.it
Purohit Milind	Univ. of South Carolina	purohit@sc.edu
Roney Michael	University of Victoria	mroney@uvic.ca
Rong Gang	IHEP	rongg@mail.ihep.ac.cn
Sborzacchi Francesco	INFN-LNF	francesco.sborzacchi@lnf.infn.it
Schwartz Alan	Univer. of Cincinnati	schwartz@physics.uc.edu
Sciascia Barbara	INFN-LNF	barbara.sciascia@lnf.infn.it
Shipsey Ian	Purdue University	shipsey@purdue.edu
Stocchi Achille	LAL	stocchi@lal.in2p3.fr
Valente Paolo	INFN - Roma I	paolo.valente@roma1.infn.it
Ventura Silvia	INFN-LNF	silvia.ventura@lnf.infn.it
Weiler Andreas	TU Munich	aweiler@ph.tum.de
Wisniewski William	SLAC	wjw@slac.stanford.edu
Yamamoto Hitoshi	Tohoku University	yhitoshi@awa.tohoku.ac.jp
Yamanaka Taku	Osaka University	taku@hep.sci.osaka-u.ac.jp

FRASCATI PHYSICS SERIES VOLUMES

Volume I
Heavy Quarks at Fixed Target
Eds.: S. Bianco and F.L. Fabbri
Frascati, May 31–June 2, 1993
ISBN—88–86409–00–1

Volume II – Special Issue
Les Rencontres de Physique de la Vallée d'Aoste – Results and Perspectives in Particle Physics
Ed.: M. Greco
La Thuile, Aosta Valley, March 5 –11, 1995
ISBN—88–86409–03–6

Volume III
Heavy Quarks at Fixed Target
Ed.: B. Cox
University of Virginia, Charlottesville
October 7–10, 1994, 11
ISBN—88–86409–04–4

Volume IV
Workshop on Physics and Detectors for DAΦNE
Eds.: R. Baldini, F. Bossi, G. Capon, G. Pancheri
Frascati, April 4–7, 1995
ISBN—88–86409–05–2

Volume V – Special Issue
Les Rencontres de Physique de la Vallée d'Aoste – Results and Perspectives in Particle Physics
Ed.: M. Greco
La Thuile, Aosta Valley, March 3–9, 1996
ISBN—88–86409–07–9

Volume VI
Calorimetry in High Energy Physics
Eds.: A. Antonelli, S. Bianco, A. Calcaterra, F.L. Fabbri
Frascati, June 8–14, 1996
ISBN—88–86409–10–9

Volume VII
Heavy Quarks at Fixed Target
Ed.: L. Kőpke
Rhinefels Castle, St. Goar, October 3–6, 1996
ISBN—88–86409–11–7

Volume VIII
ADONE a milestone on the particle way
Ed.: V. Valente 1997
ISBN—88–86409–12–5

Volume IX – Special Issue
Les Rencontres de Physique de la Vallée d'Aoste – Results and Perspectives in Particle Physics
Ed.: M. Greco
La Thuile, Aosta Valley, March 2–8, 1997
ISBN–88–86409–13–3

Volume X
Advanced ICFA Beam Dynamics
Workshop on Beam Dynamics Issue for e^+e^- Factories
Eds.: L. Palumbo, G. Vignola
Frascati, October 20–25, 1997
ISBN—88–86409–14–1

Volume XI
Proceedings of the XVIII International Conference on Physics in Collision
Eds.: S. Bianco, A. Calcaterra, P. De Simone, F. L. Fabbri
Frascati, June 17–19, 1998
ISBN—88–86409–15–X

Volume XII – Special Issue
Les Rencontres de Physique de la Vallée d'Aoste – Results and Perspectives in Particle Physics
Ed.: M. Greco
La Thuile, Aosta Valley, March 1–7, 1998
ISBN—88–86409–16–8

Volume XIII
Bruno Touschek and the Birth of thee$^+ e^-$
Ed.: G. Isidori
Frascati, 16 November, 1998
ISBN—88–86409–17–6

Volume XIV – Special Issue
Les Rencontres de Physique de la Vallée d'Aoste – Results and Perspectives in Particle Physics
Ed.: M. Greco
La Thuile, Aosta Valley, February 28–March 6, 1999
ISBN—88–86409–18–4

Volume XV
Workshop on Hadron Spectroscopy
Eds.: T. Bressani, A. Feliciello, A. Filippi
Frascati, March 8 2 1999
ISBN—88–86409–19–2

Volume XVI
Physics and Detectors for DAΦNE
Eds.: S. Bianco, F. Bossi, G. Capon, F.L. Fabbri, P. Gianotti, G. Isidori, F. Murtas
Frascati, November 16 –19, 1999
ISBN—88–86409–21–4

Volume XVII – Special Issue
Les Rencontres de Physique de la Vallée d'Aoste – Results and Perspectives in Particle Physics
Ed.: M. Greco
La Thuile, Aosta Valley, February 27 March 4, 2000
ISBN—88–86409–23–0

Volume XVIII
LNF Spring School
Ed.: G. Pancheri
Frascati 15–20 May, 2000
ISBN—88–86409–24–9

Volume XIX
XX Physics in Collision
Ed.: G. Barreira
Lisbon June 29–July1st. 2000
ISBN—88–86409–25–7

Volume XX
Heavy Quarks at Fixed Target
Eds.: I. Bediaga, J. Miranda, A. Reis
Rio de Janeiro, Brasil, October 9–12, 2000
ISBN—88–86409–26–5

Volume XXI
IX International Conference on Calorimetry in High Energy Physics
Eds.: B. Aubert, J. Colas, P. Nédélec, L. Poggioli
Annecy Le Vieux Cedex, France, October 9–14, 2000
ISBN—88–86409–27–3

Volume XXII – Special Issue
Les Rencontres de Physique de la Vallée d'Aoste – Results and Perspectives in Particle Physics
Ed.: M. Greco
La Thuile, Aosta Valley, March 4–10, 2001
ISBN—88–86409–28–1

Volume XXIII
XXI Physics in Collision
Ed.: Soo–Bong Kim
Seoul, Korea, June 28 30, 2001
ISBN—88–86409–30–3

Volume XXIV
International School of Space Science – 2001 Course on: Astroparticle and Gamma–ray Physics in Space
Eds.: A. Morselli, P. Picozza
L'Aquila, Italy, August 30 September 7, 2000
ISBN—88–86409–31–1

Volume XXV
TRDs for the 3rd Millennium Workshop on Advanced Transition Radiation Detectors for Accelerator and Space Applications
Eds. N. Giglietto, P. Spinelli
Bari, Italy, September 20–23, 2001
ISBN—88–86409–32–X

Volume XXVI
KAON 2001 International Conference on CP Violation
Eds.: F. Costantini, G. Isidori, M. Sozzi
Pisa Italy, June 12th 17th, 2001
ISBN—88–86409–33–8

Volume XXVII – Special Issue
Les Rencontres de Physique de la Vallée d'Aoste – Results and Perspectives in Particle Physics
Ed.: M. Greco
La Thuile, Aosta Valley, March 3–9, 2002
ISBN—88–86409–34–6

Volume XXVIII
Heavy Quarks at Leptons 2002
Eds.: G. Cataldi, F. Grancagnolo, R. Perrino, S. Spagnolo
Vietri sul mare (Italy), May 27th June 1st, 2002
ISBN—88–86409–35–4

Volume XXIX
Workshop on Radiation Dosimetry: Basic Technologies, Medical Applications, Environmental Applications
Ed.: A. Zanini
Rome (Italy), February 56, 2002
ISBN—88–86409–36–2

Volume XXIX – Suppl.
Workshop on Radiation Dosimetry: Basic Technologies, Medical Applications, Environmental Applications
Ed.: A. Zanini
Rome (Italy), February 56, 2002
ISBN—88–86409–36–2

Volume XXX – Special Issue
Les Rencontres de Physique de la Vallée d'Aoste – Results and Perspectives in Particle Physics
Ed.: M. Greco
La Thuile, Aosta Valley, March 9–15, 2003
ISBN—88–86409–39–9

Volume XXXI
Frontier Science 2002 – Charm, Beauty and CP, First International Workshop on Frontier Science
Eds.: L. Benussi, R. de Sangro, F.L. Fabbri, P. Valente
Frascati, October 6–11, 2002
ISBN—88–86409–37–0

Volume XXXII
19th International Conference on x–ray and Inner–Shell Processes
Eds.: A. Bianconi, A. Marcelli, N.L. Saini
Universitá di Roma La Sapienza June 24–28, 2002
ISBN—88–86409–39–07

Volume XXXIII
Bruno Touschek Memorial Lectures
Ed.: M. Greco, G. Pancheri
Frascati, May 11, 1987
ISBN—88–86409–40–0

Volume XXXIV – Special Issue
Les Rencontres de Physique de la Vallée d'Aoste – Results and Perspectives in Particle Physics
Ed.: M. Greco
La Thuile, Aosta Valley, February 29 – March 6, 2004
ISBN—88–86409–42–7

Volume XXXV
Heavy Quarks And Leptons 2004
Ed.: A. López
San Juan, Puerto Rico, 1–5 June 2004
ISBN—88–86409–43–5

Volume XXXVI
DAΦNE 2004: Physics At Meson Factories
Eds.: F. Anulli, M. Bertani, G. Capon, C. Curceanu–Petrascu,
F.L. Fabbri, S. Miscetti
Frascati, June 7–11, 2004
ISBN—88–86409–53–2

Volume XXXVII
Frontier Science 2004, Physics and Astrophysics in Space
Eds.: A. Morselli, P. Picozza, M. Ricci
Frascati, 14–19 June, 2004
ISBN—88–86409–52–4

Volume XXXVIII
II Workshop Italiano sulla Fisica di ATLAS e CMS
Eds.: Gianpaolo Carlino and Pierluigi Paolucci
Napoli, October 13 – 15, 2004
ISBN—88–86409–44–3

Volume XXXIX – Special Issue
Les Rencontres de Physique de la Vallée d'Aoste –
Results and Perspectives in Particle Physics
Ed.: M. Greco
La Thuile, Aosta Valley, February 27 – March 5, 2005
ISBN—88–86409–45–1

Volume XL
Frontier Science 2005 – New Frontiers in Subnuclear Physics
Eds.: A. Pullia, M. Paganoni
Milano, September 12 - 17, 2005
ISBN—88–86409–46–X